SYNTHESIS OF PROLINE-BASED N-HETEROCYCLIC CARBENE BUILDING BLOCKS AND THEIR APPLICATIONS

A Dissertation Presented to

the Faculty of the Department of Chemistry

University of Houston

In Partial Fulfillment

of the Requirements for the Degree

Doctor of Philosophy

by

Yang Zhao

May 2015

SYNTHESIS OF PROLINE-BASED N-HETEROCYCLIC CARBENE BUILDING BLOCKS AND THEIR APPLICATIONS

Yang Zhao

APPROVED:

Dr. Scott R. Gilbertson, Chairman

Dr. Chengzhi Cai

Dr. Jeremy A. May

Dr. Angela Möller

Dr. Navin Varadarajan

Dean, College of Natural Sciences and Mathematics

ACKNOWLEDGEMENTS

I would like to express my sincere gratitude to Prof. Scott R. Gilbertson, my dissertation advisor, for his constant guidance and support. His insight in this area always enlightens me. I have learned a lot from him throughout these years.

I would also like to thank Prof. Chengzhi Cai, Prof. Jeremy A. May, Prof. Angela Möller and Prof. Navin Varadarajan for serving on my dissertation committee and for valuable suggestions and discussions.

My special appreciation goes to Gino Martin R. Canlas for his friendship, useful discussions and editorial advice on this dissertation.

I thank Dr. Anton Agarkov and Dr. B. A. Bhanu Prasad for their help and cooperation throughout this research project. I am thankful to all previous and current members of the Gilbertson group.

I would like to thank Jing Yuwen for her friendship in my life. My special thanks goes to my family and friends for their never-ending support.

Finally, this dissertation is dedicated to my husband, Dr. Bo Li. Without his love and encouragement, I would not have come this far.

SYNTHESIS OF PROLINE-BASED N-HETEROCYCLIC CARBENE BUILDING BLOCKS AND THEIR APPLICATIONS

An Abstract of a Dissertation Presented to

the Faculty of the Department of Chemistry

University of Houston

In Partial Fulfillment

of the Requirements for the Degree

Doctor of Philosophy

by

Yang Zhao

May 2015

ABSTRACT

The synthesis of novel proline-based N-heterocyclic carbene ligands has been accomplished. These types of imidazolium salts can be used as building blocks for the synthesis of more sophisticated N-heterocyclic carbene precursors. The proline amino acids are shown to be compatible with peptide synthetic methods by incorporation into tripeptides. The approaches to a variety of bidentate ligand precursors was reported. A number of the ligands synthesized were bound to rhodium through transmetallation of a silver-NHC complex.

Table of Contents

LIST OF ABBREVIATIONS AND SYMBOLS

^{13}C NMR	proton decoupled ^{13}C nuclear magnetic resonance spectrum
^{1}H NMR	^{1}H nuclear magnetic resonance spectrum
^{31}P NMR	proton decoupled ^{31}P nuclear magnetic resonance spectrum
Ac	acetyl
acac	acetylacetonate
Ala	alanine
aq	aqueous
Ar	aryl
Bn	benzyl
Boc	*tert*-butyl carbamate
BozPHOS	1,2-bis[(2*S*,5*S*)-2,5-dimethylphospholano]benzene monooxide
br	broad resonance (NMR)
BSA	bis(trimethylsilyl)acetamide
cat	catalyst
Cbz, Z	benzyloxycarbonyl
COD	cyclooctadiene
d	doublet (NMR)
DCM	dichloromethane
dd	doublet of doublets (NMR)
ddd	doublet of boublets of doublets
DMAc	dimethylacetamide

DMAP	4-demethylaminopyridine
DME	dimethoxyethane
DMF	dimethylformamide
DMSO	dimethylsulfoxide
E	electrophile
EDCI	1-ethyl-3-(3-dimethylaminopropyl)carbodiimide
ee	enantiomeric excess
Et	ethyl
FAB	fast atom bombardment
FG	functional group
Fmoc	9-fluorenylmethylcarbamate
g	gram
HOBt	1-hydroxybenzotriazole
HPLC	high-pressure liquid chromatography
hr	hour
Hyp	hydroxyproline
Hz	hertz, cycles by second (NMR)
IMes	1,3-bis(2,4,6-trimethylphenyl)imidazol-2-ylidene
Imi	imidazole
J	scalar coupling constant (NMR)
LC-MS	liquid-chromatography mass spectroscopy
m	multiplet

Me	methyl
MeCN	acetonitrile
Mes	mesityl, 2,4,6-trimethylphenyl
mg	milligram
mL	milliliter
Ms	mesylate, methanesulfonate
napht	naphthyl
NHC	N-heterocyclic carbene
NMR	nuclear magnetic resonance
OSu	*N*-hydroxysuccinimide
PG	protecting group
Ph	phenyl
ppm	parts per million (NMR)
Pr	propyl
Pro	proline
q	quartet (NMR)
RT	room temperature
s	singlet (NMR)
SM	starting material
S_N	nucleophilic substitution
SPPS	solid-phase peptide synthesis
t	triplet (NMR)

TBAF	tetra-*n*-butylammonium fluoride
*t*Bu	*tert*-butyl
Tf	triflate, trifluoromethanesulfonate
TFA	trifluoroacetic acid
THF	tetrahydrofuran
TLC	thin layer chromatography
TMS	trimethylsilyl
UV	ultraviolet
wt	weight
δ	chemical shift in parts per million (NMR)
μw	microwave

LIST OF FIGURES

LIST OF SCHEMES

LIST OF TABLES

CHAPTER 1 INTRODUCTION

1.1 N-Heterocyclic Carbenes

Carbene, a molecule containing a neutral carbon atom with six valence electrons, was considered to be very reactive and short-lived due to its lone pair electrons and electrophilic character.[1–4] In the early 1960s, Wanzlick[5] firstly introduced a "nucleophilic" carbene containing a heterocycle bearing at least one nitrogen atom and described the enhanced stability. Since the first stable, crystalline N-heterocyclic carbene (Scheme 1.1) has been isolated by Arduengo[6] in 1991 and the first NHCs were used in transition metal catalysis by Herrmann et al[7] in 1995 their use has exploded.

Scheme 1.1: First isolation of N-heterocyclic carbene

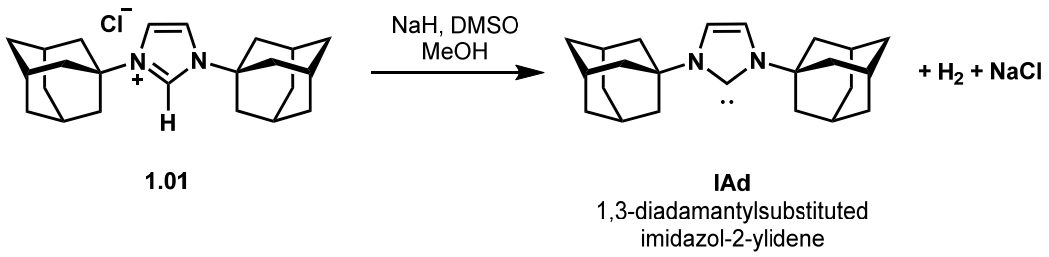

1.01

IAd
1,3-diadamantylsubstituted
imidazol-2-ylidene

The original discovery of stable NHCs was mainly focused on the imidazolium-derived carbenes **1.02**. In the past several decades, chemists have extensively worked toward the development of novel NHC achitecture.[8] Figure 1.1 illustrates some representative mono-dentate NHC structures. While the majority of heterocyclic carbenes have been the five-

membered rings, the reported NHC cores varied from five- to four-, six- and seven-membered rings. Compared to the classical imidazolidin-ylidene **1.02** and imidazol-ylidene **1.03**, some NHCs may replace one nitrogen neighboring to the carbene center with carbon, sulfur, oxygen or phosphorus atom. The structural diversity can also be shown by varying the heteroatom substituents and the NHC skeleton backbones.

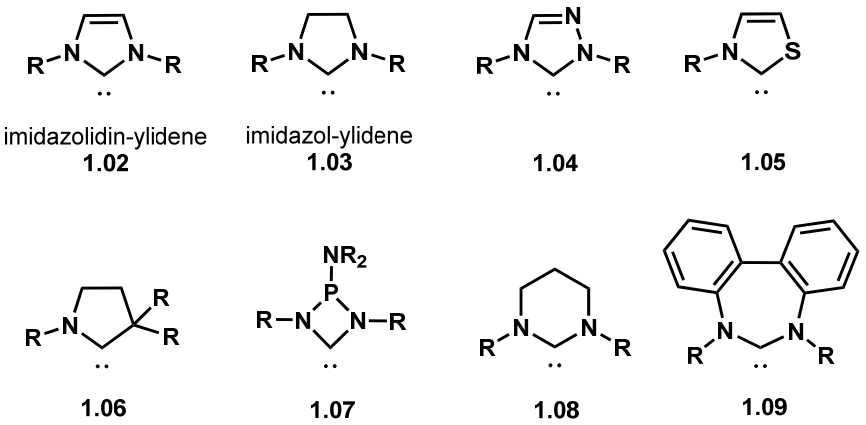

Figure 1.1: Some different mono-dentate NHCs.

The extraordinary stability of N-heterocyclic carbenes is a result of both electronic and steric effects. The steric shielding of bulky N-substituents allows for decreased chemical reactivity at the carbene and thus promotes stability. Furthermore, the electronic factors significantly contribute to the NHC stability. The empty p-orbital of carbene carbon accepts electron donation from the two adjacent nitrogen atoms. Most carbenes are electron-deficient species. However, NHCs are more electron-rich and nucleophilic (Figure 1.2). It is noteworthy that although NHCs can be isolated, they are still considered to be sensitive compounds.

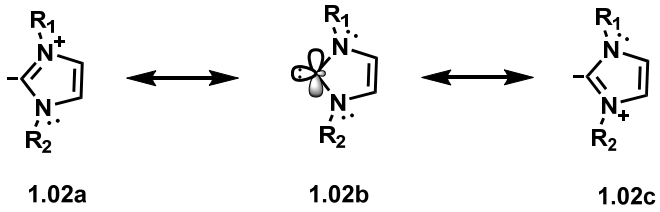

Figure 1.2: Resonance structures of N-heterocyclic carbene.

The similarities of NHCs with organophosphines and the wide utility of NHCs in organometallic chemistry lead us to work in exploring the novel NHC synthesis. Due to three properties NHCs have been used as phosphine replacements: a) NHCs are strong σ-donors, b) NHCs form robust bonds with transition metals,[9] and c) NHCs have unique shapes (Figure 1.3) leading to their large steric demand.[10–12] Another advantage of NHCs is their enhanced structural diversity, which could be easily achieved and used to facilitate the optimization of reactions. Moreover, contrary to phosphines, NHC precursors are stable without decomposition in air and consequently NHCs can be used as ligands in oxidation chemistry.

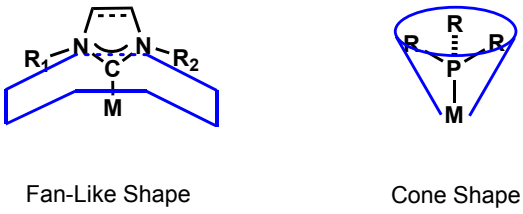

Figure 1.3: Different shapes of NHC and phosphine complexes.

1.2 Previous Method for N-Heterocyclic Carbene Precursors

The increasing interest in NHCs has dramatically motivated development of creative and flexible synthetic methods for their synthesis. The most common method for the formation of NHC ligands is the *in situ* deprotonation of the corresponding azolium salts (Scheme 1.2). The challenging part of synthesizing NHCs may be the construction of their precursors, especially the cyclization step.[13] Of the different classes of mono-, bi- and multi-dentate NHCs, we have focused on synthesis and applications of imidazolium and imidazolidinium salts derived NHCs. They are usually considered to be the most important and most often employed NHCs.

Scheme 1.2: Deprotonation of azolium salts

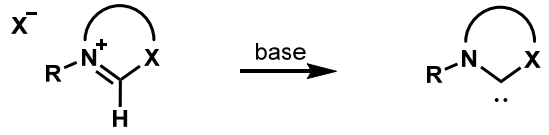

1.10 **1.11**

X= NR', O, S, CR'R'', PR'

A straightforward classification of the synthetic strategies toward NHC precursors is by the final unit being induced into the heterocycle skeleton (Scheme 1.3). There has been considerable success in the development of cyclization methodologies by condensation of desired backbones with *N*, *N'*-disubstituted formamidine (route **a**).[3,14–19] Incorporation of an amino unit in the final cyclization to prepare imidazolium salts via a heterocyclic interconversion (route **b**) was initially reported by Fürstner and coworkers.[20] This methodology is compatible with a number of functional groups and could provide a wide variety of structures, however, only a few examples using this strategy exist.[21–23]

Scheme 1.3: Syntheses of NHC precursors

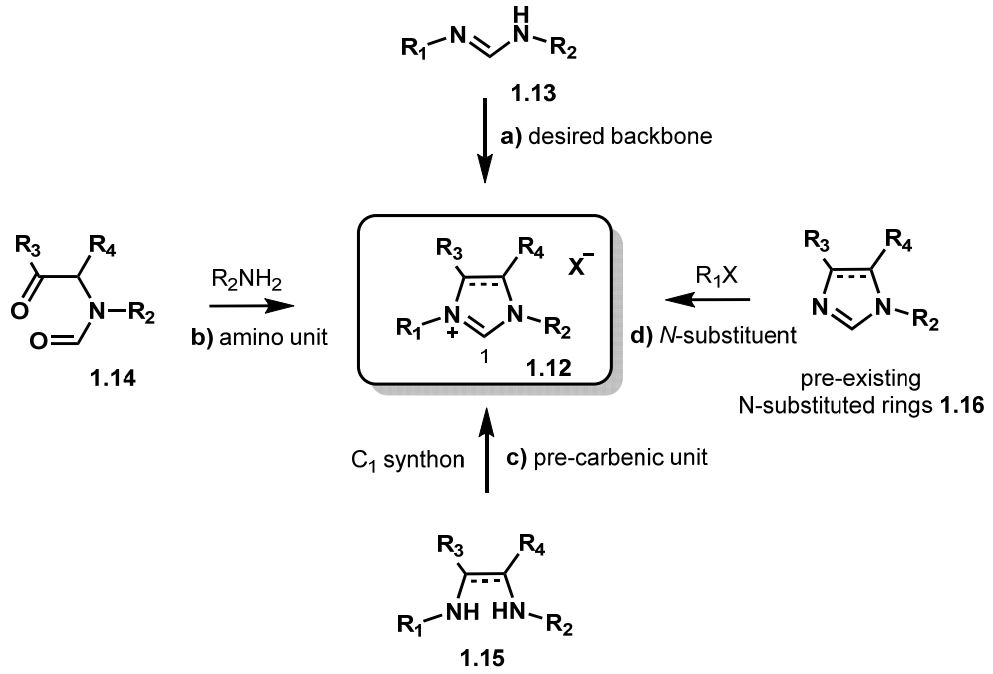

The most common method of cyclization to form NHC precursors is the final installation of C_1 synthon (route **c**). Trialkyl orthoformate is applied as precarbenic unit and treated with N, N'-disubstituted diamine in the presence of proton and counter ion sources to form the saturated NHC precursors **1.18** (Scheme 1.4). This methodology is widely used to synthesize unsymmetrical imidazolidinium salts due to its high tolerance of both aryl and alkyl *N*-substituents and various functional groups.[9,23–44]

Scheme 1.4: Synthesis of saturated NHC precursors via installation of C_1

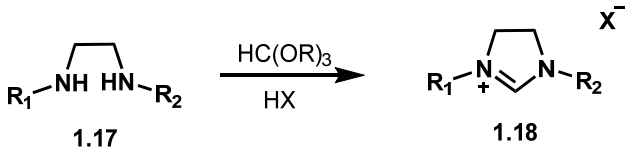

The imidazolium salts may be obtained by treatment of 1,2-diimine (Scheme 1.5) with 1,1-bis(electrophile) such as chloromethylethyl ether[25,45–52] and chloromethyl pivalate[28,50,53–64] or with paraformaldehyde.[65–76]

Scheme 1.5: Synthesis of unsaturated NHC precursors via installation of C_1

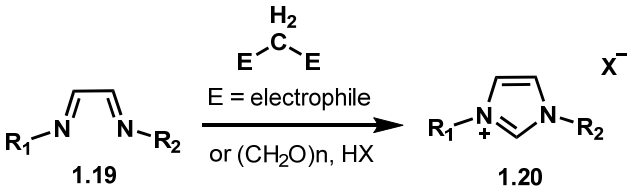

Rather than being constructed by cyclization, the azolium salts can also be generated by alkylating the existed heterocycles (Scheme 1.3, route **d**).[77] This strategy allows the convenient variation of one *N*-substituent to prepare collections of unsymmetrical NHC precursors.

1.3 Applications of NHCs in Asymmetric Catalysis

In recent years, N-heterocyclic carbenes have been widely utilized as nucleophilic organocatalysts[78–80] and as effective ligands in numerous transition metal catalyzed transformations (Scheme 1.6).[81–83]

Scheme 1.6: First report of NHC in transition metal catalysis

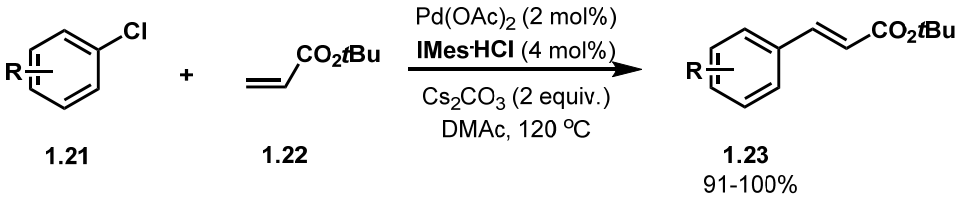

In 1996, Enders and Herrmann designed a novel type of NHC ligand with chiral *N*-substituents and reported the pioneering asymmetric catalysis using chiral NHC to induce stereoselectivity (Scheme 1.7).[84] Other chiral NHCs of this type have been used as ligands in transition metal catalyzed hydrosilylation,[85] arylation,[86,87] allylic alkylation[88] It has been found that the NHC ligands with more steric demanding substituents are more efficient in stereo-directing. However, this type of ligand generally only provides moderate stereoselectivity.

Scheme 1.7: Enantioselective hydrosilylation using chiral NHC as ligand

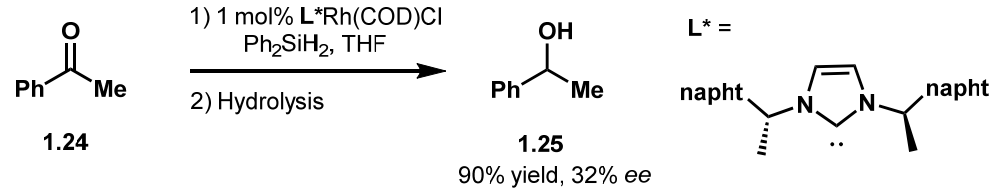

Burgess and coworkers reported the first highly enantioselective metal-NHC catalysis (Scheme 1.8).[89] This type of ligand is a combination of NHC with an oxazoline which is a highly efficient building block for ligands in asymmetric catalysis.[90] The bidentate ligand provides a better chiral environment for the catalytic reaction. Since then, a significant number of asymmetric catalytic transformations with high stereoselectivities have emerged.[91]

Scheme 1.8: Asymmetric catalytic hydrogenation by Burgess

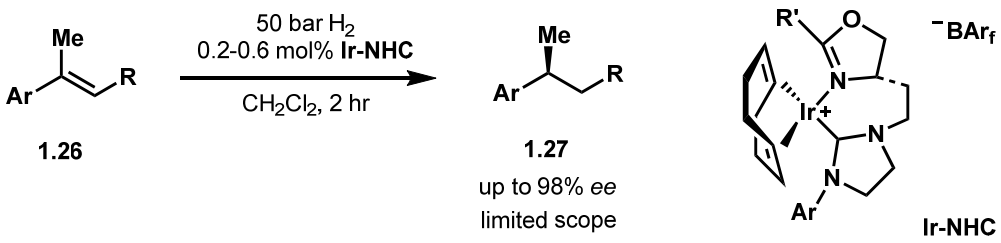

Another interesting type of NHC ligand is the one containing axial or planar chirality such as **1.31**. The Rh-NHC catalyzed conjugated addition to cyclohexanone gave excellent yield and selectivity.[92]

Scheme 1.9: Asymmetric conjugated addition to cyclohexanone

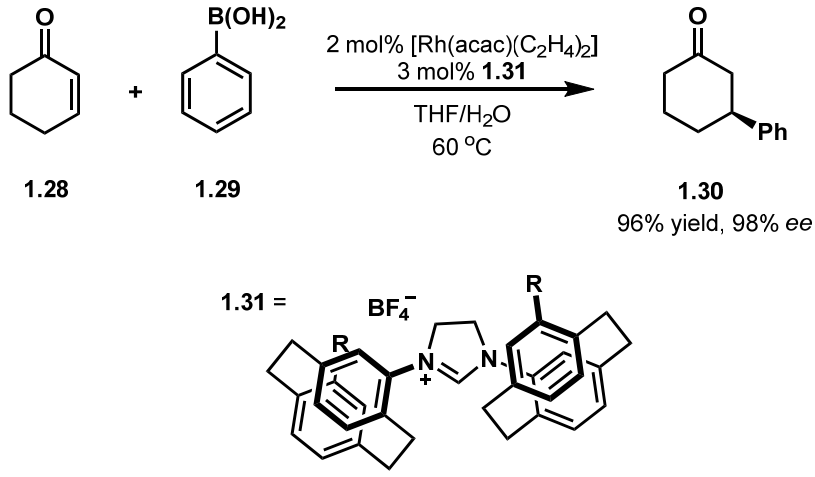

In conclusion, asymmetric catalysis using NHC as ligand is a rapid developing field. Whereas numerous efficient ligands systems have been developed, methods for the facile synthesis of chiral NHC ligands that can be screened their reactivity and stereoselectivity in transition metal catalysis are still needed.

CHAPTER 2 SYNTHESIS OF NHC BUILDING BLOCKS

2.1 Proline Derivatives

$_L$-Proline is structurally distinctive among the α-proteinogenic amino acids. The unique cyclic structure of proline side provides conformational rigidity, that allows proline to be commonly found at the turn position in stable β-turn peptide secondary structures.[93–97]

Proline and hydroxyproline are important components in collagen.[98] *trans*-4-hydroxy-$_L$-proline is the most common diastereomer (Figure 2.1) and its derivatives are available and inexpensive. A number of suppliers provide Hyp with a variety of protecting groups on the amine and the carboxylic acid.

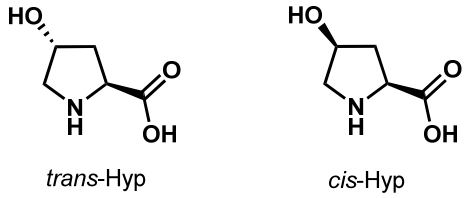

trans-Hyp *cis*-Hyp

Figure 2.1: Two diastereomers of 4-hydroxy-$_L$-proline.

It is noted that two configurations of peptide bond (*C*-*N*) exist in peptides, proteins[99,100] and other nonpeptide amino acid derivatives. Despite the dominance of *trans*-isomer in most amino acid residues, a higher occurrence of the *cis*-isomer is found[101] for proline

and hydroxyproline residues (Figure 2.2). Due to the secondary amine functionality of proline results in a smaller energy difference between the *cis*- and *trans*-isomers of the amide bond. Both isomers may be observed by NMR due to the slow *cis*-*trans* isomerization at room temperature. Characterization of the proline derivatives at elevated temperature may result in the coalescence of the *cis*- and *trans*-isomers.

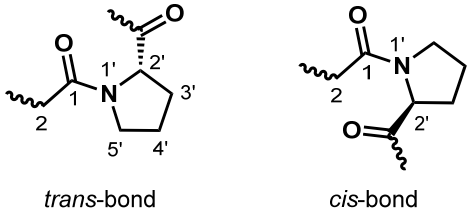

Figure 2.2: Two configurations of the peptide bond.

Since the discovery of proline-catalyzed asymmetric aldol reactions by List, Lerner, and Barbas in 2000,[102] proline has played a significant role in the development of highly enantioselective organocatalysis.[103–105] Additionally, proline-based small ligands have been effective in transition metal-catalyzed transformations. For example, our group has developed a series of phosphine-proline-oxazoline ligands **2.01** (Figure 2.3) that can be used in palladium-catalyzed asymmetric allylation and Heck reactions.[106–109]

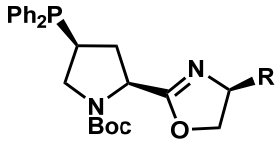

2.01

R = *i*-Pr, Ph, *t*-Bu, *etc*

Figure 2.3: Proline-based phosphine-oxazoline ligands.

2.2 Design of NHC Building Blocks

The chemistry that we reported in this dissertation is the development of novel NHC precursors **2.02** and **2.03** that can be directly used as ligands for transition metals, and also serve as building blocks for the synthesis of other structurally diverse ligands (Scheme 2.1).

Scheme 2.1: Conversion of NHC building blocks into other structures

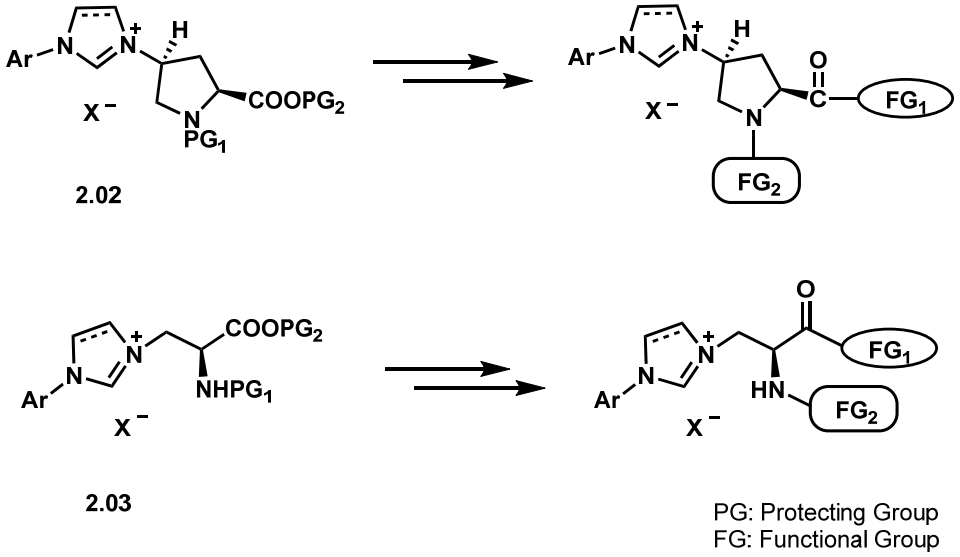

NHC ligands are beginning to be used in a wide variety of different types of catalytic chemistry. This increasing interest in NHCs has dramatically motivated the emergence of creative and flexible synthetic methods for their synthesis.[13] However, the nearly flat shape of NHCs while coordinated to transition metals has hindered their development as ligands in asymmetric catalysis.

Because our NHCs are incorporated into amino acids, where the amine group and the acid can be joined to other structures, one advantage of our strategy is the facile synthesis of a collection of new chiral NHC ligands based on the amino acid as a modular NHC building block. These collections can be rapidly screened for improved reactivity and selectivity. Additionally, the NHC precursors obtained from this modular synthesis could be complementary to naturally occurring amino acid side chains such as imidazole and basic amines. Our group has successfully developed a number of approaches to synthesize amino acids bearing nucleophilic side chains,[109–113] such as phosphine-proline-oxazoline ligands **2.01** (Figure 2.3). The aim of this dissertation is to further expand the collection of amino acids to NHC-containing amino acids that have potential not only in organometallic chemistry but also in other fields of chemistry.

When an amino acid is used as a component in the NHC, it may be incorporated into different scaffolds via amide bond formation. The combination of the building blocks with other structures can be achieved by the classical solution-phase peptide synthesis or solid-phase peptide synthesis. The detailed methods and examples will be discussed in Chapter 3.

2.3 Review of One-Pot Synthesis of NHC Precursors

In 2009, a facile one-pot methodology toward the synthesis of a variety of symmetrical, unsymmetrical and chiral mono- or bidentate imidazolidinium ligands from *N*-(2-iodoethyl)aryl amine salts **2.04** was developed by Gilbertson and Prasad,[43] forming the

products **2.06** in up to 94% yield (Scheme 2.2). One major advantage of this approach is the exclusion of harsh reduction steps using $LiAlH_4$ or BH_3, which were typically applied in the previous methodologies.[13,25] This approach is easily accessed and compatible with a number of potentially reactive functional groups.

Scheme 2.2: Facile one-pot synthesis of NHC precursors

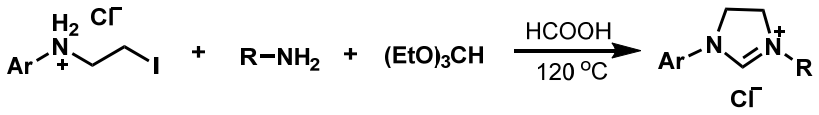

2.04 **2.05** **2.06**

According to the similar but stepwise route Plenio *et al* reported,[114] diamine **2.07** was formed via nucleophilic substitution of the iodide **2.04**, followed by a cyclization using triethyl orthoformate as the imidazolidinium precarbenic unit.

Scheme 2.3: Stepwise synthesis of imidazolidinium salts by Plenio

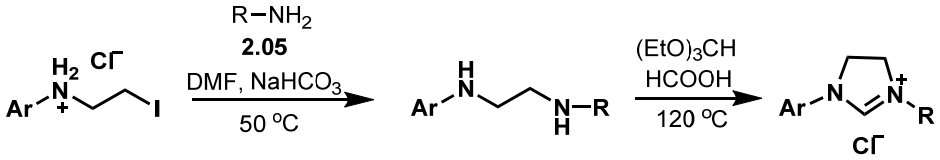

2.04 **2.07** **2.06**

2.4 Modifications of One-Pot Synthesis of NHC Precursors

Following the one-pot procedure (Scheme 2.4),[43] amino alcohol **2.09** was formed via a solvent-free reaction of aryl amine **2.08** with 2-iodoethanol. Then **2.09** was treated with iodine to provide the amino iodide which was immediately converted to ammonium salt

2.04 by bubbling gaseous hydrochloric acid through the solution. The precipitated salt was isolated by simple filtration from the solution.

Scheme 2.4: Synthesis of *N*-(2-iodoethyl)aryl amine salts

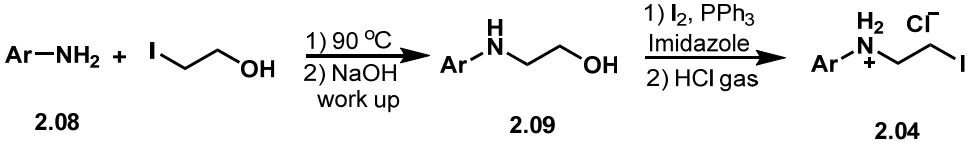

A number of imidazolidinium salts with hindered 2,4,6-trimethylphenyl substituent on one nitrogen were synthesized using this one-pot approach (Scheme 2.2) in moderate to good yields, utilizing either conventional heating or microwave-assisted heating (Table 2.1).

Table 2.1: Imidazolidinium salts by one-pot synthesis

Entry	Product	Yield (%) (conventional heating)	Yield (%) (μw-assisted heating)
1	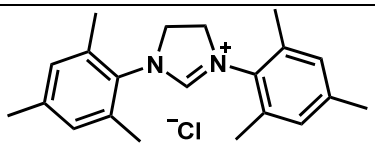	56	49
2	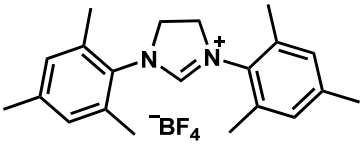	61	N/A
3	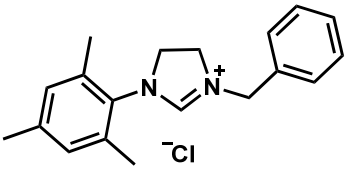	97	90
4	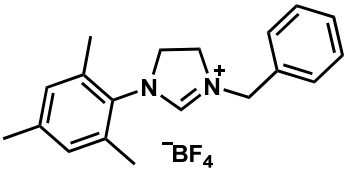	62	N/A

5	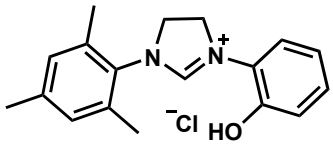	50	N/A
6	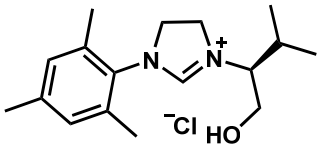	0	49
7	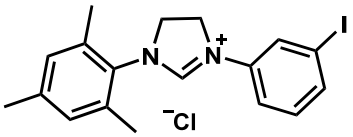	N/A	29
8	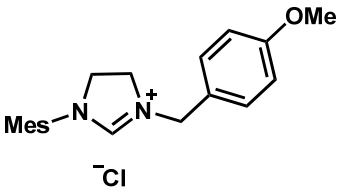	N/A	34
9	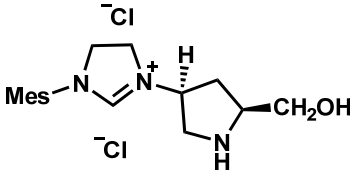	0	0

The procedure to form the imidazolidinium salts in the final cyclization step is usually facile. When solids result the products can often be precipitated and isolated by simple filtration. However, the one-pot procedure, while significantly simplifying the synthetic route, suffers some difficulty in recovering products that do not form as solids. The resulting reaction mixture can be a thick oil and a repetitive dissolving-scratching-evaporating process in a variety of different solvents may be required to obtain pure product in a solid form.

Several modifications of the procedure were found to facilitate the purification of imidazolidinium salts. Formic acid that was used as a catalyst in the reaction hampered precipitation of the salts. The complete removal of formic acid from reaction mixture *in*

vacuo has been shown to hasten the isolation of product. In addition, changing the counter ion to non-coordinating BF_4^- was also successful in facilitating the isolation of several products but with a decrease in yield due to the higher solubility of tetrafluoroborate salts in organic solvents.

Although microwave-assisted heating has been applied as an unconventional energy source in many fields of organic synthesis, such as transition-metal catalysis, heterocycle synthesis and combinatorial synthesis,[115] it has rarely been utilized in the synthesis of NHCs.[116] After the optimization of reaction temperature and reaction time, several different substrates were tested under microwave-assisted heating. The isolated yields (Table 2.1) have been shown to be comparable to those of conventional heated reactions. Microwave-assisted heating significantly reduces reaction time from 12 hours to 30 minutes or 1 hour, leading to fewer side reactions and assisting in improved product recovery.

2.5 Initial Attempts toward the NHC Building Blocks

Our initial attempt toward the synthesis of the desired NHC precursor **2.02** was to use the facile one-pot route. Literature routes were performed to synthesize both Boc-[117] and Cbz-[118] protected *cis*-4-amino proline methyl esters **2.14** and **2.15** (Scheme 2.5) from commercially available *N*-Boc-Hyp-OMe and Z-Hyp-OMe. Mesylation of those alcohols gave **2.10** and **2.11** in high yields. Nucleophilic substitution provided azides **2.12** and **2.13** in good yield. Conversion of azide to *cis*-4-aminoproline methyl esters **2.14** and **2.15**

was achieved by hydrogenation of **2.12** and **2.13** using palladium on charcoal and Raney-nickel as catalysts, respectively.

Scheme 2.5: Synthesis of *N*-protected *cis*-4-aminoproline methyl esters

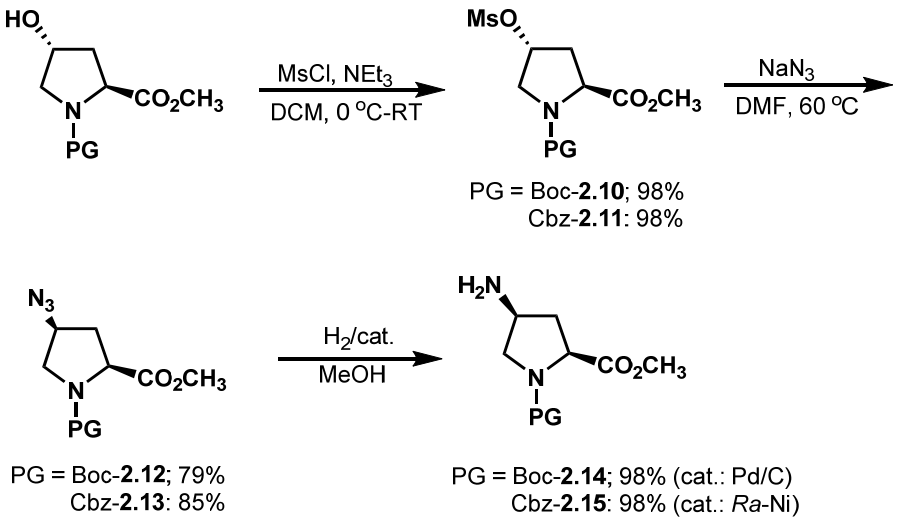

N-Boc-*cis*-4-aminoproline methyl ester **2.14** was used as nucleophile in the previously described one-pot method to access the imidazolidinium salt **2.16** (Scheme 2.6). Unfortunately, using neither conventional or microwave-assisted heating provided the desired product **2.16**. Since the Boc protecting group is sensitive to the acidic conditions, it is suspected that the protecting group was cleaved by the formic acid used as catalyst in the reaction. Cbz protected **2.15** was chosen as a replacement, however no reaction was observed to occur under a number of reaction conditions (Scheme 2.6).

Large steric size of the secondary amine may hinder the substitution, especially in the target molecule bearing both bulky mesityl and proline groups. The use of formic acid and high temperature in these reaction conditions may also be too harsh for the proline substrates.

Scheme 2.6: Attempted direct synthesis from 4-aminoproline

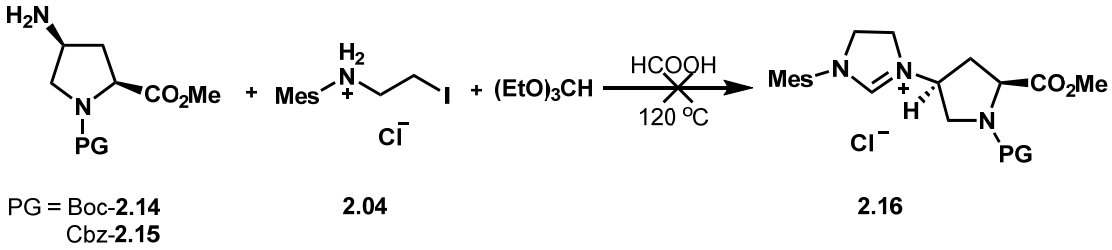

PG = Boc-**2.14**
Cbz-**2.15**

2.04

2.16

2.6 Synthesis of NHC Building Blocks via Alkylation of Imidazoles

Most of the work in this section was shown in a published paper.[119] As was mentioned in Chapter 1, alkylation of pre-existed imidazoles **2.17** (Scheme 2.7) is a simple and straightforward strategy toward the synthesis of unsymmetrical imidazolium salts. A number of alkyl chlorides,[120,121] bromides,[122–126] iodides,[89,127] and trifluoromethanesulfonates[128,129] have been found to be efficient electrophiles in this type of transformation. Surprisingly, no methanesulfonates have been reported in such reactions.

Scheme 2.7: Alkylation of Mono-Substituted Imidazole

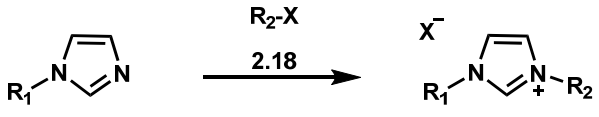

2.17

2.19

X: Cl, Br, I, OTf

We chose this strategy as an alternative route to synthesize the NHC building blocks for several reasons. The two reaction substrates, *N*-monosubstituted imidazoles and proline

[119] Zhao, Y.; Gilbertson, S. R. *Org. Lett.* **2014**, *16* (4), 1033.

derivatives with different leaving groups at 4-position, can be easily accessed from inexpensive commercially available chemicals. Strong base or acid was not necessary for these reactions, leading to fewer side reactions. Additionally, the use of the proper solvent in the purification of the salt may be simplified because of its low solubility in some organic solvents.

The mesityl group is one of the most common bulky *N*-substituents utilized in symmetrical and unsymmetrical NHCs.[54] Sterically demanding mesityl imidazole **2.20** was formed and isolated by a reported protocol in 69% yield (Scheme 2.8).[130]

Scheme 2.8: Synthesis of mesityl imidazole

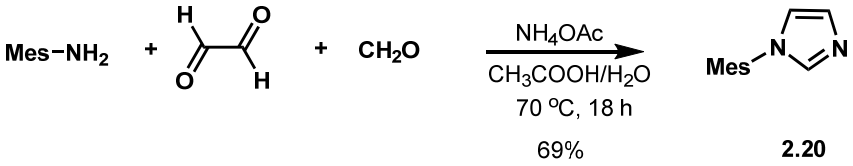

Alcohols may be turned into electrophiles for substitution reactions by converting them to mesylates. Our laboratory reported the preparation of phosphinoprolines using proline mesylate in nucleophilic substitution with alkali metal salts of diphenylphosphide.[109] Methanesulfonyl proline esters **2.10** and **2.11** were initially chosen as precursors to develop the synthetic method for NHC-proline building blocks. However, no substitution occurred with mesityl imidazole under various reaction conditions (Scheme 2.9).

Modification of the leaving group from mesylate to trifluoromethanesulfonate proved a successful route to **2.25** (Scheme 2.10).[119] Trifluoromethanesulfonation of *trans*-hydroxyproline methyl ester **2.22** provided intermediate **2.23**. Subsequent treatment of

purified triflate with mesityl imidazole, at -78 °C, followed by purification in the presence of trifluoroacetic acid provided the trifluoroacetate salt **2.25**.

Scheme 2.9: Alkylation of mesityl imidazole

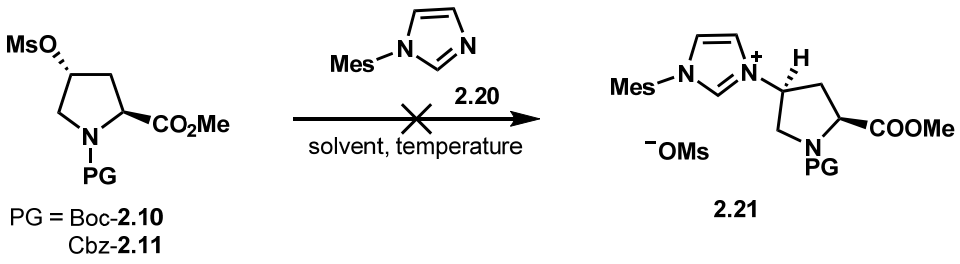

Scheme 2.10: Synthesis of NHC building block **2.25**

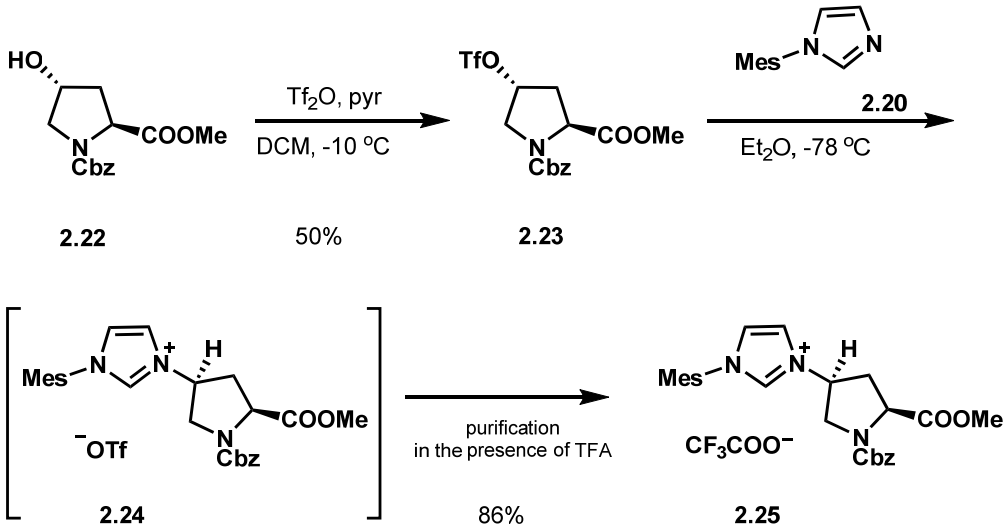

In our initial attempts, the triflation reaction was problematic due to limited stability of the triflate product. To prevent the formation of side products by decomposition or elimination of the triflate, the reaction was carried out at -10 °C and quickly purified at room temperature. Purification of **2.23** upon a very rapid column chromatography proved to be necessary in providing compound **2.24** in the subsequent substitution step. Lack of stability of the triflate compound on silica gel resulted in yields that vary with the length

of purification time. Furthermore, it proved necessary to use the freshly-prepared triflates immediately to afford the imidazolium salt and avoid decomposition.

Triflate **2.23** was not stable at room temperature. However, it was shown to be a more appropriate leaving group for our sterically demanding substrates than mesylate, since the more stable mesylate does not react with **2.20** (Scheme 2.9) even at elevated temperatures.

Since the starting materials are much more soluble in diethyl ether than imidazolium salt the triflate salt **2.24** could be easily isolated as white foam by simply washing with diethyl ether followed by complete removal of the solvent. Imidazolium trifluoroacetate salt **2.25** was obtained in high yield after preparative HPLC. The counter ions of **2.24** and **2.25** were determined by their ^{13}C-^{19}F couplings in ^{13}C NMR analyses.

Scheme 2.11: Synthesis of NHC building block **2.29**

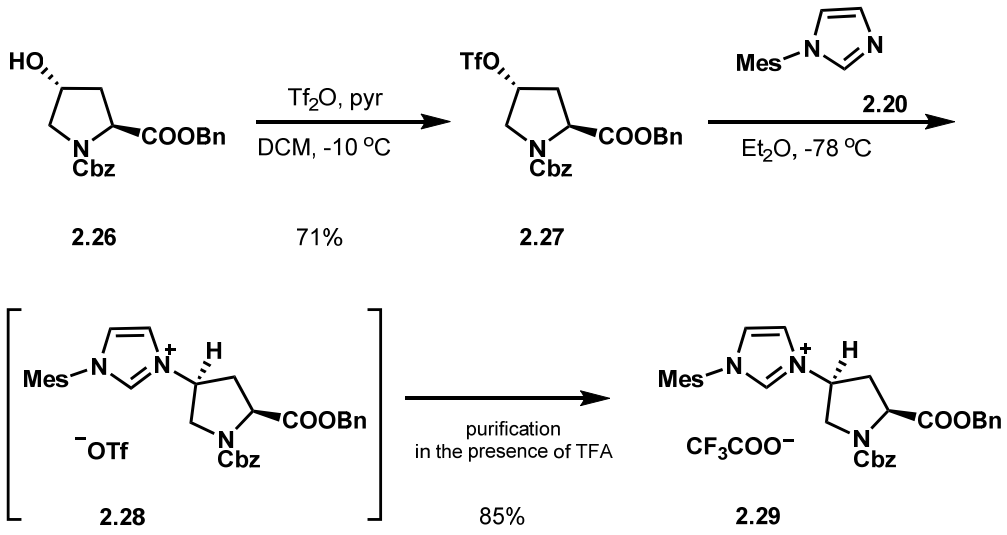

For one-step global deprotection, NHC building block **2.29** was synthesized from benzyl hydroxyproline **2.26** following a similar procedure (Scheme 2.11). This doubly-protected imidazolium was formed by treatment of triflate **2.27** with mesityl imidazole at -78 °C

and isolated by preparative HPLC in 85% yield. Preparation of **2.29** provides more flexibility for functionalization of the NHC building blocks which will be discussed in Chapter 3.

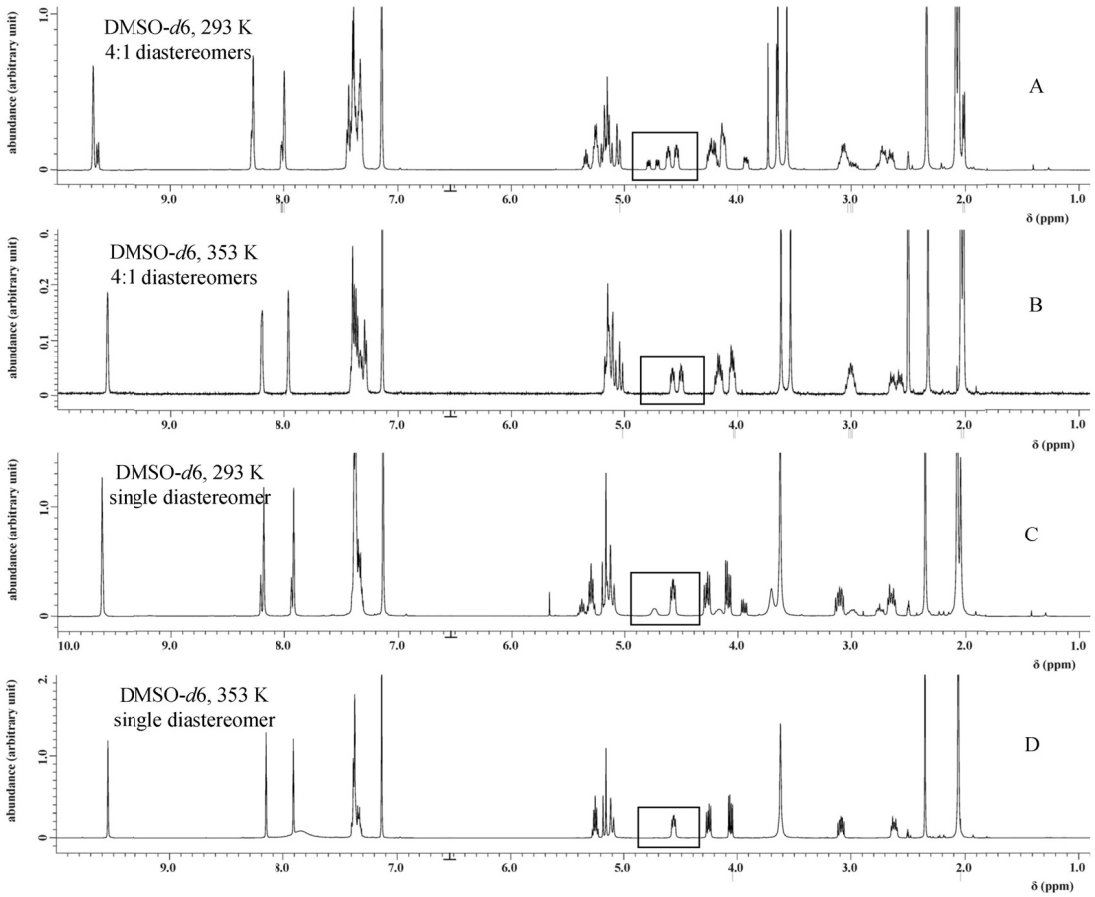

Figure 2.4: ^{1}H NMR of **2.25** at different temperatures.

The temperature at which the nucleophilic substitution is performed plays an important role in the formation of imidazolium salts **2.25** and **2.29**. A 4:1 mixture of diastereomers was obtained when the reaction was warmed to room temperature. For example, the α-H peaks of **2.25** (mixture of diastereomers) in ^{1}H NMR are highlighted in the square (**A** and **B**, Figure 2.4). For each diastereomer, the NMR spectra are reported for a mixture of two

rotomers at room temperature. In **A**, Figure 2.4 the left two groups of peaks represent two rotomers of the minor diastereomer, and the right two represent two rotomers of the major diastereomer. Coalescence of the rotomer peaks were observed at 353 K in DMSO-*d*6 (**B**, Figure 2.4) and only one group of peaks is shown for each diastereomer.

The reaction conditions were modified to minimize epimerization. When the reaction was carefully maintained at -78 °C, the diastereomeric ratio of imidazolium salt was > 20:1 and imidazolium salt could be obtained as a single diastereomer in high yield upon separation by preparative HPLC. The rotomer peaks at room temperature **C** and coalescence of the rotomer peaks at elevated temperature **D** are shown in Figure 2.4. These two spectra of the single diastereomer support the conclusion that the two groups of peaks in **B**, Figure 2.4 belong to two diastereomers instead of conformational isomers.

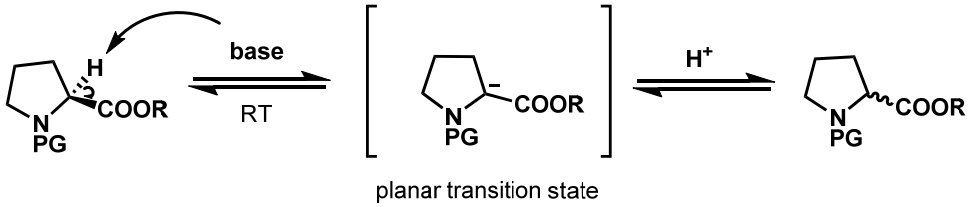

Figure 2.5: Racemization of proline on α-carbon.

The most possible position for epimerization is the proline α-carbon (Figure 2.5).[131,132] The α-proton may be removed by the basic mesityl imidazole during the reaction at room temperature leading to the racemization. Even though the imidazolium prolines have been treated with base in Chapter 3 and no epimerization was observed, this probability cannot be ruled out because that reaction was carried out at 0 ^{o}C.

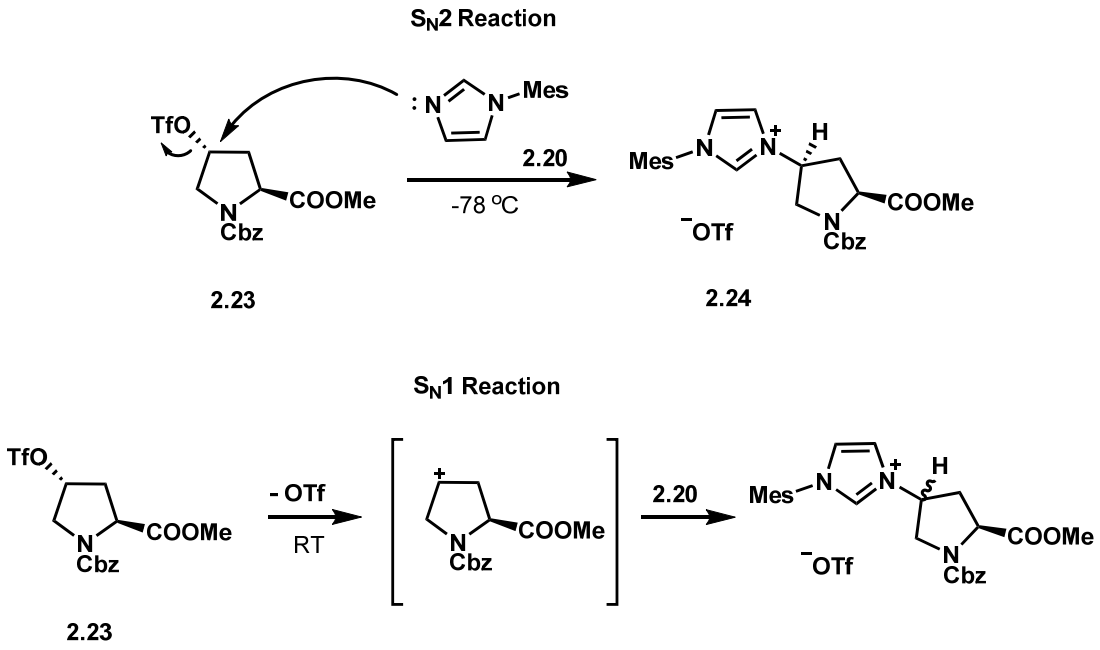

Figure 2.6: S_N1 and S_N2 reactions.

On the other hand, this epimerization may be rationalized by the competition between S_N1 and S_N2 pathways in the substitution reaction (Figure 2.5). The S_N2 reaction leads to the inversion of the electrophile stereochemistry by backside attack on **2.23**, providing the desired *cis*-product. S_N1 pathway would yield a 1:1 mixture of the two diastereomers. In this imidazolium formation reactions the substitution could follow either S_N1 or S_N2 pathways or a combination of them.

In addition to the proline-based NHC precursors, using iodide **2.30** as electrophile alanine-based imidazolium salt **2.31** was synthesized by alkylation of mesityl imidazole (Scheme 2.12). Although we have mainly focused on the proline-containing NHC precursors, this alanine-imidazolium also has a potential in constructing bidentate β-turn

peptide ligands and small ligands. Further modification of reaction conditions may be performed to improve the reaction conversion.

Scheme 2.12: Synthesis of alanine-based imidazolium salt

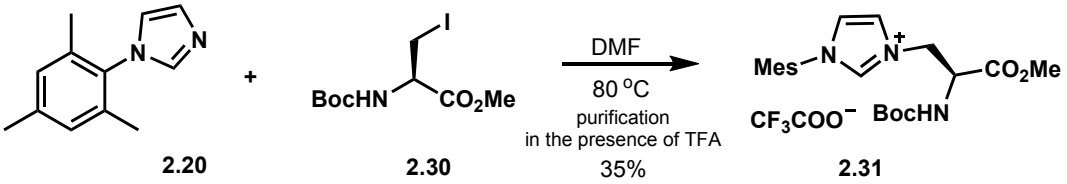

The sterically hindered NHC building blocks have been successfully synthesized and fully characterized. The generality of this approach may be applied to reactions with other proline-containing substrates and other amino acids.

2.7 Experimental Section

General Procedures:

All reagents were purchased from Sigma-Aldrich, Acros, Aapptec and Strem and used as received unless otherwise noted. Thin-layer chromatography was performed on silica gel 60 F_{254} pre-coated plates (0.25 mm) from Silicycle and components were visualized by UV light (254 nm) and/or 10% phosphomolybdic acid in ethanol stain. Flash chromatography was performed using Silicycle silica gel 230-400 (particle size 40-63 μm) mesh. Analytical high-pressure liquid chromatography was performed on an Agilent 1100 Series instrument equipped with a Variable Wavelength Detector. Preparative HPLC was performed on a Gilson instrument equipped with a 321 pump, UV/VIS-155 detector and FC-204 fraction collector. ^{1}H and ^{13}C NMR were recorded on JEOL ECX-

400 NMR spectrometer (400 MHz for ^{1}H NMR and 100 MHz for ^{13}C NMR) or JEOL ECX-500 NMR spectrometer (500 MHz for ^{1}H NMR and 125 MHz for ^{13}C NMR) in chloroform-*d* at ambient temperature and/or 318 K (45 ˚C) or in DMSO-*d*6 at ambient temperature and 353 K (80 ˚C, if necessary). In chloroform-*d*, chemical shifts were referenced to the residual chloroform-H peak at 7.26 ppm for ^{1}H NMR and 77.16 ppm for ^{13}C NMR. In DMSO-*d*6, chemical shifts were referenced to the residual DMSO-H peak at 2.50 ppm for ^{1}H NMR and 39.52 ppm for ^{13}C NMR. Chemical shifts are reported in parts per million (ppm, δ). Multiplicity are indicated as s = singlet, d = doublet, t = triplet, q = quartet, m = multiplet, br = broad resonance and the coupling constants (*J*) are reported in Hz. Liquid chromatography-mass spectrometry (LC-MS) was performed on a Thermo Finningan Surveyor instrument equipped with MSQ Plus single quadrupole detector. High resolution mass spectral data were recorded on an Agilent 6530 Accurate Mass Q-TOF LC/MS (high resolution ESI) and a Micromass (now Waters) Autospec Ultima mass Spectrometer (high resolution CI) from University of Texas at Austin, Mass Spectrometry Facility (MSF) of the Department of Chemistry & Biochemistry.

1-(2,4,6-Trimethylphenyl)-1*H*-imidazole (2.03)

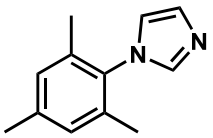

A mixture of glacial acetic acid (10 mL), 37% aqueous formaldehyde (3 mL) and 37% aqueous glyoxal (4.6 mL) was heated to 70 ˚C. A solution of 2,4,6-trimethylaniline (5.39

g, 40.0 mmol), ammonium acetate (3.08 g, 40.0 mmol) in 2 mL water and glacial acetic acid (10 mL) was added dropwise after which the reaction mixture was heated at 70 ˚C for 18 hours. After cooling to room temperature the resulting brown solution was added very slowly to a stirred solution of 29.4 g $NaHCO_3$ in 300 mL water. Brownish solid was precipitated and filtered. Evaporation of water gave crude product which was purified by column chromatography (eluent: 5% MeOH in DCM) to yield product (5.56 g, 75%): ^{1}H NMR (400 MHz, $CDCl_3$) δ 7.43 (s, 1H), 7.23 (s, 1H), 6.96 (s, 2H), 6.89 (s, 1H), 2.33 (s, 3H), 1.98 (s, 6H); ^{13}C NMR (125 MHz, $CDCl_3$) δ 138.62, 137.25, 135.16, 133.20, 129.34, 128.81, 119.84, 20.84, 17.13; LC/MS (ESI) calculated for $C_{12}H_{15}N_2$ $[M+H]^+$ 187.12, found 187.21 (t_R = 9.51 min); HRMS ($^+$ESI) calculated for $C_{12}H_{15}N_2$ $[M+H]^+$ 187.1230, found 187.1229.

(2*S*,4*R*)-1-benzyl-2-methyl-4-(trifluoromethylsulfonyloxy)pyrrolidine-1,2-dicarboxylate (2.23)

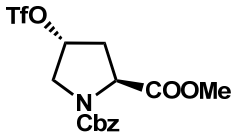

To a solution of Z-Hyp-OMe (2.06 g, 7.38 mmol) and pyridine (1.19 mL, 14.8 mmol) in 30 mL of DCM triflic anhydride (1.86 mL, 11.1 mmol) was added at -10 ˚C. The resulting yellowish solution was stirred in an ethanol/ice bath for 4 hours, followed by washing with 20 mL of saturated $NaHCO_3$ (aq.) and 20 mL of brine then dried over $MgSO_4$. After evaporating the solvent, the orange residue was dissolved in a small

amount of DCM and subjected to column chromatography using DCM as eluent. Triflate intermediate was collected as a colorless oil (1.51 g, 50%).

The NMR spectra are reported for a mixture of two rotamers: ^{1}H NMR (500 MHz, $CDCl_3$) δ 7.29-7.38 (m, 5H), 5.48 (br s, 1H), 5.02-5.28 (m, 2H), 4.58 (dd, *J* = 8.0, 8.0 Hz, 0.5H), 4.52 (dd, *J* = 8.0, 8.0 Hz, 0.5H), 4.06 (d, *J* = 13.8 Hz, 0.5H), 3.96 (d, *J* = 13.2 Hz, 0.5H), 3.87 (dd, *J* = 14.3, 4.0 Hz, 1H), 3.78 (s, 1.5H), 3.55 (s, 1.5H), 2.66-2.73 (m, 1H), 2.33-2.40 (m, 1H); ^{13}C NMR (125 MHz, $CDCl_3$) δ 171.91, 171.84, 154.33, 153.86, 135.92, 135.85, 128.66, 128.57, 128.41, 128.35, 128.13, 128.09, 118.45 (q, $J_{C\text{-}F}$ = 319 Hz), 86.39, 85.87, 67.89, 67.84, 57.31, 57.02, 52.93, 52.84, 52.57, 52.54, 37.60, 36.44.

3-((3*S*,5*S*)-1-(benzyloxycarbonyl)-5-(methoxycarbonyl)pyrrolidin-3-yl)-1-mesityl-1*H*-imidazol-3-ium trifluoroacetate (2.25, 4:1 mixture of diastereomers)

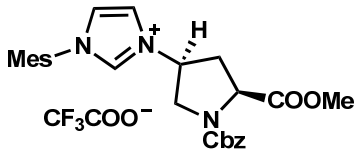

A solution of mesityl imidazole (616 mg, 3.31 mmol) in dry Et_2O was added to the solution of **2.23** (1.51 g, 3.68 mmol) in Et_2O at -78 ˚C. The reaction mixture was warmed to room temperature and stirred for 24 hours. The resulting light yellowish oil was washed three times with Et_2O and dried under vacuum to give a white form. The compound was purified by preparative HPLC (Column: XBridge BEH C_{18} OBD Prep 5 μm, 19 x 150 mm; wavelength: 215 nm, 254 nm; temperature: ambient; solvent A: 0.1%

trifluoroacetic acid in H_2O, solvent B: 0.1% trifluoroacetic acid in MeCN; flow rate: 12 mL/min. Held at 0% B for 1 min, ramped to 100% B over 17 min, ramped to 0% B over 1 min and held for 1 min.) to give pure product as white foam (1.77 g, 90%). The product is a mixture of two diastereomers (~4:1).

The NMR spectra are reported for a mixture of two rotamers: ^{1}H NMR (400 MHz, DMSO-*d*6, 293 K) δ 9.69 (s, 1H, major), 9.64 (d, *J* = 7.5 Hz, 1H, minor), 8.29 (d, *J* = 1.7 Hz, 1H, minor), 8.28 (s, 1H, major), 8.01-8.02 (m, 1H, minor), 7.99 (s, 1H, major), 7.33-7.39 (m, 5H), 7.14 (s, 2H), 5.34 (dddd, *J* = 6.3, 6.3, 6.3, 6.3 Hz, 1H, minor), 5.25 (m, 1H, major), 5.15-5.35 (m, 2H), 4.79 (dd, *J* = 8.6, 4.6 Hz, 0.5H, minor), 4.71 (dd, *J* = 9.2, 4.0 Hz, 0.5H, minor), 4.62 (dd, *J* = 8.6, 5.2 Hz, 0.5H, major), 4.55 (dd, *J* = 9.2, 5.7 Hz, 0.5H, major), 4.12-4.25 (m, 2H), 3.73 (s, 0.5H, minor), 3.66 (s, 0.5H, minor), 3.65 (s, 0.5H, major), 3.57 (s, 0.5H, major), 3.03-3.12 (m, 1H, major), 2.94-3.00 (m, 1H, minor), 2.66-2.72 (m, 1H), 2.34 (s, 3H), 2.08 (s, 3H, major), 2.06 (s, 3H, major), 2.02 (s, 3H, minor), 2.01 (s, 3H, minor); ^{13}C NMR (100 MHz, DMSO-*d*6, 293 K) δ 172.16, 172.07, 171.91, 171.72, 158.75 (q, $J_{C\text{-}F}$ = 35 Hz), 154.08, 153.91, 153.60, 153.52, 140.46, 137.45, 137.33, 136.53, 134.68, 134.53, 131.34, 131.29, 129.29, 128.54, 128.46, 128.12, 128.05, 128.00, 127.84, 127.75, 127.52, 127.43, 124.49, 124.45, 124.32, 122.41, 122.18, 122.18, 122.12, 116.14 (q, $J_{C\text{-}F}$ = 292 Hz), 66.80, 66.71, 57.95, 57.65, 57.51, 57.23, 57.07, 52.39, 52.21, 51.98, 51.34, 50.73, 50.33, 35.39, 35.13, 34.48, 34.15, 20.57, 16.97, 16.88;

^{1}H NMR (400 MHz, DMSO-*d*6, 353 K) δ 9.61 (s, 1H), 8.22 (m, 1H, minor), 8.20 (m, 1H, major), 7.93 (m, 1H, minor), 7.91 (m, 1H, major), 7.31-7.39 (m, 5H), 7.14 (s, 2H), 5.38 (dddd, *J* = 6.4, 6.4, 6.4, 6.4 Hz, 1H, minor), 5.30 (dddd, *J* = 6.4, 6.4, 6.4, 6.4 Hz, 1H,

major), 5.09-5.20 (m, 2H), 4.75 (br s, 1H, minor), 4.58 (dd, *J* = 8.9, 5.7 Hz, 1H, major), 4.27 (dd, *J* = 11.7, 6.6 Hz, 1H, major), 4.17 (br, 1H, minor), 4.09 (dd, *J* = 11.5, 5.5 Hz, 1H, major), 3.94 (dd, *J* = 11.5, 5.5 Hz, 1H, minor), 3.70 (s, 3H, minor), 3.63 (s, 3H, major), 3.07-3.15 (m, 1H, major), 2.96-3.04 (m, 1H, minor), 2.72-2.79 (m, 1H, minor), 2.62-2.68 (m, 1H, major), 2.36 (s, 3H), 2.08 (s, 6H, major), 2.05 (s, 6H, minor); ^{13}C NMR (100 MHz, DMSO-*d*6, 353 K) δ 171.43, 158.21 (q, $J_{C\text{-}F}$ = 35 Hz), 153.51, 140.17, 137.10, 136.99, 136.21, 134.24, 134.13, 130.97, 130.93, 128.95, 128.06, 127.62, 127.23, 124.24, 124.06, 122.05, 121.87, 115.90 (q, $J_{C\text{-}F}$ = 292 Hz), 66.49, 57.29, 57.13, 51.83, 51.71, 50.42, 34.75, 20.14, 16.48;

3-((3*S*,5*S*)-1-(benzyloxycarbonyl)-5-(methoxycarbonyl)pyrrolidin-3-yl)-1-mesityl-1*H*-imidazol-3-ium trifluoroacetate (2.25)

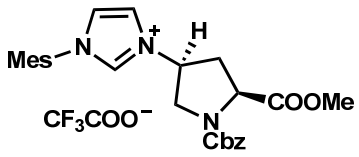

A solution of mesityl imidazole (142 mg, 0.763 mmol) in 10 mL of anhydrous Et_2O was added to the solution of **2.23** (349 mg, 0.848 mmol) in 15 mL of Et_2O at -78 ˚C. After 3 hours the reaction mixture was warmed to room temperature and the solvent was removed under reduced pressure. The resulting light yellowish oil was washed with Et_2O (3 x 20 mL) and dried under vacuum to give a white form (diastereomeric ratio is ~ 20:1).

The NMR spectra are reported for a mixture of two rotamers (only major diastereomer is recorded): ^{1}H NMR (500 MHz, DMSO-*d*6, 293 K) δ 9.59 (s, 1H), 8.22 (s, 1H), 7.97 (s, 1H), 7.45 – 7.25 (m, 5H), 7.14 (s, 2H), 5.21–5.11 (m, 2H), 5.06 (dd, *J* = 30.1, 12.9 Hz, 1H), 4.59 (dd, *J* = 8.9, 5.5 Hz, 0.5H), 4.51 (dd, *J* = 8.8, 5.8 Hz, 0.5H), 4.24–4.10 (m, 1H), 4.09–3.99 (m, 1H), 3.62 (s, 1.5H), 3.54 (s, 1.5H), 3.10–2.93 (m, 1H), 2.72–2.61 (m, 0.5H), 2.61–2.55 (m, 0.5H), 2.33 (s, 3H), 2.04 (s, 3H), 2.02 (s, 3H); ^{13}C NMR (125 MHz, DMSO-*d*6, 293 K) δ 171.90, 171.56, 158.02 (q, J_{C-F} = 32.9 Hz), 153.89, 153.44, 140.30, 137.21, 136.38, 134.52, 131.19, 129.18, 128.46, 128.38, 128.06, 127.92, 127.76, 127.31, 124.17, 122.27, 116.70 (q, J_{C-F} = 297.0 Hz), 66.67, 66.57, 57.73, 57.35, 56.91, 52.21, 50.56, 50.15, 35.16, 34.27, 20.60, 16.92;

^{1}H NMR (500 MHz, DMSO-*d*6, 353 K) δ 9.53 (s, 1H), 8.15 (dd, *J* = 1.6, 1.6 Hz, 1H), 7.91 (dd, *J* = 1.6, 1.6 Hz, 1H), 7.42–7.28 (m, 5H), 7.13 (s, 2H), 5.25–5.18 (m, 1H), 5.18–5.05 (m, 2H), 4.56 (dd, *J* = 8.7, 5.8 Hz, 1H), 4.22 (ddd, *J* = 23.3, 11.6, 11.6 Hz, 1H), 4.03 (dd, *J* = 11.7, 5.6 Hz, 1H), 3.61 (s, 3H), 3.07 (ddd, *J* = 14.0, 9.0, 6.9 Hz, 1H), 2.64–2.55 (m, 1H), 2.35 (s, 3H), 2.05 (s, 6H); ^{13}C NMR (125 MHz, DMSO-*d*6, 353 K) δ 171.25, 157.57 (q, J_{C-F} = 33.0 Hz), 153.30, 139.98, 136.85, 136.05, 134.08, 130.82, 128.82, 127.95, 127.52, 127.11, 123.92, 121.92, 116.28 (q, J_{C-F} = 297.0 Hz), 66.35, 57.10, 56.96, 51.67, 50.24, 34.55, 20.11, 16.42;

The compound was purified by preparative HPLC (Column: XBridge BEH C_{18} OBD Prep 5 μm, 19 x 150 mm; wavelength: 215 nm, 254 nm; temperature: ambient; solvent A: 0.1% trifluoroacetic acid in H_2O, solvent B: 0.1% trifluoroacetic acid in MeCN; flow rate:

12 mL/min. Held at 0% B for 1 min, ramped to 100% B over 17 min, ramped to 0% B over 1 min and held for 1 min.) to give pure product as white foam (481 mg, 86%).

The NMR spectra are reported for a mixture of two rotamers: ^{1}H NMR (500 MHz, DMSO-*d*6, 293 K) δ 9.56 (s, 1H), 8.20 (s, 1H), 7.96 (s, 1H), 7.50-7.20 (m, 5H), 7.14 (s, 2H), 5.18-5.10 (m, 1H), 5.06 (dd, *J* = 29.5, 12.8 Hz, 2H), 4.59 (dd, *J* = 8.9, 5.4 Hz, 0.5H), 4.51 (dd, *J* = 8.8, 5.6 Hz, 0.5H), 4.17 (ddd, *J* = 12.4, 12.4, 6.5 Hz, 1H), 4.05 (dd, *J* = 11.6, 5.8, 5.8 Hz, 1H), 3.62 (s, 1.5H), 3.54 (s, 1.5H), 3.20-2.91 (m, 1H), 2.70-2.60 (m, 0.5H), 2.58 (dd, *J* = 13.1, 6.5 Hz, 0.5H), 2.33 (s, 3H), 2.04 (d, *J* = 2.8 Hz, 3H), 2.02 (d, *J* = 2.3 Hz, 3H); ^{13}C NMR (125 MHz, DMSO-*d*6, 293 K) δ 172.00, 171.65, 158.55 (q, $J_{C\text{-}F}$ = 35.9 Hz), 154.00, 153.54, 140.40, 137.32, 136.49, 134.62, 131.28, 129.25, 128.52, 128.43, 128.10, 127.97, 127.81, 127.38, 124.26, 122.35, 122.08, 119.52, 115.92 (q, $J_{C\text{-}F}$ = 291.9 Hz), 66.75, 66.66, 57.87, 57.45, 57.13, 57.00, 52.23, 50.67, 50.26, 40.02, 35.29, 34.39, 20.60, 16.96;

^{1}H NMR (500 MHz, DMSO-*d*6, 353 K) δ 9.55 (s, 1H), 8.16 (dd, *J* = 1.7, 1.7 Hz, 1H), 7.91 (dd, *J* = 1.7, 1.7 Hz, 1H), 7.49-7.25 (m, 5H), 7.14 (s, 2H), 5.25 (dddd, *J* = 6.3, 6.3, 6.3, 6.3 Hz, 1H), 5.13 (dd, *J* = 33.1, 12.6 Hz, 2H), 4.57 (dd, *J* = 8.8, 5.7 Hz, 1H), 4.25 (dd, *J* = 11.8, 6.7 Hz, 1H), 4.06 (dd, *J* = 11.8, 5.5 Hz, 1H), 3.62 (s, 3H), 3.09 (ddd, *J* = 13.9, 9.0, 6.9 Hz, 1H), 2.70-2.53 (m, 1H), 2.35 (s, 3H), 2.05 (s, 6H); ^{13}C NMR (125 MHz, DMSO-*d*6, 353 K) δ 171.34, 157.96 (q, $J_{C\text{-}F}$ = 35.9 Hz), 153.42, 140.08, 136.93, 136.13, 134.16, 130.89, 128.89, 128.01, 127.57, 127.17, 124.00, 121.98, 119.34, 115.64 (q, $J_{C\text{-}F}$ = 292.3 Hz), 66.42, 57.05, 51.69, 50.33, 34.62, 20.12, 16.44;

LC/MS (ESI) calculated for $C_{26}H_{30}N_3O_4$ $[M\text{-}CF_3COO]^+$ 448.22, found 447.99 (t_R = 10.22 min); HRMS ($^+$ESI) calculated for $C_{26}H_{30}N_3O_4$ $[M\text{-}CF_3COO]^+$ 448.2231, found 448.2241.

(2*S*,4*R*)-dibenzyl-4-(trifluoromethylsulfonyloxy)pyrrolidine-1,2-dicarboxylate (2.27)

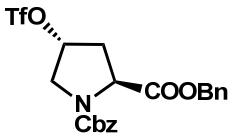

To a solution of N-Cbz-(2*S*,4*R*)-4-hydroxyl-proline benzyl ester (1.92 g, 5.40 mmol) and pyridine (0.870 mL, 10.8 mmol) in 22 mL of DCM triflic anhydride (1.36 mL, 8.10 mmol) was added at -10 ˚C. The resulting yellowish solution was stirred in an ethanol/ice bath for 3 hours, followed by washing with 15 mL of saturated $NaHCO_3$ (aq.) and 15 mL of brine then dried over $MgSO_4$. After evaporating the solvent, the orange residue was dissolved in a small amount of DCM and subjected to column chromatography using DCM as eluent. Triflate intermediate was collected as a colorless oil (1.87 g, 71%).

The NMR spectra are reported for a mixture of two rotamers: ^{1}H NMR (500 MHz, $CDCl_3$) δ 7.32-7.39 (m, 8H), 7.27-7.30 (m, 1H), 7.20-7.21 (m, 1H), 5.46 (br s, 1H), 5.16-5.29 (m, 2H), 5.07 (s, 1H), 5.00 (s, 1H), 4.64 (dd, *J* = 8.0, 8.0 Hz, 0.5H), 4.57 (dd, *J* = 8.0, 8.0 Hz, 0.5H), 4.07 (d, *J* = 13.2 Hz, 0.5H), 3.97 (d, *J* = 13.8 Hz, 0.5H), 3.88 (ddd, *J* = 13.8, 4.0, 4.0 Hz, 1H), 2.66-2.73 (m, 1H), 2.30-2.39 (m, 1H); ^{13}C NMR (125 MHz, $CDCl_3$) δ 171.33, 171.17, 154.36, 153.89, 135.95, 135.88, 135.19, 134.97, 128.78, 128.71, 128.64, 128.37, 128.18, 128.13, 118.49 (q, $J_{C\text{-}F}$ = 319 Hz), 86.32, 85.78, 67.94, 67.86, 67.62, 67.50, 57.48, 57.17, 53.00, 52.62, 37.65, 36.43.

3-((3*S*,5*S*)-1,5-bis(benzyloxycarbonyl)pyrrolidin-3-yl)-1-mesityl-1*H*-imidazol-3-ium trifluoromethanesulfonate (2.28, 4:1 mixture of diastereomers)

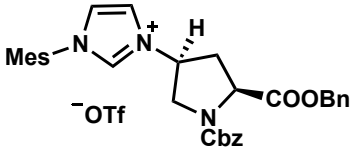

A solution of mesityl imidazole (644 mg, 3.46 mmol) in dry Et_2O was added to the solution of **2.27** (1.87 g, 3.84 mmol) in Et_2O at -78 ˚C. The reaction mixture was warmed to room temperature and stirred for 24 hours. Resulting light yellowish oil was washed with Et_2O (3 times) and dried under vacuum to give pure product (2.11 g, 91%) as a white foam. The product is a mixture of two diastereomers (~4:1).

The NMR spectra are reported for a mixture of two rotamers: ^{1}H NMR (500 MHz, DMSO-*d*6, 293 K) δ 9.59 (s, 0.5H, major), 9.57 (s, 0.5H, major), 9.52 (s, 0.5H, minor), 9.51 (s, 0.5H, minor), 8.22 (br s, 1H, minor), 8.20 (br s, 0.5H, major), 8.19 (br s, 0.5H, major), 7.98-7.99 (m, 1H, minor), 7.95 (br s, 0.5H, major), 7.94 (br s, 0.5H, major), 7.25-7.42 (m, 10H), 7.14 (s, 2H), 5.12-5.29 (m, 3H), 5.02-5.05 (m, 2H), 4.79 (dd, *J* = 34.6, 8.6 Hz, 0.5H, minor), 4.78 (dd, *J* = 34.4, 9.2 Hz, 0.5H, minor), 4.65 (dd, *J* = 8.6, 5.2 Hz, 0.5H, major), 4.59 (dd, *J* = 8.6, 5.7 Hz, 0.5H, major), 4.16-4.23 (m, 1H), 4.06-4.11 (m, 1H), 3.04-3.10 (m, 1H, major), 2.93-3.00 (m, 1H, minor), 2.70-2.75 (m, 1H, minor), 2.64-2.69 (m, 0.5H, minor), 2.54-2.61 (m, 0.5H, major), 2.33 (s, 3H), 2.03 (br, 6H, major), 1.93-2.05 (m, 6H, minor); ^{13}C NMR (100 MHz, DMSO-*d*6, 293 K) δ 171.39, 170.99, 153.96, 153.51, 140.32, 137.19, 136.41, 136.32, 135.61, 135.42, 134.57, 134.41, 131.20,

129.20, 128.53, 128.40, 128.28, 128.09, 127.92, 127.81, 127.34, 124.22, 122.24, 66.64, 66.47, 66.35, 57.72, 50.54, 50.09, 35.31, 34.41, 20.61, 16.95;

^{1}H NMR (500 MHz, DMSO-*d*6, 353 K) δ 9.50 (s, 1H, major), 9.48 (s, 1H, minor), 8.16 (dd, *J* = 1.7, 1.7 Hz, 1H, minor), 8.12 (dd, *J* = 1.7, 1.7 Hz, 1H, major), 7.92 (dd, *J* = 1.7, 1.7 Hz, 1H, minor), 7.88 (dd, *J* = 1.7, 1.7 Hz, 1H, major), 7.32-7.36 (m, 10H), 7.14 (s, 2H), 5.28-5.32 (m, 1H, minor), 5.19-5.24 (m, 1H, major), 5.11 (br, 2H), 4.78 (br, 1H, minor), 4.63 (dd, *J* = 9.2, 5.7 Hz, 1H, major), 4.25 (dd, *J* = 12.0, 6.9 Hz, 1H, major), 4.13 (br, 1H, minor), 4.05 (dd, *J* = 12.0, 5.7 Hz, 1H, major), 3.93 (dd, *J* = 11.5, 5.2 Hz, 1H, minor), 3.08-3.14 (m, 1H, major), 2.98 (m, 1H, minor), 2.74 (m, 1H, minor), 2.57-2.62 (m, 1H, major), 2.35 (s, 3H), 2.04 (s, 6H, major), 2.01 (m, 6H, minor); ^{13}C NMR (100 MHz, DMSO-*d*6, 353 K) δ 170.72, 153.37, 140.00, 136.79, 136.16, 136.01, 135.18, 134.09, 133.99, 133.63, 130.80, 128.83, 128.04, 127.96, 127.76, 127.52, 127.36, 127.12, 123.95, 121.87, 66.38, 66.07, 57.07, 50.22, 34.74, 20.12, 16.44;

LC/MS (ESI) calculated for $C_{32}H_{34}N_3O_4$ $[M\text{-}CF_3SO_3]^+$ 524.25, found 523.99 (t_R = 10.56 min); HRMS ($^+$ESI) calculated for $C_{32}H_{34}N_3O_4$ $[M\text{-}CF_3SO_3]^+$ 524.2544, found 524.2542.

3-((3*S*,5*S*)-1,5-bis(benzyloxycarbonyl)pyrrolidin-3-yl)-1-mesityl-1*H*-imidazol-3-ium trifluoroacetate (2.29, 4:1 mixture of diastereomers)

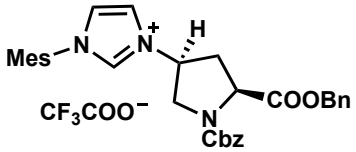

The triflate **2.27** was subjected to preparative HPLC (Column: XBridge BEH C_{18} OBD Prep 5 μm, 19 x 150 mm; Wavelength: 215 nm, 254 nm; Temperature: ambient; Solvent A: 0.1% trifluoroacetic acid in H_2O, Solvent B: 0.1% trifluoroacetic acid in MeCN; Flow rate: 12 mL/min. Held at 0% B for 1 min, ramped to 100% B over 17 min, ramped to 0% B over 1 min and held for 1 min.) to give pure product as white foam (1.81g, 82% for two steps). The product is a mixture of two diastereomers (~4:1).

The NMR spectra are reported for a mixture of two rotamers: ^{1}H NMR (500 MHz, DMSO-*d*6, 293 K) δ 9.57 (s, 0.5H, major), 9.56 (s, 0.5H, major), 9.52 (s, 0.5H, minor), 9.50 (s, 0.5H, minor), 8.19 (br s, 1H, minor), 8.18 (br s, 0.5H, major), 8.17 (br s, 0.5H, major), 7.95-7.96 (m, 1H, minor), 7.92 (br s, 0.5H, major), 7.91 (br s, 0.5H, major), 7.22-7.39 (m, 10H), 7.10 (s, 2H), 4.97-5.25 (m, 5H), 4.78 (dd, *J* = 8.6, 4.6 Hz, 0.5H, minor), 4.71 (dd, *J* = 8.6, 4.6 Hz, 0.5H, minor), 4.61 (dd, *J* = 8.9, 5.4 Hz, 0.5H, major), 4.54 (dd, *J* = 8.9, 6.0 Hz, 0.5H, major), 4.12-4.19 (m, 1H), 4.01-4.06 (m, 1H, major), 3.84-3.89 (m, 1H, minor), 2.99-3.06 (m, 1H, major), 2.90-2.96 (m, 1H, minor), 2.69-2.71 (m, 0.5H, minor), 2.67-2.68 (m, 0.5H, minor), 2.60-2.65 (m, 0.5H, major), 2.52-2.57 (m, 0.5H, major), 2.29 (s, 3H), 1.99-2.01 (br, 6H, major), 1.95 (s, 3H, minor),1.94 (s, 3H, minor); ^{13}C NMR (100 MHz, DMSO-*d*6, 293 K) δ 171.40, 171.00, 158.29 (q, $J_{C\text{-}F}$ = 35 Hz), 153.97, 153.92, 153.52, 153.40, 140.32, 137.24, 136.32, 135.63, 134.57, 134.43, 131.22, 129.20, 128.53, 128.42, 128.29, 128.09, 127.93, 127.80, 127.35, 124.23, 122.25, 116.06 (q, $J_{C\text{-}F}$ = 293 Hz), 66.65, 66.48, 66.36, 57.72, 57.49, 57.04, 50.55, 50.11, 35.32, 34.43, 20.61, 16.96, 16.87;

^{1}H NMR (500 MHz, DMSO-*d*6, 353 K) δ 9.49 (s, 1H, major), 9.48 (s, 1H, minor), 8.13 (dd, *J* = 1.7, 1.7 Hz, 1H, minor), 8.09 (dd, *J* = 1.7, 1.7 Hz, 1H, major), 7.89 (dd, *J* = 1.7, 1.7 Hz, 1H, minor), 7.85 (dd, *J* = 1.7, 1.7 Hz, 1H, major), 7.28-7.32 (m, 10H), 7.10 (s, 2H), 5.28 (dddd, *J* = 6.3, 6.3, 6.3, 6.3 Hz, 1H, minor), 5.20 (dddd, *J* = 6.3, 6.3, 6.3, 6.3 Hz, 1H, major), 5.07 (br s, 4H), 4.74 (br, 1H, minor), 4.59 (dd, *J* = 8.6, 5.7 Hz, 1H, major), 4.21 (dd, *J* = 11.5, 6.9 Hz, 1H, major), 4.09 (br, 1H, minor), 4.01 (dd, *J* = 11.5, 5.7 Hz, 1H, major), 3.89 (dd, *J* = 11.5, 5.2 Hz, 1H, minor), 3.05-3.10 (m, 1H, major), 2.93-2.96 (m, 1H, minor), 2.69-2.71 (m, 1H, minor), 2.53-2.58 (m, 1H, major), 2.31 (s, 3H), 2.00 (s, 6H, major), 1.98 (s, 6H, minor); ^{13}C NMR (100 MHz, DMSO-*d*6, 353 K) δ 170.73, 157.71 (q, $J_{C\text{-}F}$ = 35 Hz), 153.38, 140.00, 136.85, 136.72, 136.02, 135.19, 134.10, 134.00, 130.82, 128.84, 128.05, 127.97, 127.76, 127.52, 127.37, 127.13, 124.11, 121.88, 115.78 (q, $J_{C\text{-}F}$ = 294 Hz), 66.39, 66.21, 66.08, 57.08, 50.24, 34.71, 20.13, 16.44, 16.39;

3-((3*S*,5*S*)-1,5-bis(benzyloxycarbonyl)pyrrolidin-3-yl)-1-mesityl-1*H*-imidazol-3-ium trifluoroacetate (2.29)

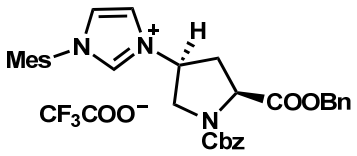

A solution of mesityl imidazole (274 mg, 1.48 mmol) in 15 mL of anhydrous Et_2O was added to the solution of **2.27** (675 mg, 1.64 mmol) in 20 mL of Et_2O at -78 ˚C. After 3 hours the reaction mixture was warmed to room temperature and the solvent was

removed under reduced pressure. The resulting light yellowish oil was washed with Et_2O (3 x 20 mL) and dried under vacuum to give a white foam (diastereomeric ratio is ~20:1).

The NMR spectra are reported for a mixture of two rotamers (only major diastereomer is recorded): ^{1}H NMR (500 MHz, DMSO-*d*6, 293 K) δ 9.63 (d, *J* = 5.5 Hz, 1H), 8.23 (d, *J* = 6.0 Hz, 1H), 7.96 (d, *J* = 5.5 Hz, 1H), 7.49–7.22 (m, 10H), 7.14 (s, 2H), 5.24 – 5.00 (m, 5H), 4.65 (ddd, *J* = 14.5, 7.2, 7.2 Hz, 0.5H), 4.60 (dd, *J* = 8.7, 5.9 Hz, 0.5H), 4.21 (ddd, *J* = 18.2, 11.8, 6.5 Hz, 1H), 4.10 (ddd, *J* = 11.4, 11.4, 5.1 Hz, 1H), 3.15–2.97 (m, 1H), 2.74–2.64 (m, 0.5H), 2.65–2.56 (m, 0.5H), 2.33 (s, 3H), 2.04 (dd, *J* = 6.1, 6.1 Hz, 6H); ^{13}C NMR (125 MHz, DMSO-*d*6, 293 K) δ 171.43, 171.02, 158.44 (q, $J_{C\text{-}F}$ = 34.9 Hz), 154.01, 153.54, 140.34, 137.30, 136.35, 135.65, 135.46, 134.59, 131.24, 129.22, 128.53, 128.41, 128.28, 128.08, 127.95, 127.83, 127.79, 127.37, 124.25, 122.28, 116.21 (q, $J_{C\text{-}F}$ = 293.6 Hz), 66.74, 66.67, 66.51, 66.38, 57.77, 57.55, 57.09, 50.62, 50.17, 35.37, 34.47, 20.59, 16.95;

^{1}H NMR (500 MHz, DMSO-*d*6, 353 K) δ 9.56 (s, 1H), 8.15 (s, 1H), 7.90 (d, *J* = 1.3 Hz, 1H), 7.43–7.26 (m, 10H), 7.13 (s, 2H), 5.26 (ddd, *J* = 6.4, 6.4, 6.4 Hz, 1H), 5.12 (br s, 4H), 4.63 (ddd, *J* = 20.3, 10.2, 10.2 Hz, 1H), 4.27 (dd, *J* = 11.7, 6.7 Hz, 1H), 4.07 (dd, *J* = 11.8, 5.6 Hz, 1H), 3.13 (ddd, *J* = 14.0, 8.9, 7.0 Hz, 1H), 2.66–2.58 (m, 1H), 2.35 (s, 3H), 2.05 (s, 6H); ^{13}C NMR (125 MHz, DMSO-*d*6, 353 K) δ 170.77, 157.88 (q, $J_{C\text{-}F}$ = 34.8 Hz), 140.03, 136.92, 136.06, 135.23, 134.13, 130.85, 128.86, 128.06, 127.98, 127.76, 127.53, 127.39, 127.15, 123.99, 121.90, 115.95 (q, $J_{C\text{-}F}$ = 294.0 Hz), 66.42, 66.12, 57.15, 50.30, 34.68, 20.12, 16.44;

It was then subjected to preparative HPLC (Column: XBridge BEH C_{18} OBD Prep 5 μm, 19 x 150 mm; wavelength: 215 nm, 254 nm; temperature: ambient; solvent A: 0.1% trifluoroacetic acid in H_2O, solvent B: 0.1% trifluoroacetic acid in MeCN; flow rate: 12 mL/min. Held at 0% B for 1 min, ramped to 100% B over 17 min, ramped to 0% B over 1 min and held for 1 min.) to give pure product as white foam (806 mg, 85%).

The NMR spectra are reported for a mixture of two rotamers: ^{1}H NMR (500 MHz, DMSO-*d*6, 293 K) δ 9.65 (d, *J* = 5.4 Hz, 1H), 8.24 (d, *J* = 5.6 Hz, 1H), 7.96 (d, *J* = 5.3 Hz, 1H), 7.35 (m, 10H), 7.14 (s, 2H), 5.25–5.18 (m, 1H), 5.18–5.10 (m, 2H), 5.10–4.99 (m, 2H), 4.66 (dd, *J* = 8.9, 5.4 Hz, 0.5H), 4.60 (dd, *J* = 8.7, 5.9 Hz, 0.5H), 4.22 (ddd, *J* = 18.2, 11.7, 6.4 Hz, 1H), 4.11 (ddd, *J* = 11.4, 11.4, 5.2 Hz, 1H), 3.16–3.02 (m, 1H), 2.74–2.66 (m, 0.5H), 2.65–2.58 (m, 0.5H), 2.33 (s, 3H), 2.05 (dd, *J* = 6.3, 6.3 Hz, 6H); ^{13}C NMR (125 MHz, DMSO-*d*6, 293 K) δ 171.45, 171.05, 158.51 (q, $J_{C\text{-}F}$ = 34.9 Hz), 154.04, 153.56, 140.36, 137.32, 136.46, 136.37, 135.67, 135.48, 134.61, 131.26, 129.23, 128.54, 128.43, 128.29, 128.24, 128.09, 127.96, 127.85, 127.80, 127.39, 124.27, 122.30, 116.24 (q, $J_{C\text{-}F}$ = 293.7 Hz), 66.76, 66.68, 66.53, 66.40, 57.80, 57.57, 57.12, 50.64, 50.20, 35.41, 34.50, 20.60, 16.96;

^{1}H NMR (500 MHz, DMSO-*d*6, 353 K) δ 9.58 (s, 1H), 8.15 (dd, *J* = 1.7, 1.7 Hz, 1H), 7.90 (dd, *J* = 1.6, 1.6 Hz, 1H), 7.35 (m, 10H), 7.13 (s, 2H), 5.28 (dddd, *J* = 6.3, 6.3, 6.3, 6.3 Hz, 1H), 5.12 (br s, 4H), 4.64 (dd, *J* = 8.9, 5.8 Hz, 1H), 4.27 (dd, *J* = 11.7, 6.7 Hz, 1H), 4.07 (dd, *J* = 11.7, 5.6 Hz, 1H), 3.14 (ddd, *J* = 14.2, 8.8, 7.1 Hz, 1H), 2.67–2.58 (m, 1H), 2.35 (s, 3H), 2.06 (s, 6H); ^{13}C NMR (125 MHz, DMSO-*d*6, 353 K) δ 170.79, 157.95 (q, $J_{C\text{-}F}$ = 34.8 Hz), 153.44, 140.06, 136.95, 136.07, 135.25, 134.15, 130.87, 128.88,

128.07, 128.00, 127.78, 127.54, 127.40, 127.16, 124.01, 121.91, 115.98 (q, $J_{C\text{-}F}$ = 294.1 Hz), 66.44, 66.14, 57.16, 50.33, 34.77, 20.12, 16.45;

LC/MS (ESI) calculated for $C_{32}H_{34}N_3O_4$ $[M\text{-}CF_3COO]^+$ 524.25, found 524.01 (t_R = 10.65 min); HRMS ($^+$ESI) calculated for $C_{32}H_{34}N_3O_4$ $[M\text{-}CF_3COO]^+$ 524.2544, found 524.2554.

(*S*)-3-(2-(*tert*-butoxycarbonylamino)-3-methoxy-3-oxopropyl)-1-mesityl-1*H*-imidazol-3-ium trifluoroacetate (2.31)

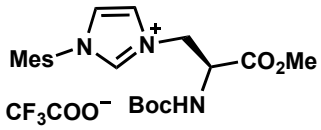

A solution of mesityl imidazole (37.2 mg, 0.20 mmol) and *N*-(*tert*-butoxycarbonyl)-3-iodo-L-alanine methyl ester (65.8 mg, 0.20 mmol) in 0.2 mL of anhydrous DMF was heated at 80 ˚C. After 12 hours, the solvent was evaporated and the resulting brownish oil was washed with diethyl ether (3 times). It was then subjected to preparative HPLC (Column: XBridge BEH C_{18} OBD Prep 5 μm, 19 x 150 mm; wavelength: 215 nm, 254 nm; temperature: ambient; solvent A: 0.1% trifluoroacetic acid in H_2O, solvent B: 0.1% trifluoroacetic acid in MeCN; flow rate: 12 mL/min. Held at 0% B for 1 min, ramped to 100% B over 17 min, ramped to 0% B over 1 min and held for 1 min.) to give pure product as colorless oil (35.2 mg, 35%):

^{1}H NMR (500 MHz, DMSO-*d*6) δ 9.35 (s, 1H), 8.03 (s, 1H), 7.94 (s, 1H), 7.60 (d, *J* = 8.6 Hz, 1H), 7.15 (s, 2H), 4.74 (dd, *J* = 15.9, 5.3 Hz, 1H), 4.71 – 4.65 (m, 1H), 4.42 (dd, *J* =

12.9, 9.2 Hz, 1H), 3.71 (s, 3H), 2.33 (s, 3H), 2.02 (s, 3H), 2.00 (s, 3H), 1.34 (s, 9H); ^{13}C NMR (125 MHz, DMSO-*d*6) δ 169.62, 157.98 (q, $J_{C\text{-}F}$ = 33.2 Hz), 155.35, 140.40, 138.17, 134.37, 134.27, 131.09, 129.33, 129.30, 123.89, 123.74, 116.75 (q, $J_{C\text{-}F}$ = 297.6 Hz), 79.14, 53.16, 52.63, 49.20, 28.04, 20.64, 16.90, 16.84; LC/MS (ESI) calculated for $C_{21}H_{30}N_3O_4$ $[M\text{-}CF_3COO]^+$ 388.22, found 388.14 (t_R = 10.26 min); HRMS ($^+$ESI) calculated for $C_{21}H_{30}N_3O_4$ $[M\text{-}CF_3COO]^+$ 388.2231, found 388.2231.

APPENDIX A: NMR SPECTRA FOR CHAPTER 2

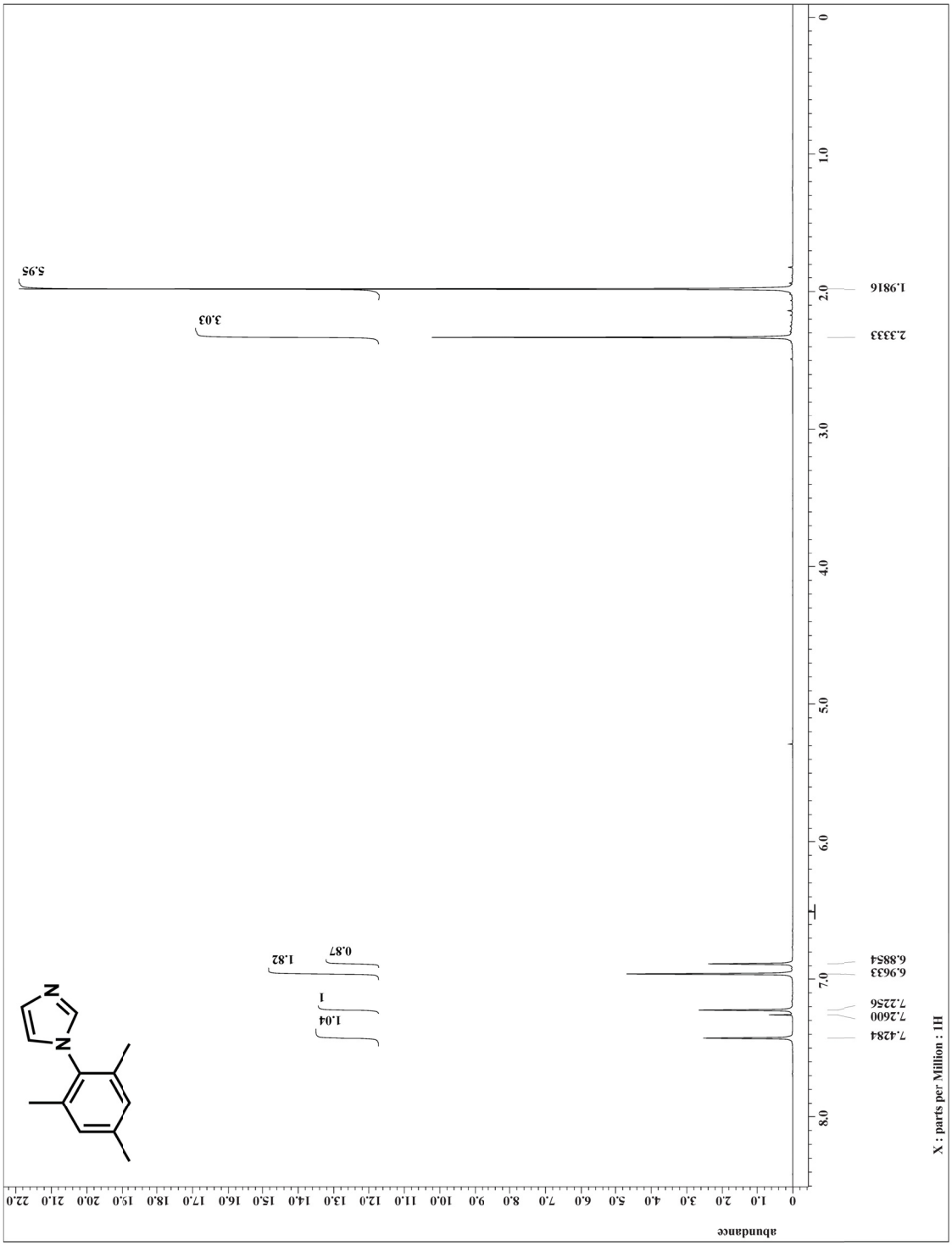

Figure 2.7: ^{1}H NMR (400 MHz, $CDCl_3$) of 1-(2,4,6-trimethylphenyl)-1*H*-imidazole (**2.03**).

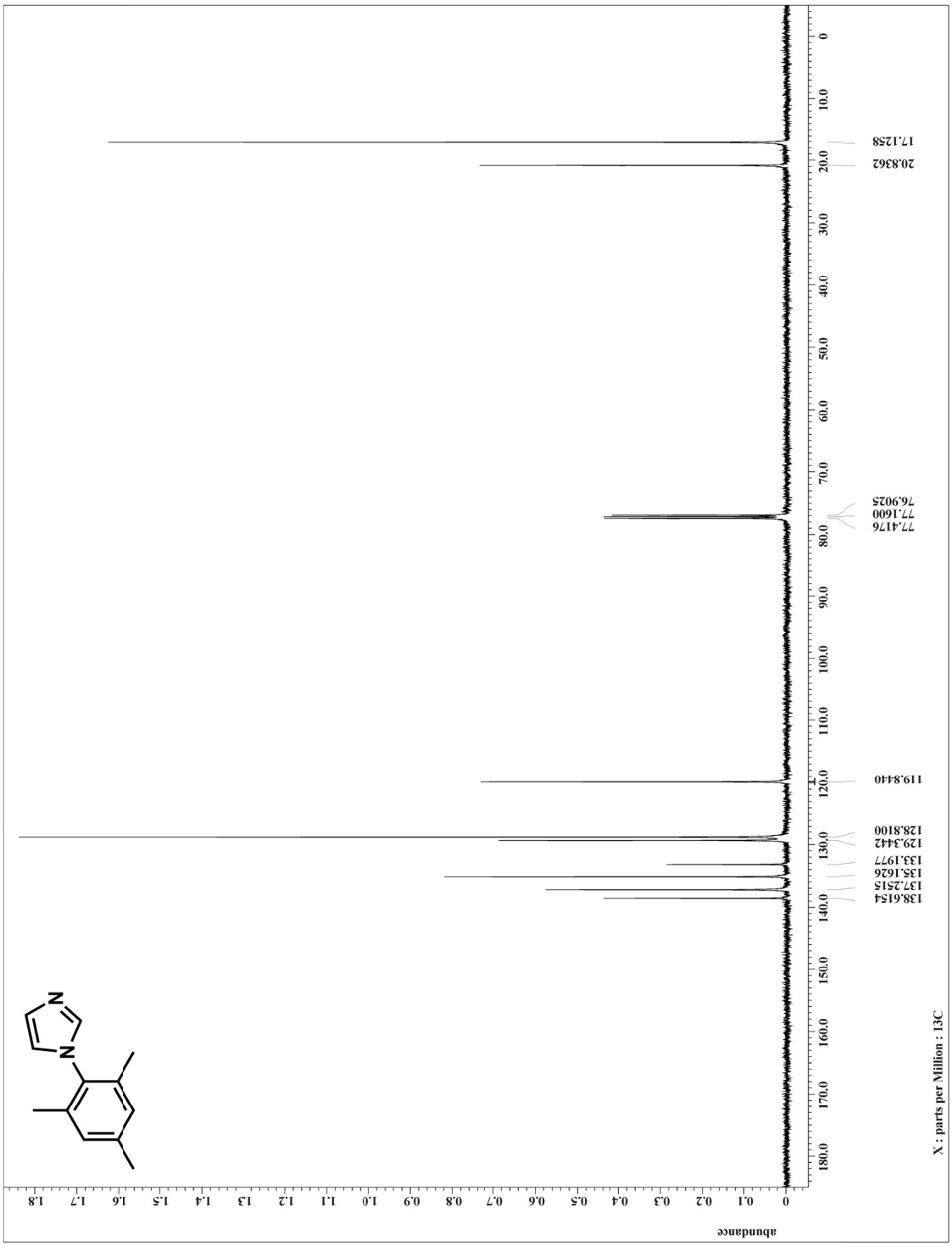

Figure 2.8: ^{13}C NMR (125 MHz, $CDCl_3$) of 1-(2,4,6-trimethylphenyl)-1*H*-imidazole (**2.03**).

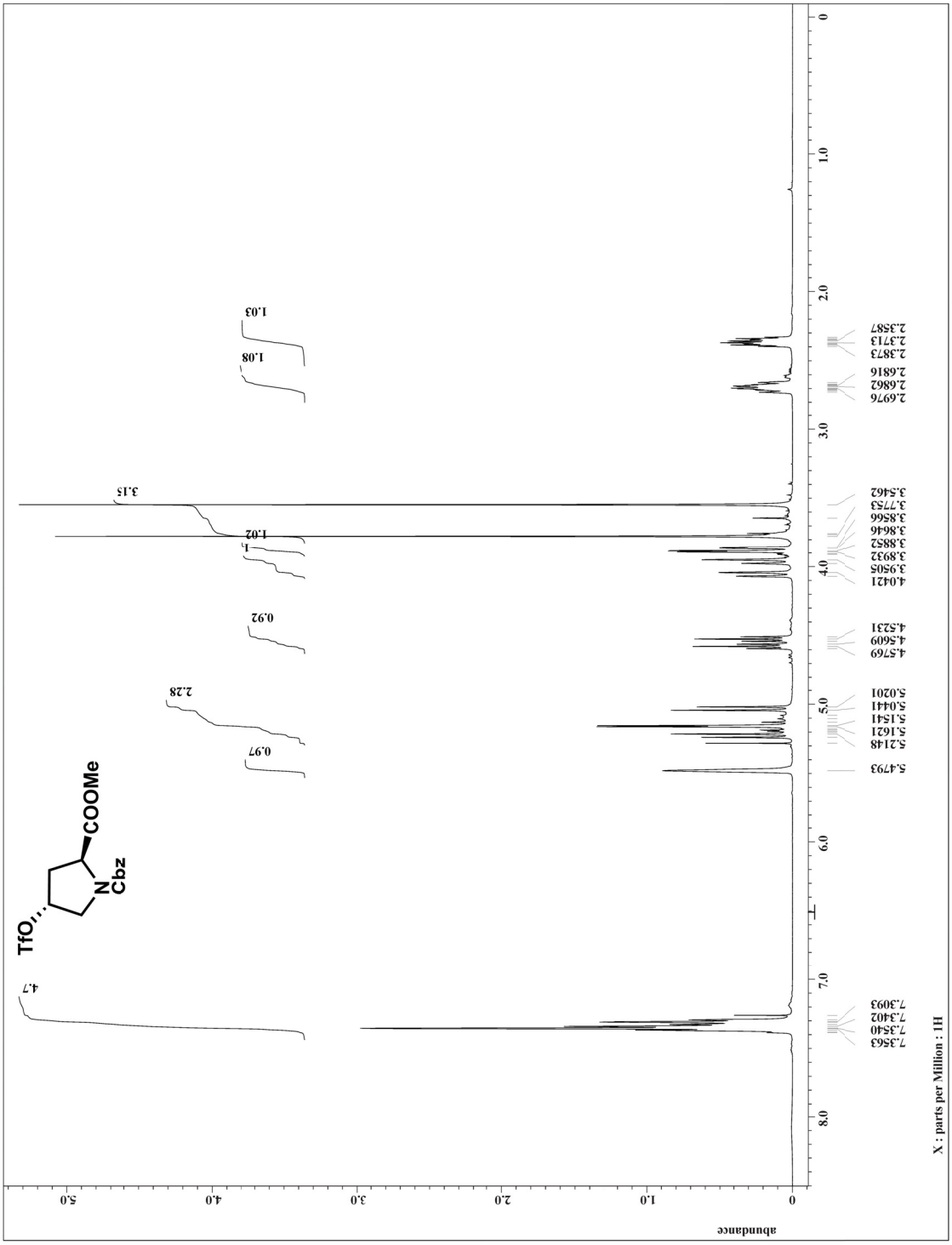

Figure 2.9: ^{1}H NMR (500 MHz, $CDCl_3$) of (2*S*,4*R*)-1-benzyl-2-methyl-4-(trifluoromethylsulfonyloxy)pyrrolidine-1,2-dicarboxylate (**2.23**).

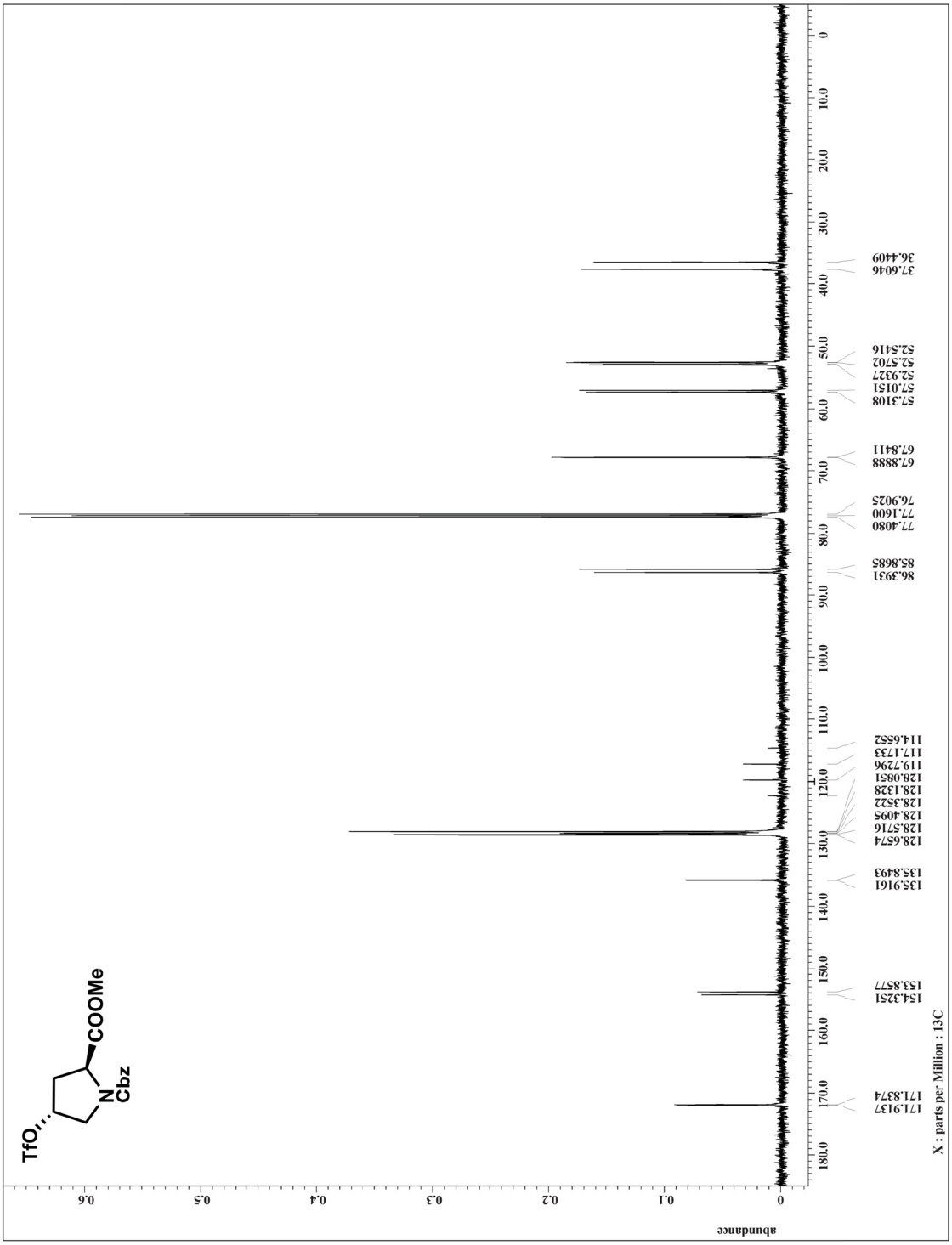

Figure 2.10: ^{13}C NMR (125 MHz, $CDCl_3$) of (2*S*,4*R*)-1-benzyl-2-methyl-4-(trifluoromethylsulfonyloxy)pyrrolidine-1,2-dicarboxylate (**2.23**).

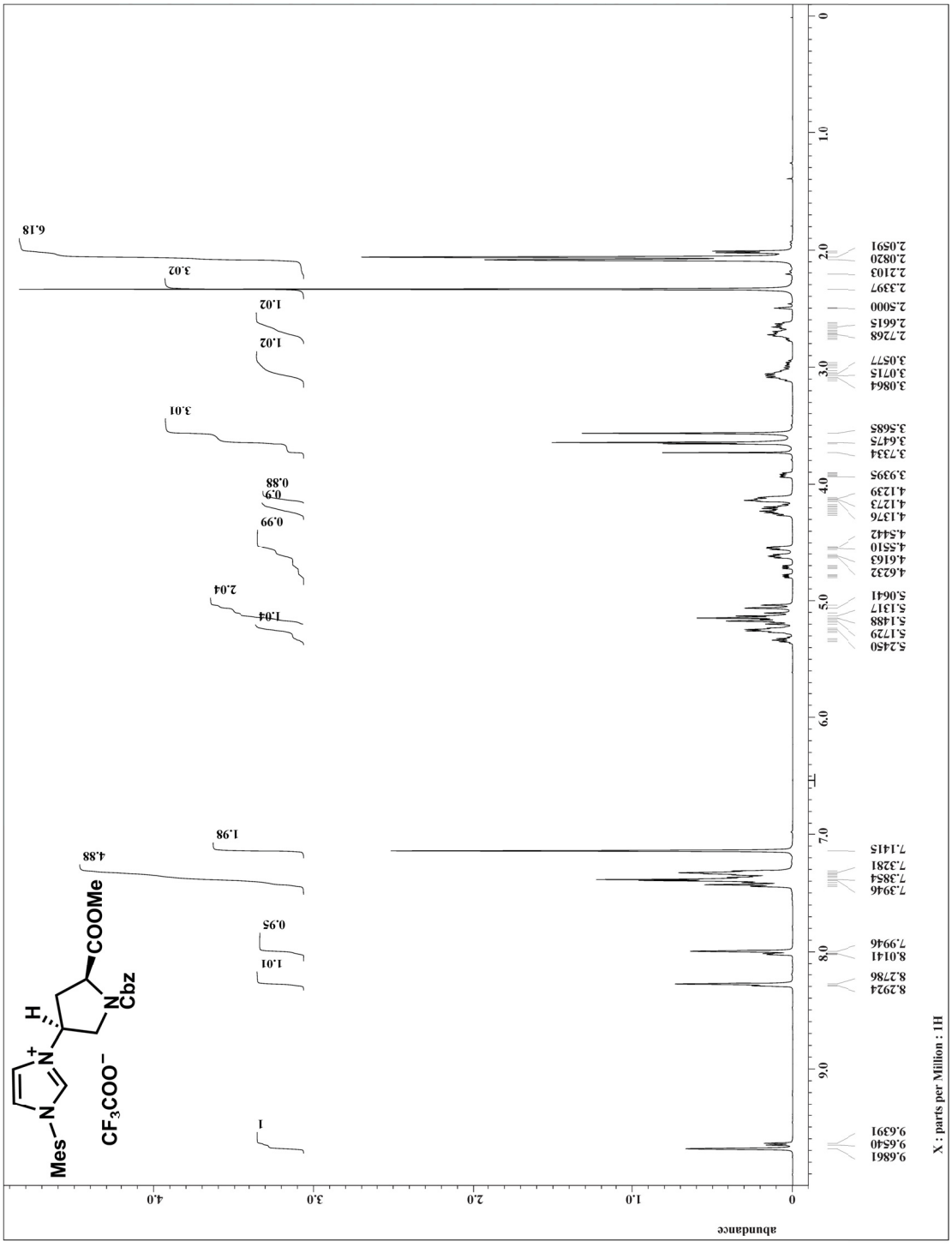

Figure 2.11: ^{1}H NMR (400 MHz, DMSO-*d*6, 293 K) of 3-((3*S*,5*S*)-1-(benzyloxycarbonyl)-5-(methoxycarbonyl)pyrrolidin-3-yl)-1-mesityl-1*H*-imidazol-3-ium trifluoroacetate (**2.25**, 4:1 mixture of diastereomers).

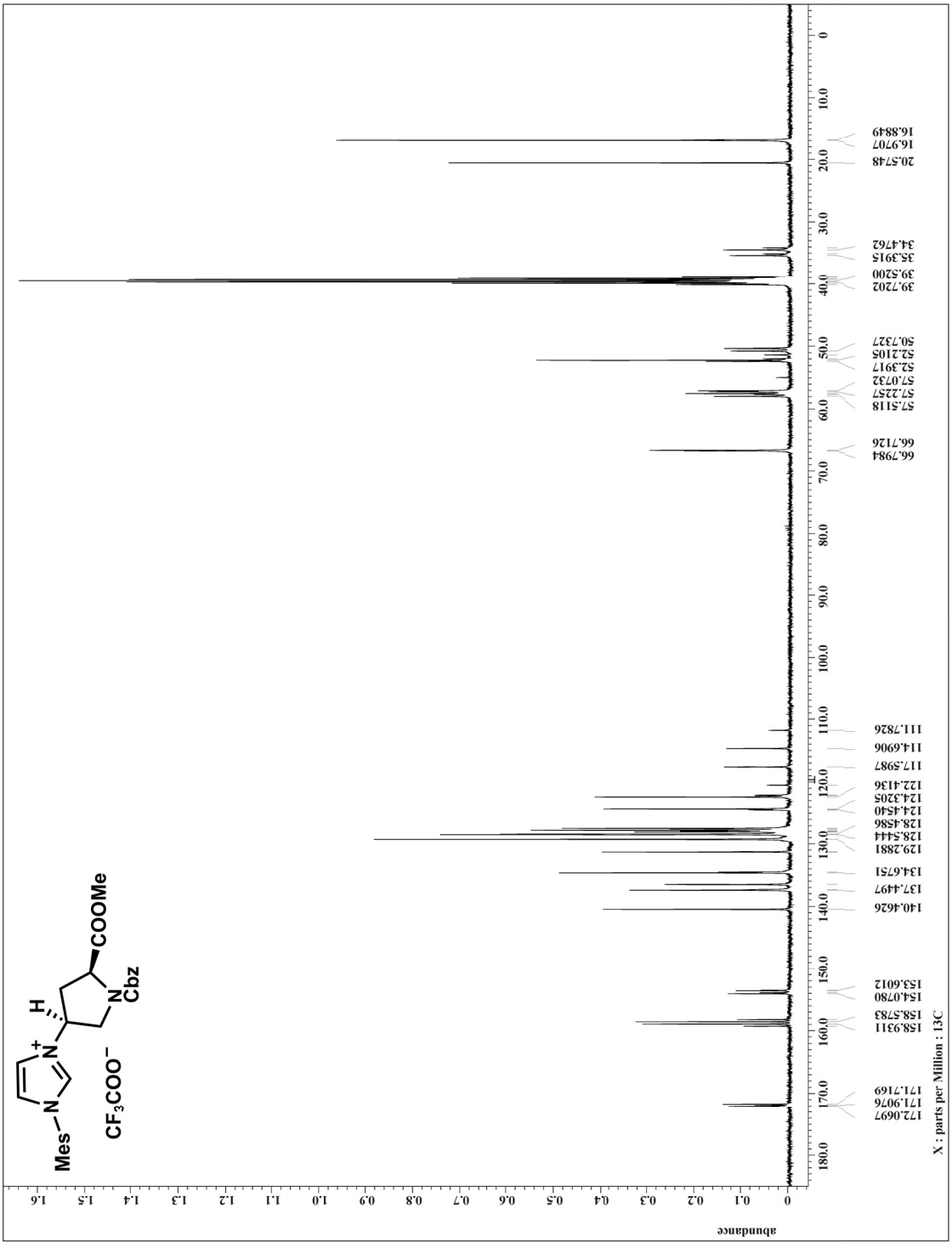

Figure 2.12: ^{13}C NMR (100 MHz, DMSO-*d*6, 293 K) of 3-((3*S*,5*S*)-1-(benzyloxycarbonyl)-5-(methoxycarbonyl)pyrrolidin-3-yl)-1-mesityl-1*H*-imidazol-3-ium trifluoroacetate (**2.25**, 4:1 mixture of diastereomers).

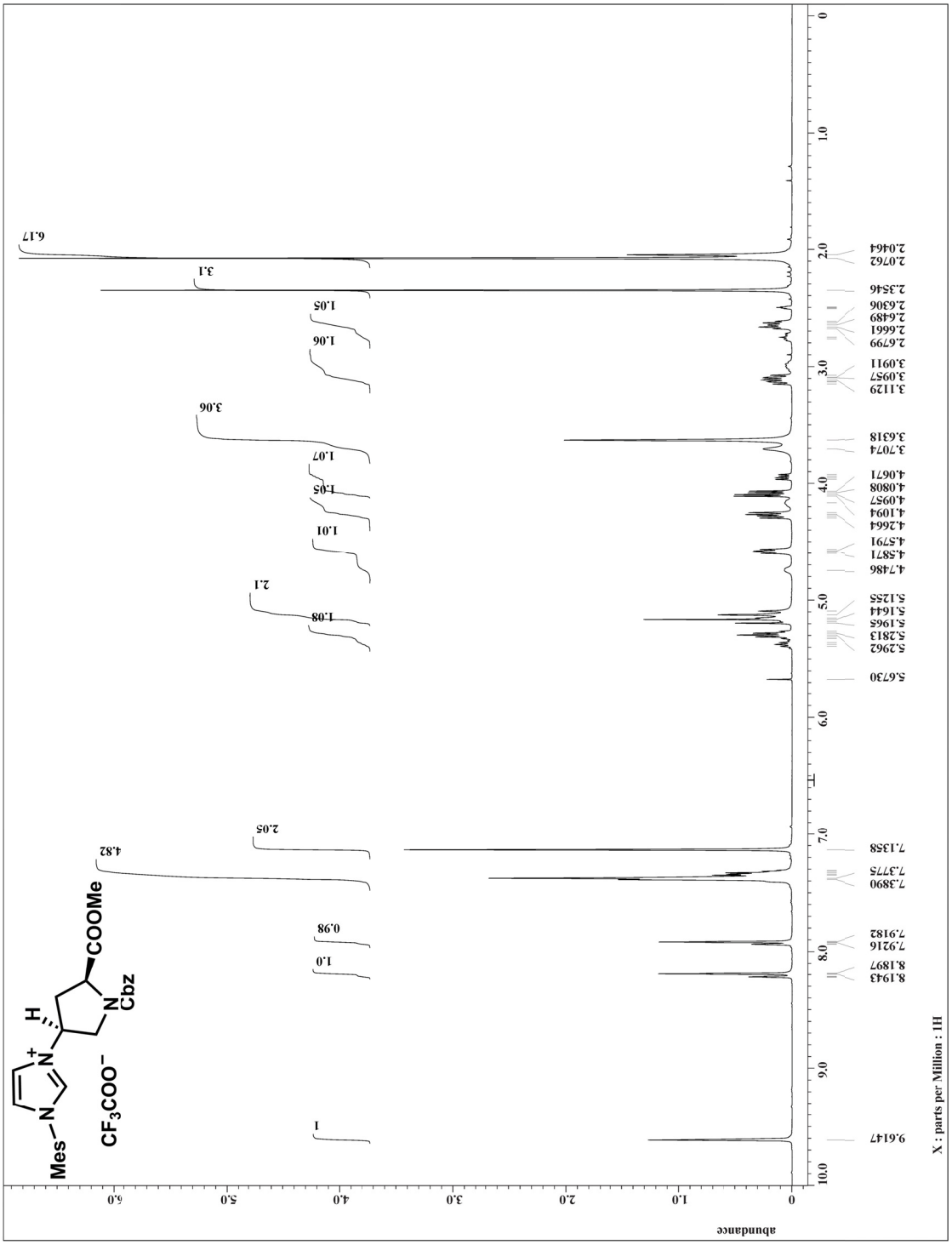

Figure 2.13: ^{1}H NMR (400 MHz, DMSO-*d*6, 353 K) of 3-((3*S*,5*S*)-1-(benzyloxycarbonyl)-5-(methoxycarbonyl)pyrrolidin-3-yl)-1-mesityl-1*H*-imidazol-3-ium trifluoroacetate (**2.25**, 4:1 mixture of diastereomers).

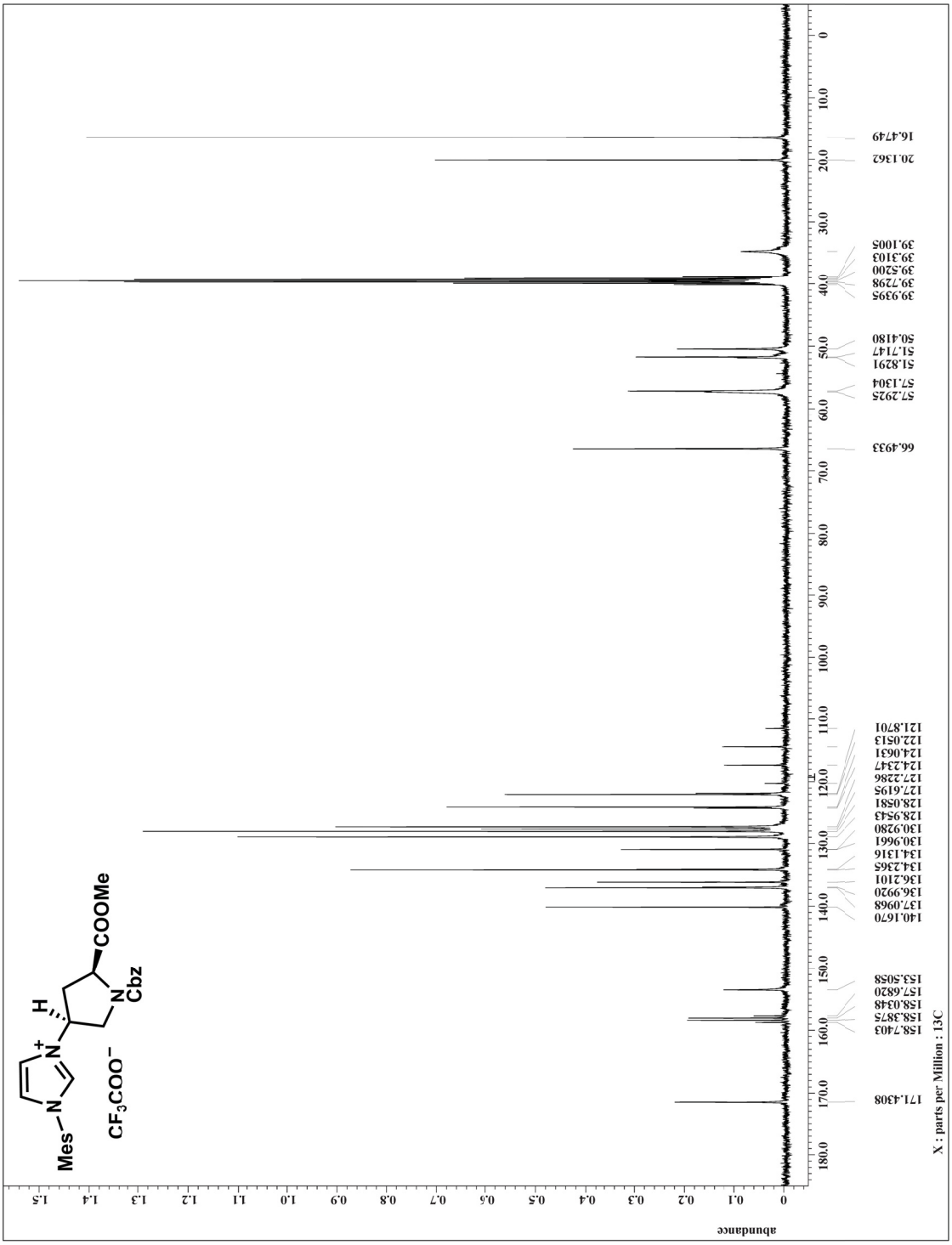

Figure 2.14: ^{13}C NMR (100 MHz, DMSO-*d*6, 353 K) of 3-((3*S*,5*S*)-1-(benzyloxycarbonyl)-5-(methoxycarbonyl)pyrrolidin-3-yl)-1-mesityl-1*H*-imidazol-3-ium trifluoroacetate (**2.25**, 4:1 mixture of diastereomers).

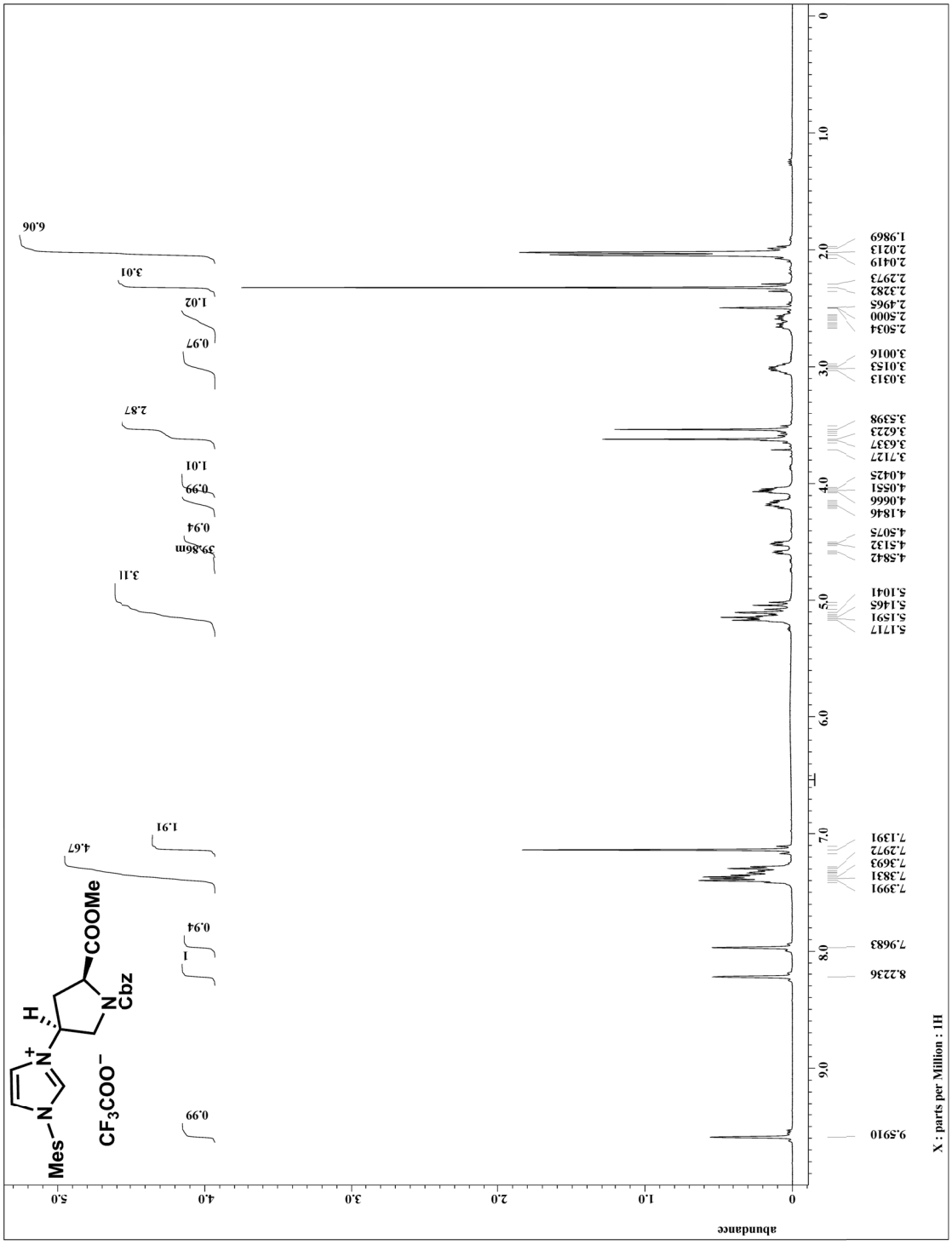

Figure 2.15: ^{1}H NMR (500 MHz, DMSO-*d*6, 293 K) of 3-((3*S*,5*S*)-1-(benzyloxycarbonyl)-5-(methoxycarbonyl)pyrrolidin-3-yl)-1-mesityl-1*H*-imidazol-3-ium trifluoroacetate (**2.25**, 20:1 mixture of diastereomers).

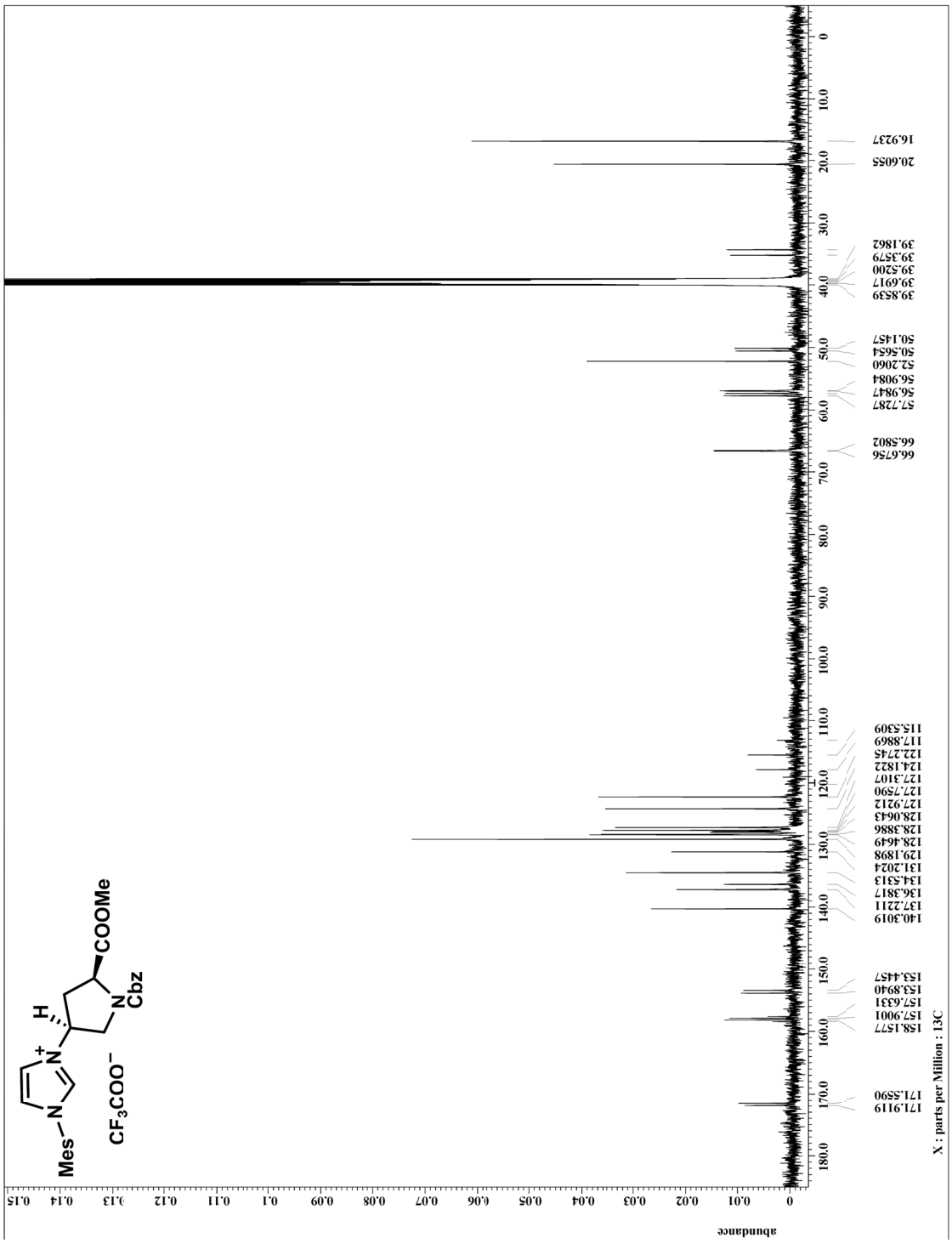

Figure 2.16: ^{13}C NMR (125 MHz, DMSO-*d*6, 293 K) of 3-((3*S*,5*S*)-1-(benzyloxycarbonyl)-5-(methoxycarbonyl)pyrrolidin-3-yl)-1-mesityl-1*H*-imidazol-3-ium trifluoroacetate (**2.25**, 20:1 mixture of diastereomers).

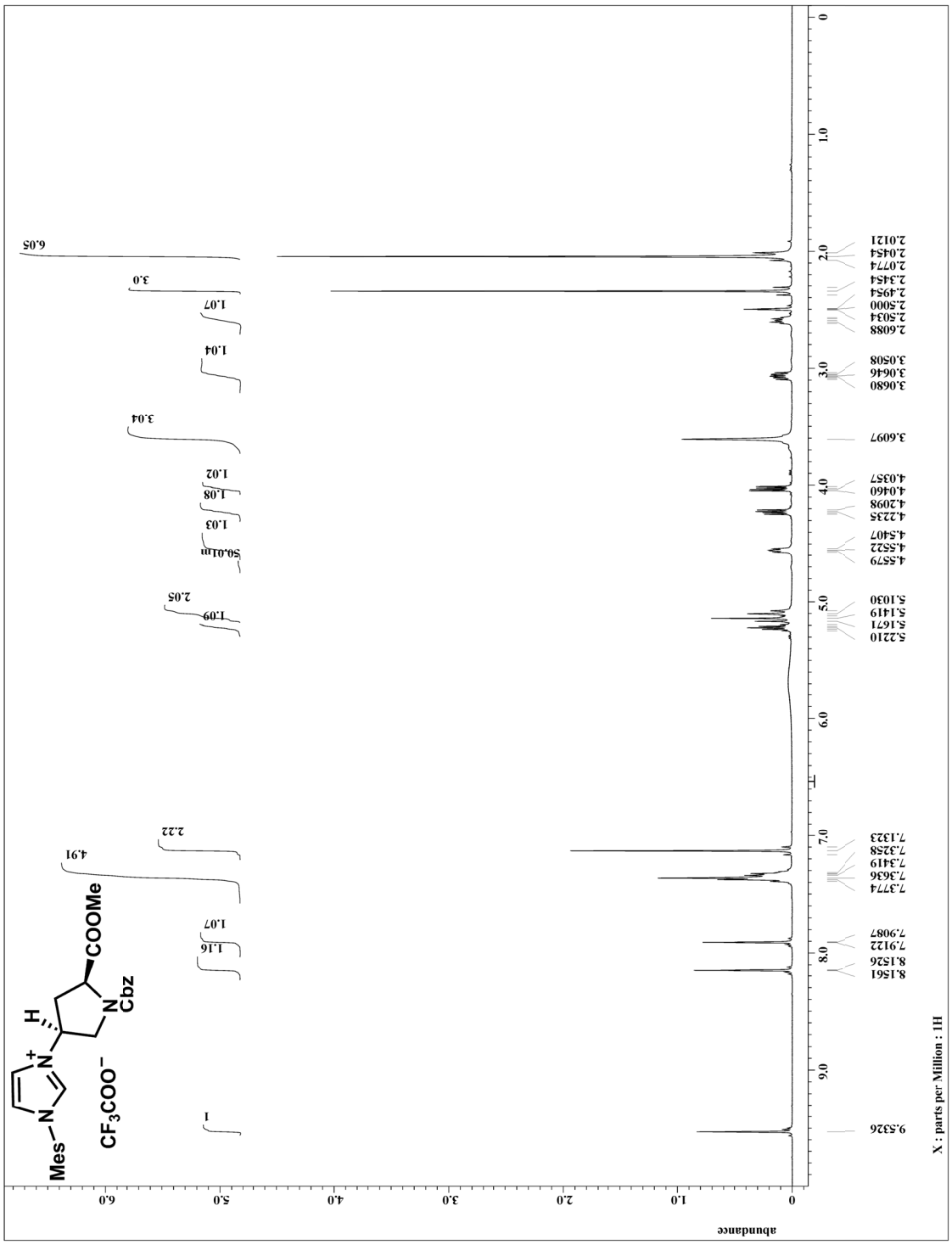

Figure 2.17: ^{1}H NMR (500 MHz, DMSO-*d*6, 353 K) of 3-((3*S*,5*S*)-1-(benzyloxycarbonyl)-5-(methoxycarbonyl)pyrrolidin-3-yl)-1-mesityl-1*H*-imidazol-3-ium trifluoroacetate (**2.25**, 20:1 mixture of diastereomers).

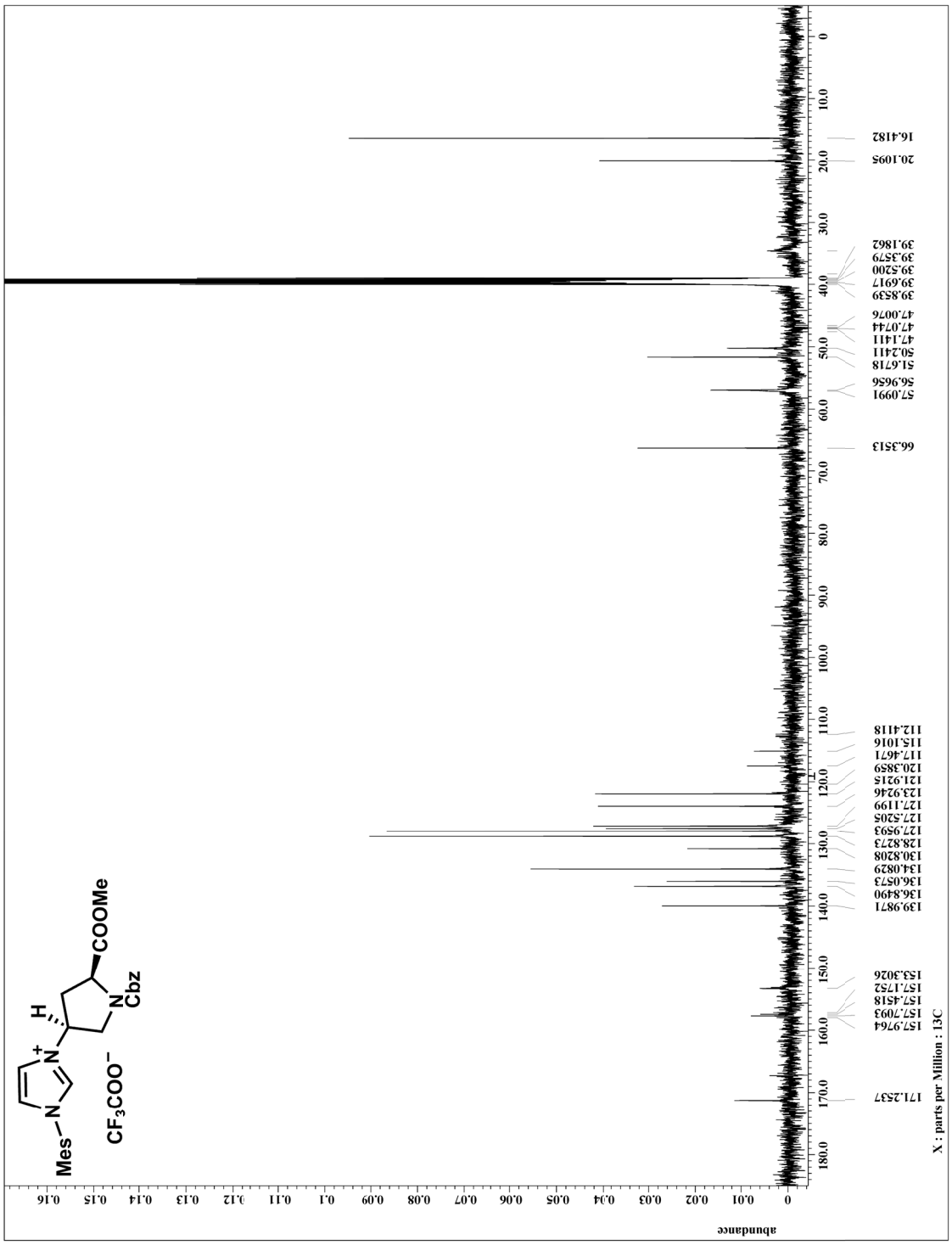

Figure 2.18: ^{13}C NMR (125 MHz, DMSO-*d*6, 353 K) of 3-((3*S*,5*S*)-1-(benzyloxycarbonyl)-5-(methoxycarbonyl)pyrrolidin-3-yl)-1-mesityl-1*H*-imidazol-3-ium trifluoroacetate (**2.25**, 20:1 mixture of diastereomers).

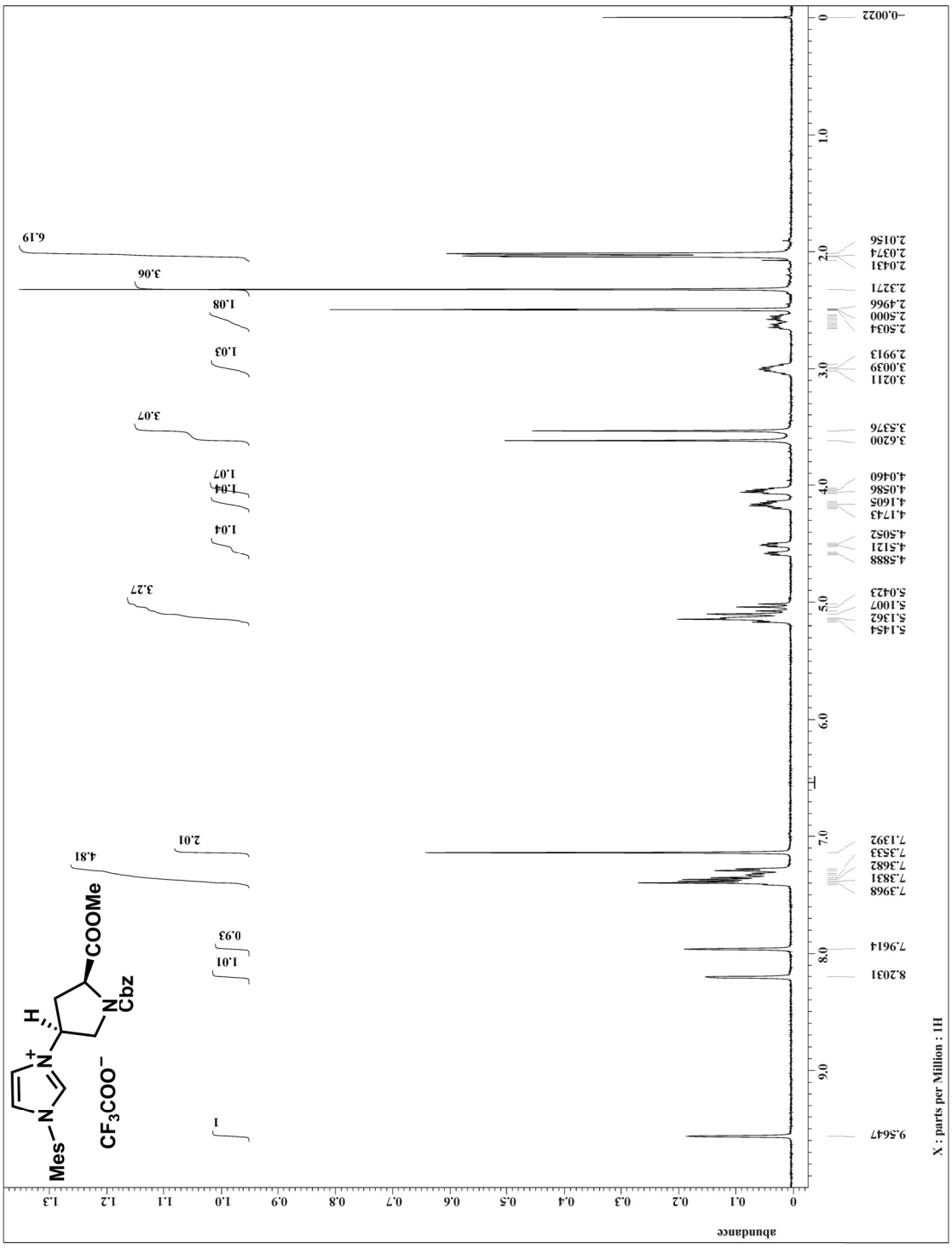

Figure 2.19: ^{1}H NMR (500 MHz, DMSO-*d*6, 293 K) of 3-((3*S*,5*S*)-1-(benzyloxycarbonyl)-5-(methoxycarbonyl)pyrrolidin-3-yl)-1-mesityl-1*H*-imidazol-3-ium trifluoroacetate (**2.25**).

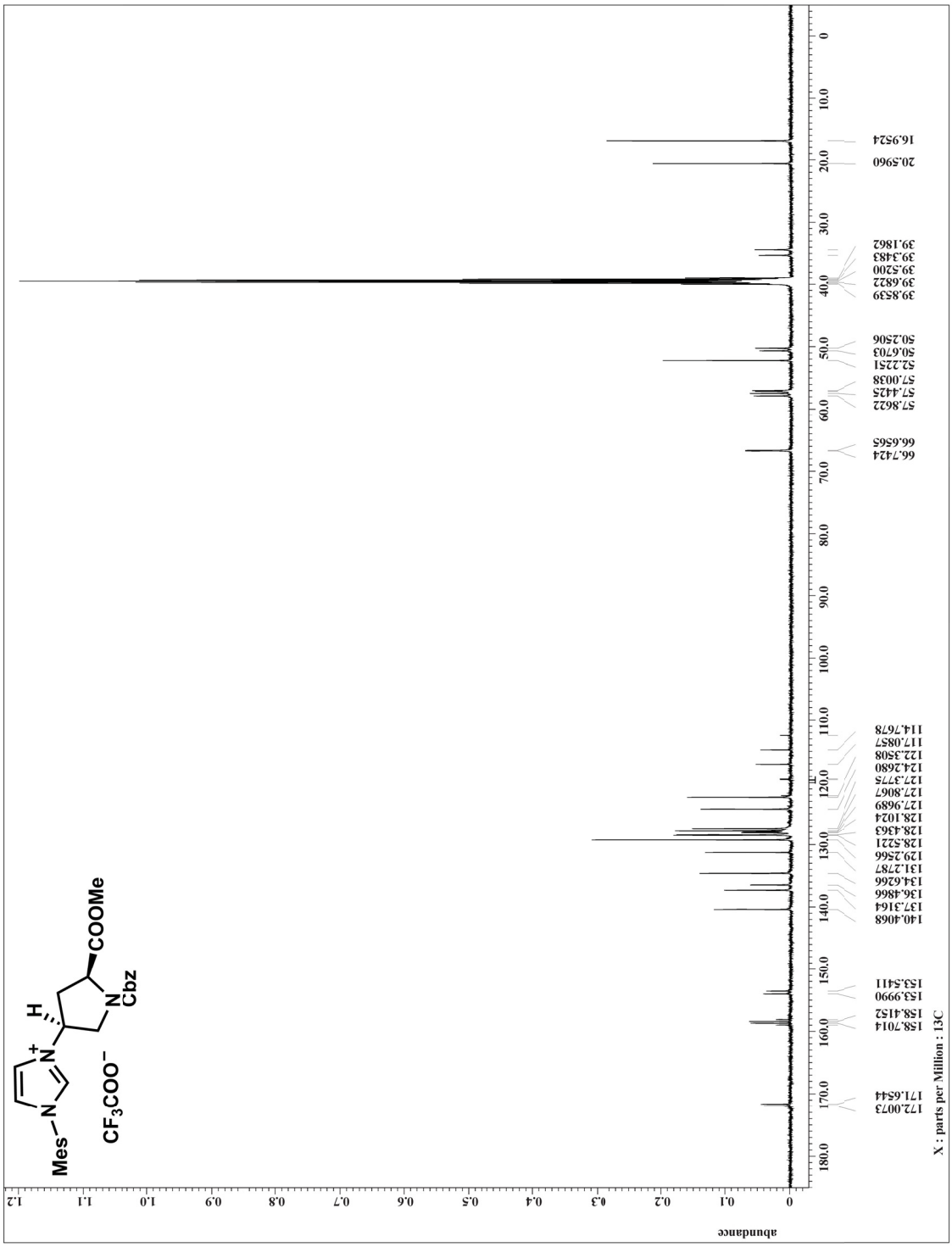

Figure 2.20: ^{13}C NMR (125 MHz, DMSO-*d*6, 293 K) of 3-((3*S*,5*S*)-1-(benzyloxycarbonyl)-5-(methoxycarbonyl)pyrrolidin-3-yl)-1-mesityl-1*H*-imidazol-3-ium trifluoroacetate (**2.25**).

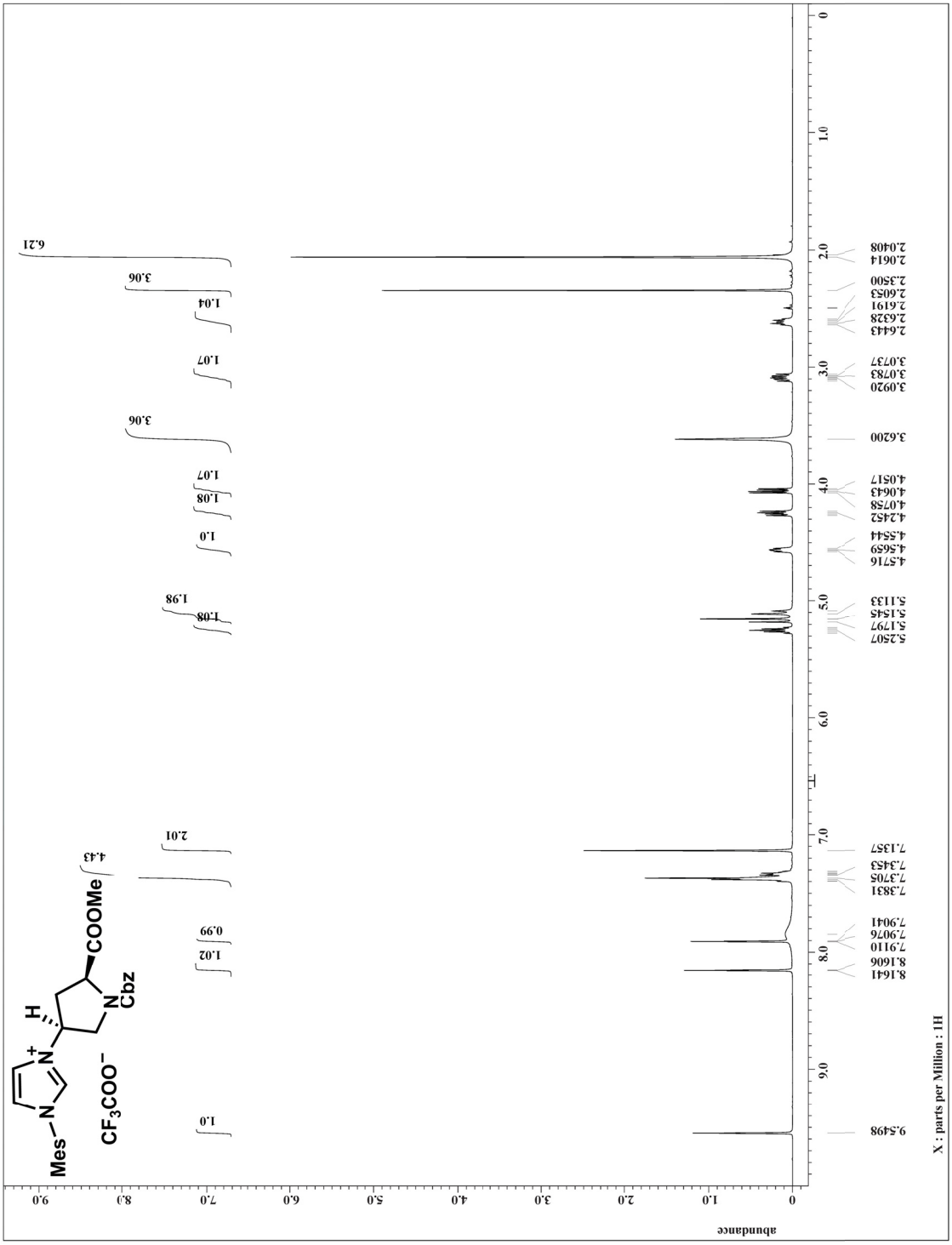

Figure 2.21: ^{1}H NMR (500 MHz, DMSO-*d*6, 353 K) of 3-((3*S*,5*S*)-1-(benzyloxycarbonyl)-5-(methoxycarbonyl)pyrrolidin-3-yl)-1-mesityl-1*H*-imidazol-3-ium trifluoroacetate (**2.25**).

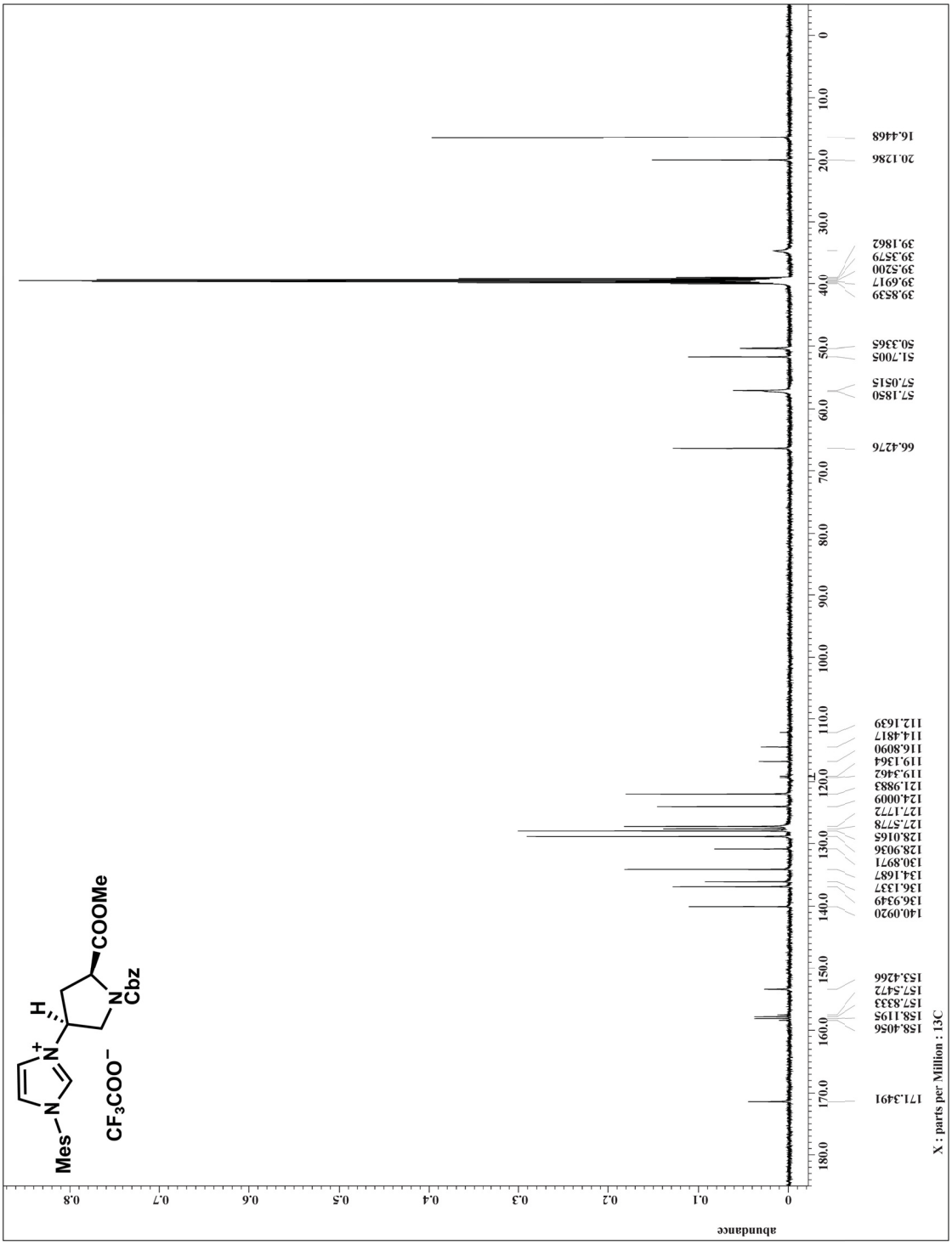

Figure 2.22: ^{13}C NMR (125 MHz, DMSO-*d*6, 353 K) of 3-((3*S*,5*S*)-1-(benzyloxycarbonyl)-5-(methoxycarbonyl)pyrrolidin-3-yl)-1-mesityl-1*H*-imidazol-3-ium trifluoroacetate (**2.25**).

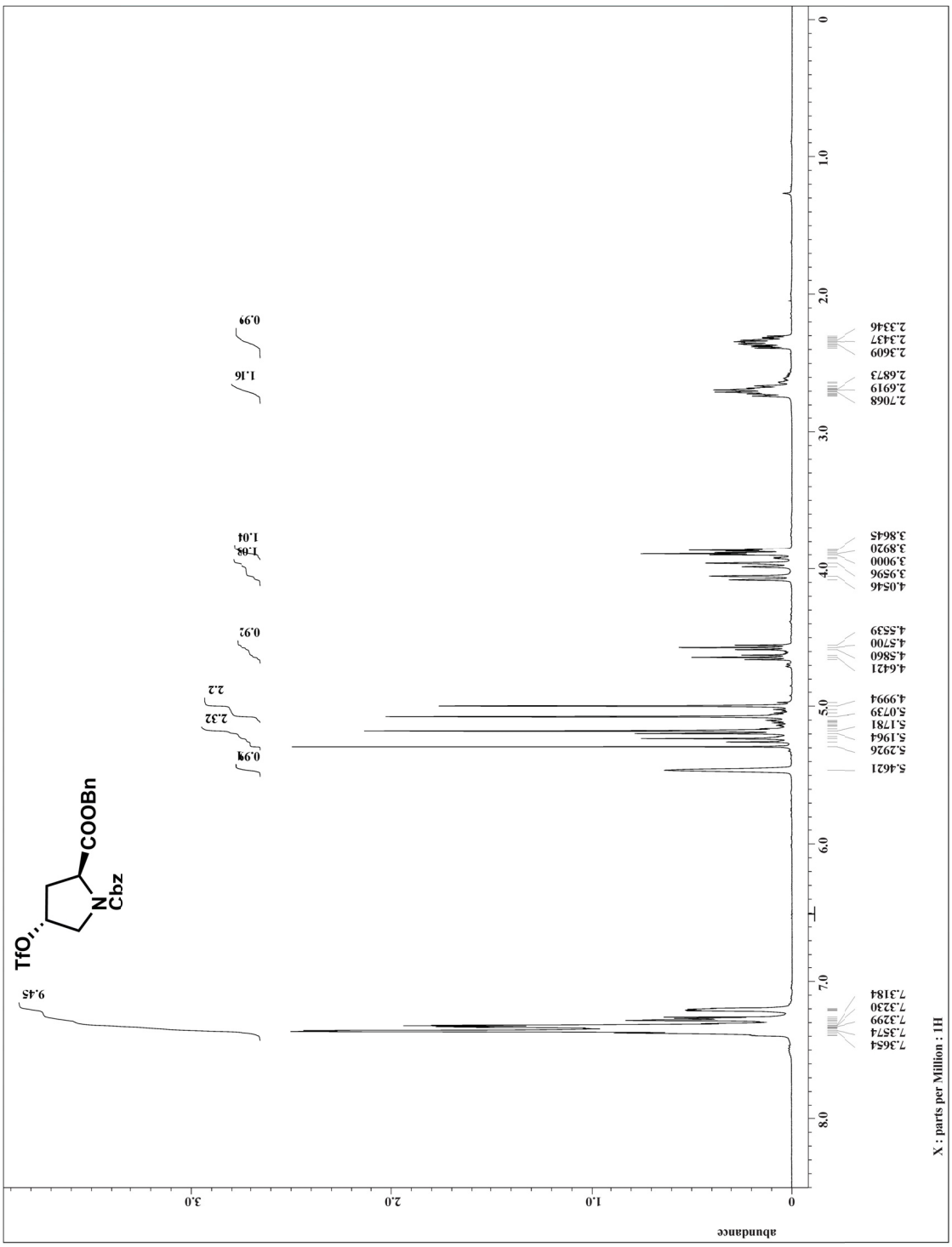

Figure 2.23: ^{1}H NMR (500 MHz, $CDCl_3$) of (2*S*,4*R*)-dibenzyl-4-(trifluoromethylsulfonyloxy)pyrrolidine-1,2-dicarboxylate (**2.27**).

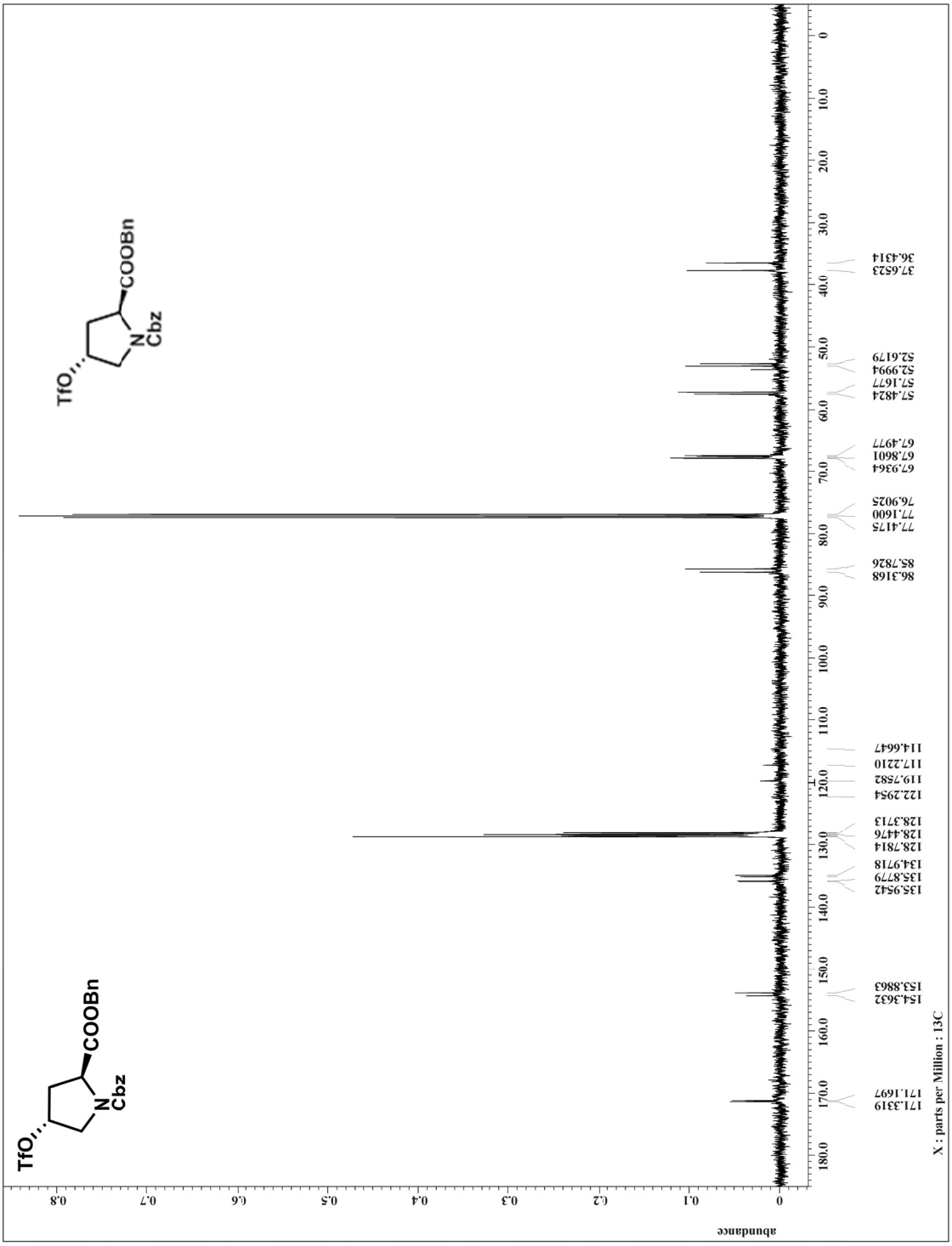

Figure 2.24: ^{13}C NMR (125 MHz, $CDCl_3$) of (2*S*,4*R*)-dibenzyl-4-(trifluoromethylsulfonyloxy)pyrrolidine-1,2-dicarboxylate (**2.27**).

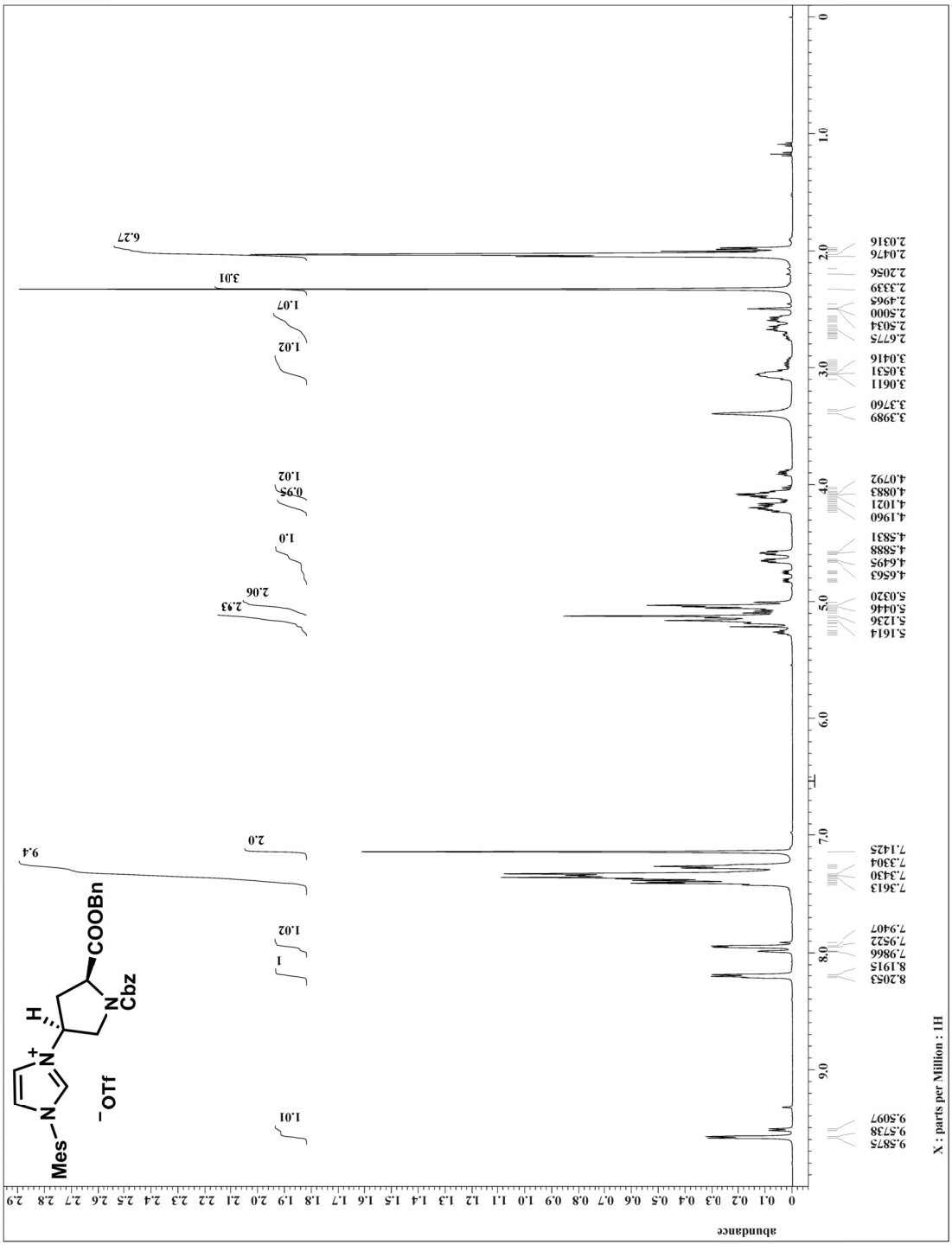

Figure 2.25: ^{1}H NMR (500 MHz, DMSO-*d*6, 293 K) of 3-((3*S*,5*S*)-1,5-bis(benzyloxycarbonyl)pyrrolidin-3-yl)-1-mesityl-1*H*-imidazol-3-ium trifluoromethanesulfonate (**2.28**, 4:1 mixture of diastereomers).

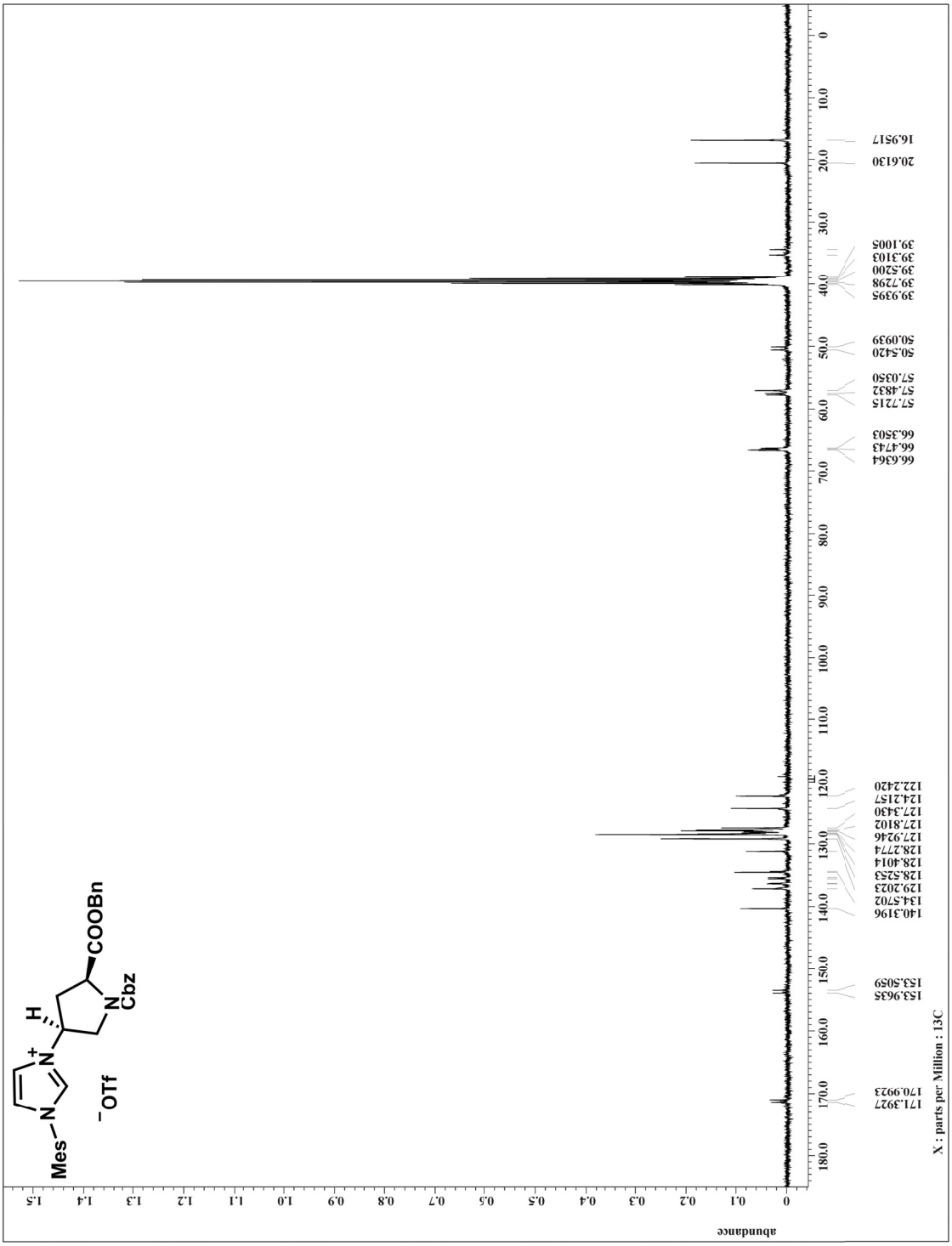

Figure 2.26: ^{13}C NMR (100 MHz, DMSO-*d*6, 293 K) of 3-((3*S*,5*S*)-1,5-bis(benzyloxycarbonyl)pyrrolidin-3-yl)-1-mesityl-1*H*-imidazol-3-ium trifluoromethanesulfonate (**2.28**, 4:1 mixture of diastereomers).

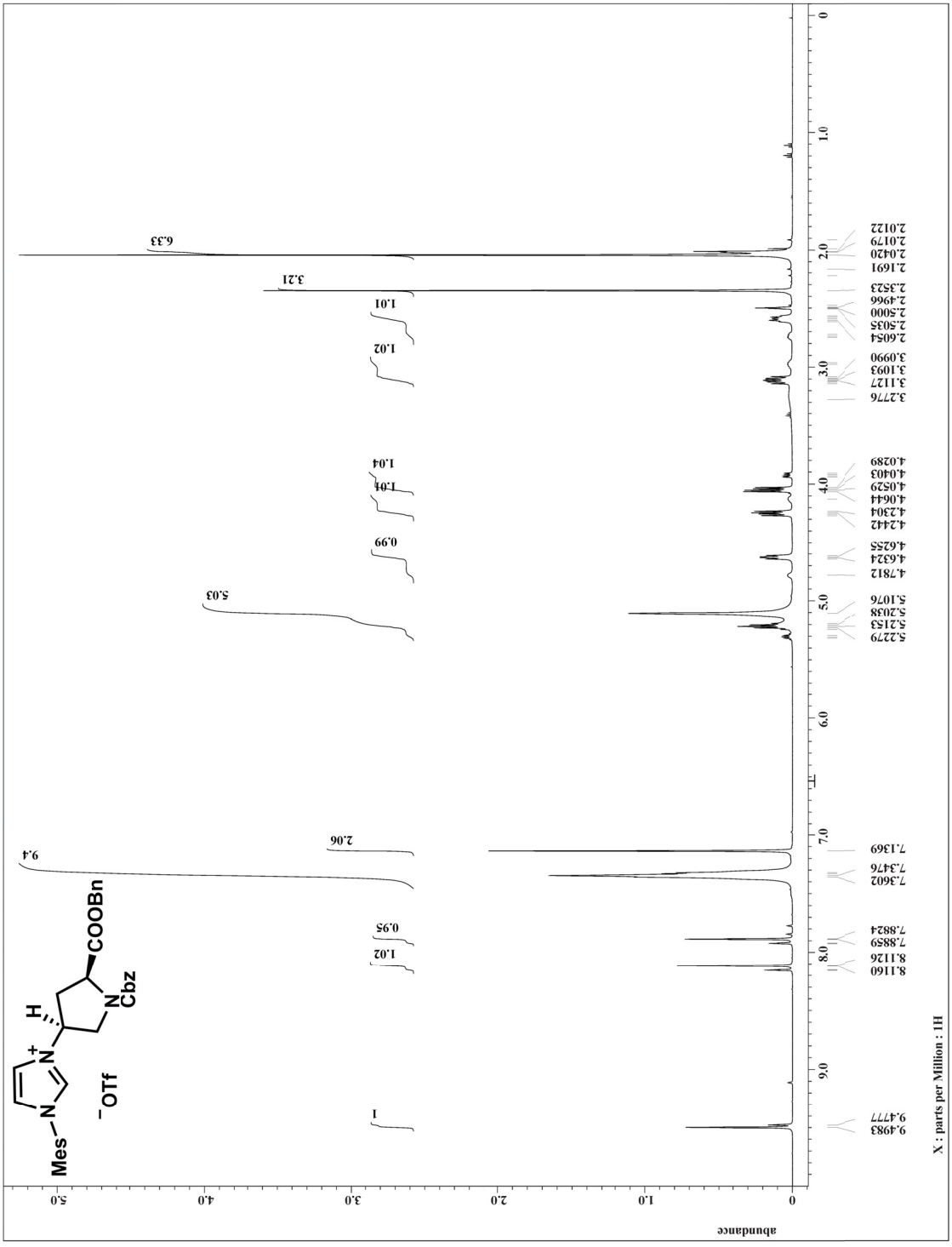

Figure 2.27: ^{1}H NMR (500 MHz, DMSO-*d*6, 353 K) of 3-((3*S*,5*S*)-1,5-bis(benzyloxycarbonyl)pyrrolidin-3-yl)-1-mesityl-1*H*-imidazol-3-ium trifluoromethanesulfonate (**2.28**, 4:1 mixture of diastereomers).

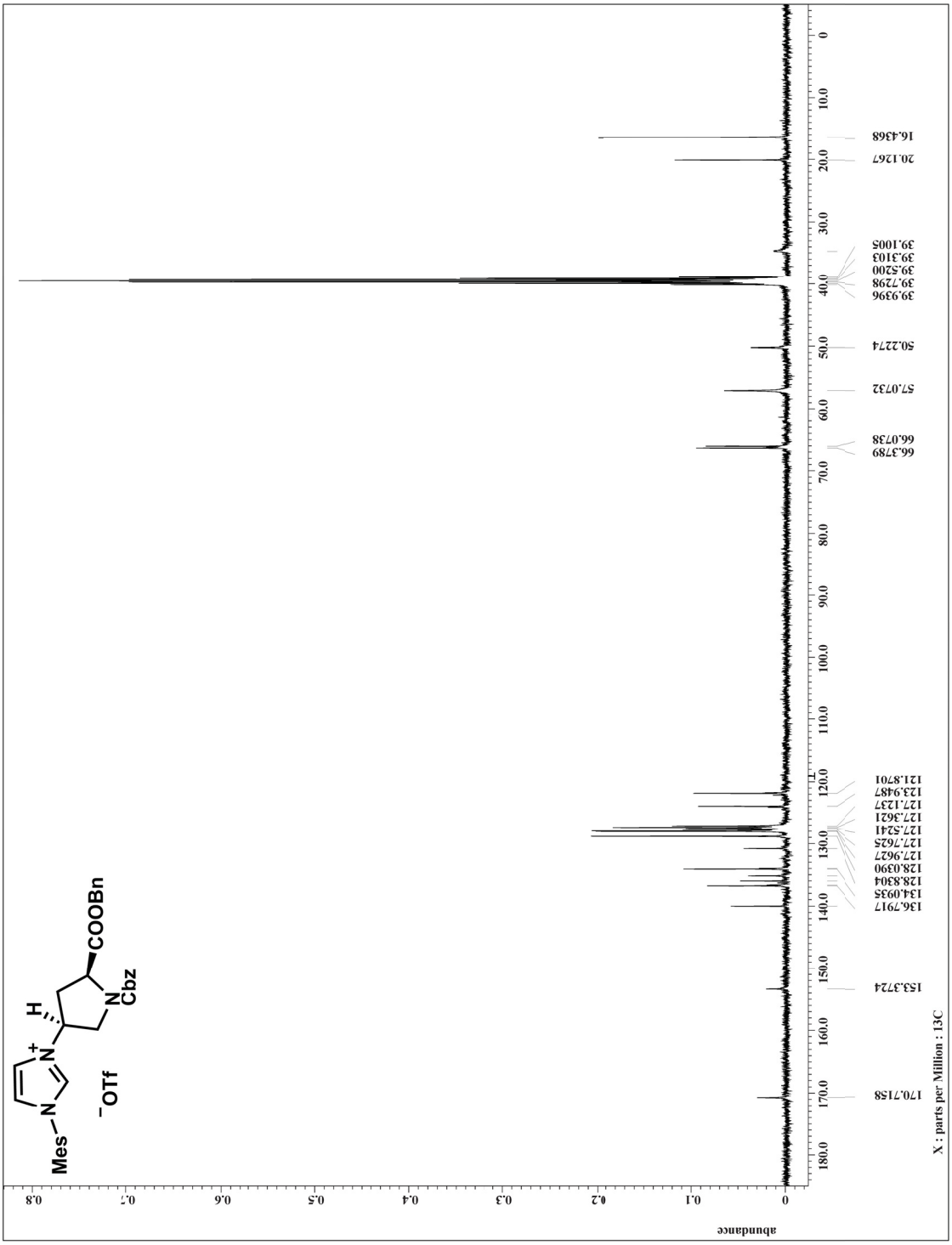

Figure 2.28: ^{13}C NMR (100 MHz, DMSO-*d*6, 353 K) of 3-((3*S*,5*S*)-1,5-bis(benzyloxycarbonyl)pyrrolidin-3-yl)-1-mesityl-1*H*-imidazol-3-ium trifluoromethanesulfonate (**2.28**, 4:1 mixture of diastereomers).

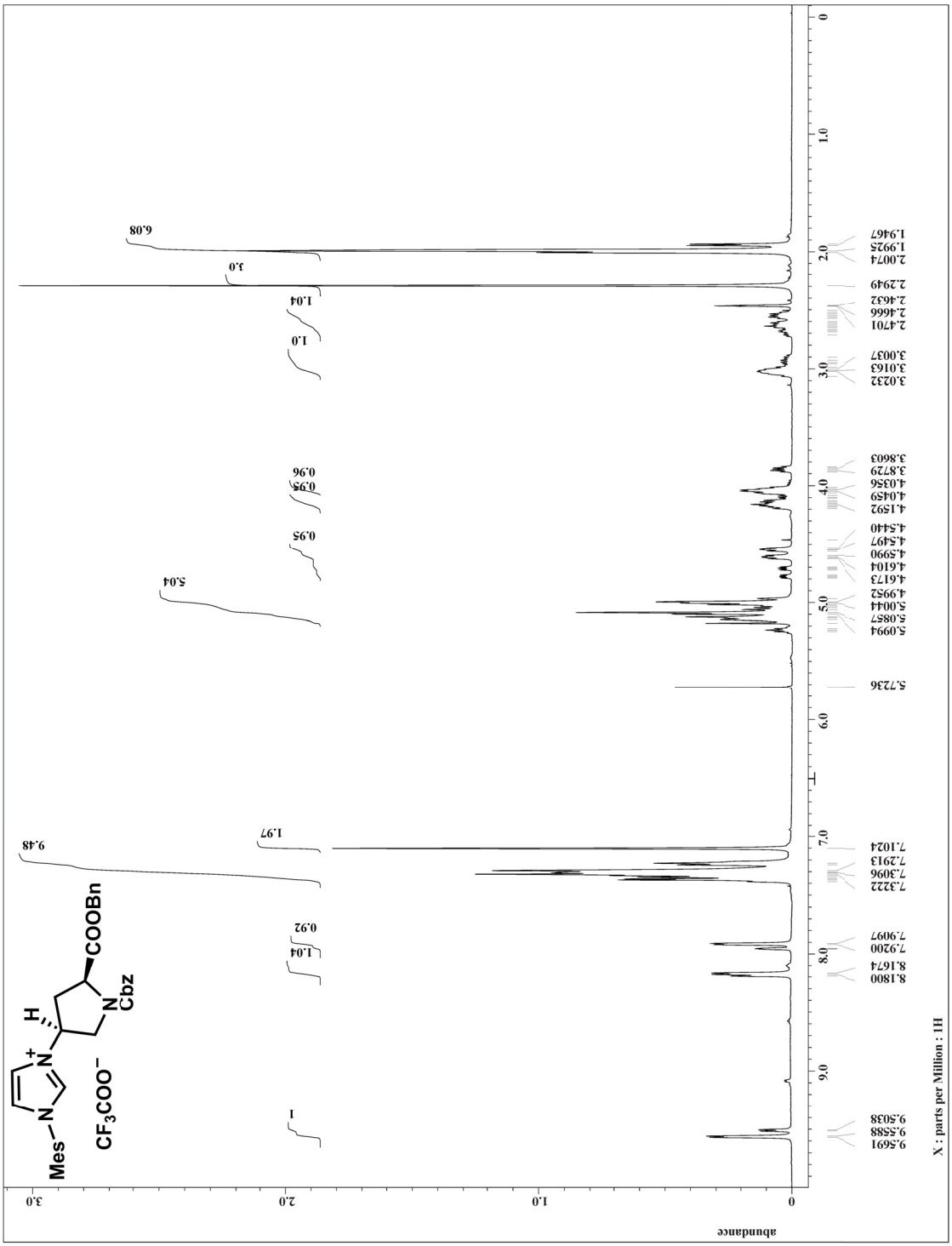

Figure 2.29: ^{1}H NMR (500 MHz, DMSO-*d*6, 293 K) of 3-((3*S*,5*S*)-1,5-bis(benzyloxycarbonyl)pyrrolidin-3-yl)-1-mesityl-1*H*-imidazol-3-ium trifluoroacetate (**2.29**, 4:1 mixture of diastereomers).

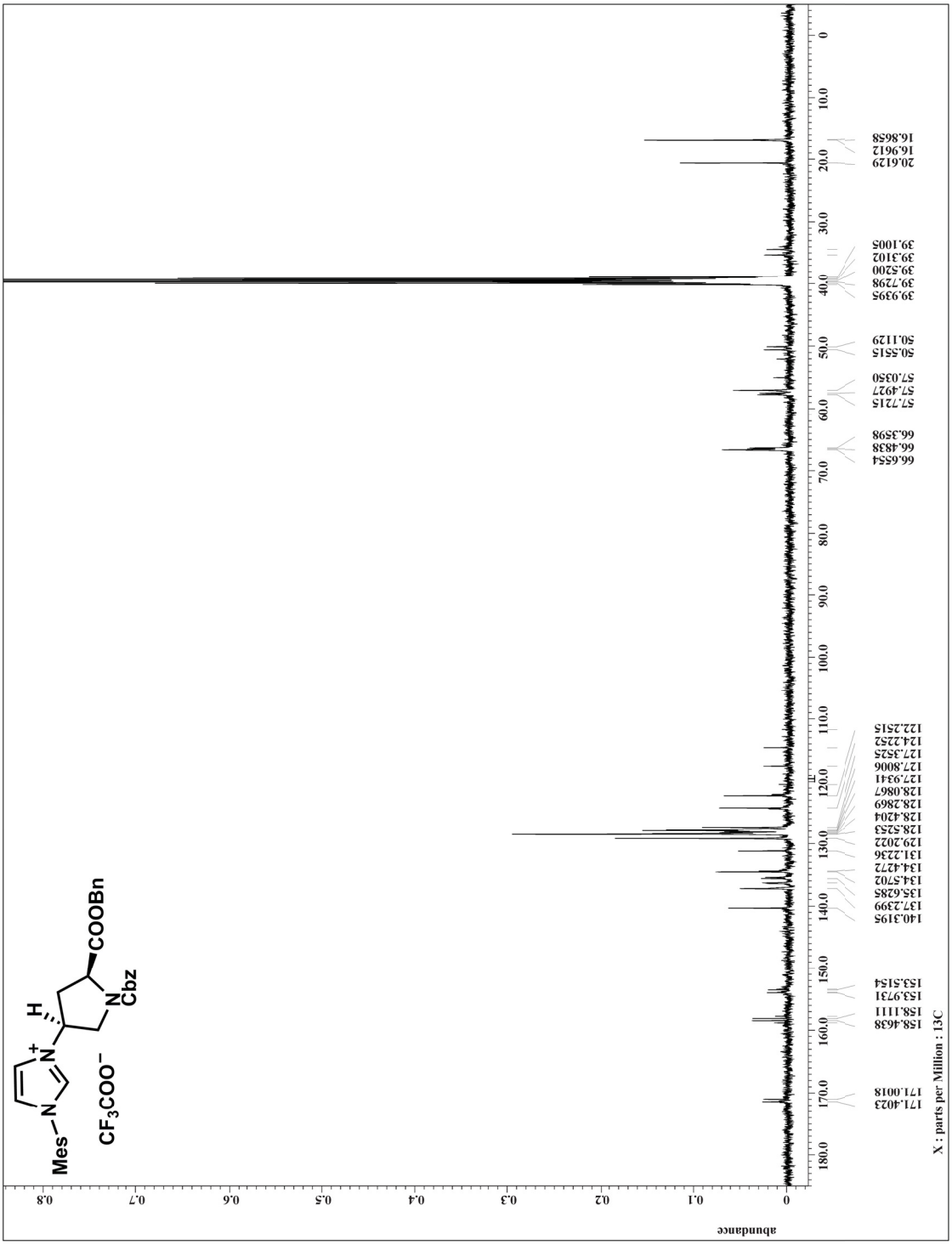

Figure 2.30: ^{13}C NMR (100 MHz, DMSO-*d*6, 293 K) of 3-((3*S*,5*S*)-1,5-bis(benzyloxycarbonyl)pyrrolidin-3-yl)-1-mesityl-1*H*-imidazol-3-ium trifluoroacetate (**2.29**, 4:1 mixture of diastereomers).

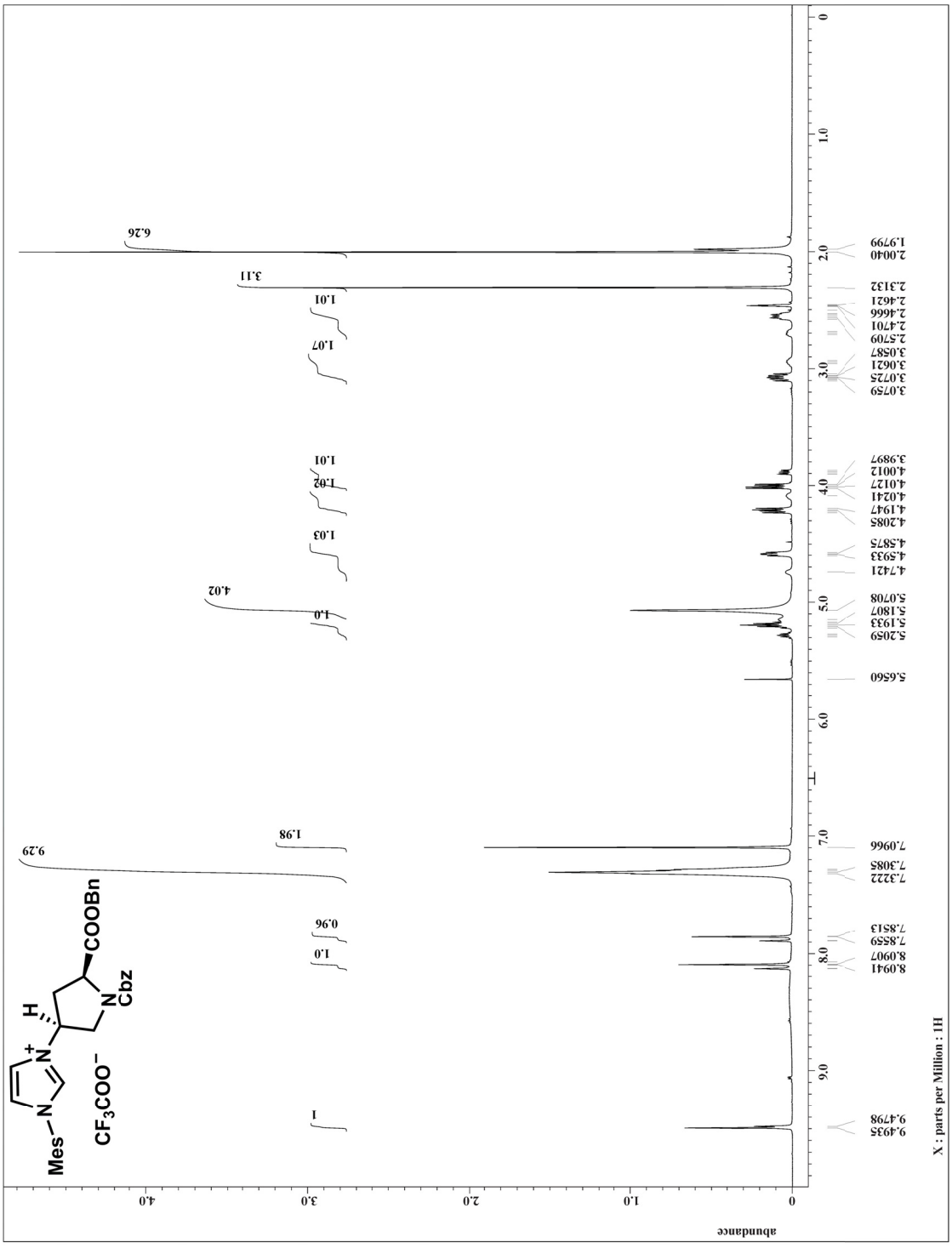

Figure 2.31: ^{1}H NMR (500 MHz, DMSO-*d*6, 353 K) of 3-((3*S*,5*S*)-1,5-bis(benzyloxycarbonyl)pyrrolidin-3-yl)-1-mesityl-1*H*-imidazol-3-ium trifluoroacetate (**2.29**, 4:1 mixture of diastereomers).

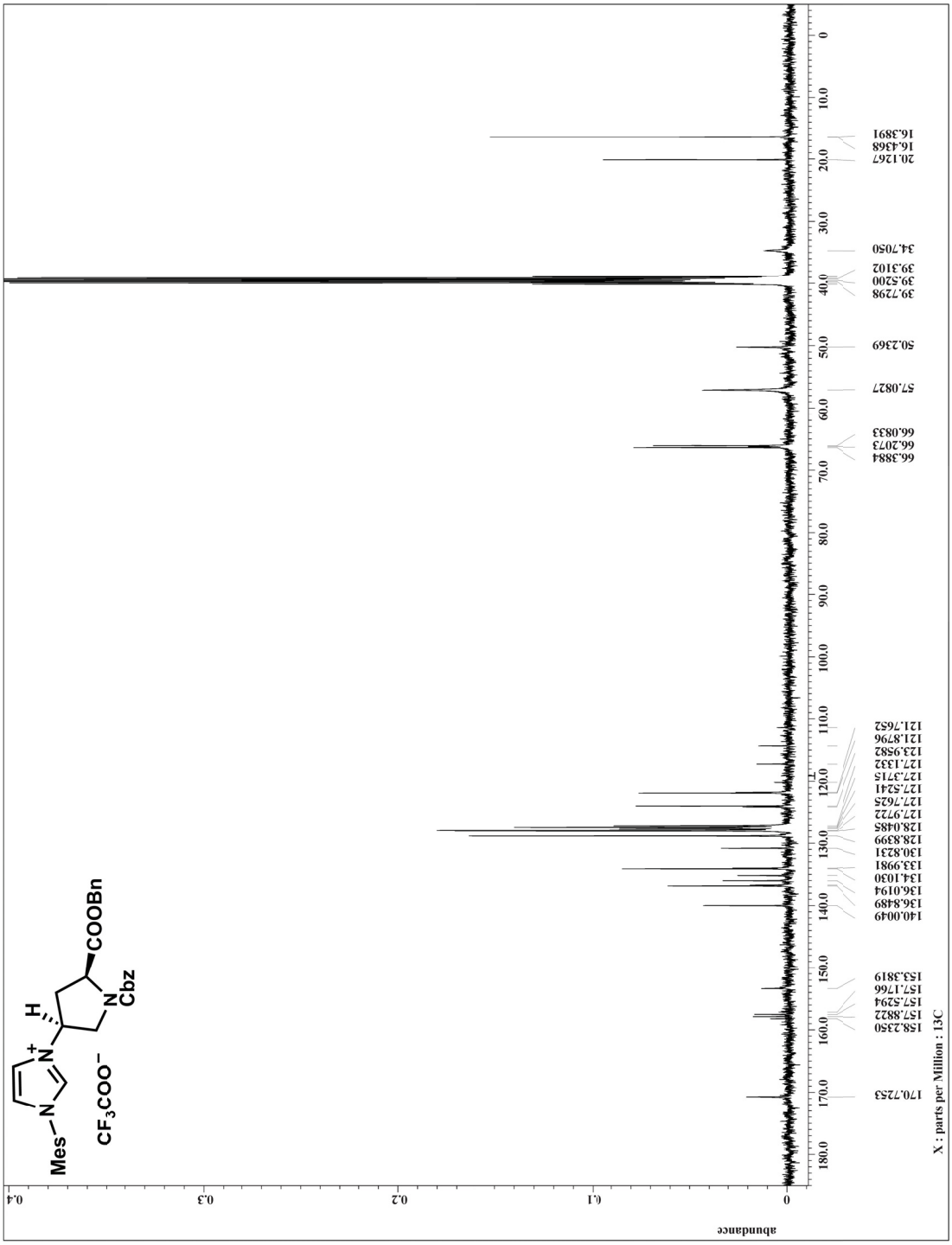

Figure 2.32: ^{13}C NMR (100 MHz, DMSO-*d*6, 353 K) of 3-((3*S*,5*S*)-1,5-bis(benzyloxycarbonyl)pyrrolidin-3-yl)-1-mesityl-1*H*-imidazol-3-ium trifluoroacetate (**2.29**, 4:1 mixture of diastereomers).

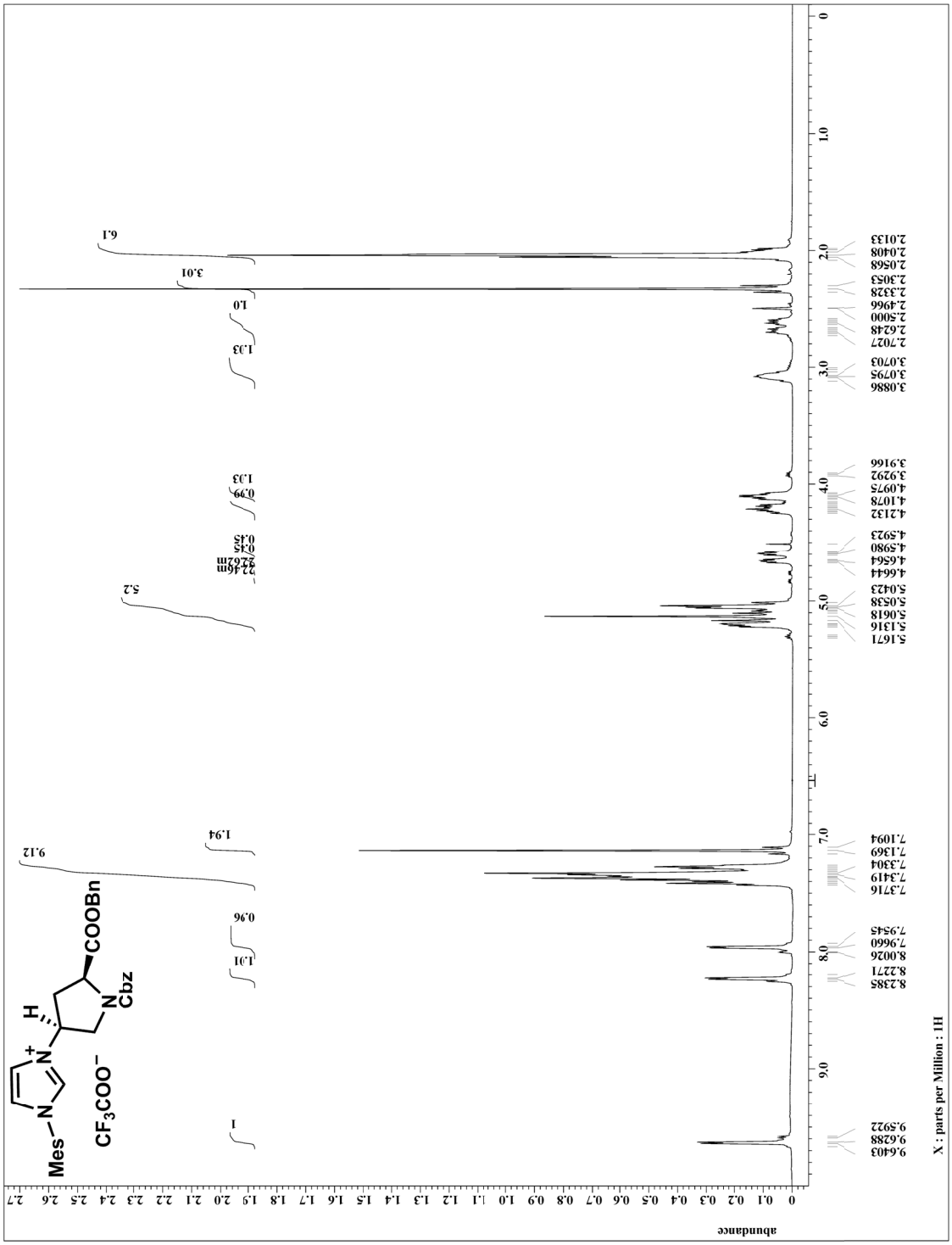

Figure 2.33: ^{1}H NMR (500 MHz, DMSO-*d*6, 293 K) of 3-((3*S*,5*S*)-1,5-bis(benzyloxycarbonyl)pyrrolidin-3-yl)-1-mesityl-1*H*-imidazol-3-ium trifluoroacetate (**2.29**, 20:1 mixture of diastereomers).

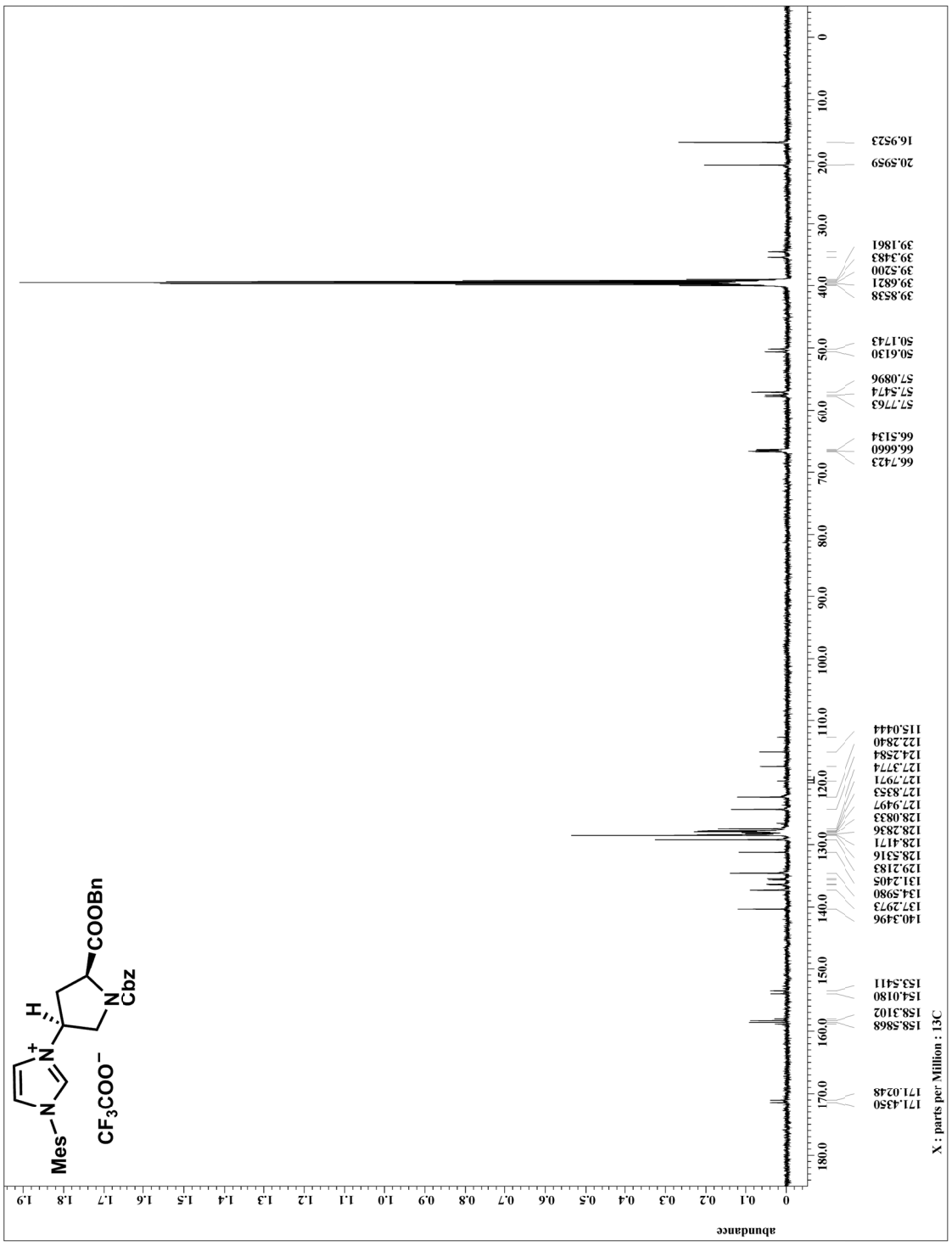

Figure 2.34: ^{13}C NMR (125 MHz, DMSO-*d*6, 293 K) of 3-((3*S*,5*S*)-1,5-bis(benzyloxycarbonyl)pyrrolidin-3-yl)-1-mesityl-1*H*-imidazol-3-ium trifluoroacetate (**2.29**, 20:1 mixture of diastereomers).

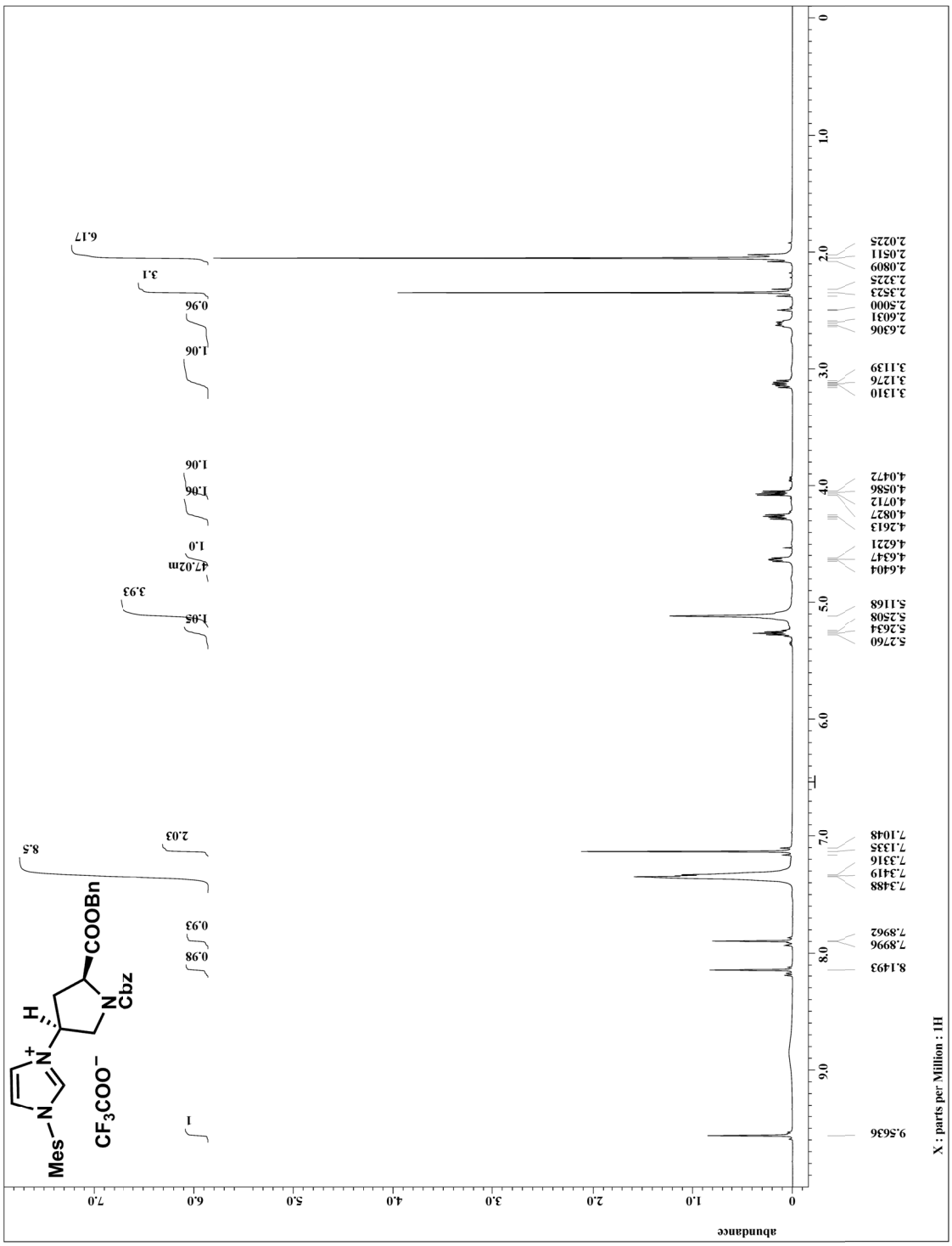

Figure 2.35: ^{1}H NMR (500 MHz, DMSO-*d*6, 353 K) of 3-((3*S*,5*S*)-1,5-bis(benzyloxycarbonyl)pyrrolidin-3-yl)-1-mesityl-1*H*-imidazol-3-ium trifluoroacetate (**2.29**, 20:1 mixture of diastereomers).

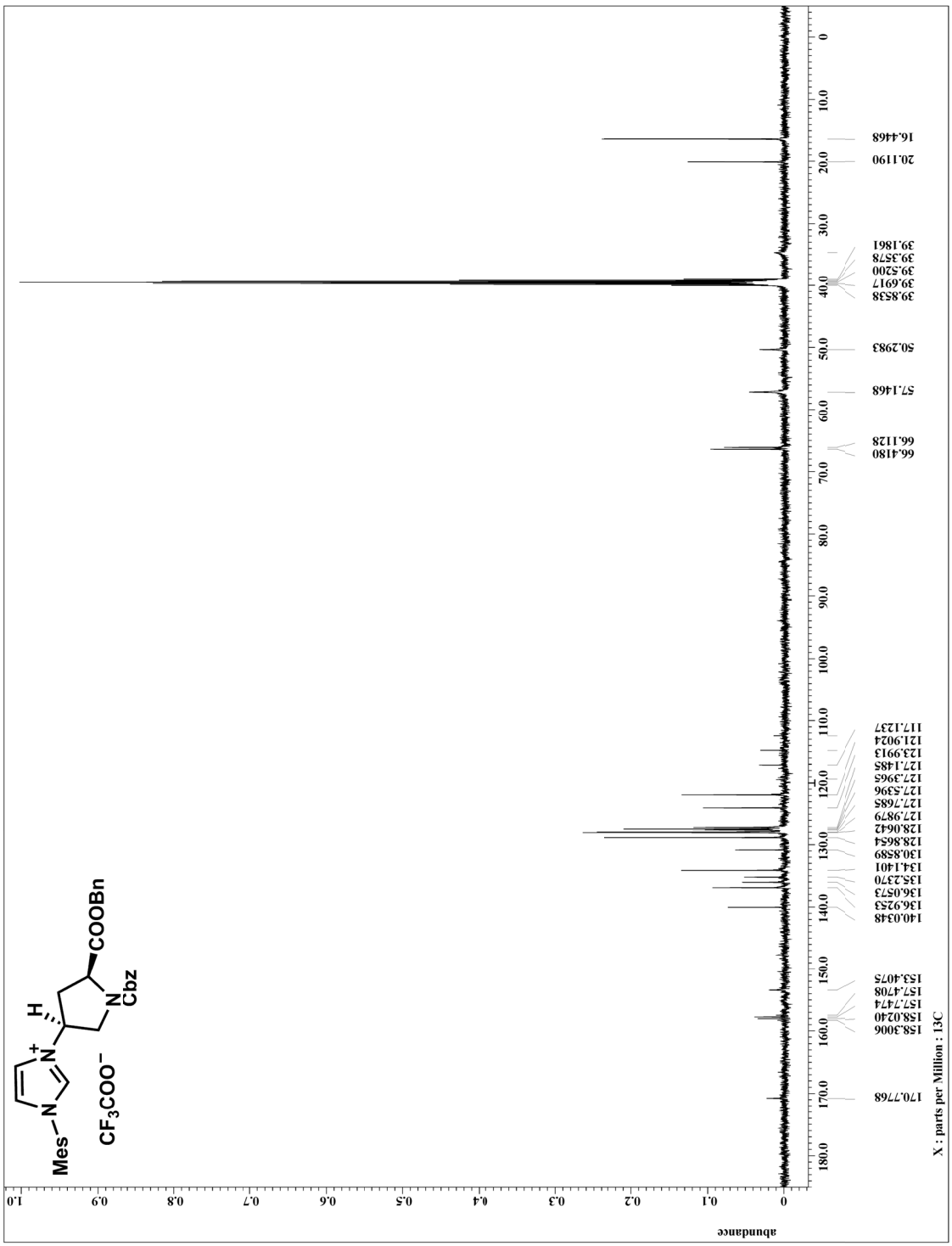

Figure 2.36: ^{13}C NMR (125 MHz, DMSO-*d*6, 353 K) of 3-((3*S*,5*S*)-1,5-bis(benzyloxycarbonyl)pyrrolidin-3-yl)-1-mesityl-1*H*-imidazol-3-ium trifluoroacetate (**2.29**, 20:1 mixture of diastereomers).

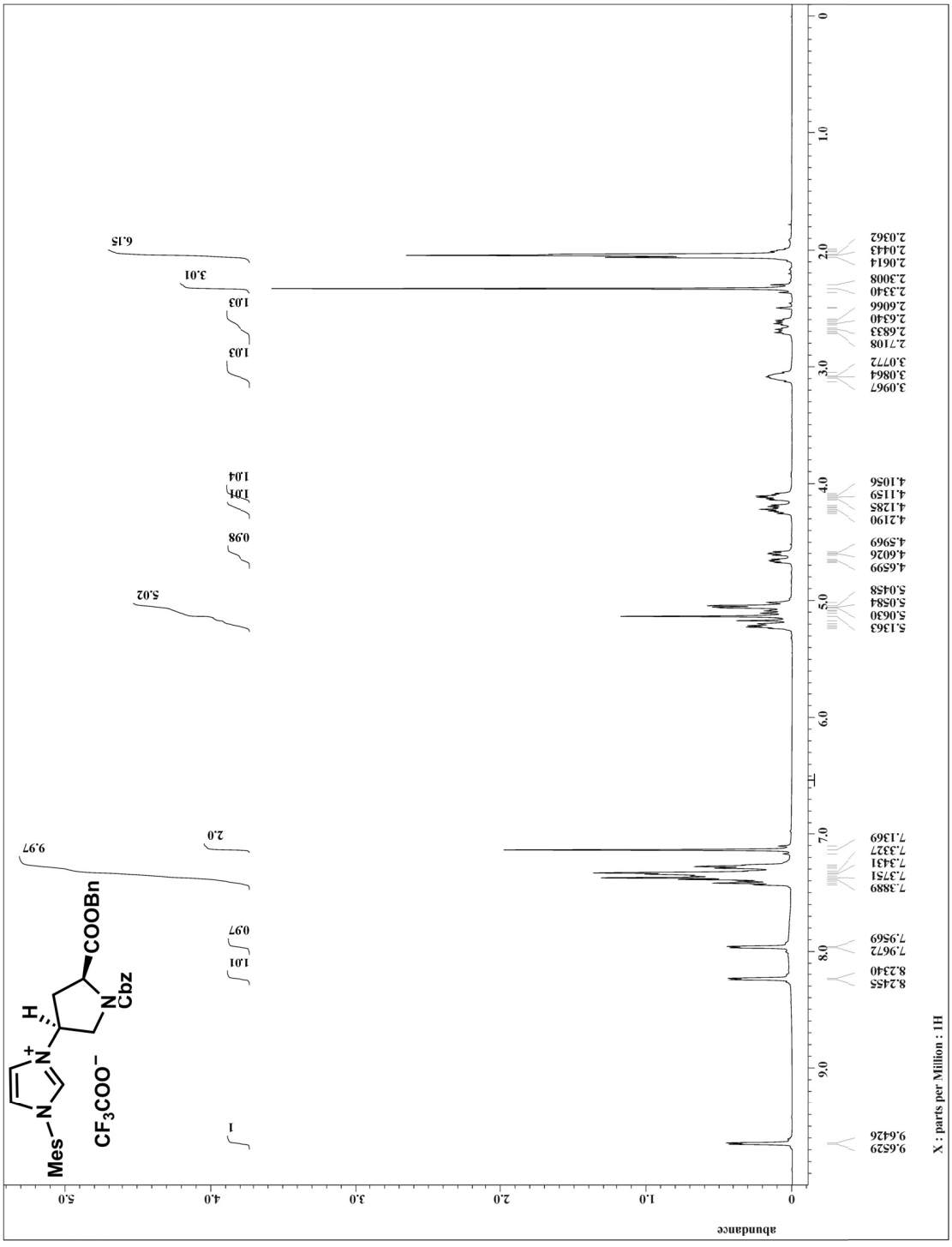

Figure 2.37: ^{1}H NMR (500 MHz, DMSO-*d*6, 293 K) of 3-((3*S*,5*S*)-1,5-bis(benzyloxycarbonyl)pyrrolidin-3-yl)-1-mesityl-1*H*-imidazol-3-ium trifluoroacetate (**2.29**).

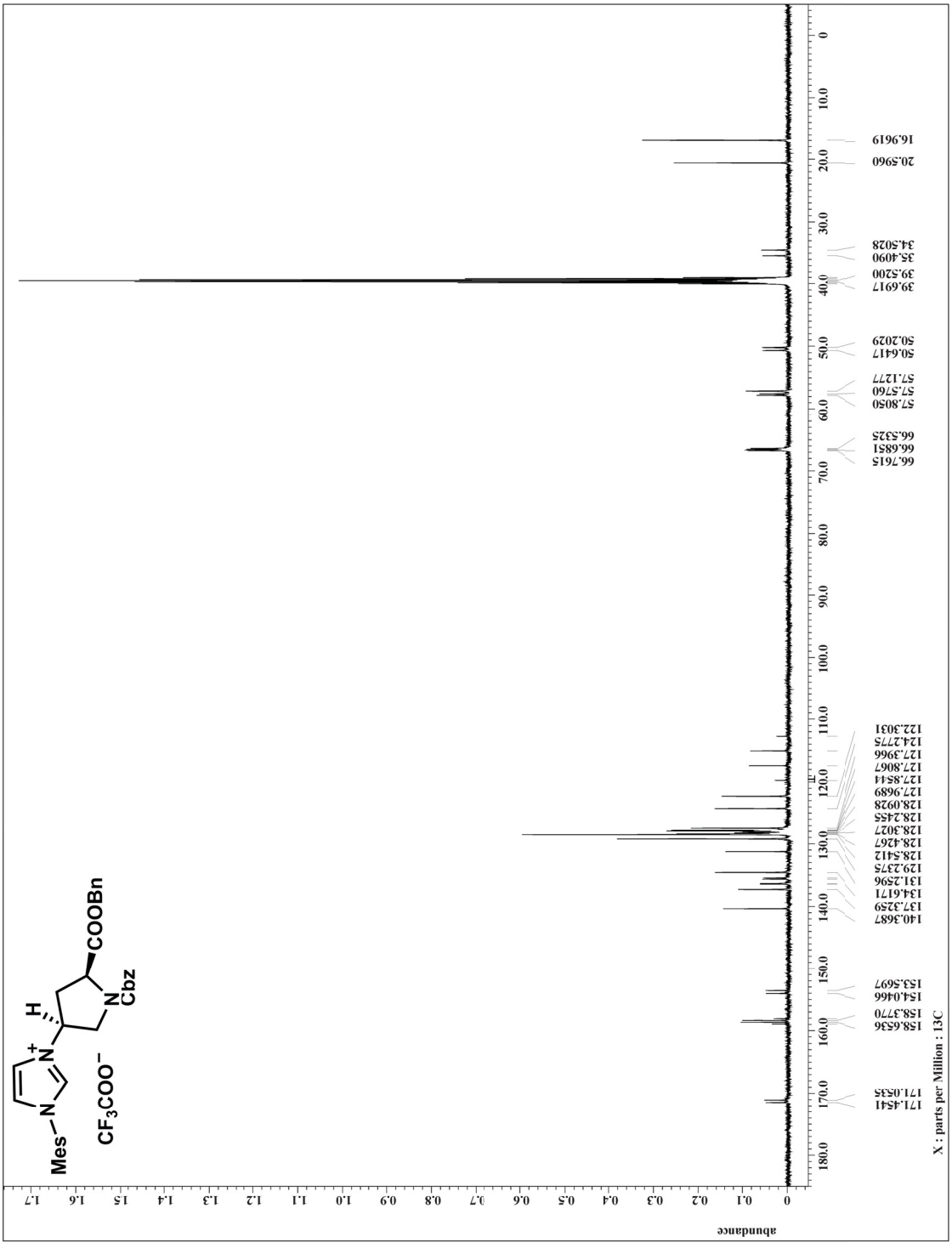

Figure 2.38: ^{13}C NMR (125 MHz, DMSO-*d*6, 293 K) of 3-((3*S*,5*S*)-1,5-bis(benzyloxycarbonyl)pyrrolidin-3-yl)-1-mesityl-1*H*-imidazol-3-ium trifluoroacetate (**2.29**).

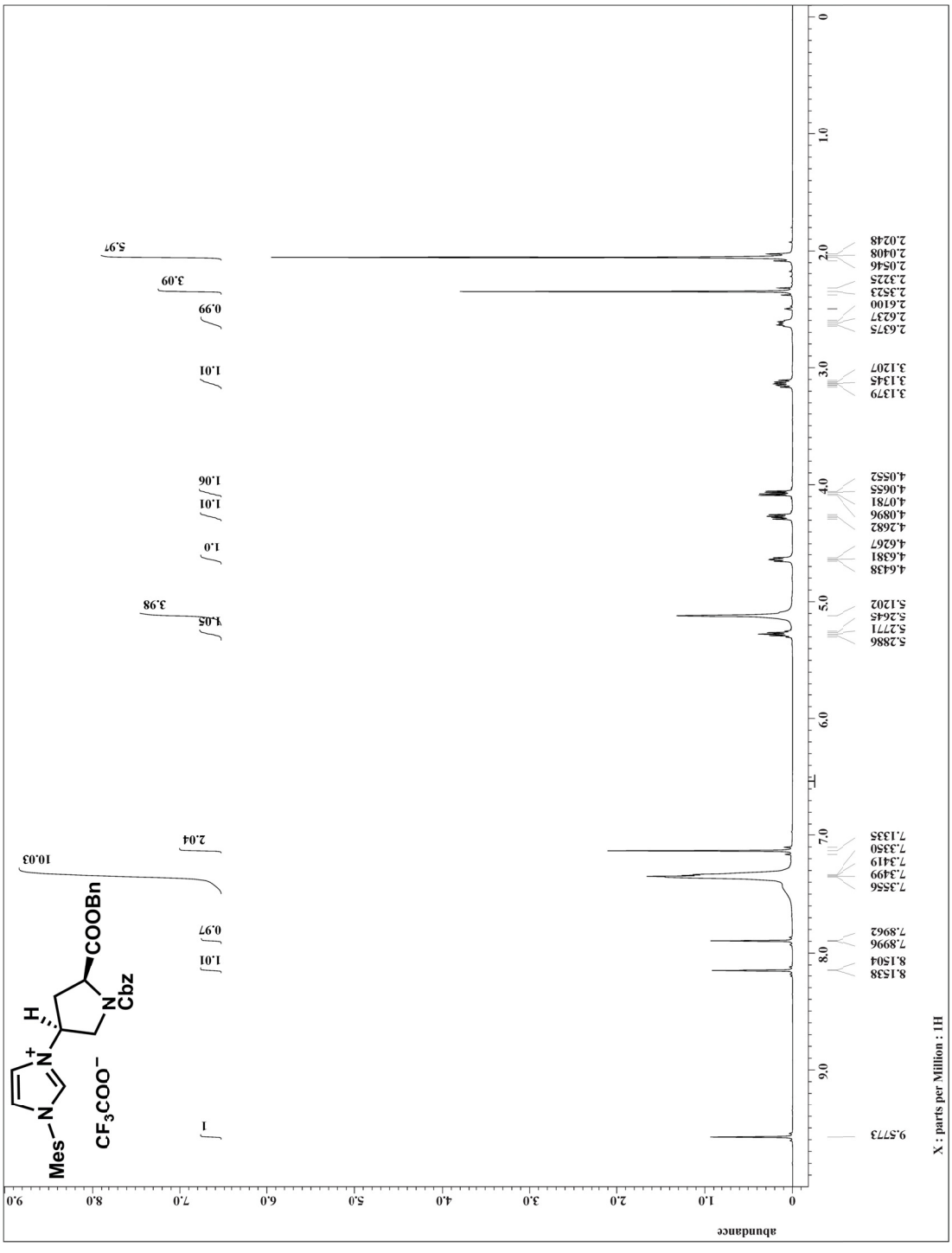

Figure 2.39: ^{1}H NMR (500 MHz, DMSO-*d*6, 353 K) of 3-((3*S*,5*S*)-1,5-bis(benzyloxycarbonyl)pyrrolidin-3-yl)-1-mesityl-1*H*-imidazol-3-ium trifluoroacetate (**2.29**).

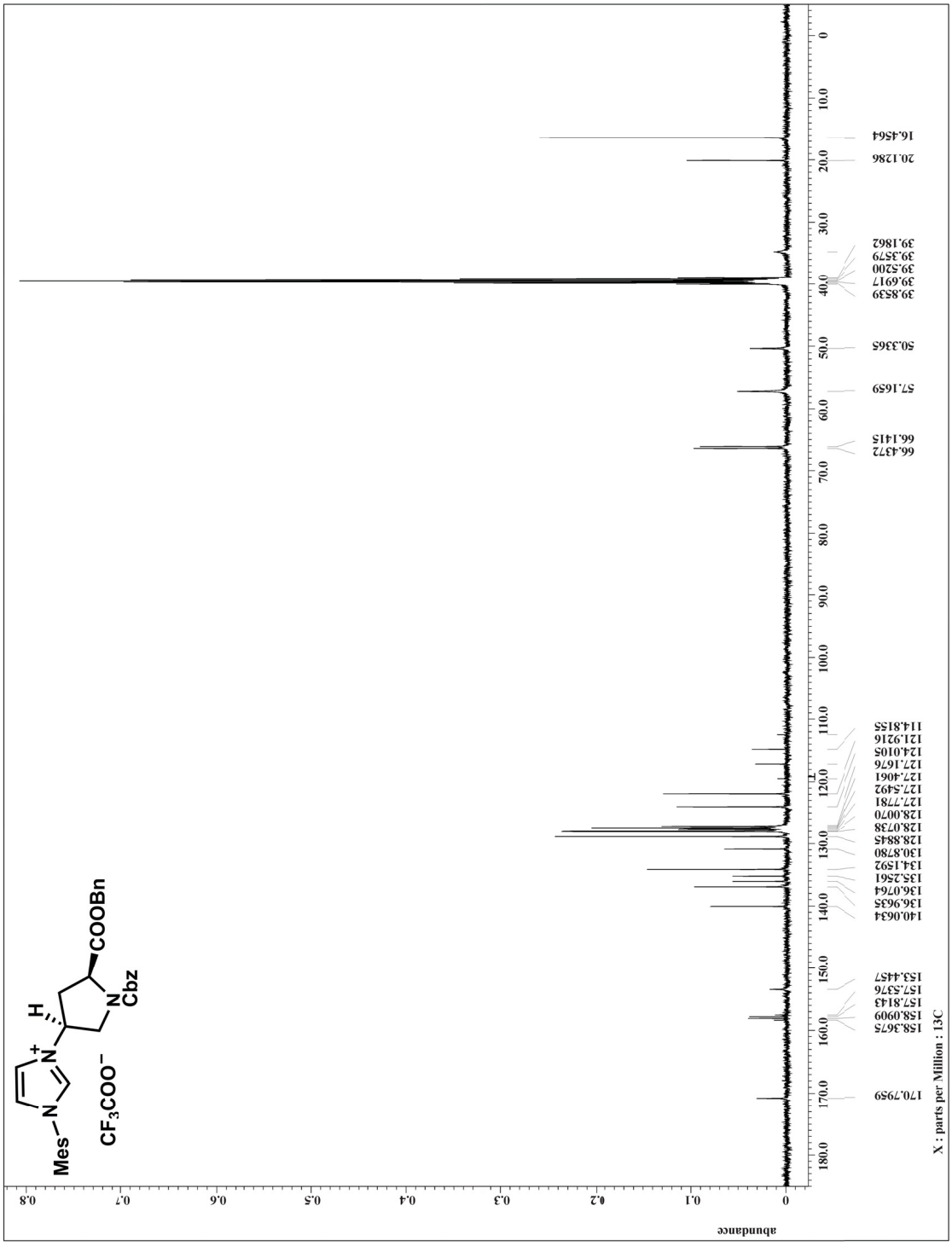

Figure 2.40: ^{13}C NMR (125 MHz, DMSO-*d*6, 353 K) of 3-((3*S*,5*S*)-1,5-bis(benzyloxycarbonyl)pyrrolidin-3-yl)-1-mesityl-1*H*-imidazol-3-ium trifluoroacetate (**2.29**).

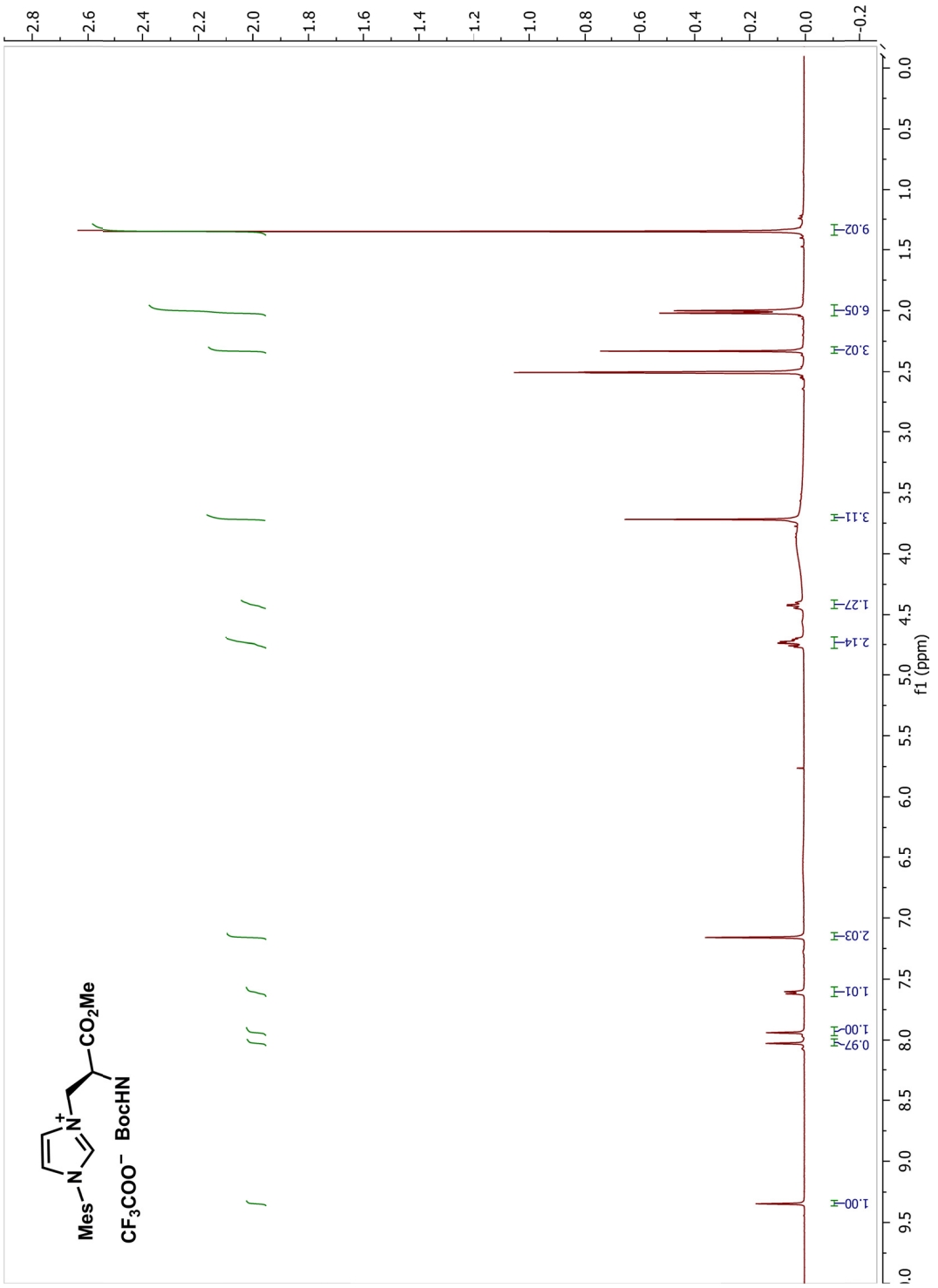

Figure 2.41: ^{1}H NMR (500 MHz, DMSO-*d*6) of (*S*)-3-(2-(*tert*-butoxycarbonylamino)-3-methoxy-3-oxopropyl)-1-mesityl-1*H*-imidazol-3-ium trifluoroacetate (**2.31**).

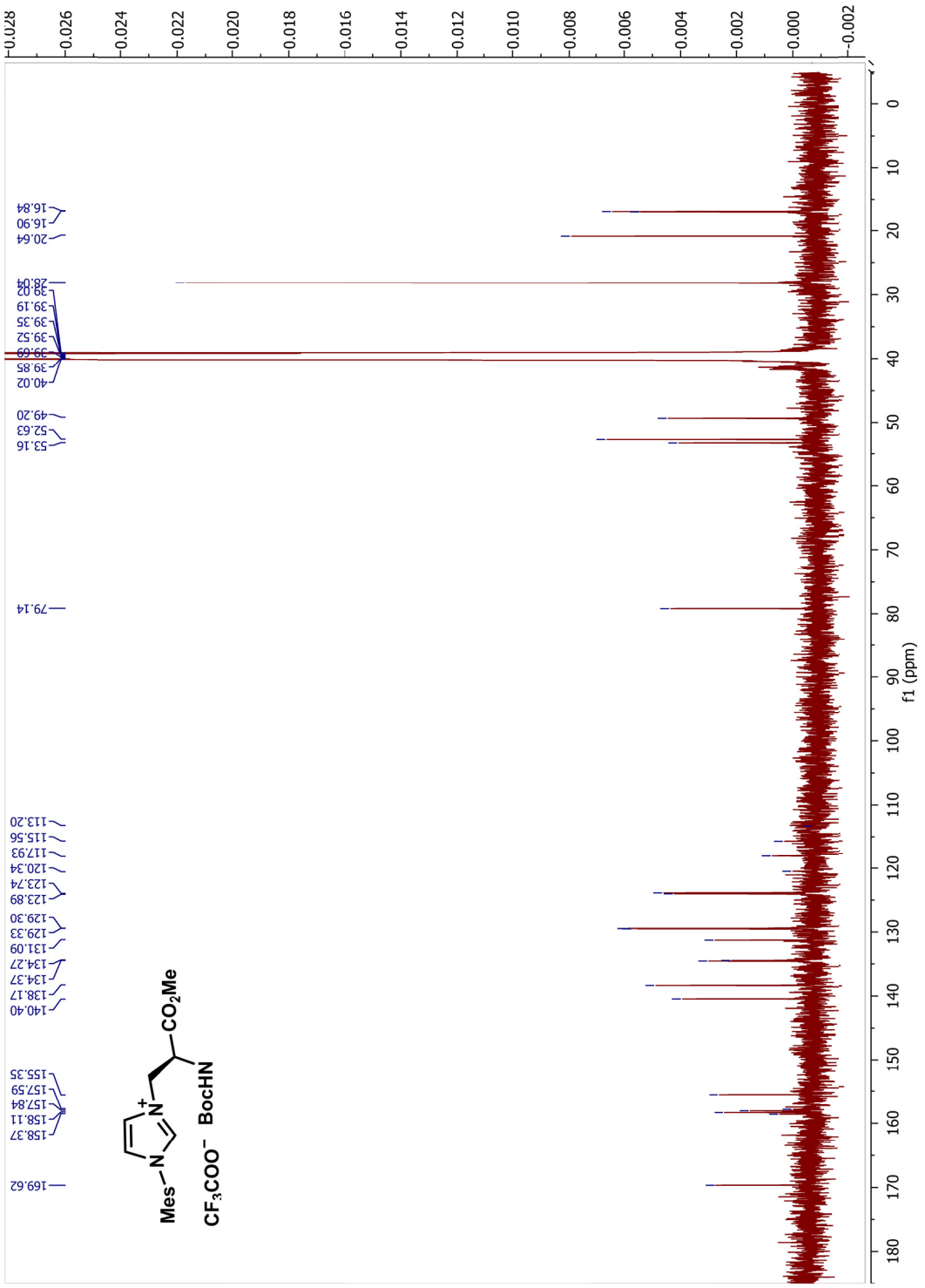

Figure 2.42: ^{13}C NMR (125 MHz, DMSO-*d*6) of (*S*)-3-(2-(*tert*-butoxycarbonylamino)-3-methoxy-3-oxopropyl)-1-mesityl-1*H*-imidazol-3-ium trifluoroacetate (**2.31**).

CHAPTER 3 SYNTHESIS OF PROLINE-BASED NHC PRECURSORS

3.1 Review of Amino Acids and Peptides in Asymmetric Catalysis

The concept of enzymatic catalysis is an important nature-inspired lesson for chemists. The imitation of enzymes has invaluably contributed to the tremendous success of single amino acid and short peptide (<50 amino acids in length) being used as highly effective and selective catalysts in chemical transformations.[133] The known advantages of these catalysts are easy access, fine-tuning and good stability in moisture and air.

Scheme 3.1: The Hajos-Parrish-Eder-Sauer-Wiechert reaction

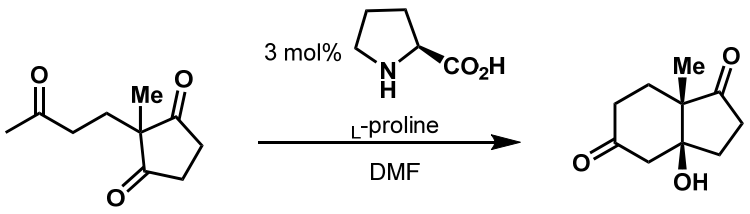

3.01 99% yield 93% *ee* **3.02**

Natural single amino acids and modified amino acid residues have been considered as simplified enzyme mimics.[134] As early as 1971,[135–137] Hajos, Parrish, Eder, Sauer and Wiechert reported the pioneering use of $_{L}$-proline as catalyst for the intramolecular aldol

reactions (Scheme 3.1). Proline derivatives have gathered most attention among the naturally-occurring single amino acids in regard to asymmetric catalysis.[138]

Small peptides have also been reported to function in asymmetric organic catalysis.[109,133,139] Miller and coworkers have reported the use of small peptides as nucleophilic catalysts for acyl,[140,141] phosphoryl[142,143] transfers and Baylis-Hillman reactions.[144,145] Several representative examples of peptide-based organocatalysts reported by other chemists are used for sulfinyl transfer,[146] aldol reactions,[147] and epoxidations.[148,149]

Scheme 3.2: Pd-peptide catalyzed addition to cyclic allyl acetates

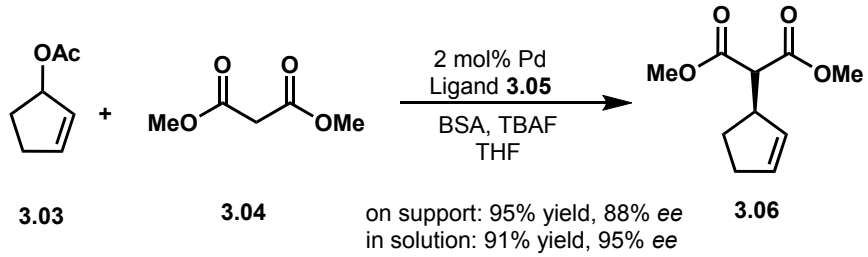

3.03 **3.04** on support: 95% yield, 88% *ee* in solution: 91% yield, 95% *ee* **3.06**

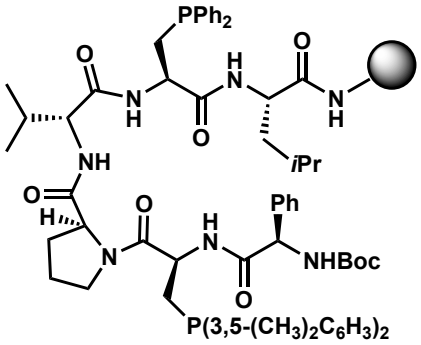

Ligand 3.05

In addition to the success of peptide-based organocatalysis, transition metal binding peptides have been used to control or mimic enzyme activity and perform reactions that

are not typically seen in biological systems.[111,113,150–156] Our group has reported libraries of bisphosphine-peptide ligand systems in coordination with palladium to facilitate reactions in a stereoselective fashion. An example has been shown in Scheme 3.2.

Both natural and unnatural amino acids can be embedded in the peptide primary structure to serve as building blocks as well as to introduce new chirality into the primary structure of the peptide sequences. It appears that the stereoselectivity is mainly determined by the secondary structure of the peptides. A well defined secondary structure with a certain degree of flexibility is found to be key to successful chiral scaffolds. As shown in Scheme 3.2, β-turn secondary structure was efficient in controlling the chiral environment near the transition metal and thus leading to the observed stereoselectivity for the transformations. It is noted that turn-like peptide structures were also utilized in the Miller asymmetric organocatalysis work[140,157].

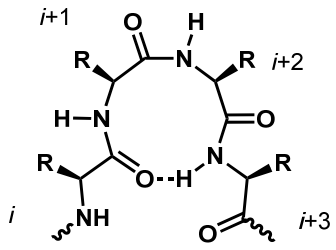

Figure 3.1: β-turn secondary structure.

Turns are one common secondary structure in proteins and small peptides. In the nomenclature, they are called β-Turns (Figure 3.1) if the turn structure is composed of four amino acids (*i*, *i*+1, *i*+2, *i*+3). In the majority of cases turn structures are stabilized by torsion angle and hydrogen bonding patterns formed within both sides of the loop.

Due to its cyclic structure and secondary amino functionality, proline is a good turn inducer in the *i*+1 position.

In the ligand systems developed by our group (**3.08**, Scheme 3.3), at the turn $_{L}$-proline and a $_{D}$-amino acid occupied the *i*+1 and *i*+2 positions, respectively. The two phosphine binding sites were positioned in *i* and *i*+3. Upon solid-phase peptide synthesis with diverse amino acid residues, the library of peptide sequences was screened to optimize the reactivity and selectivity.

Scheme 3.3: Syntheses of peptide sequence **3.08**

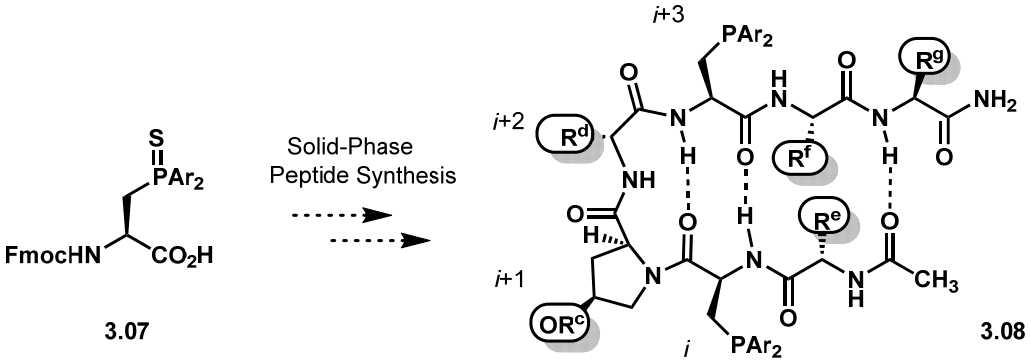

Research with amino acid-based catalysis has been expanded to the combination of single amino acids with other functionality. Hoveyda[158–160] and Jacobsen[161] research groups reported the utilization of chiral amino acid-urea ligands in transition metal catalyzed transformations. Our group has focused on the development of a proline-based phosphine-oxazoline bidentate ligand system **3.11** and their uses in asymmetric allylation (Scheme 3.4) and the Heck reaction.[106–108]

Scheme 3.4: Pd-catalyzed asymmetric allylation

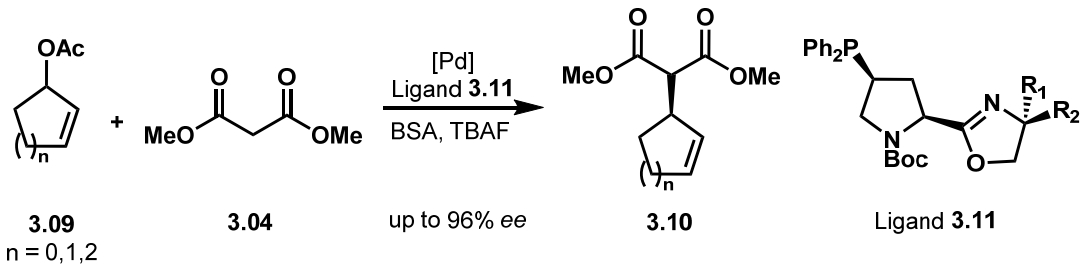

Based on the preliminary results, it was found that the nucleophilic natural amino acids are limited to those bearing side chains such as imidazole and basic amines. Thus in recent years chemists have investigated the design and preparation of novel nucleophilic amino acids. Some examples are found in the Miller work. Our group has successfully developed a system of phosphine-containing amino acids (Figure 3.2).[109–113] In Chapter 2, we reported another type of potential nucleophilic amino acid, imidazolium containing amino acids. These imidazolium salts are NHC precursors and the amino acid structures allow these molecules to be used as building block in synthetic small peptides as well as combined with other coordinating functionalities, to yield the precursors for a variety of NHC ligands.

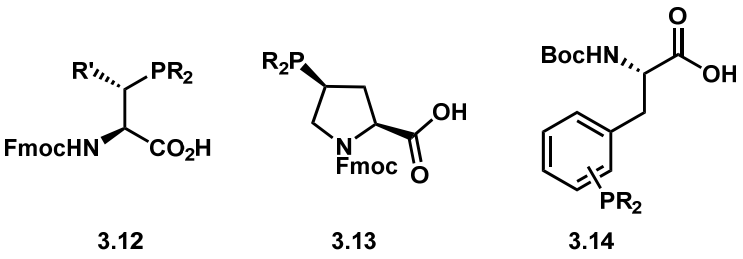

Figure 3.2: Several amino acid residues bearing nucleophilic side chains.

3.2 Incorporation of NHC Building Blocks into Peptide Structures

Most of the work in this section was shown in a published paper.[119] Two important strategies of the amide bond formation: in-solution peptide synthesis and solid-phase peptide synthesis are both applied in the case of NHC-containing peptide formation. Figure 3.3 shows the targeted NHC-proline residues with different protecting groups as well as their uses, which will be discussed individually.

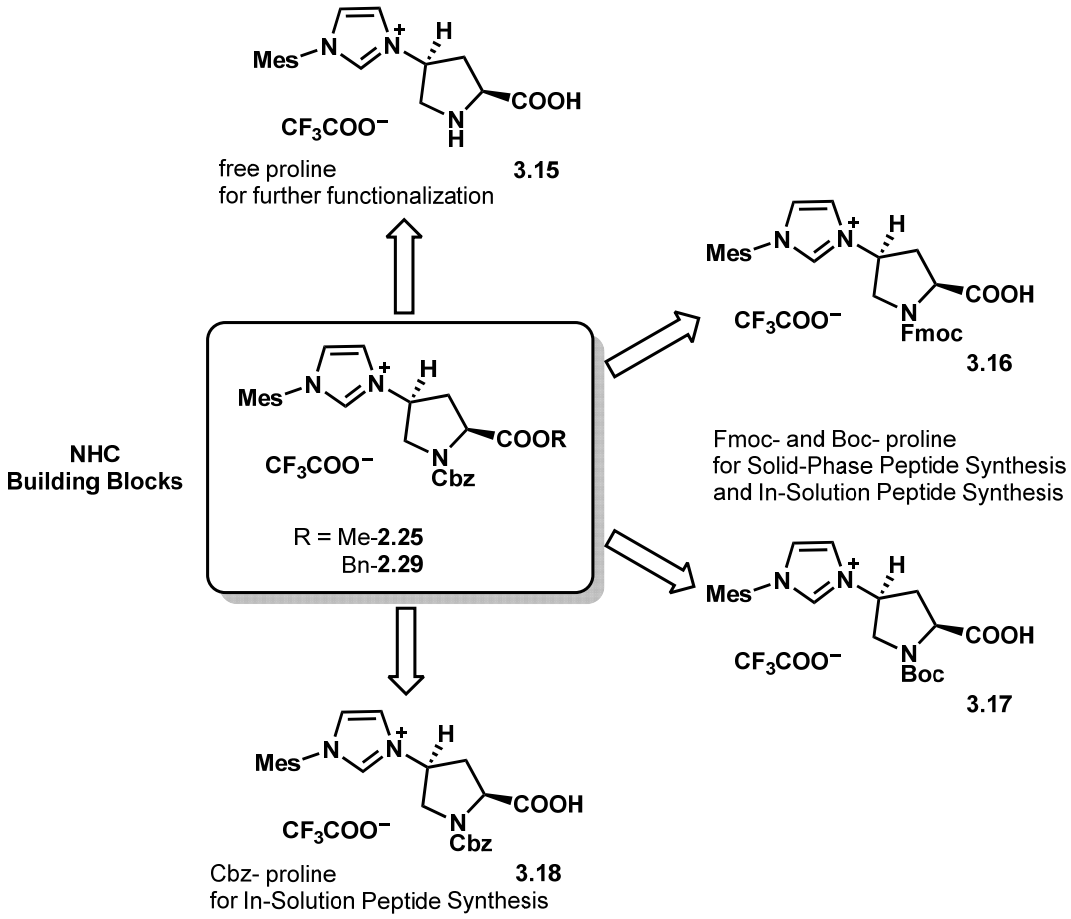

Figure 3.3: Applications of NHC building blocks in peptide chemistry.

[119] Zhao, Y.; Gilbertson, S. R. *Org. Lett.* 2014, *16* (4), 1033.

Solution peptide synthesis and solid-phase peptide synthesis (SPPS) are well-developed and highly efficient techniques for the preparation of oligopeptides. Single amino acids that are mono-protected on either *N*- or *C*-terminus can be used as building blocks in both techniques. Linear, solution-phase synthesis is a repetitive process of single amide bond formation, protecting group removal and purification. It is convenient for the synthesis of oligopeptides. However, as the length of peptides increases, the yield decreases and the process becomes tedious. In the case of solid phase peptide synthesis the procedure is performed on a solid support, where the protecting group, after cleavage, and other unreacted components not attached to the resin maybe washed off without the need for purification of the intermediate.

Scheme 3.5: Proposed synthesis of peptide **3.19** and **3.20**

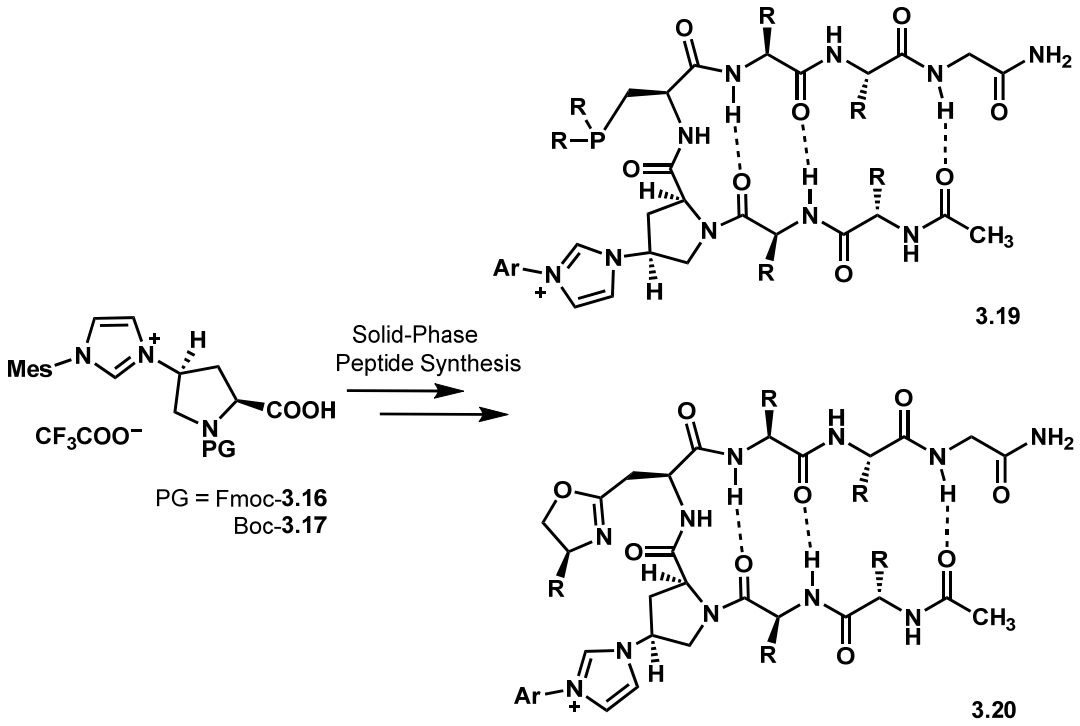

The formation of an imidazolium salt can be challenging, especially if it is desired to be incorporated into a complicated structure such as peptide. Thus the convenient incorporation into peptide structure that contains an imidazolium salt via amide bond formation is a promising advantage of our NHC-proline building block.

On the basis of the reported stable β-turn in peptide sequence **3.08**, we have designed a collection of peptides **3.19**, **3.20** and **3.21**, which bear imidazolium side chains that could be precursors for NHCs. Two coordinating groups are located at the turn in **3.19** and **3.20**, while in **3.21** two coordinating groups are positioned down the sequence at *i* and *i+3* locations . These bifunctional ligands contain an NHC and either phosphine or an oxazoline. These NHC scaffolds may also be diversified by changing the amino acids in the sequence providing a library of NHC precursors.

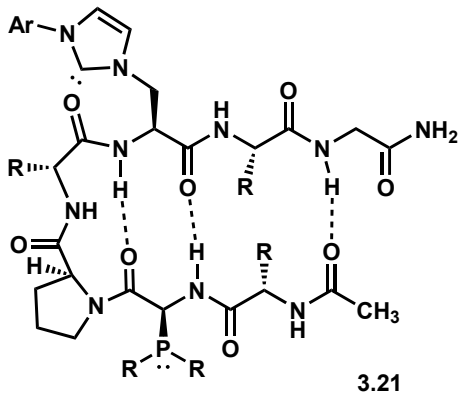

3.21

Figure 3.4: Bifunctional peptide with coordinating groups positioned down the sequence.

In solid phase peptide synthesis the two most commonly used amine protecting groups are Fmoc and Boc. Designed imidazolium salts **3.16** and **3.17** are the building blocks for

3.19 and **3.20** (Scheme 3.5). With **2.25** in hand, we hypothesized that the simple exchange of protecting group and removal of *C*-protecting group could be easily achieved affording the desired salts. However, this proved problematic with the imidazolium salt. Regarding the imidazolium containing structures, due to the complexity of salt purification, high conversion is essential during the transformations. Since the reactant and product are both imidazolium-based and their properties could be similar, complete conversion of the reactants would significantly facilitate the isolation of the desired compound.

Scheme 3.6: Attempted protecting group removal of **2.25**

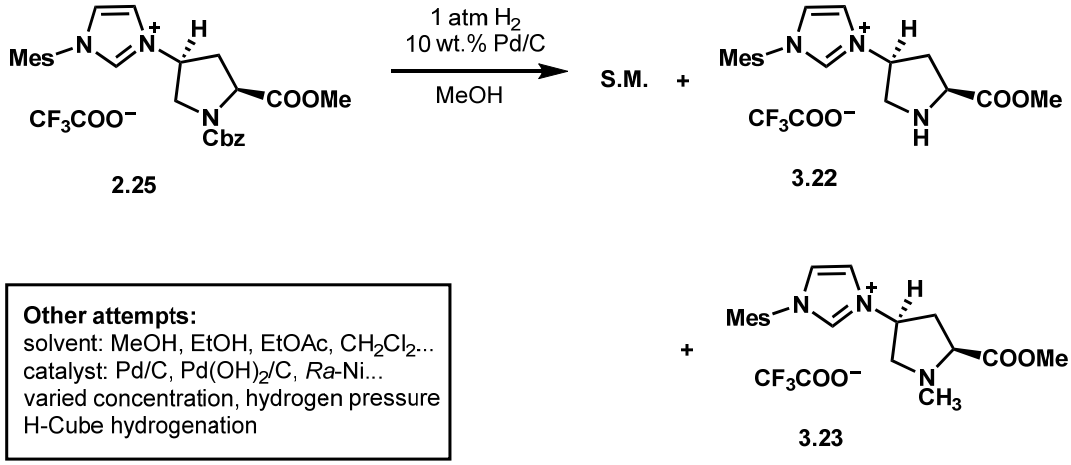

In order to use our proline containing NHC precursor we first had to remove the Cbz protecting group. The removal of Cbz protecting group was attempted (Scheme 3.6) by hydrogenolysis utilizing Pd/C as catalyst. In the initial attempt, the target *N*-deprotected **3.22** was observed, but a side product *N*-methyl proline **3.23** formed before the starting material was fully consumed. Further investigation with the assistance of LC-MS revealed that desired product **3.22** was formed within minutes but subsequently *N*-

methylation could be observed and was more rapid than starting material consumption. The ratio of starting material, *N*-deprotected **3.22** and side product **3.23** was dependent on the reaction time. After 24 hours, **3.22** was completely alkylated to afford pure **3.23** in 86% yield. Although this phenomenon is not typically seen in reactions involving proline, a literature report was found for this partial *N*-alkylation.[162] It demonstrated the formation of *N*-alkylation product by proton NMR and FAB mass spectroscopy, and mentioned that this side product had not been reported due for two reasons: usually the amide bond formation is much faster than this alkylation in peptide synthesis, and the trace amounts of water in the reaction solvent probably eliminate the side product formation. However, in our attempts varying the reaction conditions such as catalyst, reaction solvent, concentration, hydrogen pressure, and the utilization of H-Cube Continuous-flow Hydrogenation Reactor could not prevent the formation of this side product which also proved difficult to separate from the desired product.

Scheme 3.7: Complete deprotection of **2.29**

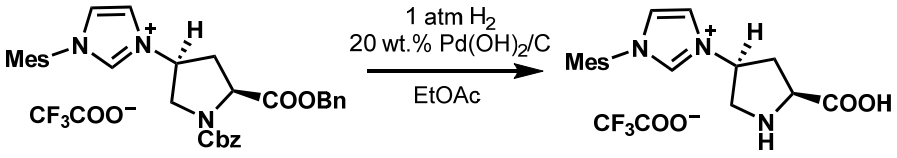

2.29 86% **3.15**

The failure in generation of completely deprotected imidazolium-proline lead to the preparation of the benzyl ester **2.29**, discussed in Chapter 2. Using optimized hydrogenolysis conditions (Scheme 3.7), **2.29** can be fully deprotected to yield free proline **3.15** with imidazolium side chain. This reaction was monitored by LC-MS and reaction went to completion before occurrence of alkylation. Proline **3.15** could

potentially be used as precursor for organocatalyst or metal ligand. It is noted that unprotected proline bearing imidazolidinium at 4-position could not be formed using the one-pot methodology in Chapter 2.

Scheme 3.8: Synthesis of *N*-Fmoc **3.16**

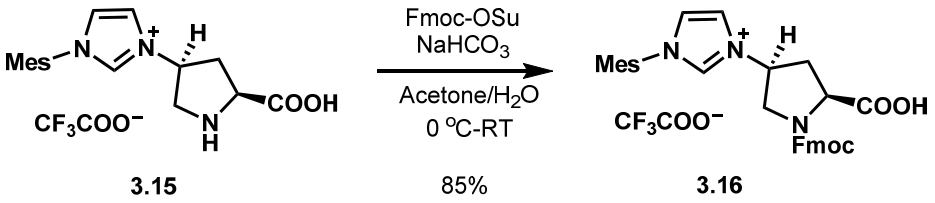

3.15 85% **3.16**

Proline **3.15** can be easily functionalized. Standard reaction condictions provided the Fmoc-protection **3.16** (Scheme 3.8).

Scheme 3.9: Synthesis of *N*-Boc **3.17**

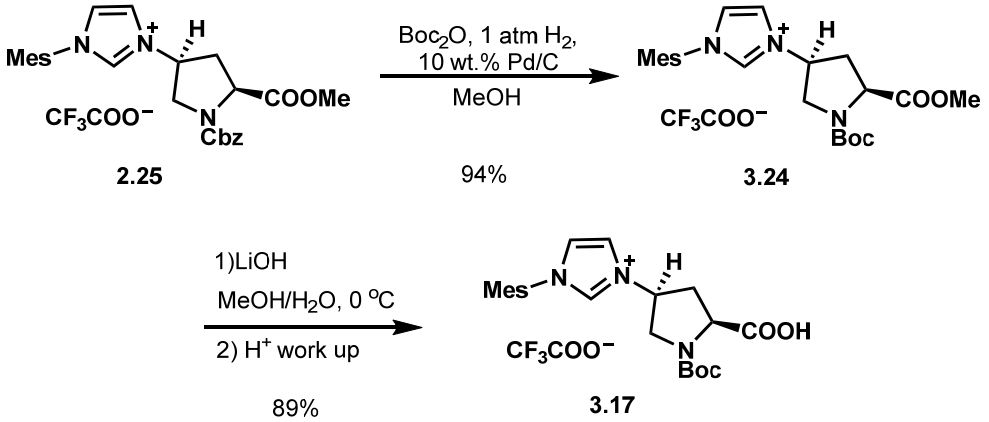

2.25 94% **3.24**

89% **3.17**

N-Boc-proline **3.17** can be accessed *via* a number of routes. Boc-protection of proline **3.15** could generate **3.17** but this strategy was not straightforward. After searching the relevant literature, we found that one-pot hydrogenolysis of Cbz in presence of Boc-anhydride can allow the swapping of protecting groups from Cbz to Boc-protection of the secondary amine (Scheme 3.9). The one-pot procedure shortened the route and

eliminated the formation of *N*-methyl side product. Mild hydrolysis of methyl ester **3.24** with lithium hydroxide provided **3.17** upon acidic workup and no further purification is needed.

Fortunately the same conditions were applicable for benzyl ester **2.29** as well (Scheme 3.10). Deprotection of both amine and acid and then Boc-protection of amine can be accessed in one pot. **3.17** was prepared with only one step from our building block **2.29** in high yield.

Scheme 3.10: One-pot synthesis of *N*-Boc **3.17**

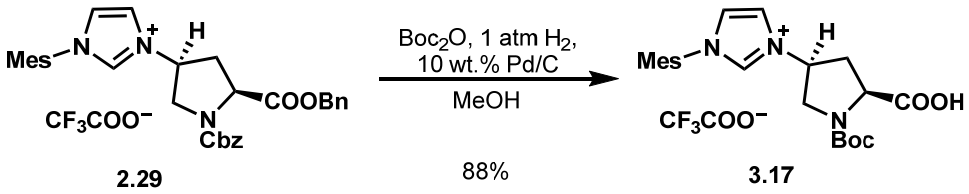

2.29 **3.17**

Acids **3.16** and **3.17** were synthesized efficiently and are intended for direct use in solid-phase peptide synthesis and generating peptides with nucleophilic side chains such as **3.19** and **3.20**.

Scheme 3.11: Synthesis of *N*-Cbz **3.18**

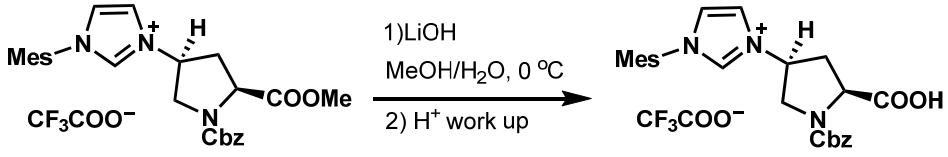

2.25 **3.18**

Treatment of **2.25** with lithium hydroxide selectively hydrolyzed the methyl ester to provide acid **3.18** without removal of Cbz group in excellent yield (Scheme 3.11). No

further purification is needed. Free acid **3.18** can be used to synthesize short peptides in solution, as well as precursor for NHCs.

The building block has also been used in classical solution-phase peptide synthesis (Scheme 3.12). Standard coupling of acid **3.18** with alanine methyl ester provided dipeptide **3.25** in high yield. Cbz-deprotection and standard coupling with N-Boc alanine provided tripeptide **3.27**.

Scheme 3.12: In-solution synthesis of tripeptide **3.27**

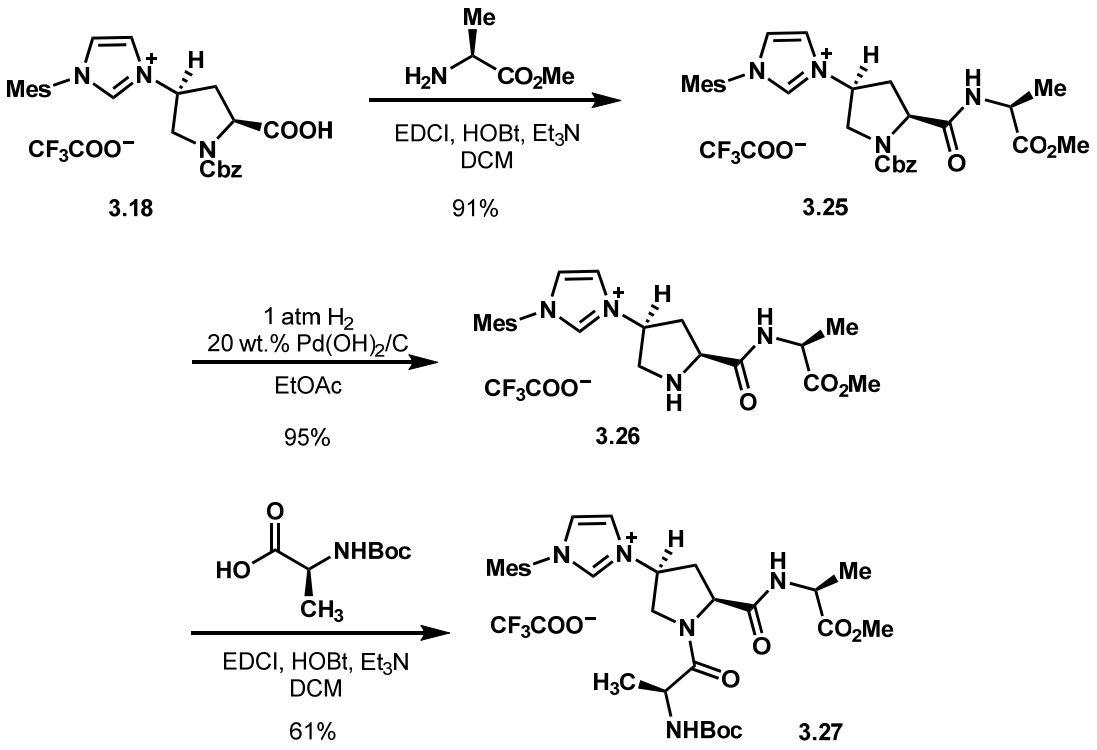

Building block acids **3.15-3.18** have been prepared and a short peptide **3.27** has been synthesized to demonstrate the uses of our NHC precursors. All of the intermediates could be used individually as precursor of organocatalyst or as ligands for transition metals by us as well as other researchers. These NHC precursors are air and moisture

stable for long periods of time. It is also noteworthy that no epimerization or decomposition was observed in any above reaction, demonstrating the robustness of our NHC building blocks.

3.3 Synthesis of NHC-Proline-Oxazoline Bidentate Ligands

Our group has successfully utilized phosphine-oxazoline bidentate ligand system **3.11** (Figure 3.5) in asymmetric palladium catalysis. Burgess and coworkers reported the NHC-oxazoline bidentate ligand **3.30**[89,127] in iridium-catalyzed hydrogenation (Scheme 3.13), which is also one of the limited examples of NHC being used in a highly selective asymmetric reaction.

Scheme 3.13: Application of NHC-oxazoline **3.30**

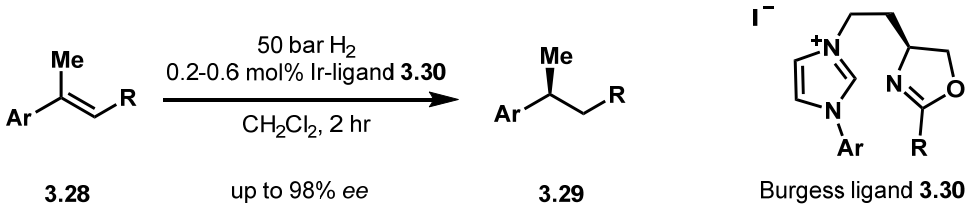

3.28 up to 98% *ee* **3.29** Burgess ligand **3.30**

Having the NHC-proline building block in hand, we then designed the bidentate ligand **3.31**. One of the structural differences of our ligands and Burgess ligands is the chiral center next to the oxazoline nitrogen. In our ligands the chirality is positioned closer to the metal and may provide a better chiral environment. Our proposed ligand system replaces phosphine in ligand **3.11** with NHC. Such a substitution would typically increase the activity of transition metal complexes over those with ligand **3.11**. A 3-D representation of **3.32** is shown in Figure 3.6. Surrounded by mesitylene, oxazoline and

Cbz protecting group, the ligand has a unique chiral environment. In addition, by changing the starting amino alcohols this type of ligands can be easily modified to obtain highly selective catalytic complexes.

Figure 3.5: Proline-based bidentate ligands.

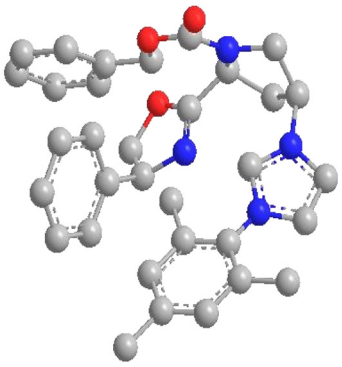

Figure 3.6: 3-D view of proposed ligand **3.32**.

The initial attempt (Scheme 3.14) started with a standard EDCI coupling of acid **3.18** and amino alcohol **3.33**. The resulting alcohol was then subjected to a previously reported condition with methanesulfonyl chloride, providing a reaction mixture of minor desired oxazoline **3.32** and major mesylate imidazolium based on LC-MS. However, the desired product decomposed upon HPLC or column chromatography. Recrystallization of the salt

was also attempted but failed. A number of other conditions that are typically utilized to generate oxazoline were unsuccessful on our substrates.

Scheme 3.14: Attempted synthesis of **3.32**

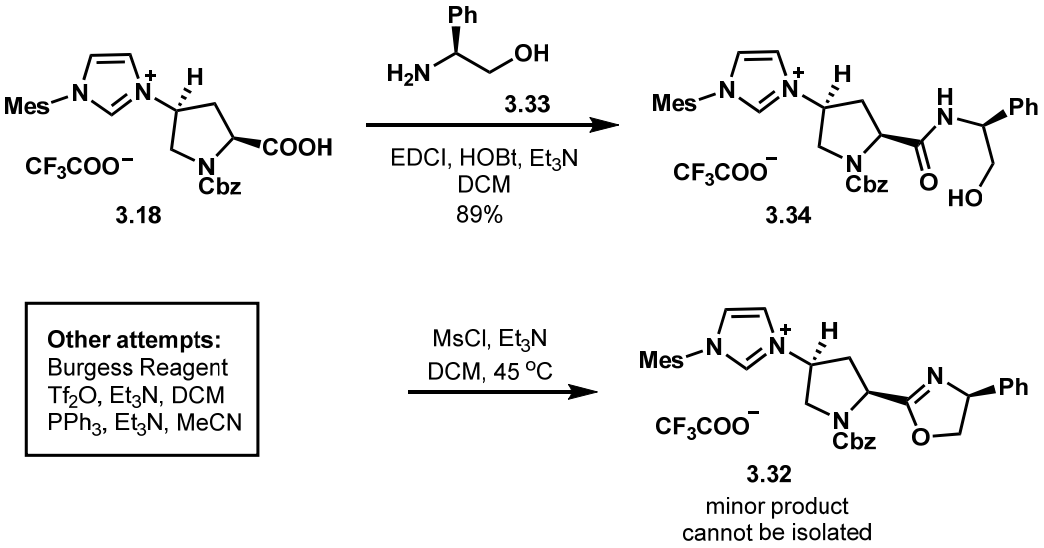

It was one of our goals to further derivatize our NHC building block by converting it into an imidazolium-proline-oxazoline system. However, due to the failure of this strategy, we decided to revise the route to obtain the ligand.

The alternative route in Scheme 3.15 failed in the triflation step due to the instability of secondary triflate. The common strategy in Scheme 3.16 was efficient in the preparation of oxazoline **3.40** but not the installation of imidazolium ring.

Scheme 3.15: Attempted synthesis of **3.38**

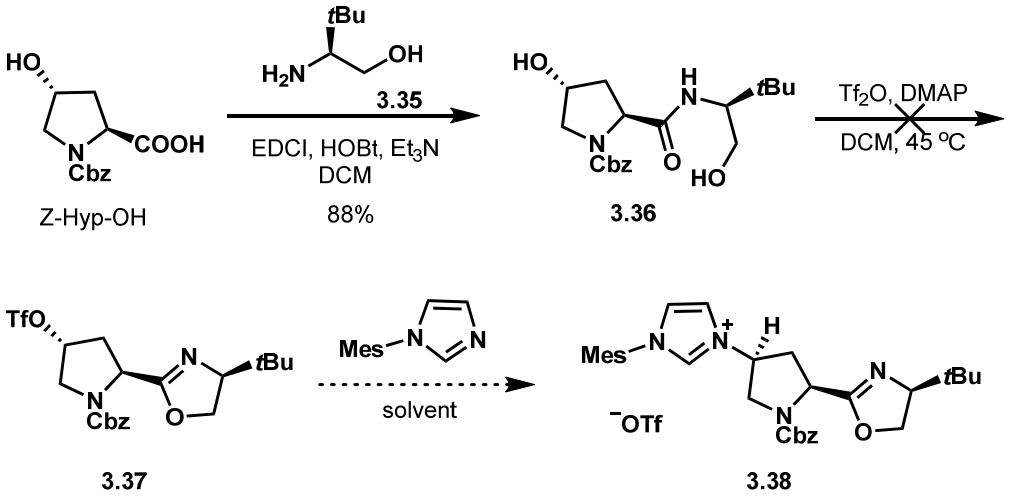

Scheme 3.16: Attempted synthesis of **3.41**

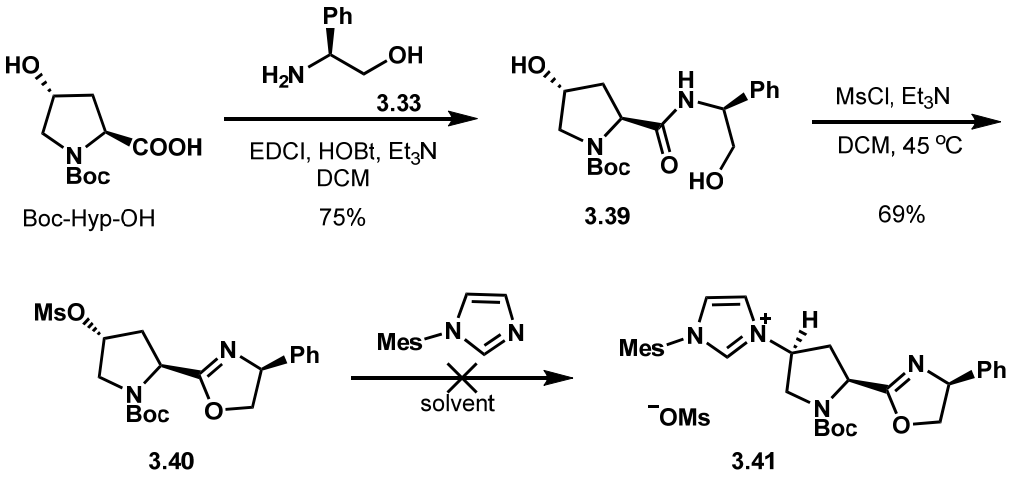

After careful consideration, we decided to work with Boc-protected **3.17** since we feel the steric hindrance due to the longer Cbz group might be one reason of failed completion in Scheme 3.14. Based on the LC-MS results, the reaction with methanesulfonyl chloride provided a higher ratio of oxazoline product **3.43** than that of **3.32**. Unfortunately we did not find an effective technique to purify the product without decomposition of oxazoline.

Scheme 3.17: Attempted synthesis of **3.43**

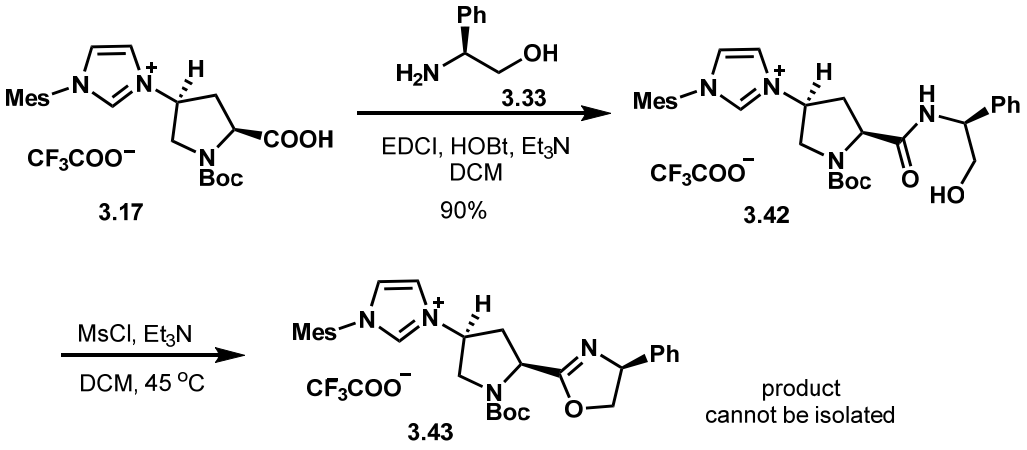

To summarize the attempts to synthesize the NHC-proline-oxazoline, complete conversion would highly facilitate the isolation of desired product. The mesylation procedure has been modified but complete conversion cannot be achieved. Substitution of protecting group with less hindered and more robust functionalities such as acetyl or alkyl might be a solution to this issue. Recrystallization and other purification techniques to isolate product **3.43** may also be promising to obtain the designed ligand.

3.4 Synthesis of NHC-Phosphine and Phosphine Oxide Bidentate Ligands

The phosphine-phosphine oxide ligand systems were found to be valuable in transition-metal catalysis due to the lability of phosphine oxide coordination that can provide an empty coordination site of metal. Our group has used the well-defined Rh-BozPHOS complex **3.46** in [4+2+2] cycloadditions (Scheme 3.18).[163]

Scheme 3.18: Rh-catalyzed [4+2+2] cycloadditions

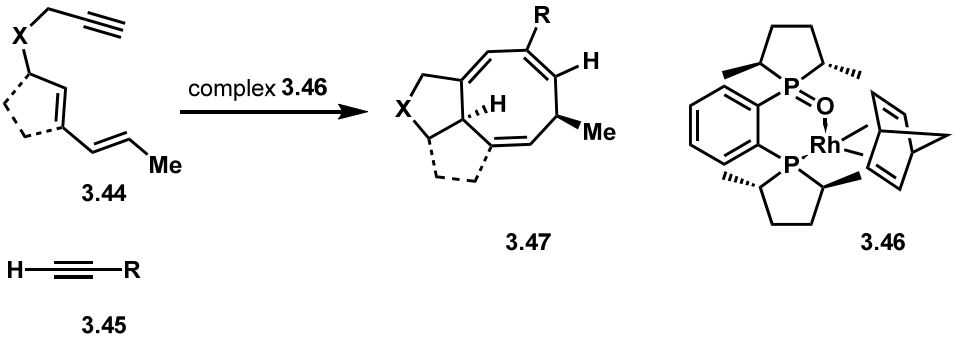

In addition to the phosphine-phosphine oxide ligand systems, the combination of NHC-phosphine (oxide) may have potential in a number of catalytic transformations including cycloadditions to construct medium-sized ring systems. Upon standard amide bond coupling, the ligand precursor **3.48** can be easily synthesized using our building block derivative and finely tuned by varying the stereocenters of the aminophosphine **3.47** (Scheme 3.19). This type of bidentate ligand should allow for better control of the ligand sterics than the monodentate NHC ligands.

Scheme 3.19: Coupling of aminophosphine (oxide) with acid

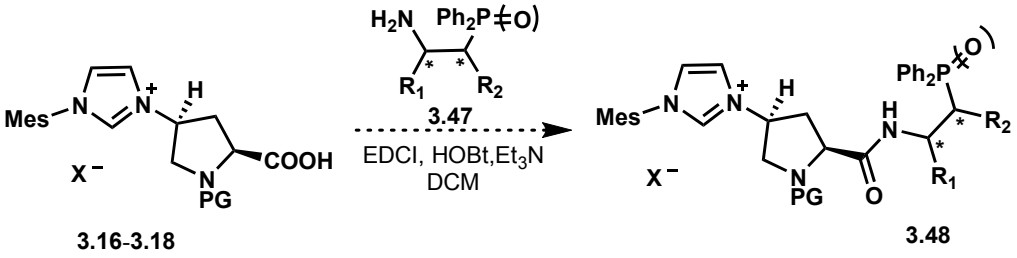

It is known that phosphines can be air-sensitive and may be oxidized to phosphine oxide. Thus our strategy was to protect the phosphine as the phosphine sulfide (Scheme 3.20). Standard coupling was performed to generate the imidazolium-containing phosphine

sulfide **3.51**. However, upon attempted hydrogenolysis, the free phosphine was never obtained with the phosphine sulfide fully recovered.

Scheme 3.20: Attempted synthesis of **3.52**

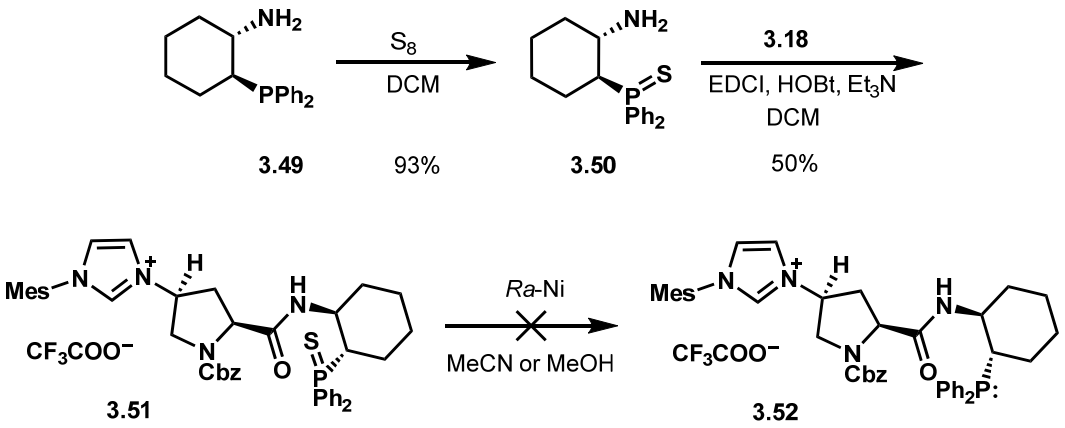

Scheme 3.21: Oxidation of phosphine ligand

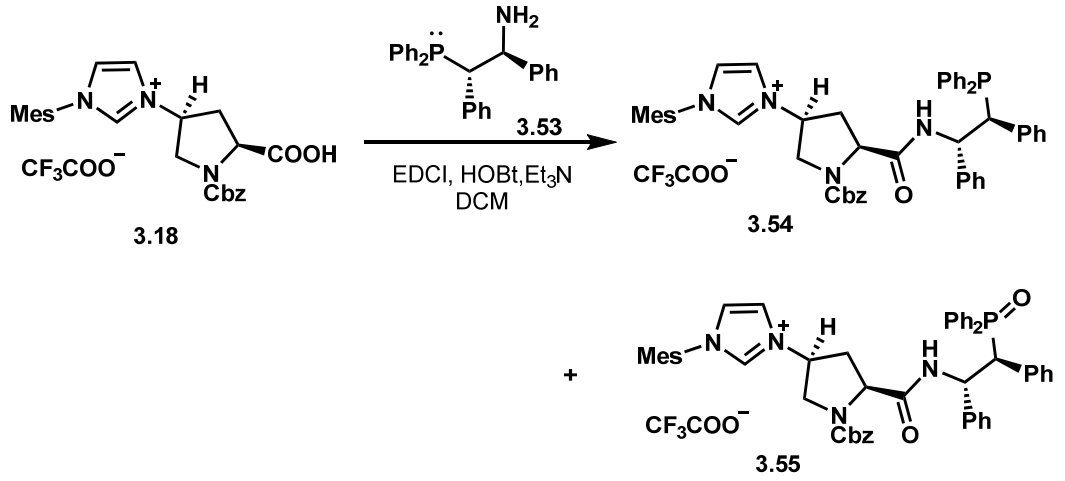

The NHC precursor **3.18** was also coupled with free phosphine **3.53** under inert atmosphere (Scheme 3.21). Not surprisingly, during the process of purification by HPLC the phosphine **3.54** was partially oxidized to **3.55**. These ligands are partially oxidized while being purified by reversed phase HPLC.

Scheme 3.22: Synthesis of aminophosphine oxide **3.57**

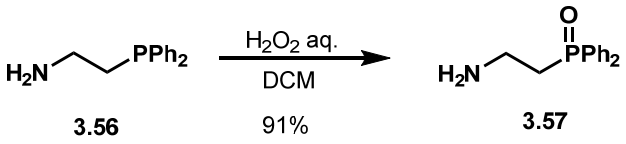

Scheme 3.23: Synthesis of aminophosphine oxide **3.60**

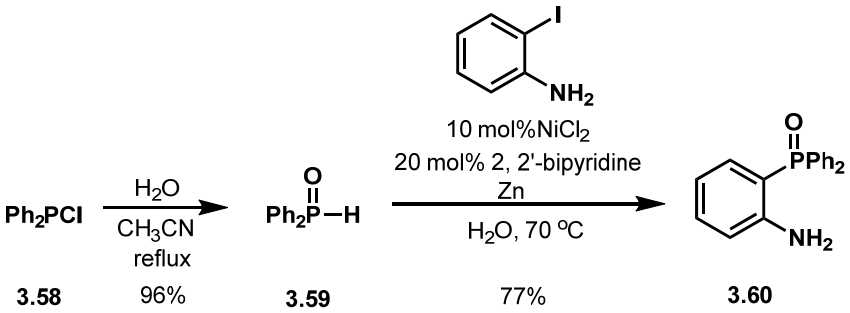

Amino phosphine oxides such as **3.57** and **3.60** [164] were synthesized. The imidazolium-phosphine oxide ligands were prepared following the standard EDCI coupling shown in Scheme 3.19 using these amino phosphine.[165] Figure 3.7 illustrates these compounds and their coupling yields respectively.

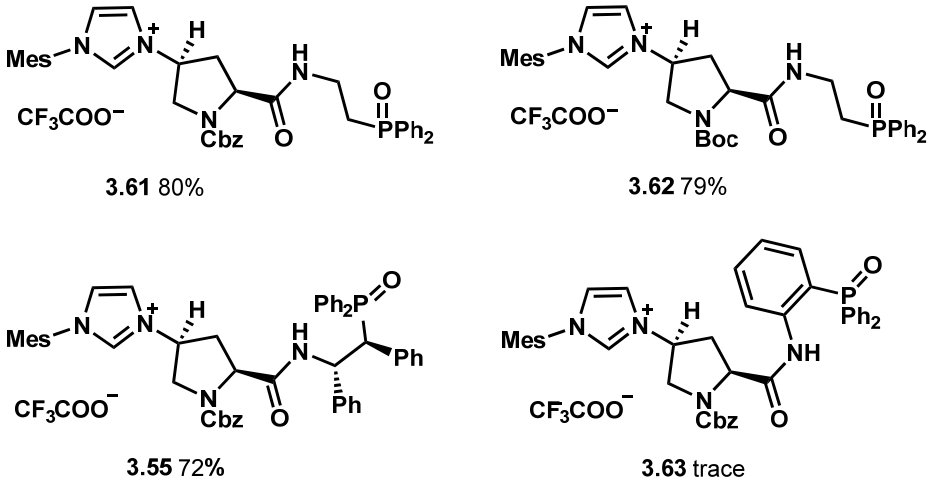

Figure 3.7: Synthetic NHC-phosphine oxide precursors.

3.5 Experimental Section

General Procedures:

All reagents were purchased from Sigma-Aldrich, Acros, Aapptec and Strem and used as received unless otherwise noted. Thin-layer chromatography was performed on silica gel 60 F_{254} pre-coated plates (0.25 mm) from Silicycle and components were visualized by UV light (254 nm) and/or 10% phosphomolybdic acid in ethanol stain. Flash chromatography was performed using Silicycle silica gel 230-400 (particle size 40-63 μm) mesh. Analytical high-pressure liquid chromatography was performed on an Agilent 1100 Series instrument equipped with a Variable Wavelength Detector. Preparative HPLC was performed on a Gilson instrument equipped with a 321 pump, UV/VIS-155 detector and FC-204 fraction collector. ^{1}H, ^{13}C and ^{31}P NMR were recorded on JEOL ECX-400 NMR spectrometer (400 MHz for ^{1}H NMR, 100 MHz for ^{13}C NMR and 161 MHz for ^{31}P NMR) or JEOL ECX-500 NMR spectrometer (500 MHz for ^{1}H NMR and 125 MHz for ^{13}C NMR) in chloroform-*d* at ambient temperature and/or 318 K (45 ˚C) or in DMSO-*d*6 at ambient temperature and 353 K (80 ˚C, if necessary). In chloroform-*d*, chemical shifts were referenced to the residual chloroform-H peak at 7.26 ppm for ^{1}H NMR and 77.16 ppm for ^{13}C NMR. In DMSO-*d*6, chemical shifts were referenced to the residual DMSO-H peak at 2.50 ppm for ^{1}H NMR and 39.52 ppm for ^{13}C NMR. ^{31}P chemical shifts were measured relative to 85% H_3PO_4 as an external reference. Chemical shifts are reported in parts per million (ppm, δ). Multiplicity are indicated as s = singlet, d = doublet, t = triplet, q = quartet, m = multiplet, br = broad resonance and the coupling

constants (*J*) are reported in Hz. Liquid chromatography-mass spectrometry (LC-MS) was performed on a Thermo Finningan Surveyor instrument equipped with MSQ Plus single quadrupole detector. High-resolution mass-spectral data were recorded on an Agilent 6530 Accurate Mass Q-TOF LC/MS (high resolution ESI) and a Micromass (now Waters) Autospec Ultima mass Spectrometer (high resolution CI) from University of Texas at Austin, Mass Spectrometry Facility (MSF) of the Department of Chemistry & Biochemistry.

Experimental Procedures:

3-((3*S*,5*S*)-5-carboxypyrrolidin-3-yl)-1-mesityl-1*H*-imidazol-3-ium trifluoroacetate (3.15)

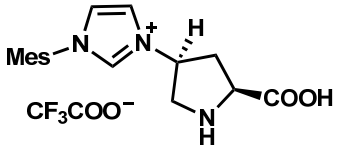

To a solution of 3-((3*S*,5*S*)-1,5-bis(benzyloxycarbonyl)pyrrolidin-3-yl)-1-mesityl-1*H*-imidazol-3-ium trifluoroacetate (141 mg, 0.220 mmol) in 7 mL of ethyl acetate was added 20 wt.% palladium hydroxide on carbon (100%, 140 mg). The reaction mixture was allowed to stir for 12 hours under atmospheric pressure of hydrogen at room temperature while monitored by analytical HPLC. After filtration through Celite 545, the solvent was evaporated under reduced pressure. Residue was washed with diethyl ether (2 x 20 mL) to give a pure product (78 mg, 86%):

^{1}H NMR (500 MHz, Acetone-*d*6) δ 9.67 (s, 1H), 8.48 (d, *J* = 1.5 Hz, 1H), 7.89 (d, *J* = 1.6 Hz, 1H), 7.11 (s, 2H), 5.85–5.79 (m, 1H), 4.78 (dd, *J* = 9.5, 8.0 Hz, 1H), 4.27 (dd, *J* = 12.9, 8.4 Hz, 1H), 4.21 (dd, *J* = 12.9, 6.3 Hz, 1H), 3.34–3.25 (m, 1H), 3.02–2.93 (m, 1H), 2.34 (s, 3H), 2.10 (s, 6H); ^{13}C NMR (125 MHz, Acetone-*d*6) δ 170.42, 161.02 (q, $J_{C\text{-}F}$ = 34.9 Hz), 141.82, 138.56, 135.62, 132.09, 130.26, 125.58, 123.35, 117.52 (q, $J_{C\text{-}F}$ = 292.3 Hz), 59.60, 59.18, 49.65, 35.66, 20.99, 17.37, 17.32;

LC/MS (ESI) calculated for $C_{17}H_{22}N_3O_2$ $[M\text{-}CF_3COO]^+$ 300.17, found 300.18 (t_R = 8.96 min); HRMS (CI^+) calculated for $C_{17}H_{22}N_3O_2$ $[M\text{-}CF_3COO]^+$ 300.1707, found 300.1708.

3-((3*S*,5*S*)-1-(((9*H*-fluoren-9-yl)methoxy)carbonyl)-5-carboxypyrrolidin-3-yl)-1-mesityl-1*H*-imidazol-3-ium trifluoroacetate (3.16)

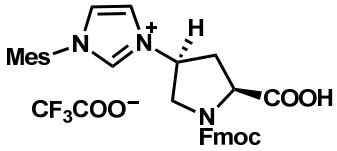

To a solution of 3-((3*S*,5*S*)-5-carboxypyrrolidin-3-yl)-1-mesityl-1*H*-imidazol-3-ium trifluoroacetate (55.3 mg, 0.133 mmol) in 4 mL of a 1:1 acetone: water mixture was added $NaHCO_3$ (22.3 mg, 0.266 mmol) and Fmoc-OSu (44.8 mg, 0.133 mmol) at 0 ˚C. The reaction mixture was allowed to stir over night at room temperature before being neutralized with 1 N HCl (aq.). After evaporation of MeOH under reduced pressure, the reaction solution was extracted twice with DCM, washed with brine, dried over $MgSO_4$ and then filtered. Compound was purified by preparative HPLC (Column: XBridge BEH

C_{18} OBD Prep 5 µm, 19 x 150 mm; wavelength: 215 nm, 254 nm; temperature: ambient; solvent A: 0.1% trifluoroacetic acid in H_2O, solvent B: 0.1% trifluoroacetic acid in MeCN; flow rate: 12 mL/min. Held at 0% B for 1 min, ramped to 100% B over 17 min, ramped to 0% B over 1 min and held for 1 min.) to give pure product (72 mg, 85%).

The NMR spectra are reported for a mixture of two rotamers: ^{1}H NMR (500 MHz, DMSO-*d*6, 293 K) δ 9.60 (d, *J* = 7.3 Hz, 1H), 8.24 (s, 1H), 7.99 (d, *J* = 7.6 Hz, 1H), 7.90 (dd, *J* = 6.6, 6.6 Hz, 2H), 7.70 (d, *J* = 7.5 Hz, 1H), 7.66 (dd, *J* = 7.3, 3.0 Hz, 1H), 7.46–7.40 (m, 2H), 7.33 (dd, *J* = 13.7, 7.1 Hz, 2H), 7.14 (d, *J* = 5.0 Hz, 2H), 5.25–5.19 (m, 0.5H), 5.18–5.13 (m, 0.5H), 4.57 (dd, *J* = 9.2, 4.8 Hz, 0.5H), 4.39 (dd, *J* = 9.2, 5.0 Hz, 0.5H), 4.35–4.13 (m, 5H), 4.09 (dd, *J* = 12.4, 4.4 Hz, 1H), 3.13–2.96 (m, 1H), 2.70 (dd, *J* = 8.8, 5.0 Hz, 0.5H), 2.64–2.58 (m, 0.5H), 2.33 (s, 3H), 2.07 (d, *J* = 6.3 Hz, 3H), 2.04 (d, *J* = 4.3 Hz, 3H); ^{13}C NMR (125 MHz, DMSO-*d*6, 293 K) δ 172.83, 172.41, 158.09 (q, J_{C-F} = 33.6 Hz), 153.90, 143.60, 140.75, 140.33, 137.14, 134.62, 131.24, 129.18, 127.85, 127.23, 124.24, 122.34, 120.25, 116.52 (q, J_{C-F} = 296.0 Hz), 67.42, 67.18, 58.11, 57.50, 57.15, 57.03, 54.96, 50.70, 50.27, 46.61, 35.51, 34.44, 20.62, 17.05;

^{1}H NMR (500 MHz, DMSO-*d*6, 353 K) δ 9.51 (s, 1H), 8.16 (s, 1H), 7.92 (dd, *J* = 1.7, 1.7 Hz, 1H), 7.88 (d, *J* = 7.6 Hz, 2H), 7.67 (d, *J* = 7.5 Hz, 2H), 7.42 (ddd, *J* = 7.4, 7.4, 4.4 Hz, 2H), 7.36–7.30 (m, 2H), 7.14 (s, 2H), 5.25–5.18 (m, 1H), 4.48 (br s, 1H), 4.34 (br s, 2H), 4.26 (br s, 1H), 4.19 (dd, *J* = 11.9, 6.6 Hz, 1H), 4.04 (dd, *J* = 11.9, 5.0 Hz, 1H), 3.07 (dd, *J* = 17.6, 11.2 Hz, 1H), 2.61 (d, *J* = 13.2 Hz, 1H), 2.35 (s, 3H), 2.06 (s, 6H); ^{13}C NMR (125 MHz, DMSO-*d*6, 353 K) δ 171.96, 157.52 (q, J_{C-F} = 33.5 Hz), 153.50, 143.30, 140.39, 139.98, 136.75, 134.14, 130.83, 128.81, 127.33, 126.74, 124.75, 123.95, 121.95,

119.67, 116.26 (q, $J_{C\text{-}F}$ = 296.5 Hz), 66.92, 57.03, 54.34, 50.35, 46.47, 34.77, 20.13, 16.50;

LC/MS (ESI) calculated for $C_{32}H_{32}N_3O_4$ $[M\text{-}CF_3COO]^+$ 522.24, found 522.22 (t_R = 10.56 min); HRMS ($^+$ESI) calculated for $C_{32}H_{32}N_3O_4$ $[M\text{-}CF_3COO]^+$ 522.2387, found 522.2387.

3-((3*S*,5*S*)-1-(*tert*-butoxycarbonyl)-5-carboxypyrrolidin-3-yl)-1-mesityl-1*H*-imidazol-3-ium trifluoroacetate (3.17)

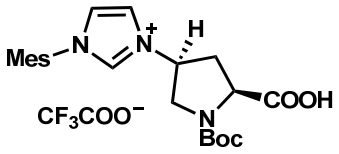

To a solution of 3-((3*S*,5*S*)-1,5-bis(benzyloxycarbonyl)pyrrolidin-3-yl)-1-mesityl-1*H*-imidazol-3-ium trifluoroacetate (59.8 mg, 0.0935 mmol) and di-*tert*-butyl dicarbonate (26.5 mg, 0.121 mmol) in 3 mL of methanol was added 10 wt.% palladium on charcoal (25%, 15 mg). The reaction mixture was allowed to stir overnight under one atmospheric pressure of hydrogen at room temperature while monitored by analytical HPLC. After filtration through Celite 545, the solvent was evaporated under reduced pressure to give white foam. The compound was subjected to preparative HPLC (Column: XBridge BEH C_{18} OBD Prep 5 µm, 19 x 150 mm; wavelength: 215 nm, 254 nm; temperature: ambient; solvent A: 0.1% trifluoroacetic acid in H_2O, solvent B: 0.1% trifluoroacetic acid in MeCN; flow rate: 12 mL/min. Held at 0% B for 1 min, ramped to 100% B over 17 min, ramped to 0% B over 1 min and held for 1 min.).

The NMR spectra are reported for a mixture of rotamers: ^{1}H NMR (500 MHz, DMSO-*d*6, 293 K) δ 9.56 (s, 1H), 8.22 (s, 1H), 7.97 (s, 1H), 7.13 (s, 2H), 5.15–5.09 (m, 1H), 4.30 (dd, *J* = 8.8, 5.8 Hz, 1H), 4.06 (dd, *J* = 15.5, 8.8 Hz, 1H), 3.91 (ddd, *J* = 23.9, 11.6, 5.3 Hz, 1H), 3.02–2.92 (m, 1H), 2.61–2.52 (m, 1H), 2.33 (s, 3H), 2.04 (s, 3H), 2.02 (s, 3H), 1.42 (s, 4.5H), 1.36 (s, 4.5H); ^{13}C NMR (125 MHz, DMSO-*d*6, 293 K) δ 173.07, 172.62, 158.26 (q, $J_{C\text{-}F}$ = 35.3 Hz), 153.26, 152.86, 140.28, 137.11, 134.59, 131.23, 129.18, 124.20, 122.33, 116.02 (q, $J_{C\text{-}F}$ = 292.9 Hz), 79.64, 57.63, 57.22, 57.07, 56.94, 50.39, 50.06, 35.14, 34.43, 28.06, 27.86, 20.62, 17.02;

^{1}H NMR (500 MHz, DMSO-*d*6, 353 K) δ 9.51 (s, 1H), 8.15 (dd, *J* = 1.4, 1.4 Hz, 1H), 7.90 (dd, *J* = 2.4, 1.1 Hz, 1H), 7.13 (s, 2H), 5.18 (dddd, *J* = 6.4, 6.4, 6.4, 6.4 Hz, 1H), 4.34 (dd, *J* = 9.0, 5.8 Hz, 1H), 3.90 (dd, *J* = 11.7, 5.7 Hz, 1H), 3.02 (ddd, *J* = 13.8, 8.9, 6.9 Hz, 1H), 2.54 (dd, *J* = 7.9, 4.7 Hz, 1H), 2.34 (s, 3H), 2.04 (s, 6H), 1.42 (s, 9H); ^{13}C NMR (125 MHz, DMSO-*d*6, 353 K) δ 172.29, 157.68 (q, $J_{C\text{-}F}$ = 35.2 Hz), 152.70, 139.96, 136.74, 134.13, 130.85, 128.81, 123.92, 121.93, 115.75 (q, $J_{C\text{-}F}$ = 293.5 Hz), 79.41, 56.97, 50.13, 34.75, 27.62, 20.12, 16.48;

LC/MS (ESI) calculated for $C_{22}H_{30}N_3O_4$ $[M\text{-}CF_3COO]^+$ 400.22, found 399.87 (t_R = 9.85 min); HRMS ($^{+}$ESI) calculated for $C_{22}H_{30}N_3O_4$ $[M\text{-}CF_3COO]^+$ 400.2231, found 400.2220.

3-((3*S*,5*S*)-1-(benzyloxycarbonyl)-5-carboxypyrrolidin-3-yl)-1-mesityl-1*H*-imidazol-3-ium trifluoroacetate (3.18)

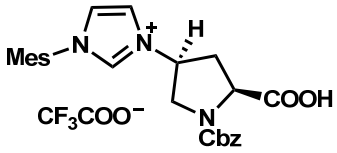

A mixture of 3-((3*S*,5*S*)-1-(benzyloxycarbonyl)-5-(methoxycarbonyl)pyrrolidin-3-yl)-1-mesityl-1*H*-imidazol-3-ium trifluoroacetate (121 mg, 0.215 mmol) and LiOH (31.8 mg, 1.07 mmol) in MeOH/H_2O (20 mL, 3/1, v/v) was stirred at 0 ˚C for 4 hours. After removing of MeOH under reduced pressure, the aqueous solution was neutralized with 1N HCl (aq.) to pH=5 and extracted with EtOAc (3 x 20 mL). The organic layer was collected, washed with water, brine in turn and dried over $MgSO_4$. Evaporation of solvent gave pure product as a white foam (111 mg, 94%).

The NMR spectra are reported for a mixture of two rotamers: ^{1}H NMR (500 MHz, DMSO-*d*6, 293 K) δ 9.60 (d, *J* = 5.6 Hz, 1H), 8.23 (d, *J* = 4.9 Hz, 1H), 7.97 (s, 1H), 7.47-7.27 (m, 5H), 7.13 (s, 2H), 5.15 (dd, *J* = 15.7, 7.3 Hz, 2H), 5.08 (dd, *J* = 12.8, 8.4 Hz, 1H), 4.50 (dd, *J* = 9.1, 5.0 Hz, 0.5H), 4.40 (dd, *J* = 8.9, 5.5 Hz, 0.5H), 4.22-4.11 (m, 1H), 4.06 (dd, *J* = 12.4, 12.4, 4.9 Hz, 1H), 3.13-2.88 (m, 1H), 2.66 (ddd, *J* = 13.4, 4.9, 4.9 Hz, 1H), 2.57 (dd, *J* = 16.3, 4.5, 4.5 Hz, 1H), 2.33 (s, 3H), 2.04 (d, *J* = 4.6 Hz, 3H), 2.02 (s, 3H); ^{13}C NMR (125 MHz, DMSO-*d*6, 293 K) δ 172.77, 172.42, 158.37 (q, $J_{C\text{-}F}$ = 36.4 Hz), 153.94, 153.70, 140.31, 137.18, 136.56, 134.61, 131.24, 129.19, 128.48, 128.38, 128.04, 127.75, 127.13, 124.21, 122.37, 122.02, 119.46, 115.73 (q, $J_{C\text{-}F}$ = 291.1 Hz), 66.57, 66.45, 57.85, 57.53, 57.15, 57.00, 50.65, 50.23, 35.41, 34.48, 20.63, 17.05;

^{1}H NMR (500 MHz, DMSO-*d*6, 353 K) δ 9.53 (s, 1H), 8.16 (dd, *J* = 1.8, 1.8 Hz, 1H), 7.90 (dd, *J* = 1.7, 1.7 Hz, 1H), 7.44-7.25 (m, 5H), 7.13 (s, 2H), 5.22 (dddd, *J* = 6.2, 6.2,

6.2, 6.2 Hz, 1H), 5.18-5.07 (m, 2H), 4.65-4.34 (m, 1H), 4.22 (dd, J = 11.8, 6.7 Hz, 1H), 4.03 (dd, J = 11.8, 5.3 Hz, 1H), 3.07 (ddd, J = 14.2, 9.0, 7.1 Hz, 1H), 2.58 (dd, J = 19.8, 12.9 Hz, 1H), 2.34 (s, 3H), 2.04 (s, 6H); ^{13}C NMR (125 MHz, DMSO-*d*6, 353 K) δ 171.98, 157.77 (q, $J_{C\text{-}F}$ = 36.4 Hz), 153.47, 139.99, 136.81, 136.23, 134.16, 130.85, 128.82, 127.96, 127.44, 127.02, 123.94, 121.99, 115.44 (q, $J_{C\text{-}F}$ = 291.7 Hz), 66.22, 57.08, 50.35, 34.84, 20.14, 16.51;

LC/MS (ESI) calculated for $C_{25}H_{28}N_3O_4$ $[M\text{-}CF_3COO]^+$ 434.21, found 433.89 (t_R = 9.97 min); HRMS ($^+$ESI) calculated for $C_{25}H_{28}N_3O_4$ $[M\text{-}CF_3COO]^+$ 434.2074, found 434.2074.

3-((3*S*,5*S*)-1-(*tert*-butoxycarbonyl)-5-(methoxycarbonyl)pyrrolidin-3-yl)-1-mesityl-1*H*-imidazol-3-ium trifluoroacetate (3.24)

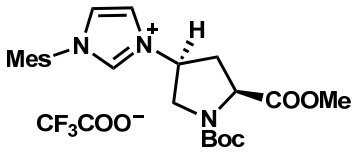

To a solution of 3-((3*S*,5*S*)-1-(benzyloxycarbonyl)-5-(methoxycarbonyl)pyrrolidin-3-yl)-1-mesityl-1*H*-imidazol-3-ium trifluoroacetate (110 mg, 0.196 mmol) and di-*tert*-butyl dicarbonate (64.2 mg, 0.294 mmol) in 5 mL of methanol was added 10 wt.% palladium on charcoal (25%, 27.5 mg). The reaction mixture was allowed to stir overnight under atmospheric pressure of hydrogen at room temperature while monitored by analytical HPLC. After filtration through Celite 545, the solvent was evaporated under reduced pressure to give white foam. The product was subjected to preparative HPLC (Column:

XBridge BEH C_{18} OBD Prep 5 μm, 19 x 150 mm; wavelength: 215 nm, 254 nm; temperature: ambient; solvent A: 0.1% trifluoroacetic acid in H_2O, solvent B: 0.1% trifluoroacetic acid in MeCN; flow rate: 12 mL/min. Held at 0% B for 1 min, ramped to 100% B over 17 min, ramped to 0% B over 1 min and held for 1 min.) to give pure product (97 mg, 94%).

The NMR spectra are reported for a mixture of two rotamers: ^{1}H NMR (500 MHz, DMSO-*d*6, 293 K) δ 9.58 (s, 1H), 8.22 (dd, *J* = 1.5, 1.5 Hz, 1H), 7.97 (s, 1H), 7.14 (s, 2H), 5.19–5.11 (m, 1H), 4.40 (ddd, *J* = 8.5, 8.5, 4.4 Hz, 1H), 4.12– 4.04 (m, 1H), 4.00–3.92 (m, 1H), 3.64 (s, 2H), 3.62 (s, 1H), 3.05–2.92 (m, 1H), 2.57 (ddd, *J* = 22.9, 13.2, 6.5 Hz, 1H), 2.33 (s, 3H), 2.05 (s, 3H), 2.03 (s, 3H), 1.42 (s, 4.5H), 1.35 (s, 4.5H); ^{13}C NMR (125 MHz, DMSO-*d*6, 293 K) δ 172.26, 171.85, 158.57 (q, $J_{C\text{-}F}$ = 292.4 Hz), 153.32, 152.72, 140.40, 137.27, 134.63, 131.28, 129.27, 124.27, 122.33, 116.02 (q, $J_{C\text{-}F}$ = 292.4 Hz), 80.02, 79.89, 57.67, 57.21, 56.95, 52.15, 50.41, 50.14, 35.11, 34.36, 28.02, 27.82, 20.61, 16.98, 16.95;

^{1}H NMR (500 MHz, DMSO-*d*6, 353 K) δ 9.53 (s, 1H), 8.14 (dd, *J* = 1.6, 1.6 Hz, 1H), 7.90 (dd, *J* = 1.5, 1.5 Hz, 1H), 7.13 (s, 2H), 5.21 (dddd, *J* = 6.5, 6.5, 6.5, 6.5 Hz, 1H), 4.42 (ddd, *J* = 11.8, 5.9, 5.9 Hz, 1H), 4.13 (ddd, *J* = 14.5, 7.3, 7.3 Hz, 1H), 3.92 (dd, *J* = 11.7, 5.8 Hz, 1H), 3.66 (s, 3H), 3.04 (ddd, *J* = 13.9, 8.7, 7.0 Hz, 1H), 2.61–2.52 (m, 1H), 2.34 (s, 3H), 2.05 (s, 6H), 1.41 (s, 9H); ^{13}C NMR (125 MHz, DMSO-*d*6, 353 K) δ 171.63, 158.02 (q, $J_{C\text{-}F}$ = 35.5 Hz), 152.64, 140.08, 136.90, 134.16, 130.91, 128.90, 124.01, 121.96, 115.75 (q, $J_{C\text{-}F}$ = 292.8 Hz), 79.70, 56.94, 51.59, 50.16, 34.67, 27.60, 20.13, 16.44;

LC/MS (ESI) calculated for $C_{23}H_{32}N_3O_4$ $[M\text{-}CF_3COO]^+$ 414.24, found 413.60 (t_R = 10.22 min); HRMS ($^+$ESI) calculated for $C_{23}H_{32}N_3O_4$ $[M\text{-}CF_3COO]^+$ 414.2387, found 414.2391.

3-((3*S*,5*S*)-1-(benzyloxycarbonyl)-5-((*S*)-1-methoxy-1-oxopropan-2-ylcarbamoyl)pyrrolidin-3-yl)-1-mesityl-1*H*-imidazol-3-ium trifluoroacetate (3.25)

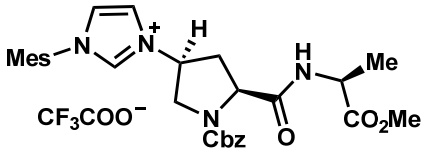

A mixture of 3-((3*S*,5*S*)-1-(benzyloxycarbonyl)-5-carboxypyrrolidin-3-yl)-1-mesityl-1*H*-imidazol-3-ium trifluoroacetate (500 mg, 0.857 mmol), EDCI (328 mg, 1.71 mmol) and HOBt (231 mg, 1.71 mmol) was stirred in 10 mL of anhydrous DCM at 0 ˚C for 5 min. In a separate flask, alanine methyl ester hydrochloride (180 mg, 1.29 mmol) was stirred for 10 min in 10 mL of anhydrous DCM after which the mixture was added to the active ester. The resulting solution was warmed to room temperature and stirred for 24 hours. After evaporation of DCM under reduced pressure, the residue was washed with 20 mL of anhydrous diethyl ether twice and then purified by preparative HPLC (Column: XBridge BEH C_{18} OBD Prep 5 μm, 19 x 150 mm; wavelength: 215 nm, 254 nm; temperature: ambient; solvent A: 0.1% trifluoroacetic acid in H_2O, solvent B: 0.1% trifluoroacetic acid in MeCN; flow rate: 12 mL/min. Held at 0% B for 1 min, ramped to 100% B over 17 min, ramped to 0% B over 1 min and held for 1 min.) to yield product (533 mg, 91%) as a white foam.

The NMR spectra are reported for a mixture of two rotamers: ^{1}H NMR (400 MHz, DMSO-*d*6, 293 K) δ 9.43 (s, 1H), 8.68 (d, *J* = 6.9 Hz, 0.5H), 8.67 (d, *J* = 6.9 Hz, 0.5H), 8.18 (br s, 0.5H), 8.16 (br s, 0.5H), 7.92 (br s, 0.5H), 7.92 (br s, 0.5H), 7.29-7.39 (m, 5H), 7.12 (s, 1H), 5.17 (br, 1H), 5.05-5.14 (m, 2H), 4.43-4.51 (m, 1H), 4.16-4.24 (m, 1H), 4.10-4.13 (br, 2H), 3.52 (s, 1.5H), 3.51 (s, 1.5H), 2.95-3.07 (m, 1H), 2.39-2.47 (m, 1H), 2.32 (s, 3H), 2.03 (s, 3H), 2.01 (s, 3H), 1.29 (d, *J* = 7.3 Hz, 1.5H), 1.18 (d, *J* = 7.3 Hz, 1.5H); ^{13}C NMR (100 MHz, DMSO-*d*6, 293 K) δ 172.97, 172.83, 171.11, 170.98, 158.38 (q, $J_{C\text{-}F}$ = 35 Hz), 153.86, 153.61, 140.24, 137.16, 136.62, 136.51, 134.75, 134.69, 131.32, 129.15, 128.47, 128.30, 128.00, 127.79, 127.73, 127.13, 123.97, 122.36, 116.14 (q, $J_{C\text{-}F}$ = 293 Hz), 66.48, 66.40, 58.35, 58.18, 57.66, 57.41, 51.95, 51.27, 50.90, 47.47, 36.55, 35.70, 30.71, 20.60, 16.95, 16.86, 16.76, 16.70;

^{1}H NMR (400 MHz, DMSO-*d*6, 353 K) δ 9.39 (s, 1H), 8.47 (d, *J* = 6.9 Hz, 1H), 8.12 (dd, *J* = 1.8, 1.8 Hz, 1H), 7.86 (dd, *J* = 1.8, 1.8 Hz, 1H), 7.29-7.36 (m, 5H), 7.12 (s, 1H), 5.21-5.25 (m, 1H), 5.09 (dd, *J* = 24.7, 12.8 Hz, 2H), 4.52 (dd, *J* = 9.6, 4.1 Hz, 1H), 4.25 (dddd, *J* = 7.3, 7.3, 7.3, 7.3 Hz, 1H), 4.20 (dd, *J* = 12.4, 6.9 Hz), 4.08 (dd, *J* = 11.9, 4.1 Hz), 3.54 (s, 3H), 3.05 (m, 1H), 2.44 (ddd, *J* = 14.2, 4.1, 4.1 Hz, 1H), 2.34 (s, 3H), 2.04 (s, 6H), 1.25 (d, *J* = 6.9 Hz, 3H); ^{13}C NMR (100 MHz, DMSO-*d*6, 353 K) δ 172.33, 170.69, 157.82 (q, $J_{C\text{-}F}$ = 35 Hz), 153.44, 139.96, 136.76, 136.24, 134.26, 130.93, 128.84, 128.78, 127.92, 127.42, 127.02, 123.74, 122.01, 115.88 (q, $J_{C\text{-}F}$ = 293 Hz), 66.16, 66.07, 57.76, 51.39, 51.36, 51.19, 47.27, 35.84, 30.11, 20.13, 16.40, 16.33;

LC/MS (ESI) calculated for $C_{29}H_{35}N_4O_5$ $[M\text{-}CF_3COO]^+$ 519.26, found 518.94 (t_R = 10.14 min); HRMS ($^{+}$ESI) calculated for $C_{29}H_{35}N_4O_5$ $[M\text{-}CF_3COO]^+$ 519.2602, found 519.2602.

1-mesityl-3-((3*S*,5*S*)-5-((*S*)-1-methoxy-1-oxopropan-2-ylcarbamoyl)pyrrolidin-3-yl)-1*H*-imidazol-3-ium trifluoroacetate (3.26)

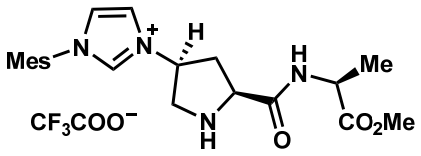

To a solution of 3-((3*S*,5*S*)-1-(benzyloxycarbonyl)-5-((*S*)-1-methoxy-1-oxopropan-2-ylcarbamoyl)pyrrolidin-3-yl)-1-mesityl-1*H*-imidazol-3-ium trifluoroacetate (528 mg, 0.790 mmol) in 30 mL of ethyl acetate was added 20 wt.% palladium hydroxide on carbon (100%, 528 mg). The reaction mixture was stirred for 18 hours under atmospheric pressure of hydrogen at room temperature. After filtration, the solvent was evaporated under reduced pressure to give a pure product (400 mg, 95%):

^{1}H NMR (500 MHz, DMSO-*d*6) δ 9.44 (s, 1H), 9.23 (d, *J* = 6.9 Hz, 1H), 8.20 (s, 1H), 7.99 (dd, *J* = 1.7, 1.7 Hz, 1H), 5.37 (ddd, *J* = 12.6, 6.3, 6.3 Hz, 1H), 4.54 (dd, *J* = 8.0, 8.0 Hz, 1H), 5.37 (ddd, *J* = 14.3, 7.2, 7.2 Hz, 1H), 3.90-3.98 (m, 2H), 3.57 (s, 1H), 3.14-3.20 (m, 1H), 2.32 (s, 3H), 2.03 (s, 6H), 1.33 (d, *J* = 7.5 Hz, 3H); ^{13}C NMR (100 MHz, DMSO-*d*6, 293 K) δ 172.44, 167.27, 158.44 (q, $J_{C\text{-}F}$ = 35 Hz), 140.38, 137.27, 134.56, 134.49, 131.11, 129.22, 124.44, 122.01, 116.70 (q, $J_{C\text{-}F}$ = 294 Hz), 57.84, 57.71, 52.16, 49.21, 48.00, 35.53, 20.61, 16.94, 16.66; LC/MS (ESI) calculated for $C_{21}H_{29}N_4O_3$ [M-CF_3COO]$^+$ 385.22, found 385.01 (t_R = 9.05 min); HRMS ($^+$ESI) calculated for $C_{21}H_{29}N_4O_3$ [M-CF_3COO]$^+$ 385.2234, found 385.2244.

3-((3*S*,5*S*)-1-((*S*)-2-(*tert*-butoxycarbonylamino)propanoyl)-5-((*S*)-1-methoxy-1-oxopropan-2-ylcarbamoyl)pyrrolidin-3-yl)-1-mesityl-1*H*-imidazol-3-ium trifluoroacetate (3.27)

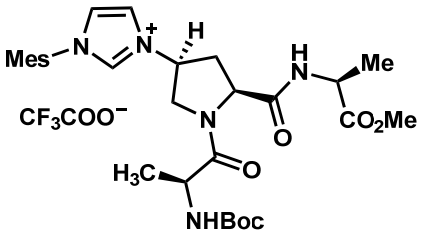

A mixture of BocN-Ala-OH (20.4 mg, 0.108 mmol), EDCI (34.3 mg, 0.180 mmol) and HOBt (24.3 mg, 0.180 mmol) was stirred in 3 mL of anhydrous DCM at 0 ˚C for 5 min. In a separate flask, 1-mesityl-3-((3*S*,5*S*)-5-((*S*)-1-methoxy-1-oxopropan-2-ylcarbamoyl)pyrrolidin-3-yl)-1*H*-imidazol-3-ium trifluoroacetate (44.8 mg, 0.0898 mmol) and triethyl amine (0.0250 mL, 0.180 mmol) were stirred for 10 min in 3 mL of anhydrous DCM after which the mixture was added to the active ester. The resulting solution was warmed to room temperature and stirred for 24 hours. After evaporation of DCM under reduced pressure, the residue was washed with 5 mL of anhydrous diethyl ether (twice) and then purified by preparative HPLC (Column: XBridge BEH C_{18} OBD Prep 5 μm, 19 x 150 mm; wavelength: 215 nm, 254 nm; temperature: ambient; solvent A: 0.1% trifluoroacetic acid in H_2O, solvent B: 0.1% trifluoroacetic acid in MeCN; flow rate: 12 mL/min. Held at 0% B for 1 min, ramped to 100% B over 17 min, ramped to 0% B over 1 min and held for 1 min.) to yield product (36 mg, 61%) as a white foam.

The NMR spectra are reported for a mixture of two rotamers: ^{1}H NMR (500 MHz, DMSO-*d*6, 293 K) δ 9.42 (s, 1H), 8.56 (s, 0.5H), 8.55 (s, 0.5H), 8.18 (s, 1H), 7.93 (s, 1H), 7.13 (s, 2H), 7.10 (s, 0.5H), 7.08 (s, 0.5H), 5.21 (ddd, *J* = 11.3, 5.7, 5.7 Hz, 1H), 4.49 (dd, *J* = 9.3, 4.8 Hz, 1H), 4.33 (dd, *J* = 13.4, 6.7 Hz, 2H), 4.23–4.15 (m, 3H), 3.52 (s, 3H), 2.93 (dd, *J* = 14.0, 7.1 Hz, 1H), 2.35 (dd, *J* = 7.2, 7.2 Hz, 1H), 2.32 (s, 3H), 2.02 (s, 6H), 1.37 (s, 9H), 1.27 (d, *J* = 7.3 Hz, 3H), 1.14 (d, *J* = 6.9 Hz, 3H); ^{13}C NMR (125 MHz, DMSO-*d*6, 293 K) δ 173.00, 171.24, 170.56, 158.16 (q, $J_{C\text{-}F}$ = 34.2 Hz), 155.21, 140.28, 137.06, 134.74, 134.61, 131.28, 129.19, 129.14, 123.97, 122.34, 116.41 (q, $J_{C\text{-}F}$ = 297.5 Hz), 78.10, 58.48, 57.78, 51.91, 50.71, 47.56, 47.50, 34.54, 28.25, 20.61, 16.93, 16.86, 16.81;

^{1}H NMR (500 MHz, DMSO-*d*6, 353 K) δ 9.38 (s, 1H), 8.33 (br s, 1H), 8.12 (s, 1H), 7.88 (s, 1H), 7.13 (s, 2H), 6.67 (br s, 1H), 5.26 (br s, 1H), 4.59 (br s, 1H), 4.36 (br s, 1H), 4.25 (ddd, *J* = 14.7, 7.4, 7.4 Hz, 1H), 4.14 (br s, 1H), 3.55 (s, 3H), 2.96 (br s, 1H), 2.34 (s, 3H), 2.04 (s, 6H), 1.39 (s, 9H), 1.31 (d, *J* = 7.3 Hz, 3H), 1.20 (d, *J* = 6.8 Hz, 3H); ^{13}C NMR (125 MHz, DMSO-*d*6, 353 K) δ 172.36, 171.08, 170.18, 157.63 (q, $J_{C\text{-}F}$ = 33.7 Hz), 154.51, 139.98, 136.69, 134.18, 130.88, 128.82, 123.75, 122.00, 116.16 (q, $J_{C\text{-}F}$ = 296.4 Hz), 77.91, 58.34, 57.61, 51.35, 50.77, 47.44, 47.27, 33.63, 27.87, 20.12, 16.38;

LC/MS (ESI) calculated for $C_{29}H_{42}N_5O_6$ $[M\text{-}CF_3COO]^+$ 556.31, found 555.98 (t_R = 10.35 min); HRMS ($^{+}$ESI) calculated for $C_{29}H_{42}N_5O_6$ $[M\text{-}CF_3COO]^+$ 556.3130, found 556.3145.

3-((3*S*,5*S*)-1-(benzyloxycarbonyl)-5-((1*S*,2*S*)-2-(diphenylphosphoryl)-1,2-diphenylethylcarbamoyl)pyrrolidin-3-yl)-1-mesityl-1*H*-imidazol-3-ium trifluoroacetate (3.55)

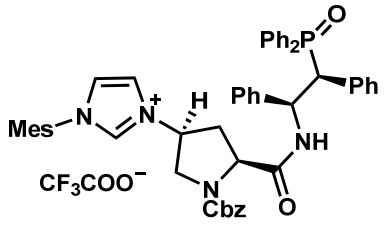

A mixture of 3-((3*S*,5*S*)-1-(benzyloxycarbonyl)-5-carboxypyrrolidin-3-yl)-1-mesityl-1*H*-imidazol-3-ium trifluoroacetate (85.0 mg, 0.155 mmol), EDCI (92.6 mg, 0.233 mmol) and HOBt (41.9 mg, 0.310 mmol) was stirred in 3 mL of anhydrous DCM at 0 ˚C for 5 min. In a separate flask, (1*S*,2*S*)-2-(diphenylphosphoryl)-1,2-diphenylethanamine (92.6 mg, 0.233 mmol) was stirred for 10 min in 3 mL of anhydrous DCM after which the mixture was added to the active ester. The resulting solution was warmed to room temperature and stirred for 24 hours. After evaporation of DCM under reduced pressure, the residue was washed with 5 mL of anhydrous diethyl ether twice and then purified by preparative HPLC (Column: XBridge BEH C_{18} OBD Prep 5 μm, 19 x 150 mm; wavelength: 215 nm, 254 nm; temperature: ambient; solvent A: 0.1% trifluoroacetic acid in H_2O, solvent B: 0.1% trifluoroacetic acid in MeCN; flow rate: 12 mL/min. Held at 0% B for 1 min, ramped to 100% B over 17 min, ramped to 0% B over 1 min and held for 1 min.) to yield product (103 mg, 72%) as a colorless oil.

The NMR spectra are reported for a mixture of two rotamers: ^{1}H NMR (400 MHz, DMSO-*d*6, 293 K) δ 9.78 (s, 0.5H), 9.73 (s, 0.5H), 8.67 (d, J = 9.0 Hz, 0.5H), 8.58 (d, J =

8.9 Hz, 0.5H), 8.13 (s, 1H), 8.09 – 7.96 (m, 2H), 7.93 (d, *J* = 7.1 Hz, 1H), 7.56 – 7.43 (m, 3H), 7.40 – 7.27 (m, 4H), 7.21 (dt, *J* = 14.0, 6.9 Hz, 11H), 7.08 – 6.82 (m, 8H), 5.68 – 5.50 (m, 1H), 5.10 (d, *J* = 7.9 Hz, 1H), 4.95 (dd, *J* = 25.5, 12.7 Hz, 1H), 4.76 (d, *J* = 6.5 Hz, 1H), 4.40 (d, *J* = 12.9 Hz, 0.5H), 4.26 (d, *J* = 6.7 Hz, 0.5H), 4.06 (dd, *J* = 12.2, 6.9 Hz, 1H), 4.01 – 3.87 (m, 1H), 2.61 – 2.51 (m, 1H), 2.36 (s, 3H), 2.23 (dd, *J* = 13.9, 6.6 Hz, 0.5H), 2.10 (dd, *J* = 24.0, 9.9 Hz, 6H), 2.03 (d, *J* = 3.5 Hz, 0.5H); ^{13}C NMR (100 MHz, DMSO-*d*6, 293 K) δ 170.58, 169.91, 158.56 (q, $J_{C\text{-}F}$ = 36.8 Hz), 154.03, 153.45, 140.17, 137.81, 136.57, 136.44, 135.94, 134.85, 134.37, 133.38, 131.58, 131.33, 130.64, 130.55, 130.23, 130.15, 129.10, 128.66, 128.55, 128.47, 128.22, 128.06, 127.85, 127.69, 127.61, 127.21, 126.78, 126.57, 124.03, 122.25, 115.71 (q, $J_{C\text{-}F}$ = 290.8 Hz) 66.66, 65.98, 58.72, 58.32, 58.08, 57.47, 55.14, 54.97, 52.19, 51.51, 48.57, 48.32, 47.93, 47.65, 35.11, 33.92, 20.69, 17.11, 1.19; ^{31}P NMR (161 MHz, DMSO-*d*6, 293 K) δ 31.99;

^{1}H NMR (400 MHz, DMSO-*d*6, 353 K) δ 9.65 (s, 1H), 8.56 (d, *J* = 8.9 Hz, 1H), 8.05 (t, *J* = 11.2 Hz, 1H), 8.01 – 7.93 (m, 2H), 7.85 (d, *J* = 1.4 Hz, 1H), 7.55 – 7.32 (m, 6H), 7.30 – 7.06 (m, 14H), 7.03 – 6.86 (m, 7H), 5.61 (dt, *J* = 13.9, 8.6 Hz, 1H), 5.21 – 5.13 (m, 1H), 5.01 (d, *J* = 12.5 Hz, 1H), 4.67 (t, *J* = 7.6 Hz, 1H), 4.24 (s, 1H), 4.15 (dd, *J* = 12.1, 7.0 Hz, 1H), 3.94 (dd, *J* = 12.0, 3.6 Hz, 1H), 2.67 (dt, *J* = 14.6, 8.5 Hz, 1H), 2.37 (s, 3H), 2.25 – 2.17 (m, 1H), 2.07 (s, 6H), 2.04 (d, *J* = 4.9 Hz, 1H); ^{13}C NMR (100 MHz, DMSO-*d*6, 353 K) δ 169.81, 157.98 (q, $J_{C\text{-}F}$ = 36.6 Hz), 153.48, 140.03, 139.96, 139.89, 137.26, 136.18, 135.62, 134.37, 134.24, 133.99, 133.31, 133.00, 131.11, 130.84, 130.27, 130.19, 129.97, 129.89, 128.78, 128.19, 128.07, 127.89, 127.39, 127.27, 127.14, 126.36, 126.18,

123.74, 121.95, 115.41 (q, $J_{C\text{-}F}$ = 291.4 Hz), 66.09, 58.29, 57.60, 55.16, 51.65, 48.79, 48.13, 34.48, 20.20, 16.56, 0.61; ^{31}P NMR (161 MHz, DMSO-*d*6, 353 K) δ 31.68;

LC/MS (ESI) calculated for $C_{51}H_{50}N_4O_4P$ $[M\text{-}CF_3COO]^+$ 813.36, found 813.50 (t_R = 11.13 min); HRMS ($^+$ESI) calculated for $C_{51}H_{50}N_4O_4P$ $[M\text{-}CF_3COO]^+$ 813.3564, found 813.3564.

(*S*)-3-(2-(*tert*-butoxycarbonylamino)-3-methoxy-3-oxopropyl)-1-mesityl-1*H*-imidazol-3-ium trifluoroacetate (3.61)

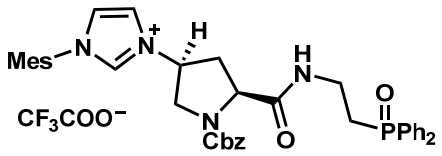

A mixture of 3-((3*S*,5*S*)-1-(benzyloxycarbonyl)-5-carboxypyrrolidin-3-yl)-1-mesityl-1*H*-imidazol-3-ium trifluoroacetate (526 mg, 0.961 mmol), EDCI (275 mg, 1.44 mmol) and HOBt (195 mg, 1.44 mmol) was stirred in 10 mL of anhydrous DCM at 0 ˚C for 5 min. In a separate flask, 2-phosphorylethylamine (251 mg, 1.02 mmol) was stirred for 10 min in 10 mL of anhydrous DCM after which the mixture was added to the active ester. The resulting solution was warmed to room temperature and stirred for 24 hours. After evaporation of DCM under reduced pressure, the residue was washed with 20 mL of anhydrous diethyl ether twice and then purified by preparative HPLC (Column: XBridge BEH C_{18} OBD Prep 5 μm, 19 x 150 mm; wavelength: 215 nm, 254 nm; temperature: ambient; solvent A: 0.1% trifluoroacetic acid in H_2O, solvent B: 0.1% trifluoroacetic acid in MeCN; flow rate: 12 mL/min. Held at 0% B for 1 min, ramped to 100% B over 17 min,

ramped to 0% B over 1 min and held for 1 min.) to yield product (597 mg, 91%) as a colorless oil.

The NMR spectra are reported for a mixture of two rotamers: ^{1}H NMR (400 MHz, DMSO-*d*6, 293 K) δ 9.61 (s, 1H), 8.41 (d, *J* = 18.3 Hz, 1H), 8.22 (s, 1H), 7.91 (s, 1H), 7.80 – 7.64 (m, 4H), 7.56 (t, *J* = 6.3 Hz, 2H), 7.52 (dt, *J* = 11.0, 4.7 Hz, 4H), 7.43 – 7.15 (m, 5H), 7.08 (s, 2H), 5.22 – 5.08 (m, 2H), 5.02 (dd, *J* = 22.0, 12.8 Hz, 1H), 4.44 – 4.31 (m, 1H), 4.18 (dd, *J* = 11.6, 6.2 Hz, 1H), 4.08 – 4.00 (m, 1H), 3.23 (dd, *J* = 31.1, 7.4 Hz, 2H), 2.94 (dt, *J* = 23.3, 11.9 Hz, 1H), 2.56 (d, *J* = 13.5 Hz, 1H), 2.46 – 2.34 (m, 1H), 2.30 (s, 3H), 2.00 (s, 3H), 1.99 (s, 3H); ^{13}C NMR (100 MHz, DMSO-*d*6, 293 K) δ 170.97, 170.73, 158.62 (q, $J_{C\text{-}F}$ = 36.9 Hz), 154.05, 153.82, 140.31, 137.38, 136.59, 134.59, 133.70, 132.73, 131.90, 131.29, 130.45, 130.36, 129.22, 128.93, 128.82, 128.50, 128.26, 128.05, 127.81, 127.18, 124.04, 122.47, 115.72 (q, $J_{C\text{-}F}$ = 290.9 Hz), 66.62, 66.43, 58.83, 58.36, 58.12, 57.27, 51.62, 51.20, 35.90, 34.98, 32.88, 29.10, 28.42, 20.62, 16.98; ^{31}P NMR (161 MHz, DMSO-*d*6, 293 K) δ 29.38, 29.12;

^{1}H NMR (400 MHz, DMSO-*d*6, 353 K) δ 9.57 (s, 1H), 8.24 – 8.18 (m, 1H), 8.18 – 8.12 (m, 1H), 7.87 – 7.81 (m, 1H), 7.70 (ddd, *J* = 11.0, 9.8, 4.2 Hz, 4H), 7.57 (ddt, *J* = 8.6, 7.2, 2.8 Hz, 2H), 7.51 (tdd, *J* = 6.8, 4.7, 2.4 Hz, 4H), 7.37 – 7.20 (m, 4H), 7.08 (s, 2H), 5.26 – 5.17 (m, 1H), 5.10 (dd, *J* = 37.4, 12.7 Hz, 2H), 4.41 (dd, *J* = 9.1, 4.7 Hz, 1H), 4.23 (dd, *J* = 12.0, 6.9 Hz, 1H), 4.02 (dd, *J* = 12.0, 4.8 Hz, 1H), 3.37 – 3.17 (m, 2H), 3.02 – 2.89 (m, 1H), 2.58 – 2.51 (m, 1H), 2.33 (s, 3H), 2.03 (s, 6H); ^{13}C NMR (100 MHz, DMSO-*d*6, 353 K) δ 170.51, 158.05 (q, $J_{C\text{-}F}$ = 36.8 Hz), 153.64, 140.02, 137.00, 136.27, 134.18, 133.56, 132.59, 131.40, 130.94, 130.09, 130.00, 128.88, 128.44, 128.33, 127.93, 127.44,

127.07, 123.77, 122.15, 115.43 (q, $J_{C\text{-}F}$ = 290.9 Hz), 66.26, 58.43, 57.40, 51.32, 35.31, 32.69, 28.99, 28.30, 20.16, 16.49; ^{31}P NMR (161 MHz, DMSO-*d*6, 353 K) δ 29.34;

LC/MS (ESI) calculated for $C_{39}H_{42}N_4O_4P$ $[M\text{-}CF_3COO]^+$ 661.29, found 661.28 (t_R = 10.27 min); HRMS ($^+$ESI) calculated for $C_{39}H_{42}N_4O_4P$ $[M\text{-}CF_3COO]^+$ 661.2938, found 661.2939.

3-((3*S*,5*S*)-1-(*tert*-butoxycarbonyl)-5-(2-(diphenylphosphoryl)ethylcarbamoyl)pyrrolidin-3-yl)-1-mesityl-1*H*-imidazol-3-ium trifluoroacetate (3.62)

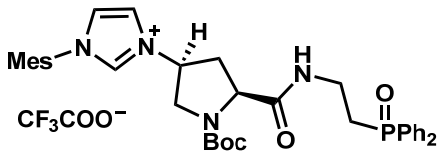

A mixture of 3-((3*S*,5*S*)-1-(*tert*-butoxycarbonyl)-5-carboxypyrrolidin-3-yl)-1-mesityl-1*H*-imidazol-3-ium trifluoroacetate (323 mg, 0.555 mmol), EDCI (212 mg, 1.11 mmol) and HOBt (150 mg, 1.11 mmol) was stirred in 10 mL of anhydrous DCM at 0 ˚C for 5 min. In a separate flask, 2-phosphorylethylamine (204 mg, 0.832 mmol) was stirred for 10 min in 10 mL of anhydrous DCM after which the mixture was added to the active ester. The resulting solution was warmed to room temperature and stirred for 24 hours. After evaporation of DCM under reduced pressure, the residue was washed with 20 mL of anhydrous diethyl ether twice and then purified by preparative HPLC (Column: XBridge BEH C_{18} OBD Prep 5 μm, 19 x 150 mm; wavelength: 215 nm, 254 nm; temperature:

ambient; solvent A: 0.1% trifluoroacetic acid in H_2O, solvent B: 0.1% trifluoroacetic acid in MeCN; flow rate: 12 mL/min. Held at 0% B for 1 min, ramped to 100% B over 17 min, ramped to 0% B over 1 min and held for 1 min.) to yield product (326 mg, 79%) as a colorless oil.

The NMR spectra are reported for a mixture of two rotamers: ^{1}H NMR (400 MHz, DMSO-*d*6, 293 K) δ 9.62 (s, 0.5H), 9.60 (s, 0.5H), 8.41 (s, 0.5H), 8.34 (s, 0.5H), 8.23 (dd, *J* = 5.0, 3.4 Hz, 1H), 7.95 – 7.63 (m, 11H), 7.60 – 7.44 (m, 8H), 7.07 (s, 2H), 5.14 (d, *J* = 4.9 Hz, 1H), 4.31 – 4.19 (m, 1H), 4.14 – 4.03 (m, 1H), 3.98 – 3.83 (m, 1H), 3.49 – 3.34 (m, 1H), 3.34 (s, 1H), 3.23 – 3.08 (m, 1H), 2.97 – 2.67 (m, 3H), 2.65 – 2.52 (m, 2H), 2.46 (dd, *J* = 9.4, 4.0 Hz, 1H), 2.89 (s, 1.5H), 2.71 (s, 1.5H), 2.01 (s, 3H), 1.99 (s, 3H), 1.39 (s, 3H), 1.34 (s, 6H); ^{13}C NMR (100 MHz, DMSO-*d*6, 293 K) δ 171.46, 171.11, 162.46, 158.73 (q, $J_{C\text{-}F}$ = 36.5 Hz), 153.23, 140.37, 137.37, 134.63, 133.74, 133.66, 132.77, 132.69, 131.98, 131.34, 130.55, 130.48, 130.39, 129.28, 128.97, 128.86, 124.11, 122.51, 115.85 (q, $J_{C\text{-}F}$ = 291.1 Hz), 79.73, 79.56, 58.62, 58.04, 57.23, 51.51, 51.21, 35.87, 35.04, 33.46, 32.95, 30.83, 29.28, 28.59, 28.46, 28.08, 27.99, 27.77, 20.64, 17.01; ^{31}P NMR (161 MHz, DMSO-*d*6, 293 K) δ 29.57, 29.30, 28.88;

^{1}H NMR (400 MHz, DMSO-*d*6, 353 K) δ 9.56 (t, *J* = 5.5 Hz, 1H), 8.19 – 8.13 (m, 2H), 7.87 – 7.82 (m, 1H), 7.80 – 7.69 (m, 5H), 7.62 – 7.46 (m, 10H), 7.44 (s, 4H), 7.09 (s, 2H), 5.23 – 5.15 (m, 1H), 4.29 (dd, *J* = 8.9, 4.9 Hz, 1H), 4.13 (dt, *J* = 20.9, 10.4 Hz, 1H), 3.91 (dd, *J* = 11.8, 5.0 Hz, 1H), 3.52 – 3.31 (m, 2H), 3.31 – 3.18 (m, 1H), 3.00 – 2.90 (m, 1H), 2.89 (s, 1H), 2.76 – 2.71 (m, 1H), 2.58 (ddd, *J* = 15.1, 8.7, 3.4 Hz, 2H), 2.33 (s, 3H), 2.02 (s, 6H), 1.39 (s, 9H); ^{13}C NMR (100 MHz, DMSO-*d*6, 353 K) δ 170.98, 162.02, 158.16

(q, $J_{C\text{-}F}$ = 36.4 Hz), 153.06, 140.07, 136.98, 134.20, 133.60, 132.63, 131.44, 130.98, 130.18, 130.12, 130.03, 128.93, 128.49, 128.37, 123.82, 122.18, 115.56 (q, $J_{C\text{-}F}$ = 291.5 Hz), 79.45, 58.41, 57.37, 51.22, 35.39, 33.26, 32.73, 30.52, 29.12, 28.42, 27.73, 20.17, 16.50; ^{31}P NMR (161 MHz, DMSO-*d*6, 353 K) δ 29.52, 29.07;

LC/MS (ESI) calculated for $C_{36}H_{44}N_4O_4P$ $[M\text{-}CF_3COO]^+$ 627.31, found 661.23 (t_R = 10.22 min); HRMS ($^+$ESI) calculated for $C_{36}H_{44}N_4O_4P$ $[M\text{-}CF_3COO]^+$ 627.3095, found 627.3096.

APPENDIX B: NMR SPECTRA FOR CHAPTER 3

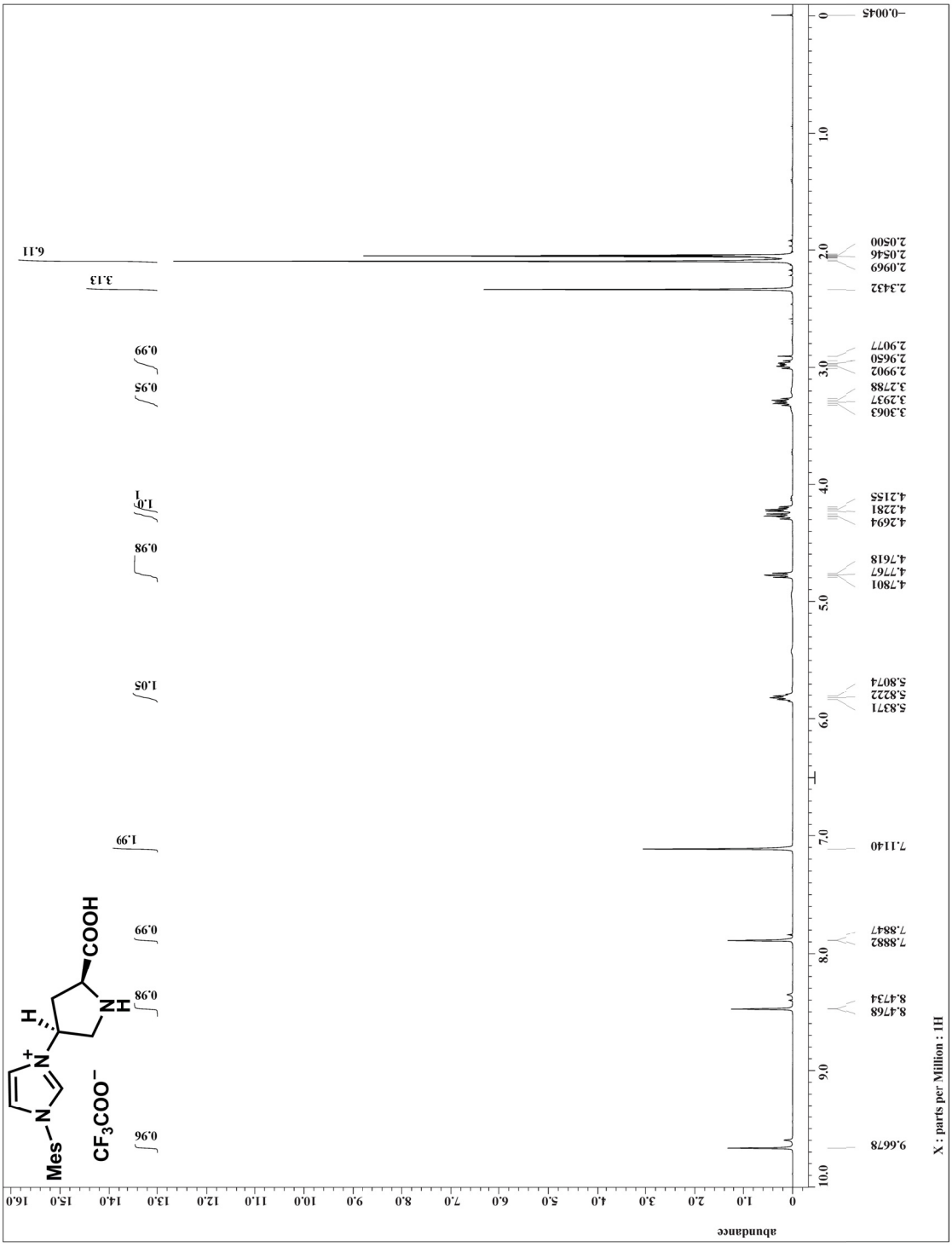

Figure 3.8: ^{1}H NMR (500 MHz, Acetone-*d6*) of 3-((3*S*,5*S*)-5-carboxypyrrolidin-3-yl)-1-mesityl-1*H*-imidazol-3-ium trifluoroacetate (**3.15**).

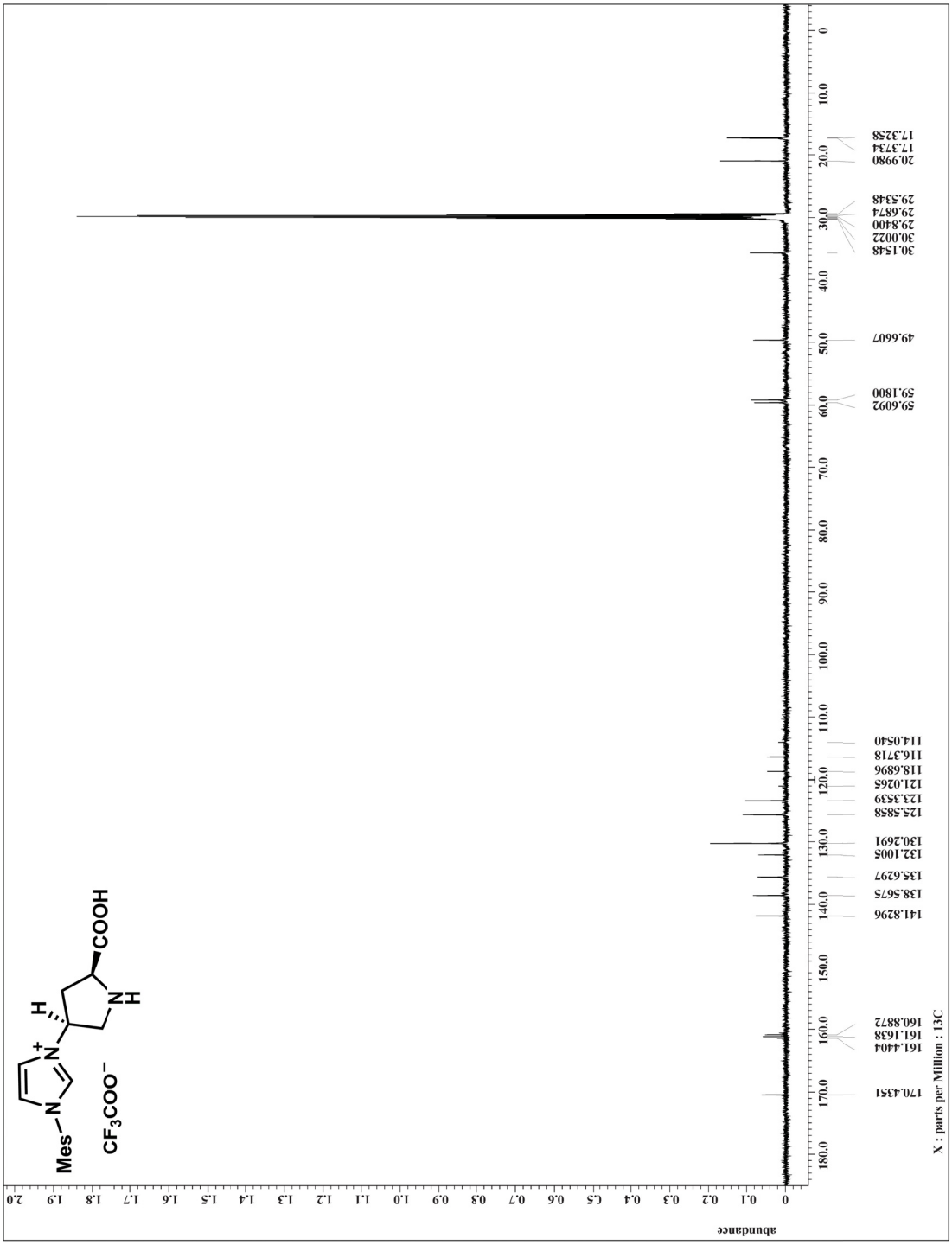

Figure 3.9: ^{13}C NMR (125 MHz, Acetone-*d*6) of 3-((3*S*,5*S*)-5-carboxypyrrolidin-3-yl)-1-mesityl-1*H*-imidazol-3-ium trifluoroacetate (**3.15**).

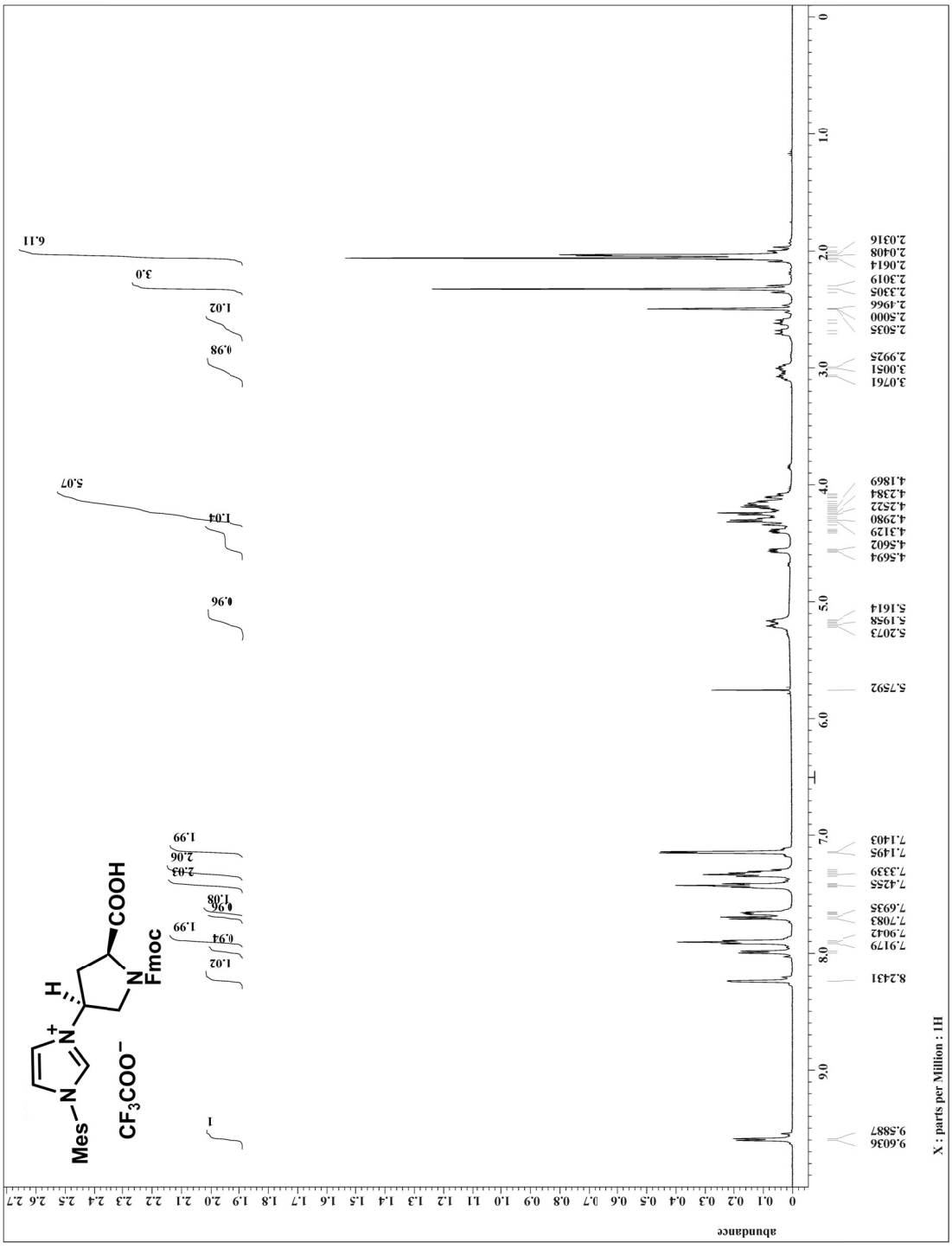

Figure 3.10: ^{1}H NMR (500 MHz, DMSO-*d*6, 293 K) of 3-((3*S*,5*S*)-1-(((9*H*-fluoren-9-yl)methoxy)carbonyl)-5-carboxypyrrolidin-3-yl)-1-mesityl-1*H*-imidazol-3-ium trifluoroacetate (**3.16**).

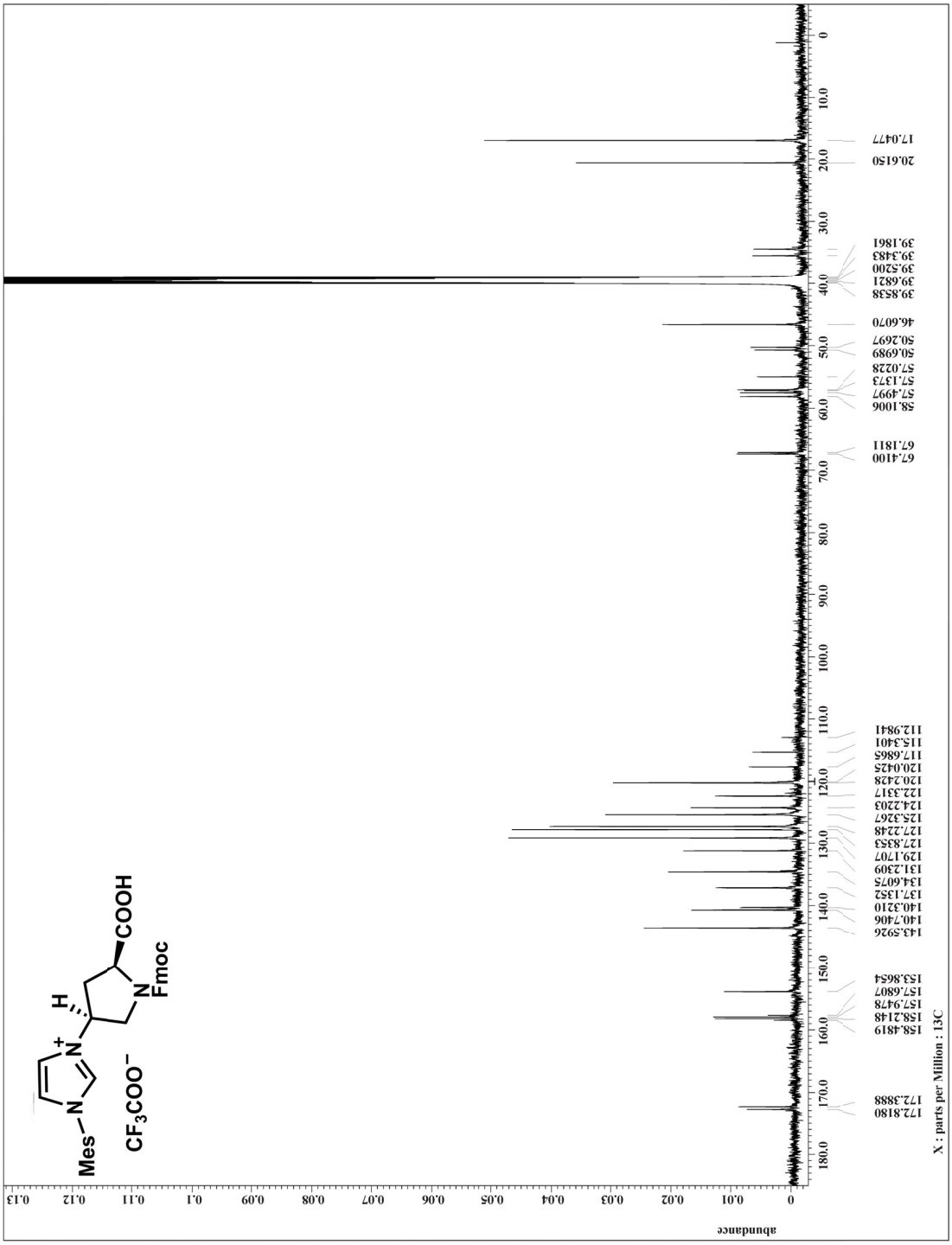

Figure 3.11: ^{13}C NMR (125 MHz, DMSO-*d*6, 293 K) of 3-((3*S*,5*S*)-1-(((9*H*-fluoren-9-yl)methoxy)carbonyl)-5-carboxypyrrolidin-3-yl)-1-mesityl-1*H*-imidazol-3-ium trifluoroacetate (**3.16**).

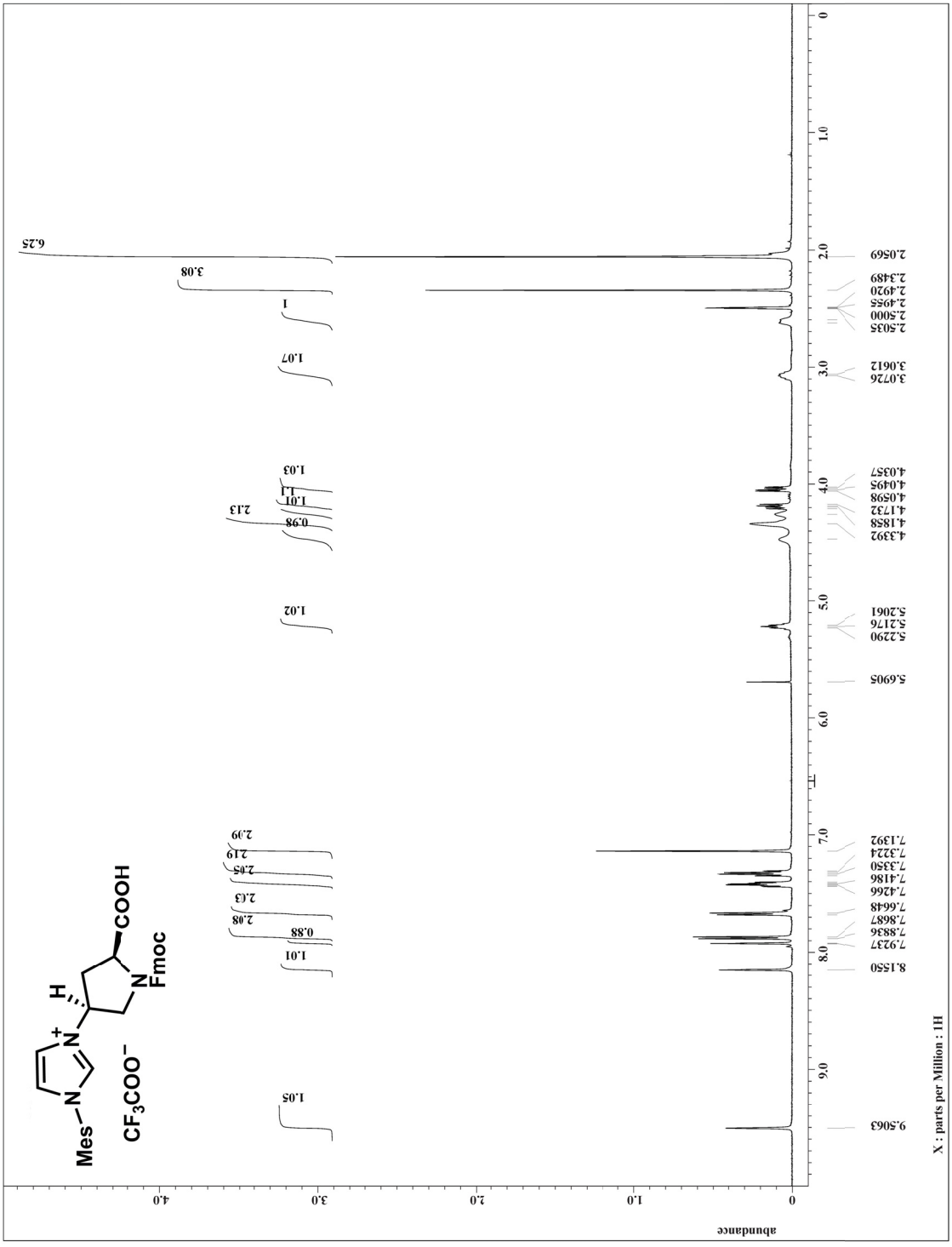

Figure 3.12: ^{1}H NMR (500 MHz, DMSO-*d*6, 353 K) of 3-((3*S*,5*S*)-1-(((9*H*-fluoren-9-yl)methoxy)carbonyl)-5-carboxypyrrolidin-3-yl)-1-mesityl-1*H*-imidazol-3-ium trifluoroacetate (**3.16**).

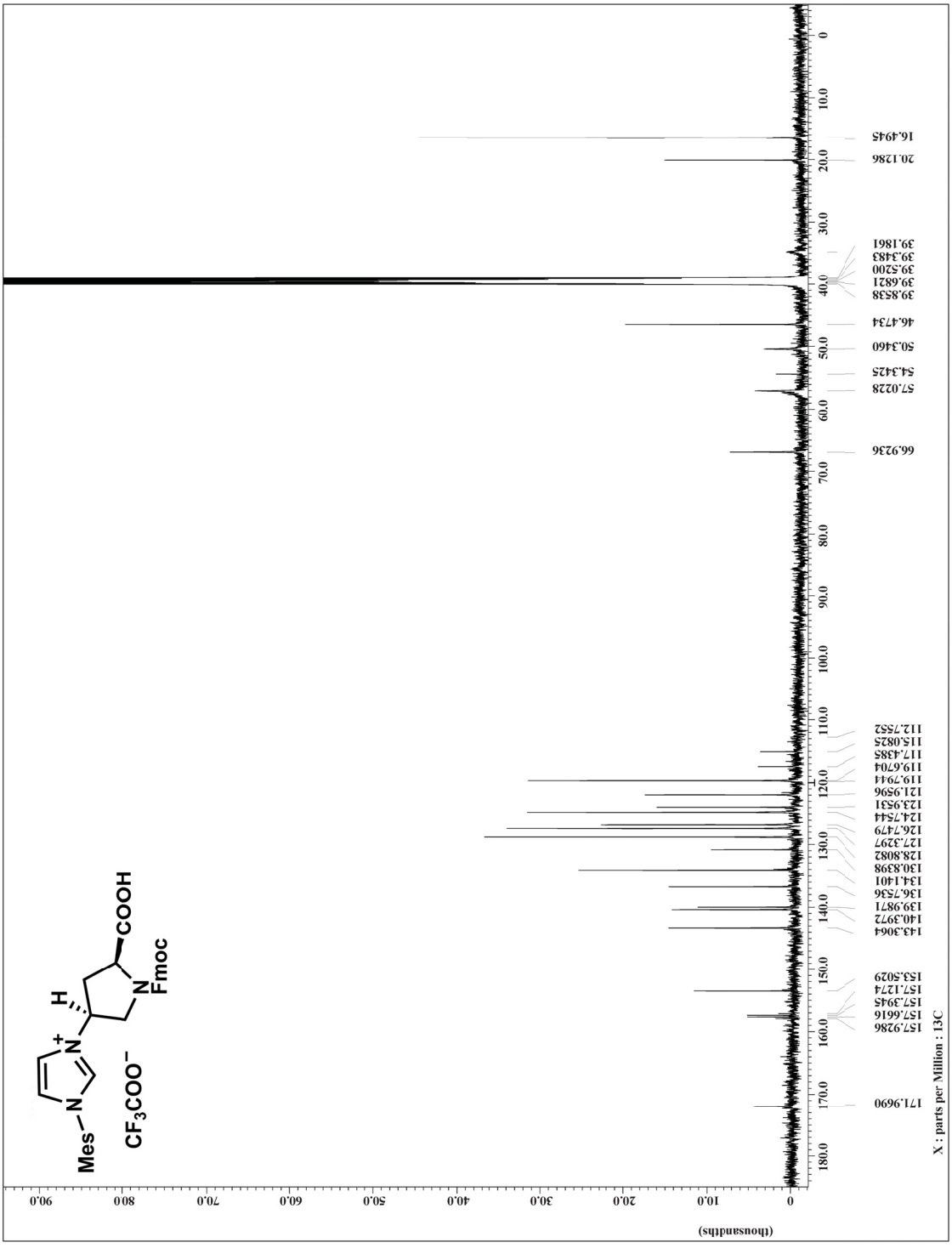

Figure 3.13: ^{13}C NMR (125 MHz, DMSO-*d*6, 353 K) of 3-((3*S*,5*S*)-1-(((9*H*-fluoren-9-yl)methoxy)carbonyl)-5-carboxypyrrolidin-3-yl)-1-mesityl-1*H*-imidazol-3-ium trifluoroacetate (**3.16**)

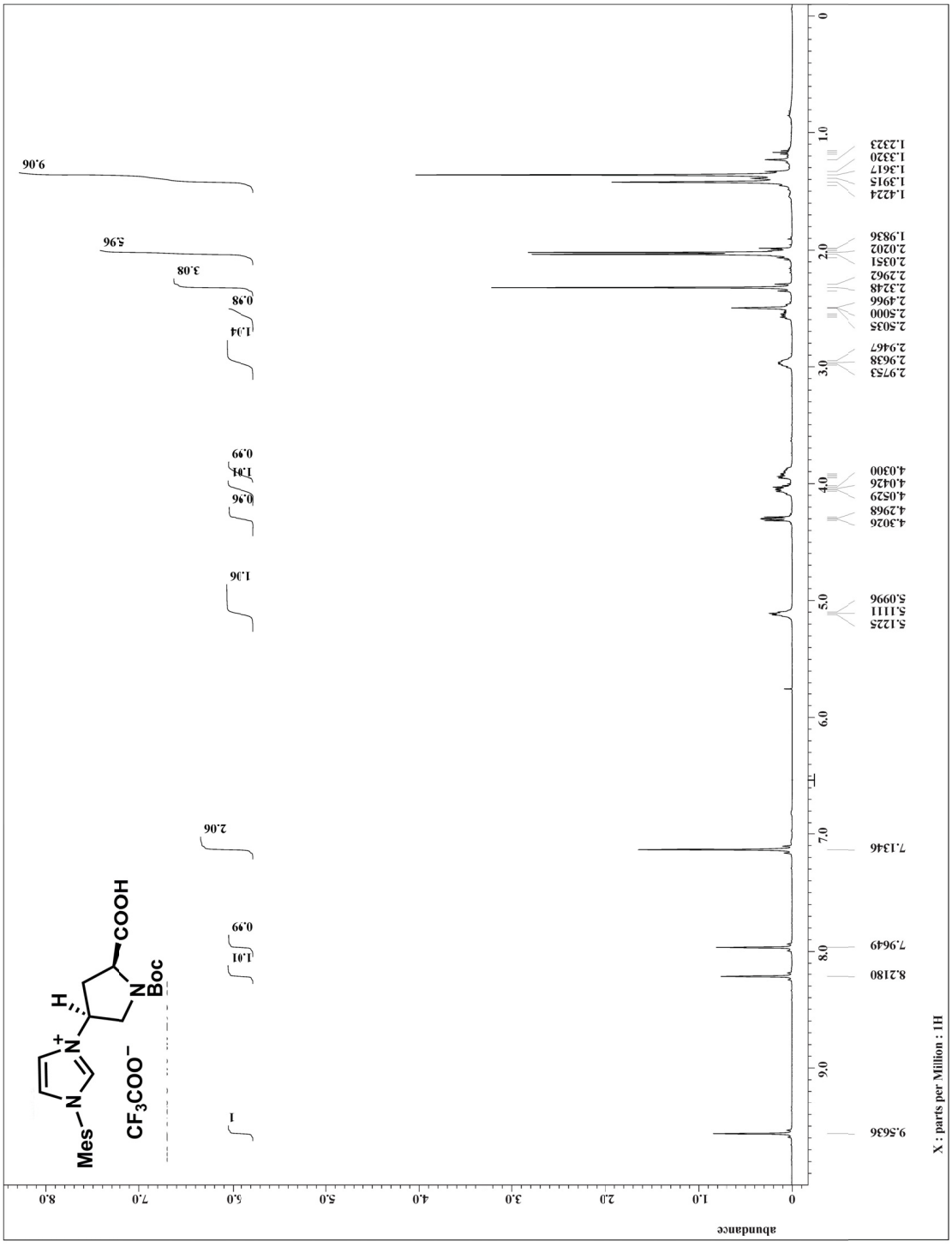

Figure 3.14: ^{1}H NMR (500 MHz, DMSO-*d*6, 293 K) of 3-((3*S*,5*S*)-1-(*tert*-butoxycarbonyl)-5-carboxypyrrolidin-3-yl)-1-mesityl-1*H*-imidazol-3-ium trifluoroacetate (**3.17**).

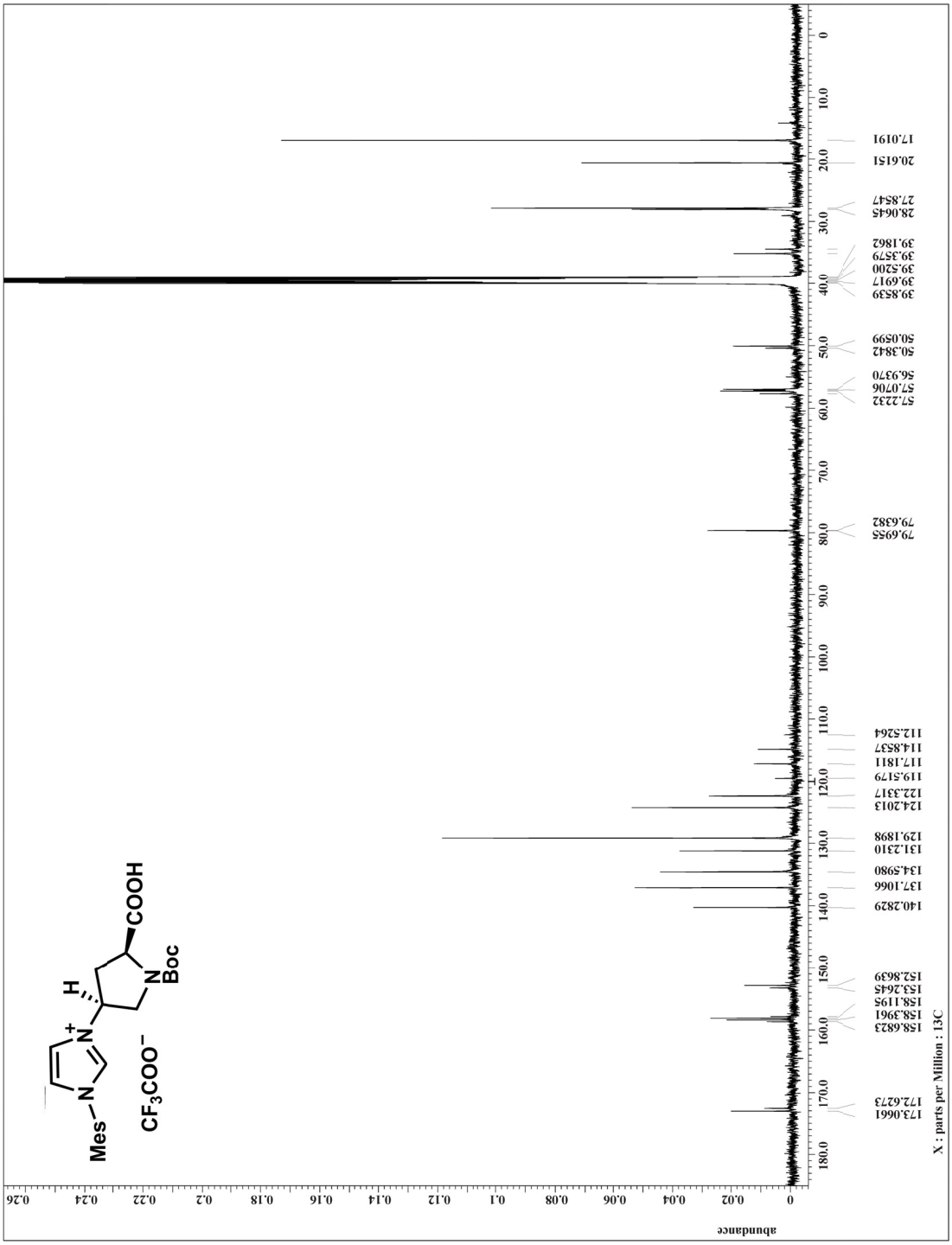

Figure 3.15: ^{13}C NMR (125 MHz, DMSO-*d*6, 293 K) of 3-((3*S*,5*S*)-1-(*tert*-butoxycarbonyl)-5-carboxypyrrolidin-3-yl)-1-mesityl-1*H*-imidazol-3-ium trifluoroacetate (**3.17**).

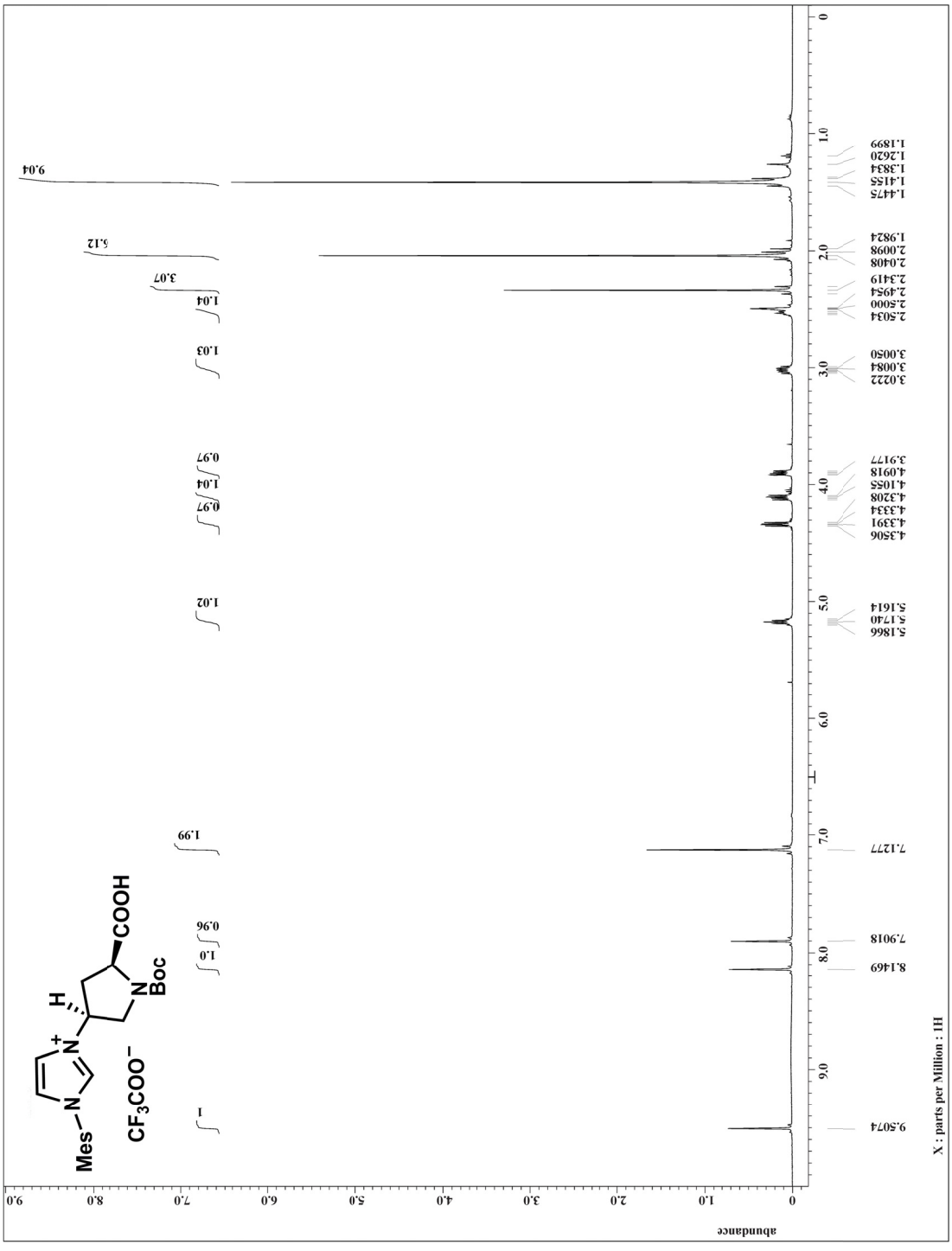

Figure 3.16: ^{1}H NMR (500 MHz, DMSO-*d*6, 353 K) of 3-((3*S*,5*S*)-1-(*tert*-butoxycarbonyl)-5-carboxypyrrolidin-3-yl)-1-mesityl-1*H*-imidazol-3-ium trifluoroacetate (**3.17**).

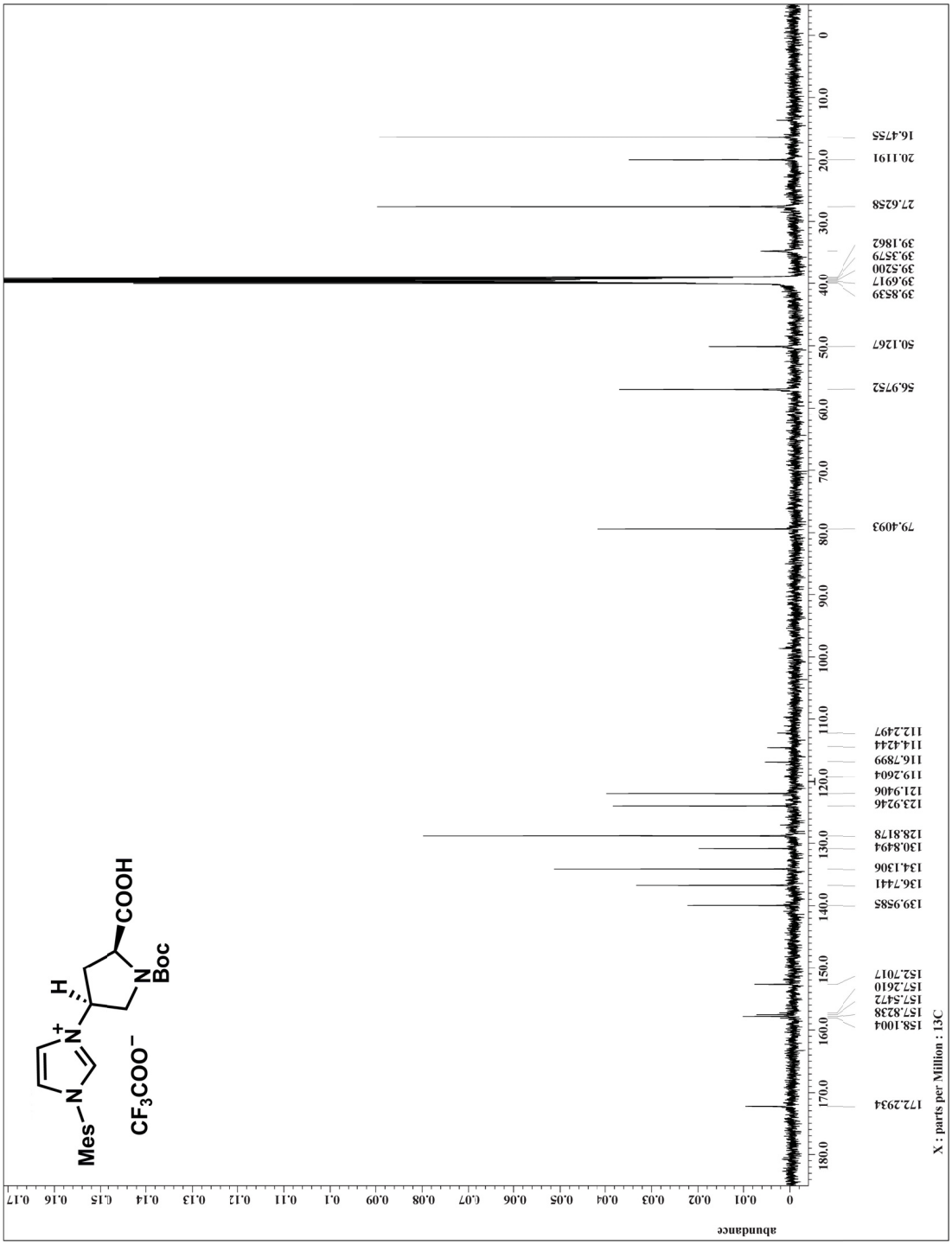

Figure 3.17: ^{13}C NMR (125 MHz, DMSO-*d*6, 353 K) of 3-((3*S*,5*S*)-1-(*tert*-butoxycarbonyl)-5-carboxypyrrolidin-3-yl)-1-mesityl-1*H*-imidazol-3-ium trifluoroacetate (**3.17**).

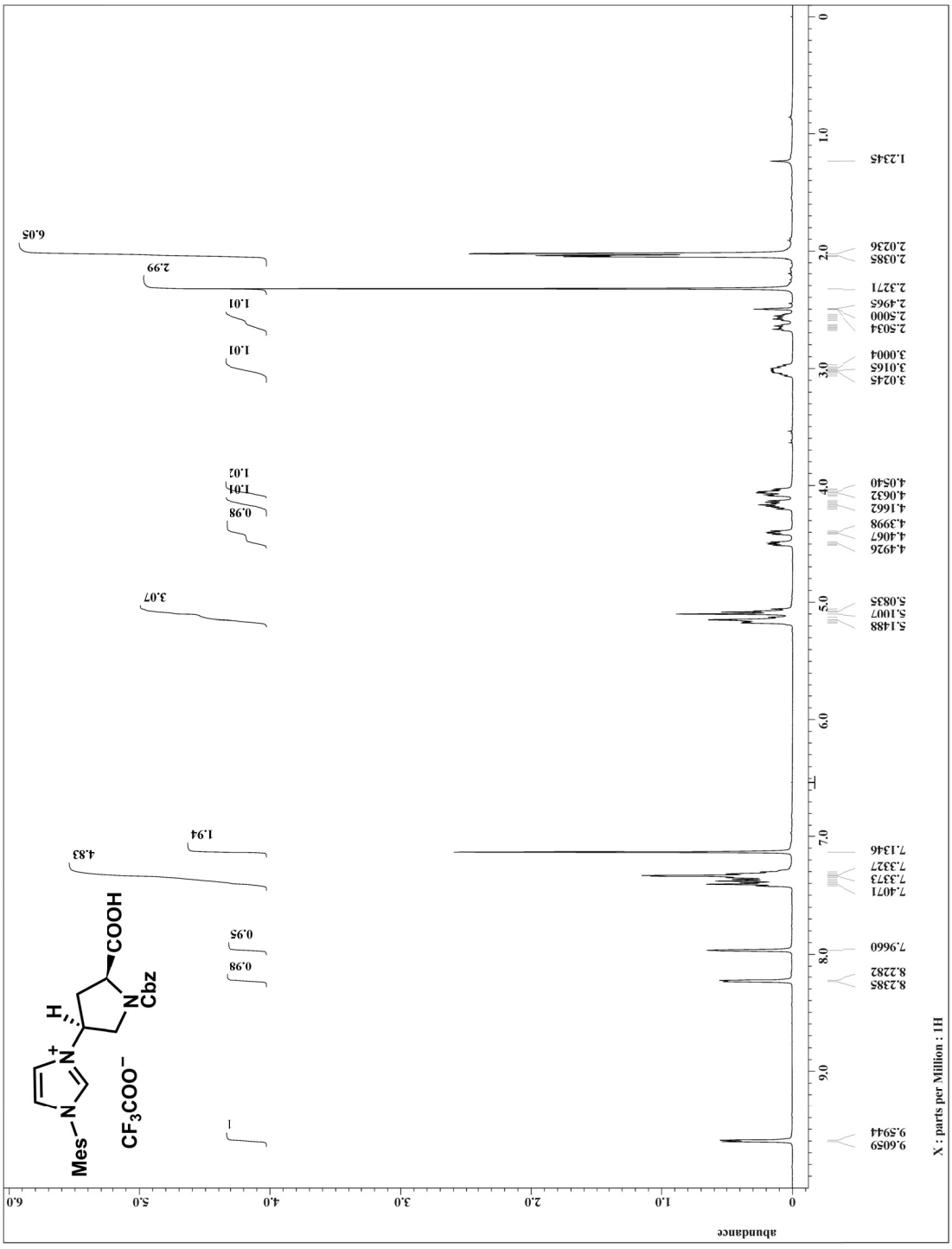

Figure 3.18: ^{1}H NMR (500 MHz, DMSO-*d*6, 293 K) of 3-((3*S*,5*S*)-1-(benzyloxycarbonyl)-5-carboxypyrrolidin-3-yl)-1-mesityl-1*H*-imidazol-3-ium trifluoroacetate (**3.18**).

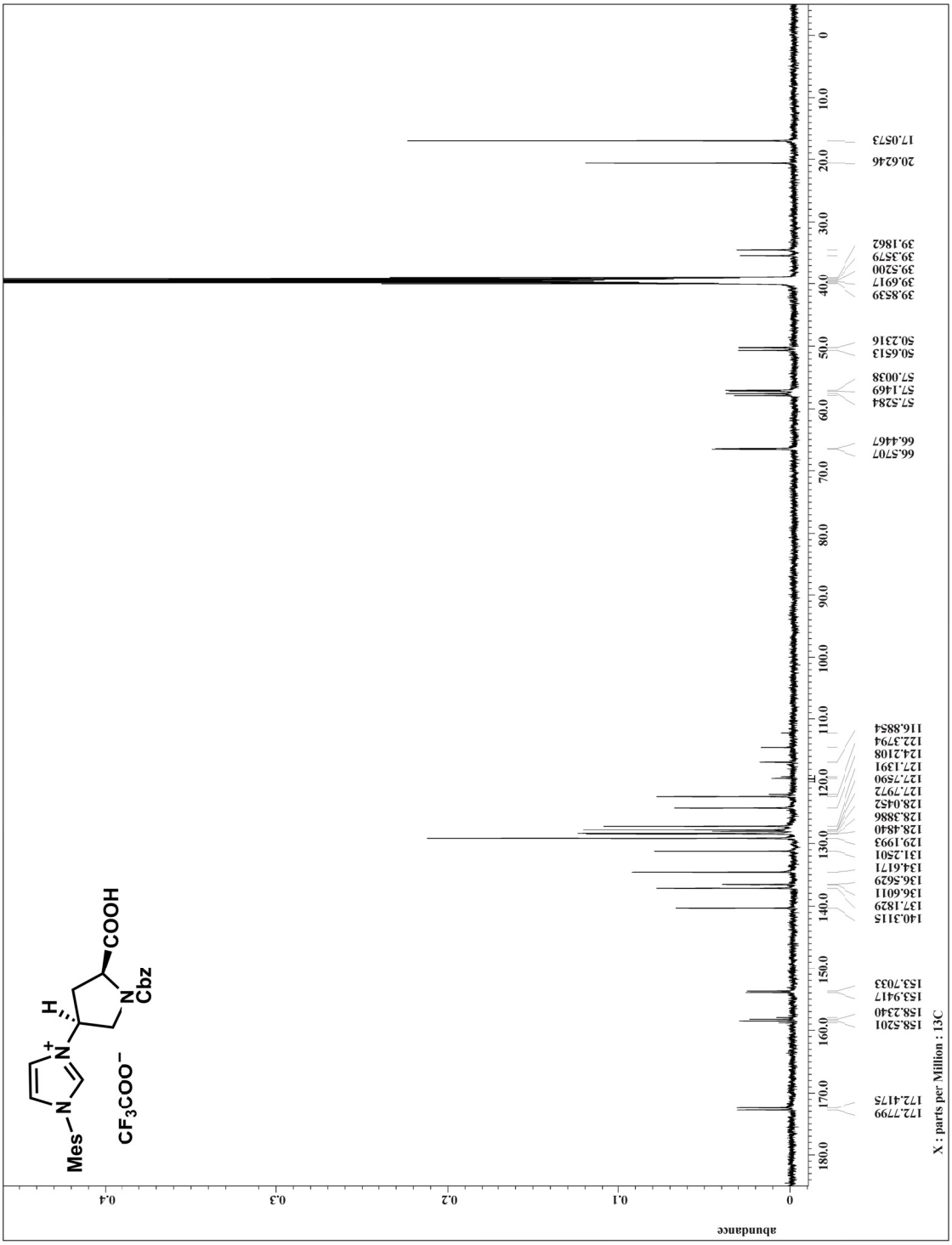

Figure 3.19: ^{13}C NMR (125 MHz, DMSO-*d*6, 293 K) of 3-((3*S*,5*S*)-1-(benzyloxycarbonyl)-5-carboxypyrrolidin-3-yl)-1-mesityl-1*H*-imidazol-3-ium trifluoroacetate (**3.18**).

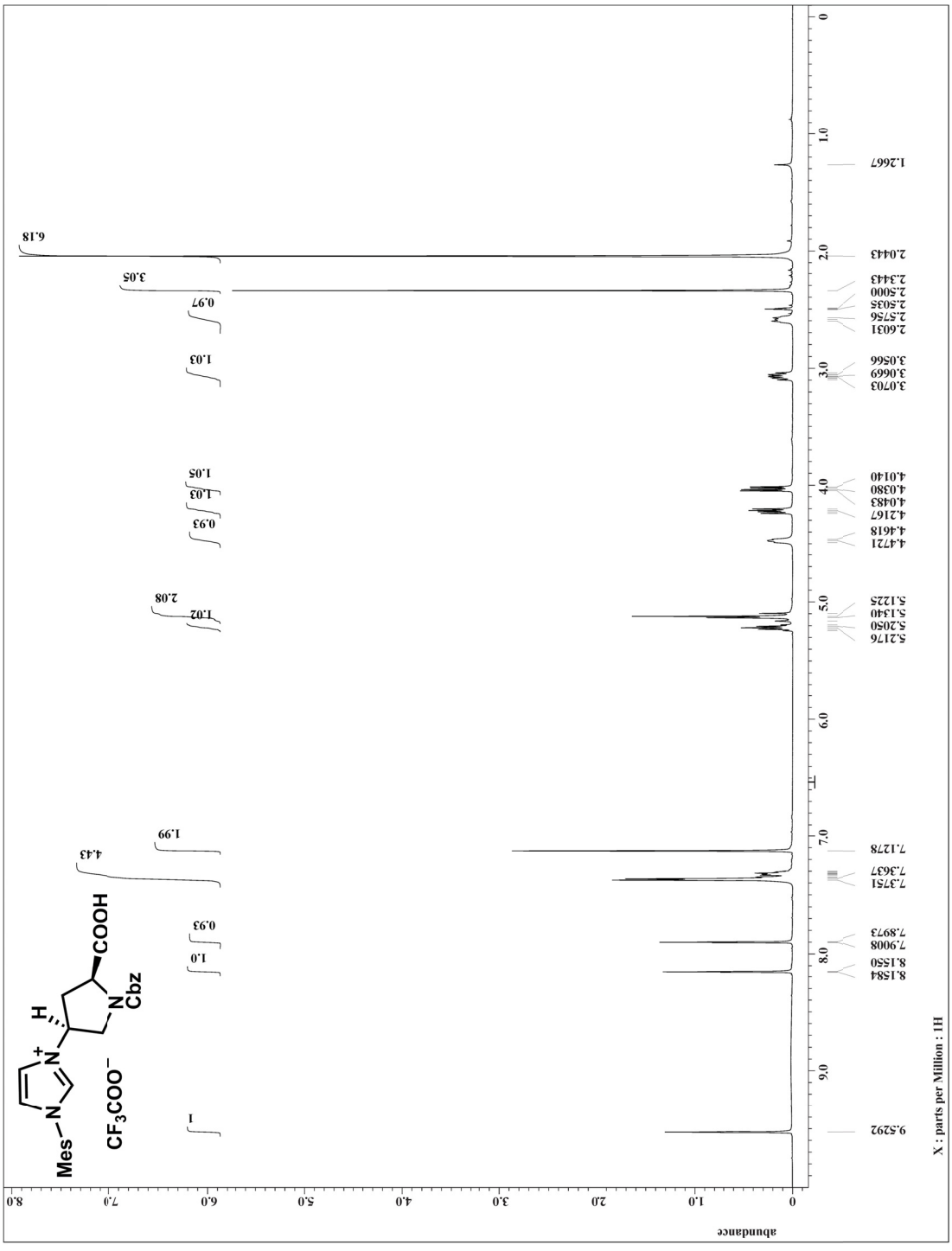

Figure 3.20: ^{1}H NMR (500 MHz, DMSO-*d*6, 353 K) of 3-((3*S*,5*S*)-1-(benzyloxycarbonyl)-5-carboxypyrrolidin-3-yl)-1-mesityl-1*H*-imidazol-3-ium trifluoroacetate (**3.18**).

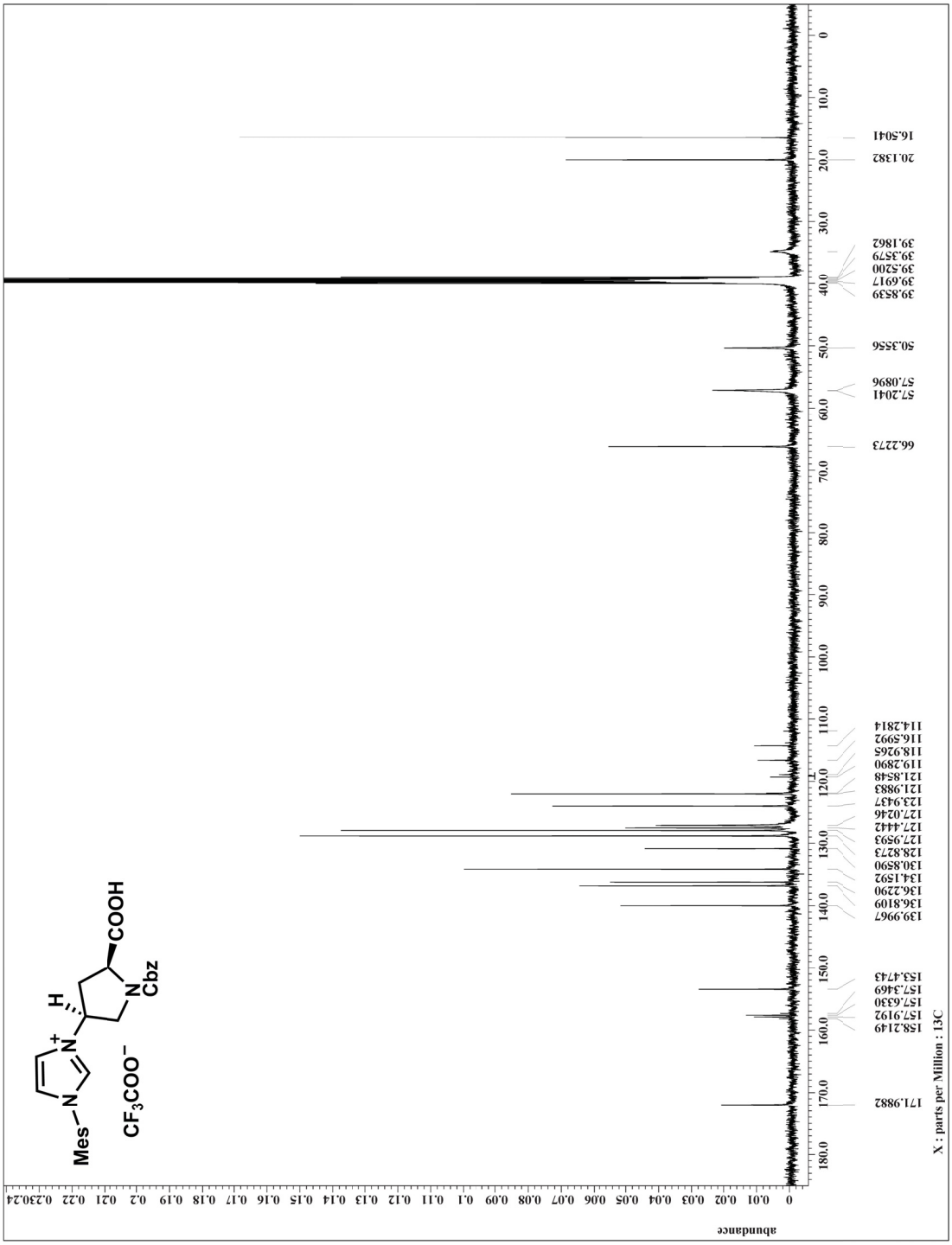

Figure 3.21: ^{13}C NMR (125 MHz, DMSO-*d*6, 353 K) of 3-((3*S*,5*S*)-1-(benzyloxycarbonyl)-5-carboxypyrrolidin-3-yl)-1-mesityl-1*H*-imidazol-3-ium trifluoroacetate (**3.18**).

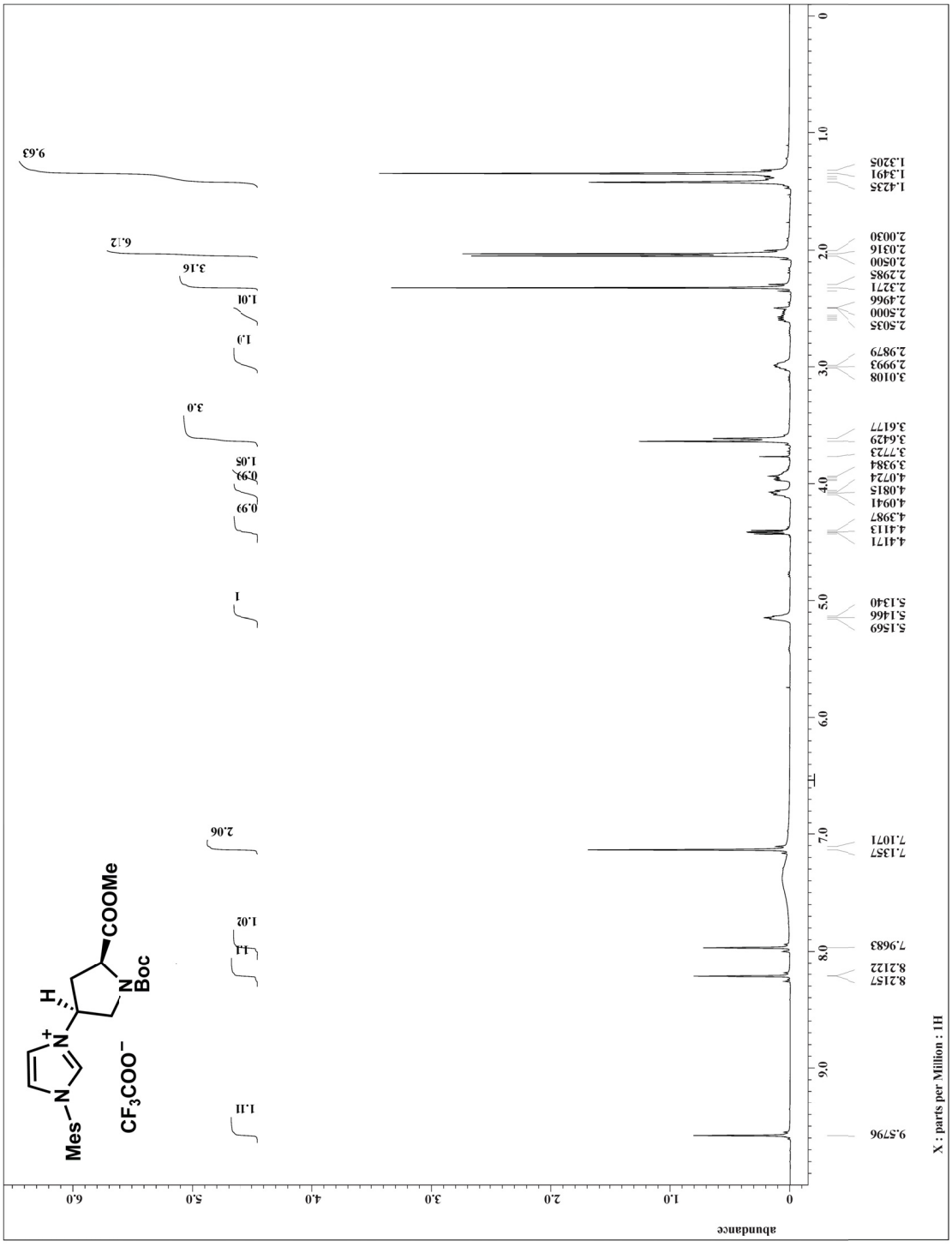

Figure 3.22: ^{1}H NMR (500 MHz, DMSO-*d*6, 293 K) of 3-((3*S*,5*S*)-1-(*tert*-butoxycarbonyl)-5-(methoxycarbonyl)pyrrolidin-3-yl)-1-mesityl-1*H*-imidazol-3-ium trifluoroacetate (**3.24**).

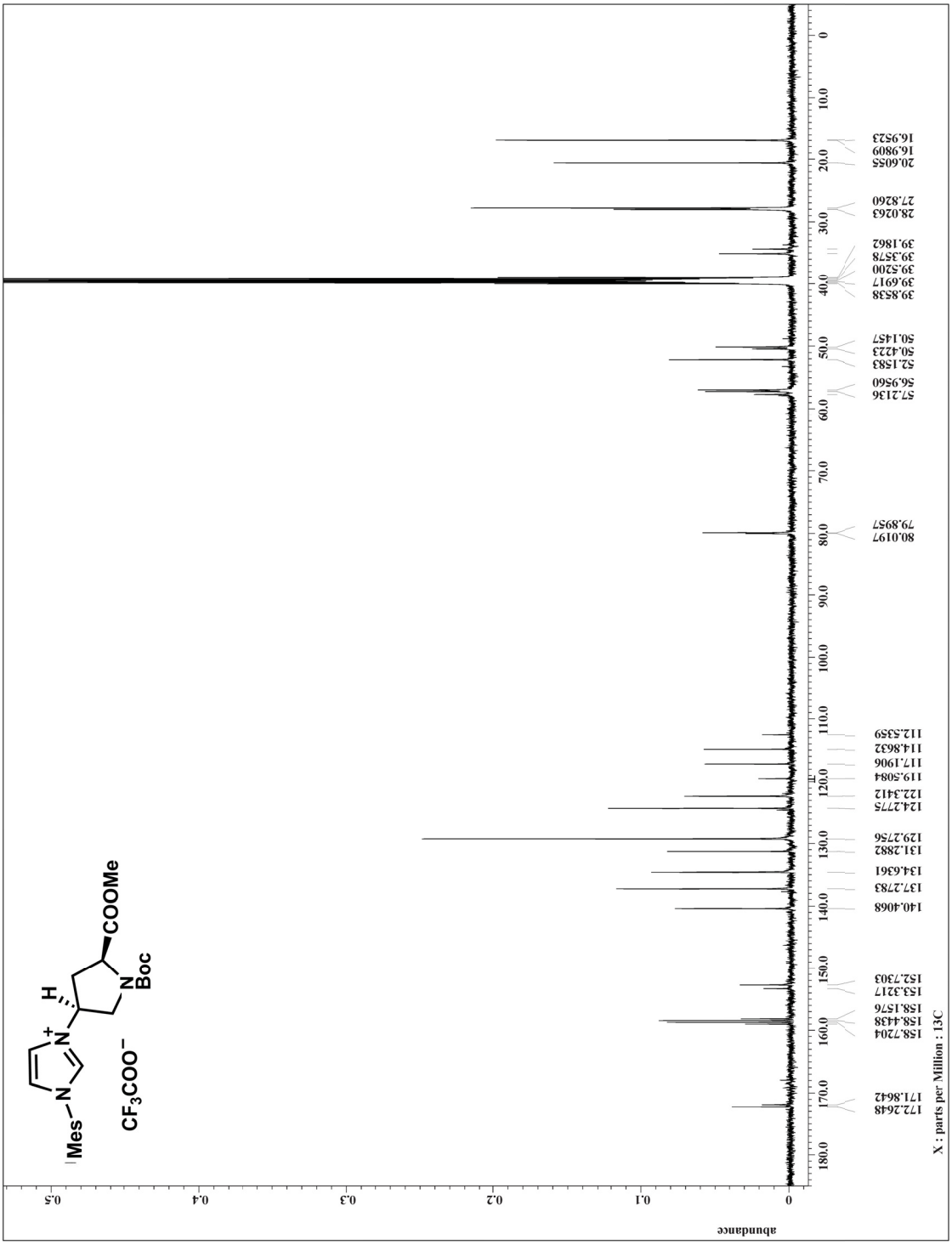

Figure 3.23: ^{13}C NMR (125 MHz, DMSO-*d*6, 293 K) of 3-((3*S*,5*S*)-1-(*tert*-butoxycarbonyl)-5-(methoxycarbonyl)pyrrolidin-3-yl)-1-mesityl-1*H*-imidazol-3-ium trifluoroacetate (**3.24**).

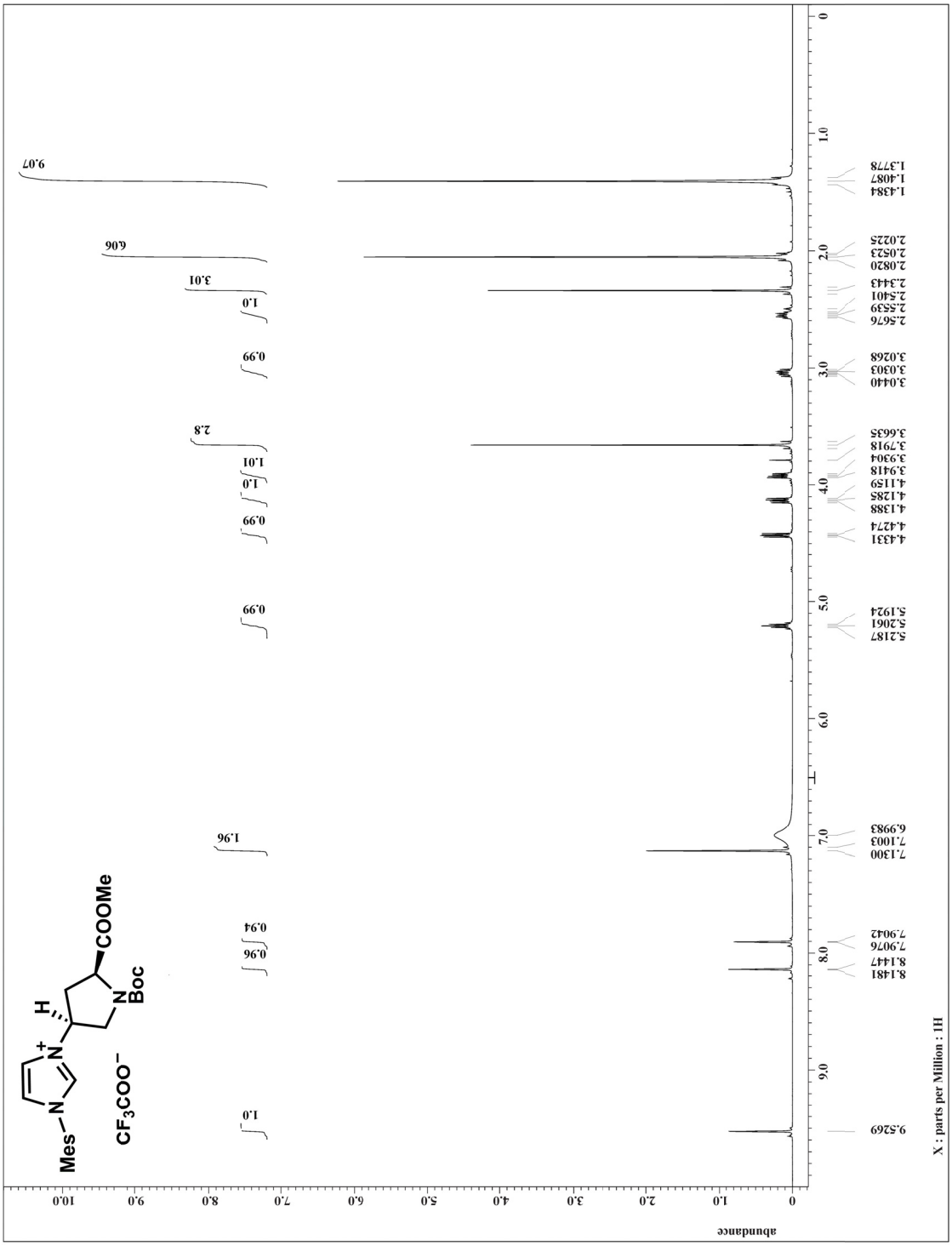

Figure 3.24: ^{1}H NMR (500 MHz, DMSO-*d*6, 353 K) of 3-((3*S*,5*S*)-1-(*tert*-butoxycarbonyl)-5-(methoxycarbonyl)pyrrolidin-3-yl)-1-mesityl-1*H*-imidazol-3-ium trifluoroacetate (**3.24**).

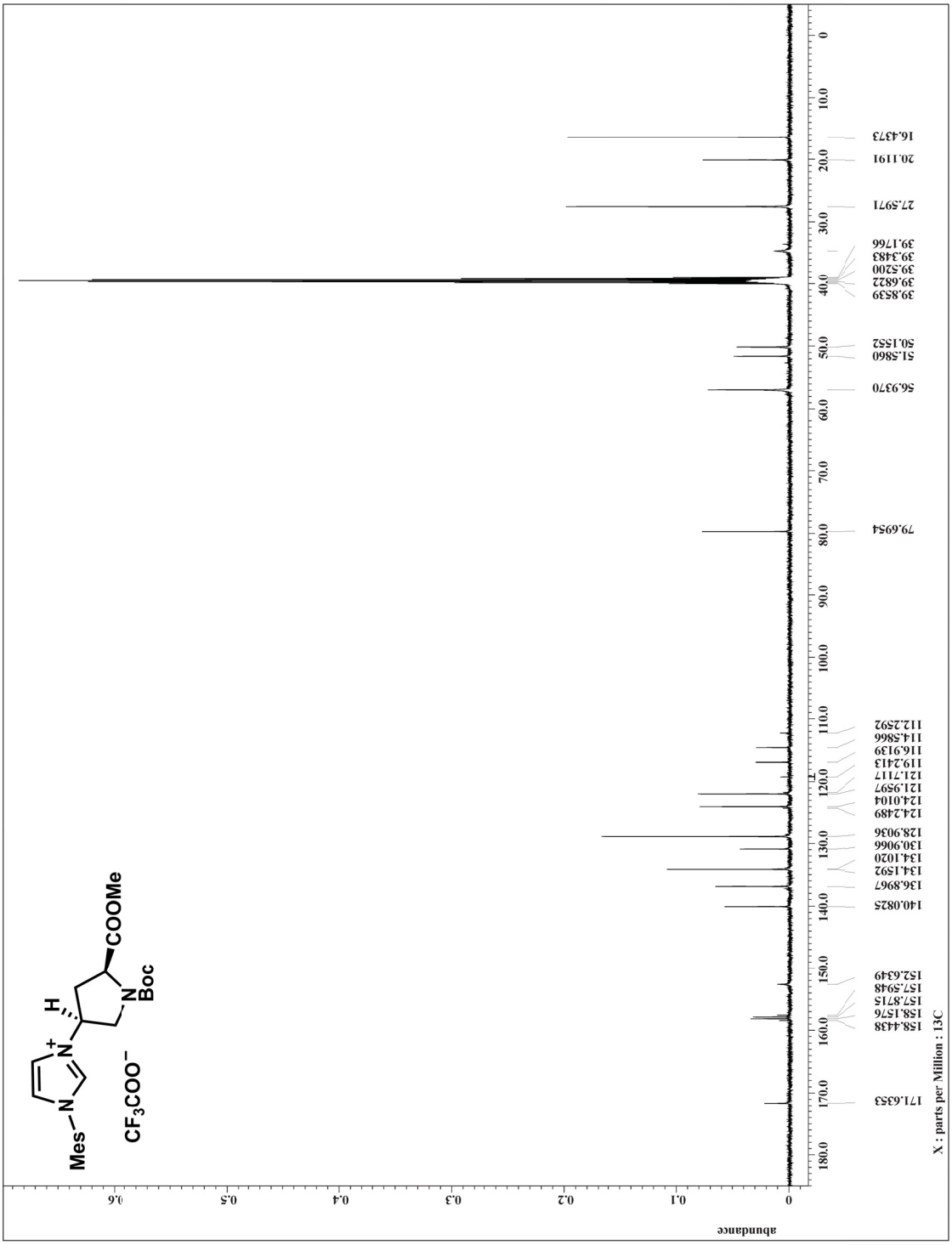

Figure 3.25: ^{13}C NMR (125 MHz, DMSO-*d*6, 353 K) of 3-((3*S*,5*S*)-1-(*tert*-butoxycarbonyl)-5-(methoxycarbonyl)pyrrolidin-3-yl)-1-mesityl-1*H*-imidazol-3-ium trifluoroacetate (**3.24**).

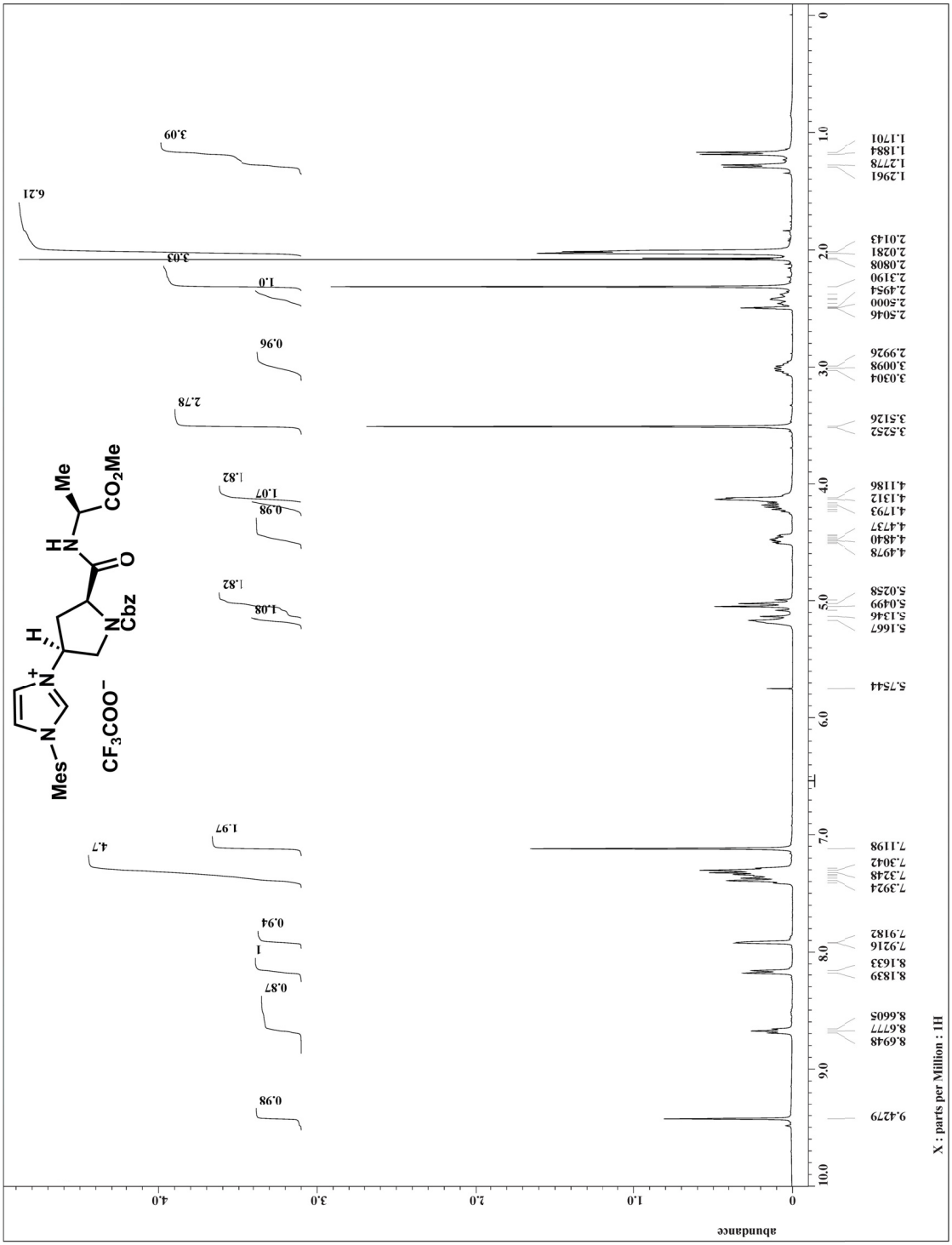

Figure 3.26: ^{1}H NMR (400 MHz, DMSO-*d*6, 293 K) of 3-((3*S*,5*S*)-1-(benzyloxycarbonyl)-5-((*S*)-1-methoxy-1-oxopropan-2-ylcarbamoyl)pyrrolidin-3-yl)-1-mesityl-1*H*-imidazol-3-ium trifluoroacetate (**3.25**).

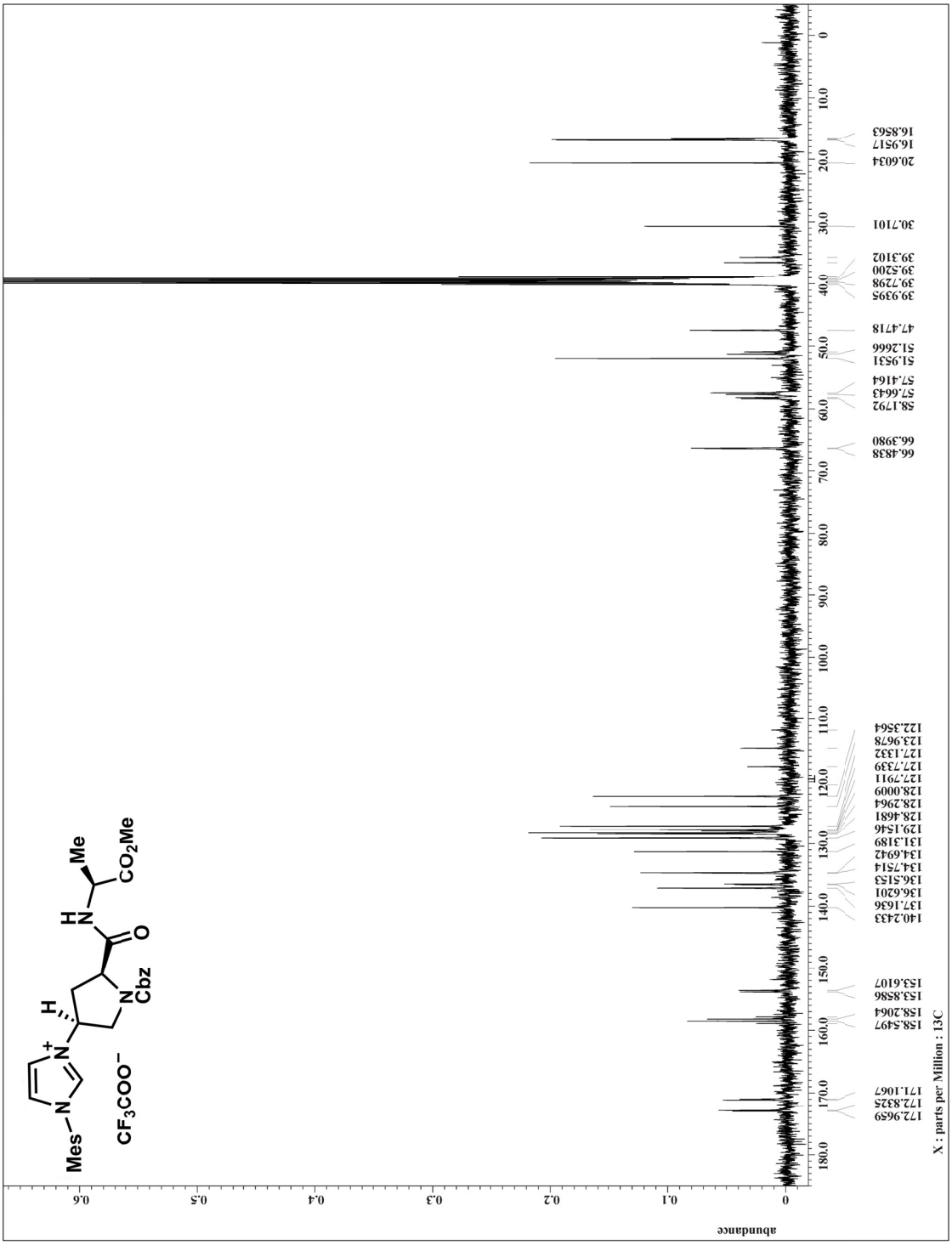

Figure 3.27: ^{13}C NMR (100 MHz, DMSO-*d*6, 293 K) of 3-((3*S*,5*S*)-1-(benzyloxycarbonyl)-5-((*S*)-1-methoxy-1-oxopropan-2-ylcarbamoyl)pyrrolidin-3-yl)-1-mesityl-1*H*-imidazol-3-ium trifluoroacetate (**3.25**).

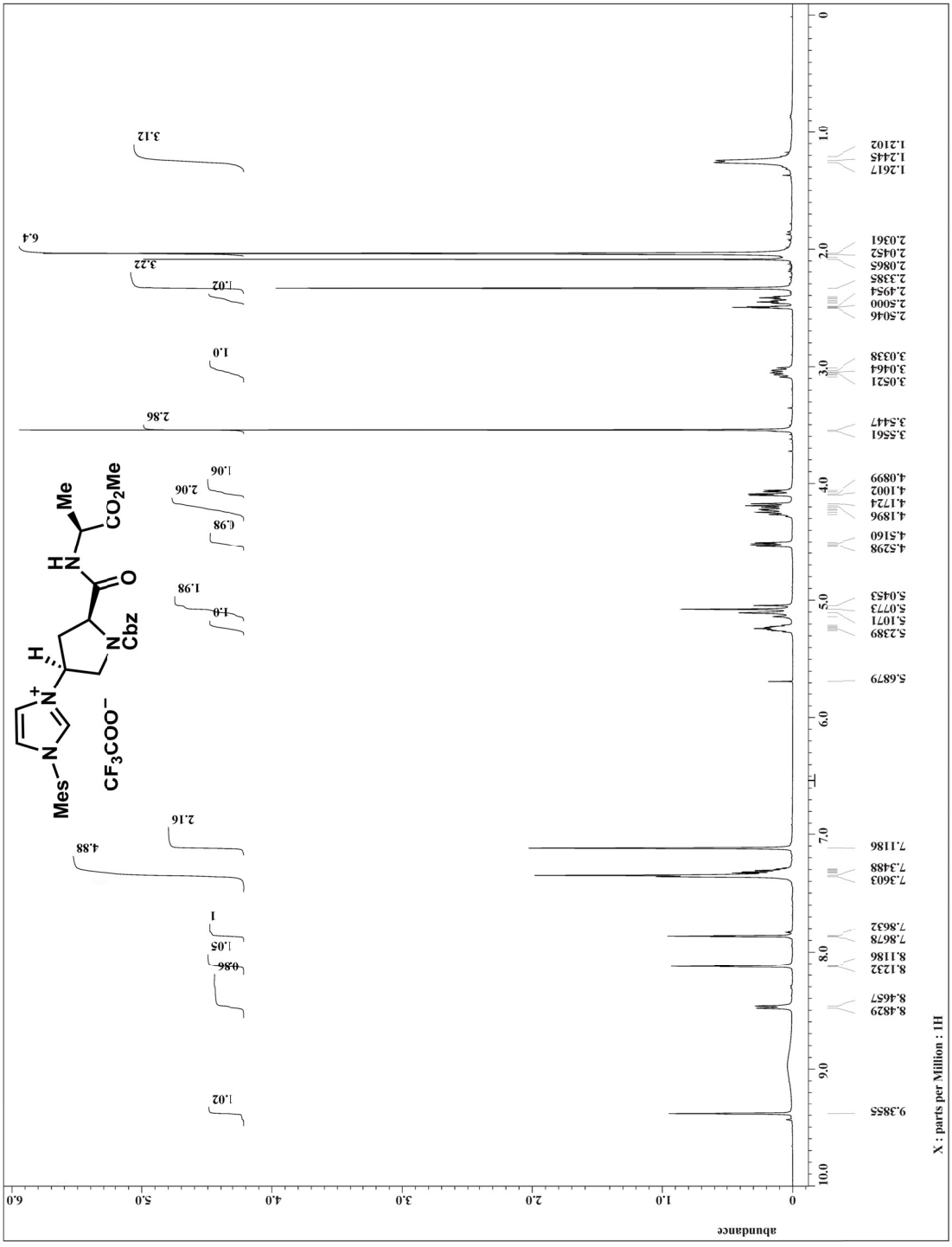

Figure 3.28: ^{1}H NMR (400 MHz, DMSO-*d*6, 353 K) of 3-((3*S*,5*S*)-1-(benzyloxycarbonyl)-5-((*S*)-1-methoxy-1-oxopropan-2-ylcarbamoyl)pyrrolidin-3-yl)-1-mesityl-1*H*-imidazol-3-ium trifluoroacetate (**3.25**).

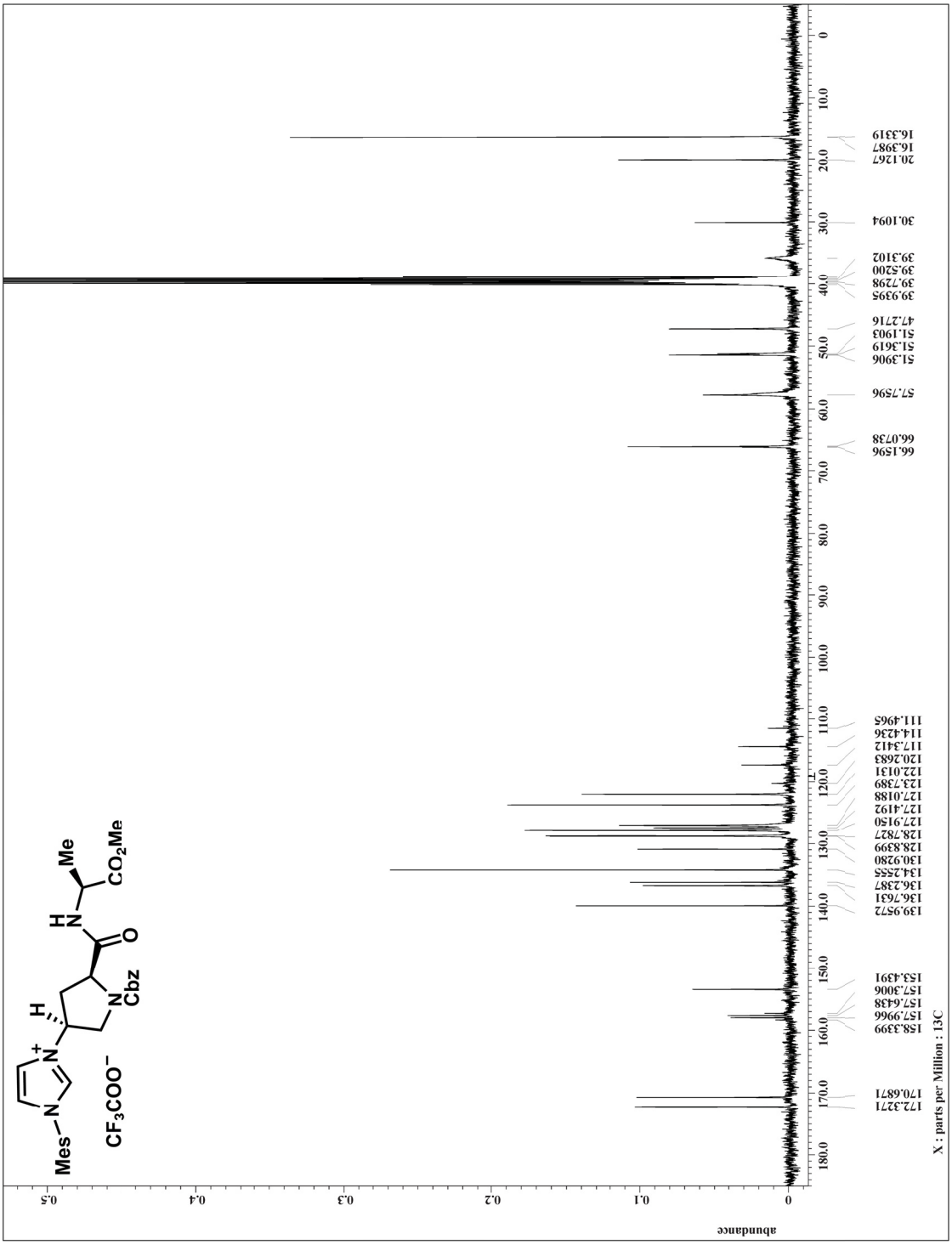

Figure 3.29: ^{13}C NMR (100 MHz, DMSO-*d*6, 353 K) of 3-((3*S*,5*S*)-1-(benzyloxycarbonyl)-5-((*S*)-1-methoxy-1-oxopropan-2-ylcarbamoyl)pyrrolidin-3-yl)-1-mesityl-1*H*-imidazol-3-ium trifluoroacetate (**3.25**).

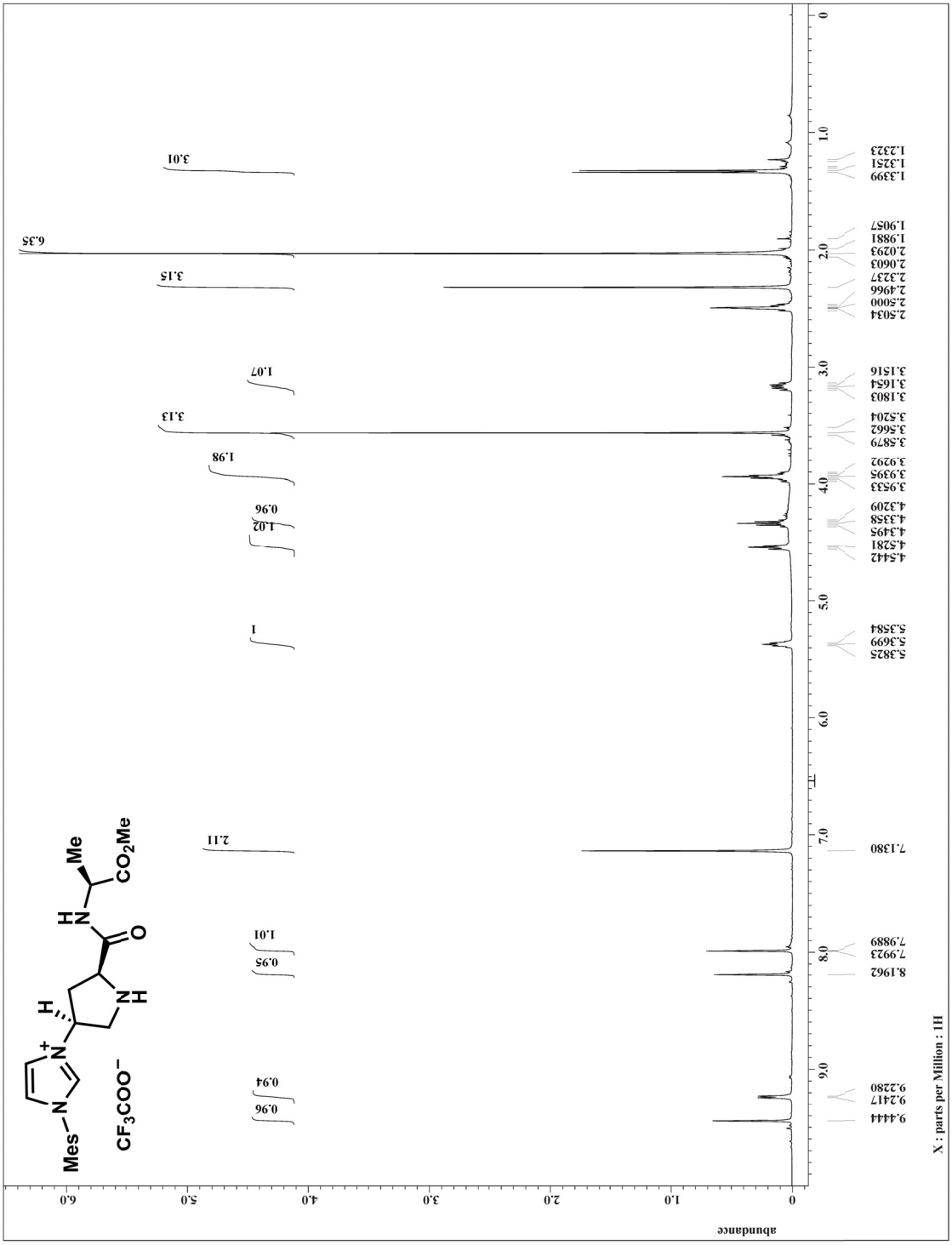

Figure 3.30: ^{1}H NMR (500 MHz, DMSO-*d*6) of 1-mesityl-3-((3*S*,5*S*)-5-((*S*)-1-methoxy-1-oxopropan-2-ylcarbamoyl)pyrrolidin-3-yl)-1*H*-imidazol-3-ium trifluoroacetate (**3.26**).

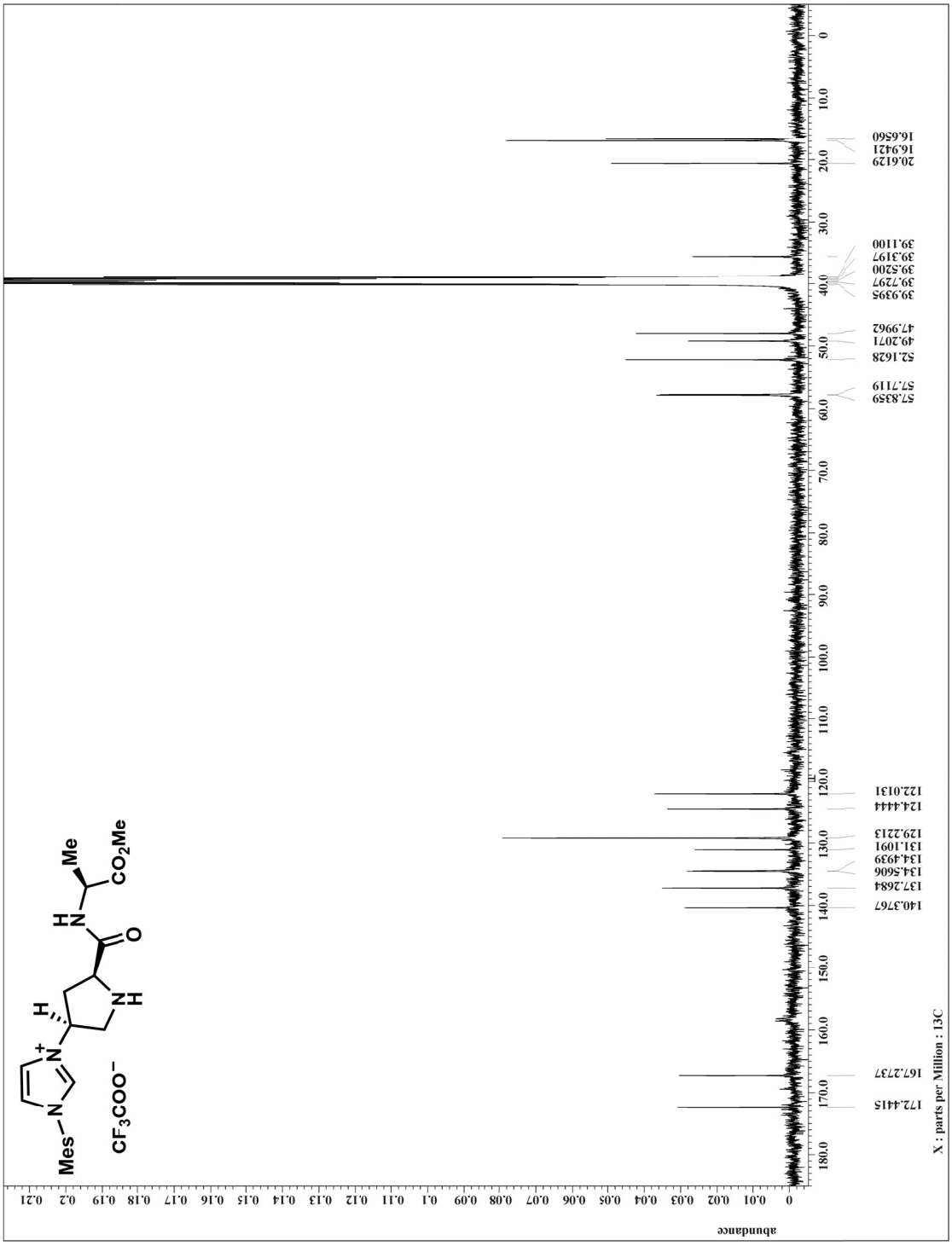

Figure 3.31: ^{13}C NMR (100 MHz, DMSO-*d*6, 293 K) of 1-mesityl-3-((3*S*,5*S*)-5-((*S*)-1-methoxy-1-oxopropan-2-ylcarbamoyl)pyrrolidin-3-yl)-1*H*-imidazol-3-ium trifluoroacetate (**3.26**).

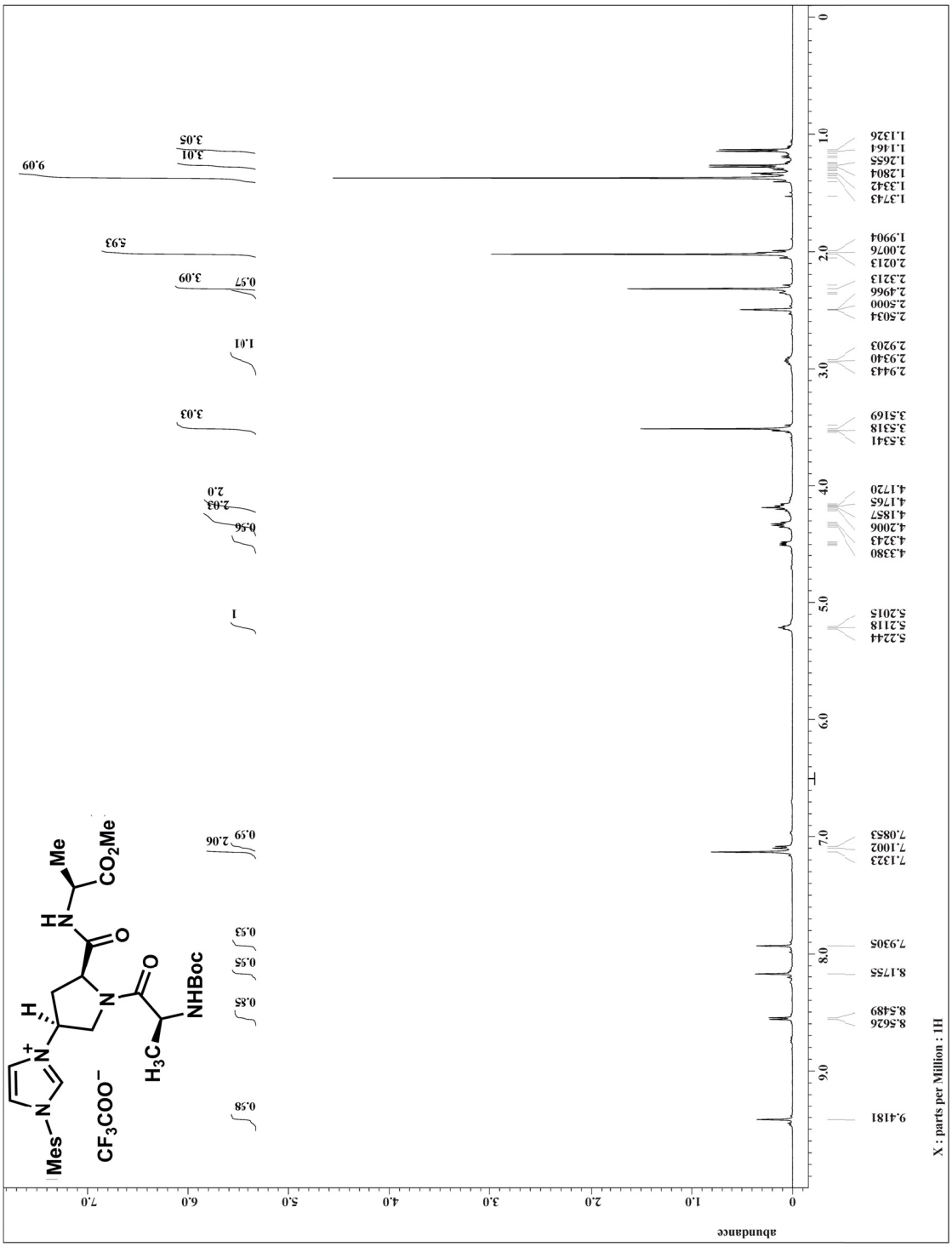

Figure 3.32: ^{1}H NMR (500 MHz, DMSO-*d*6, 293 K) of 3-((3*S*,5*S*)-1-((*S*)-2-(*tert*-butoxycarbonylamino)propanoyl)-5-((*S*)-1-methoxy-1-oxopropan-2-ylcarbamoyl)pyrrolidin-3-yl)-1-mesityl-1*H*-imidazol-3-ium trifluoroacetate (**3.27**).

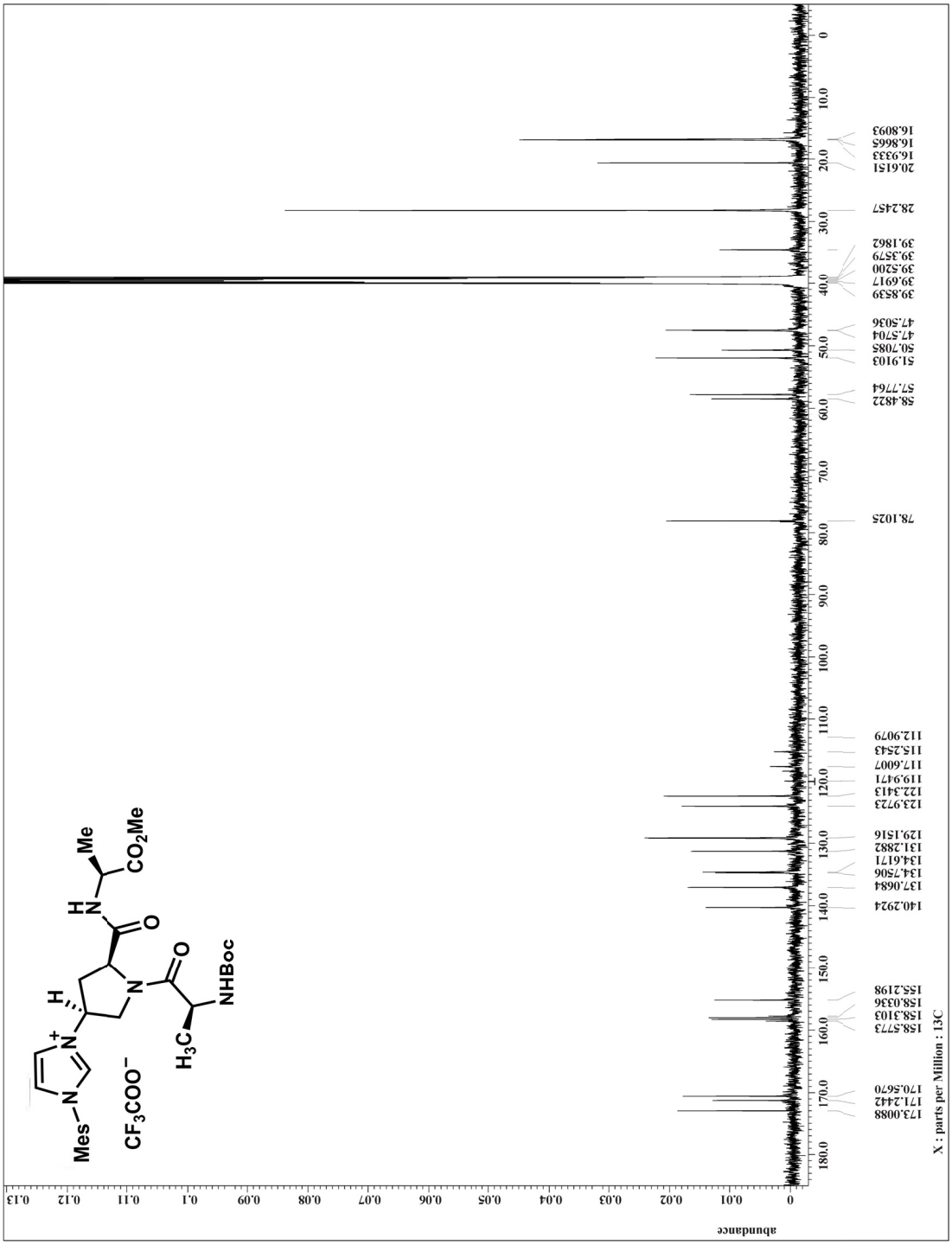

Figure 3.33: ^{13}C NMR (125 MHz, DMSO-*d*6, 293 K) of 3-((3*S*,5*S*)-1-((*S*)-2-(*tert*-butoxycarbonylamino)propanoyl)-5-((*S*)-1-methoxy-1-oxopropan-2-ylcarbamoyl)pyrrolidin-3-yl)-1-mesityl-1*H*-imidazol-3-ium trifluoroacetate (**3.27**).

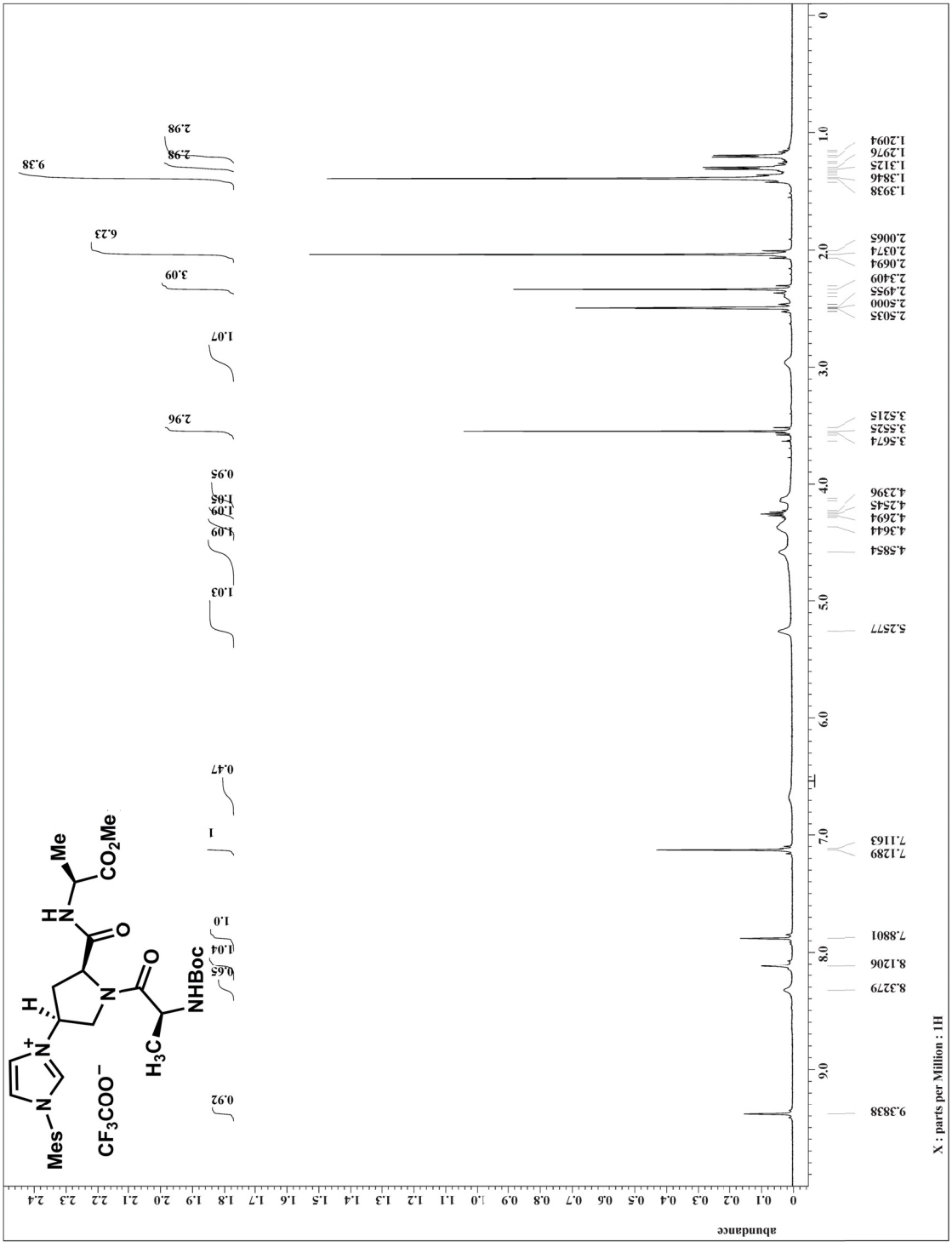

Figure 3.34: ^{1}H NMR (500 MHz, DMSO-*d*6, 353 K) of 3-((3*S*,5*S*)-1-((*S*)-2-(*tert*-butoxycarbonylamino)propanoyl)-5-((*S*)-1-methoxy-1-oxopropan-2-ylcarbamoyl)pyrrolidin-3-yl)-1-mesityl-1*H*-imidazol-3-ium trifluoroacetate (**3.27**).

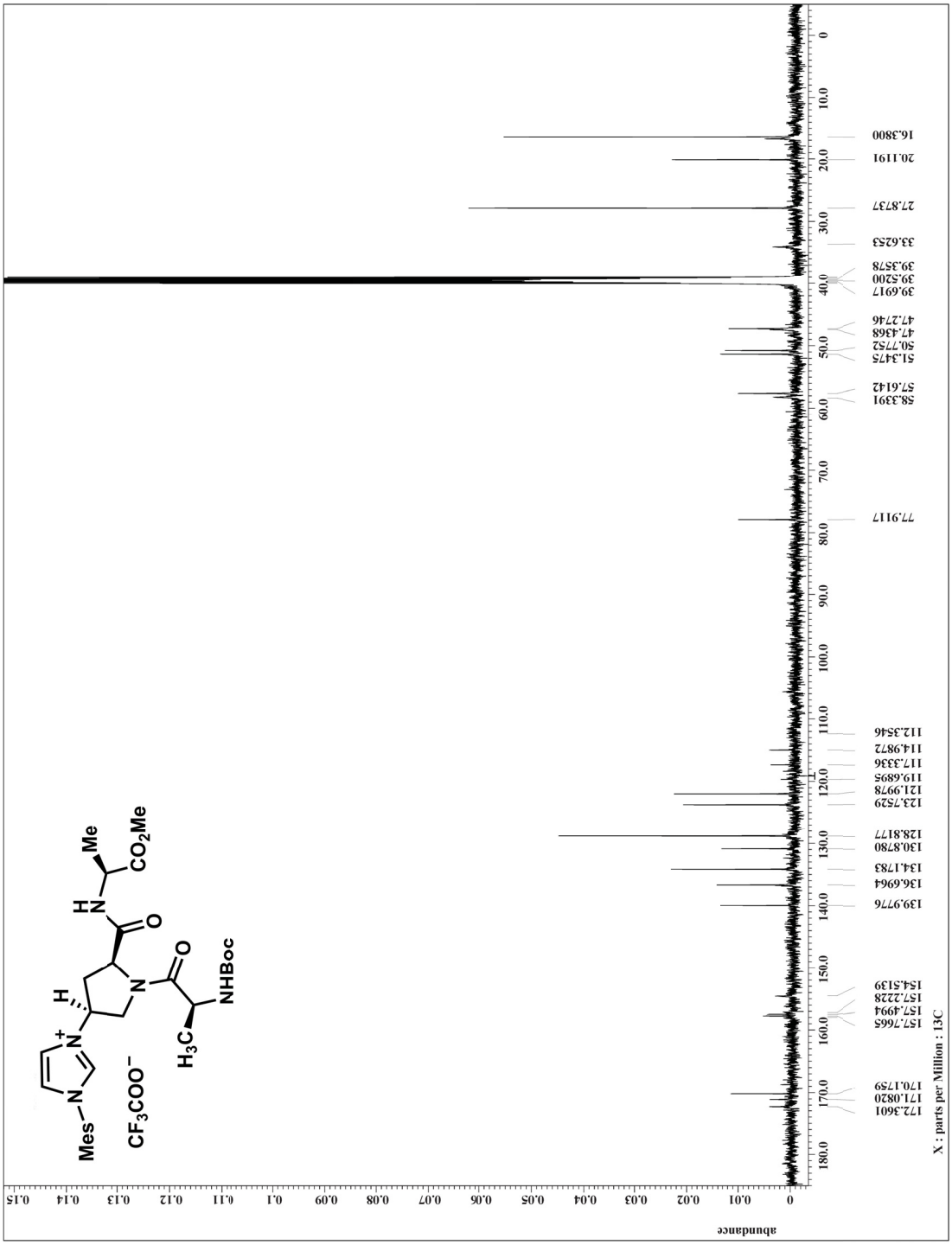

Figure 3.35: ^{13}C NMR (125 MHz, DMSO-*d*6, 353 K) of 3-((3*S*,5*S*)-1-((*S*)-2-(*tert*-butoxycarbonylamino)propanoyl)-5-((*S*)-1-methoxy-1-oxopropan-2-ylcarbamoyl)pyrrolidin-3-yl)-1-mesityl-1*H*-imidazol-3-ium trifluoroacetate (**3.27**).

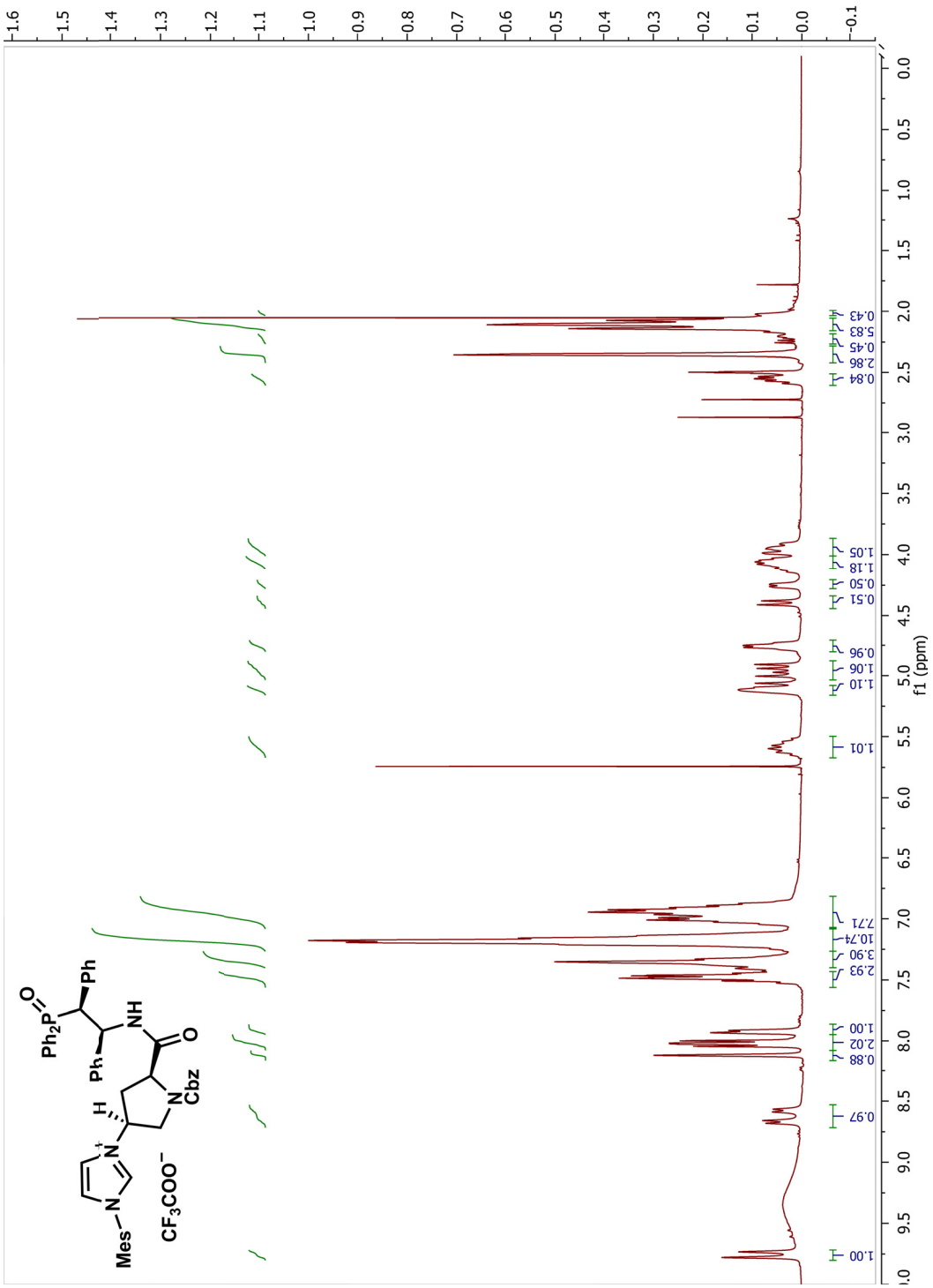

Figure 3.36: ^{1}H NMR (400 MHz, DMSO-*d*6, 293 K) of 3-((3*S*,5*S*)-1-(benzyloxycarbonyl)-5-((1*S*,2*S*)-2-(diphenylphosphoryl)-1,2-diphenylethylcarbamoyl) pyrrolidin-3-yl)-1-mesityl-1*H*-imidazol-3-ium trifluoroacetate (**3.55**).

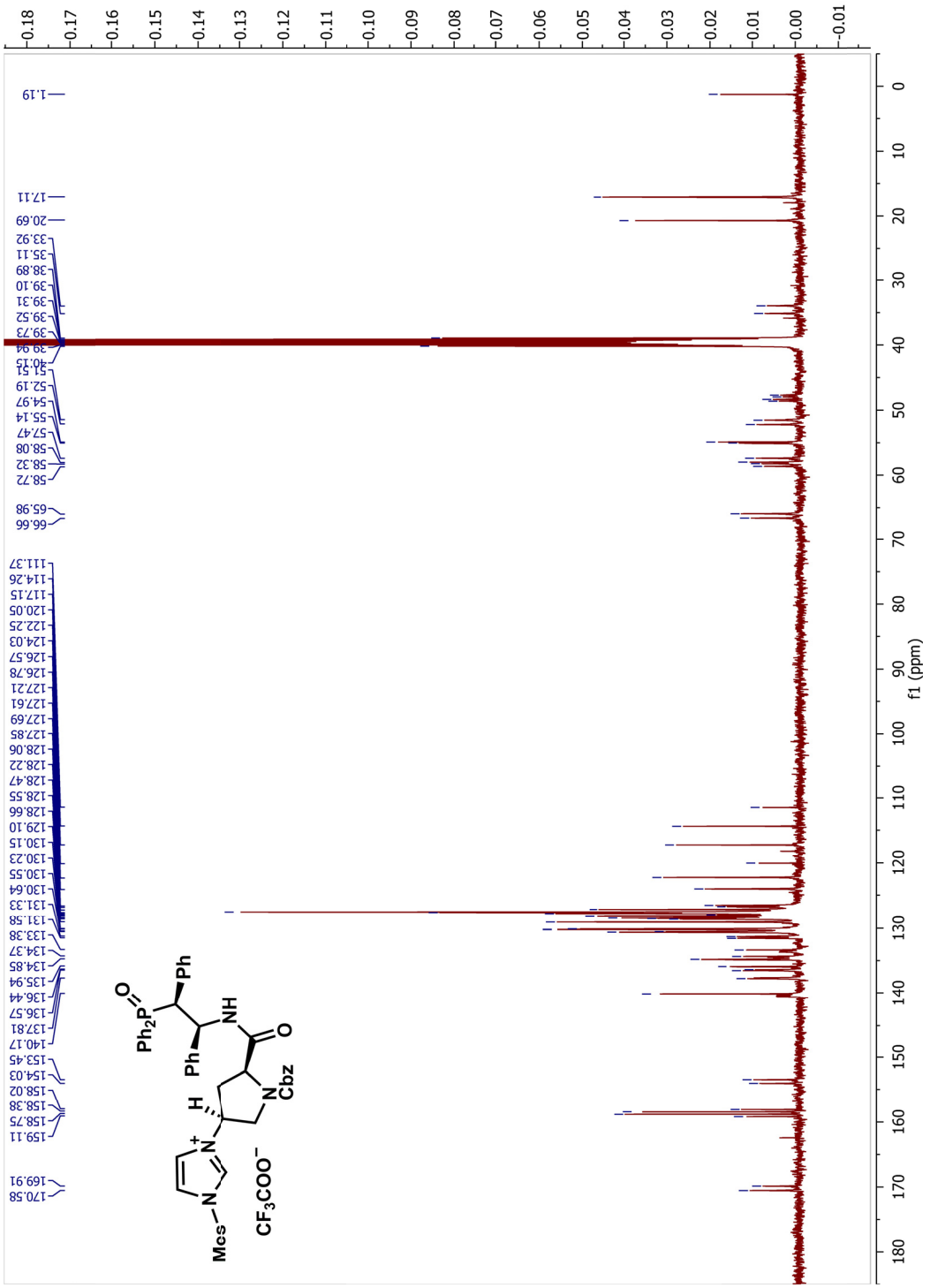

Figure 3.37: ^{13}C NMR (100 MHz, DMSO-*d*6, 293 K) of 3-((3*S*,5*S*)-1-(benzyloxycarbonyl)-5-((1*S*,2*S*)-2-(diphenylphosphoryl)-1,2-diphenylethylcarbamoyl) pyrrolidin-3-yl)-1-mesityl-1*H*-imidazol-3-ium trifluoroacetate (**3.55**).

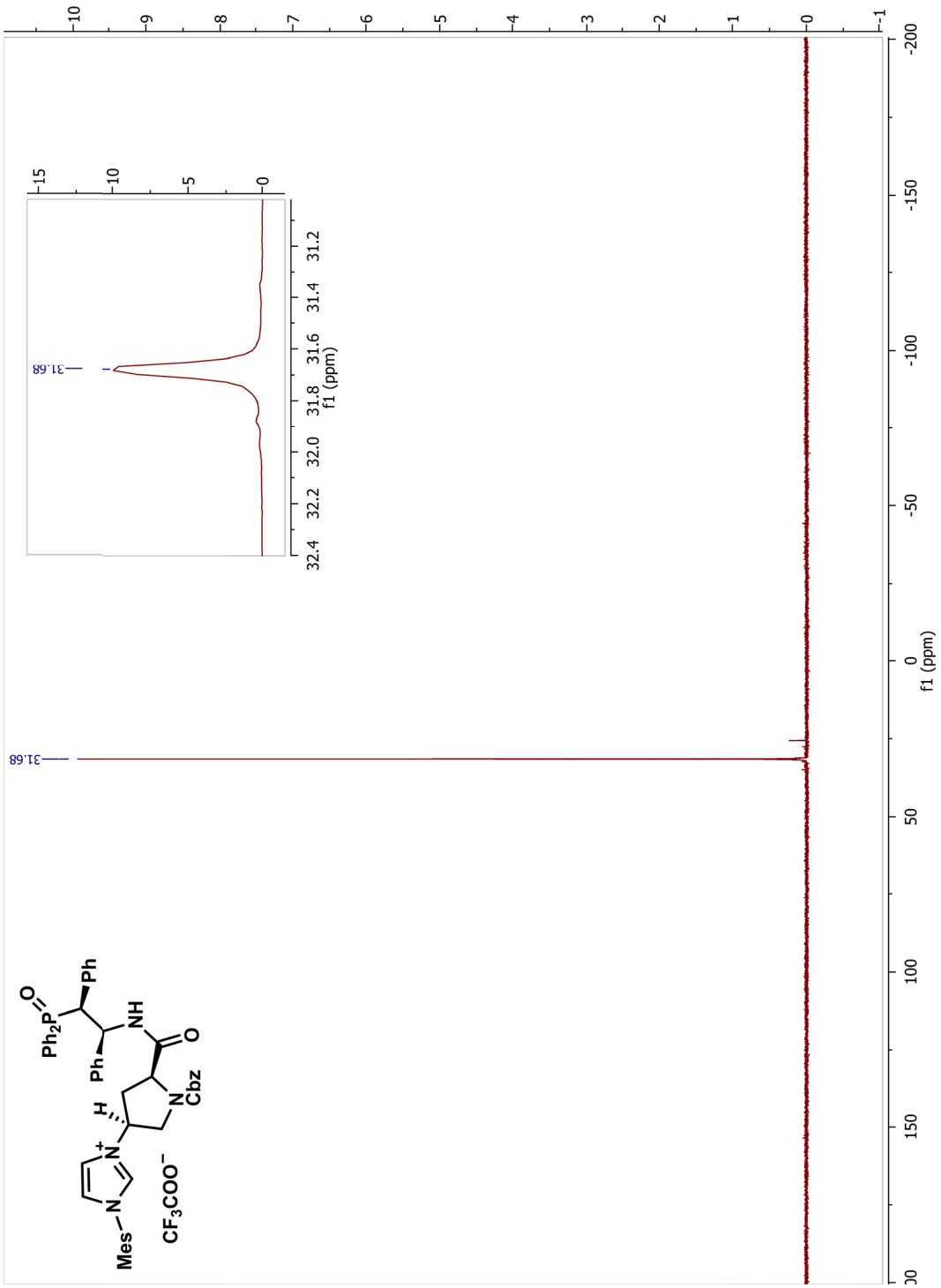

Figure 3.38: ^{31}P NMR (161 MHz, DMSO-*d*6, 293 K) of 3-((3*S*,5*S*)-1-(benzyloxycarbonyl)-5-((1*S*,2*S*)-2-(diphenylphosphoryl)-1,2-diphenylethylcarbamoyl) pyrrolidin-3-yl)-1-mesityl-1*H*-imidazol-3-ium trifluoroacetate (**3.55**).

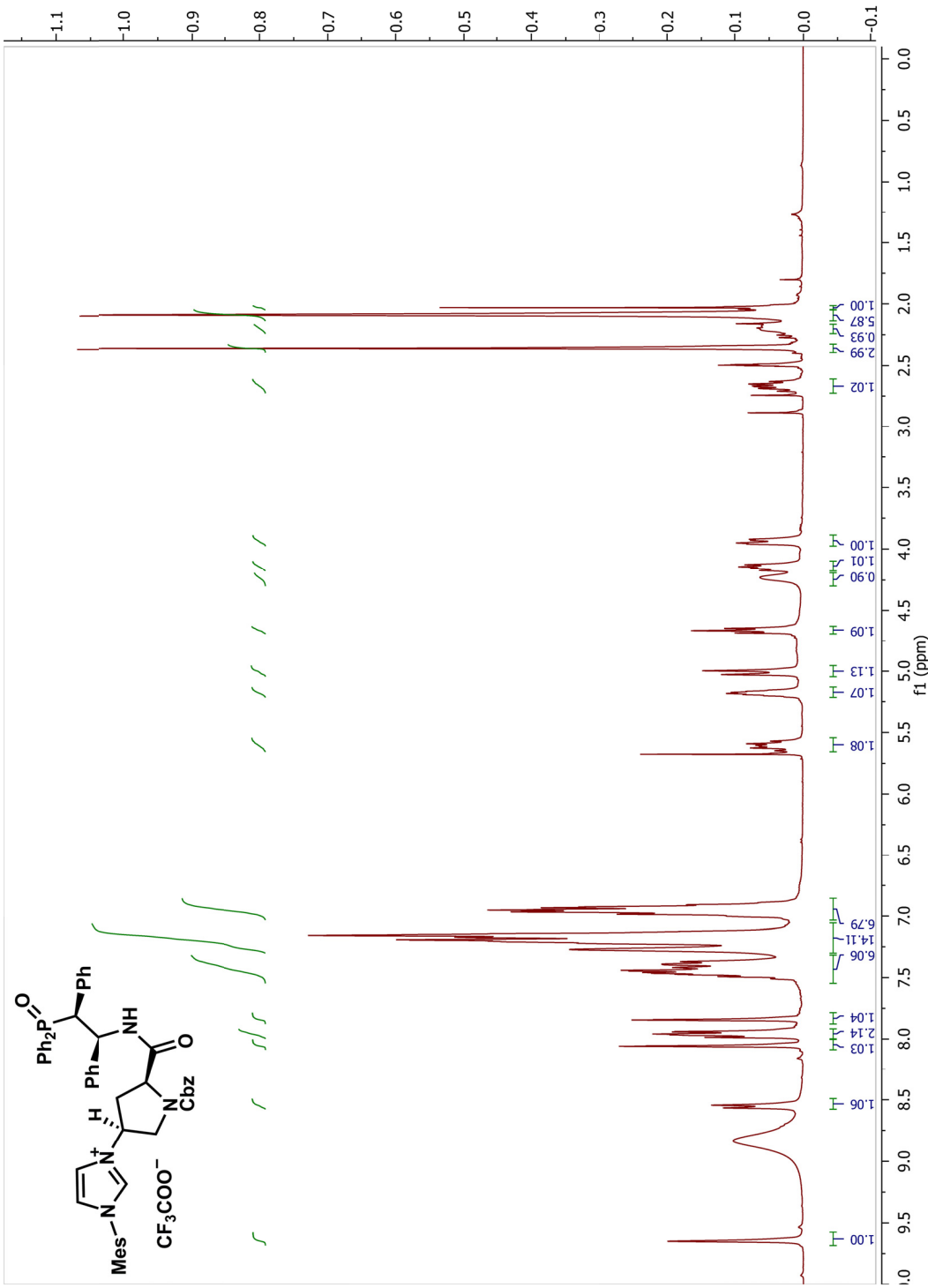

Figure 3.39: ^{1}H NMR (400 MHz, DMSO-*d*6, 353 K) of 3-((3*S*,5*S*)-1-(benzyloxycarbonyl)-5-((1*S*,2*S*)-2-(diphenylphosphoryl)-1,2-diphenylethylcarbamoyl) pyrrolidin-3-yl)-1-mesityl-1*H*-imidazol-3-ium trifluoroacetate (**3.55**).

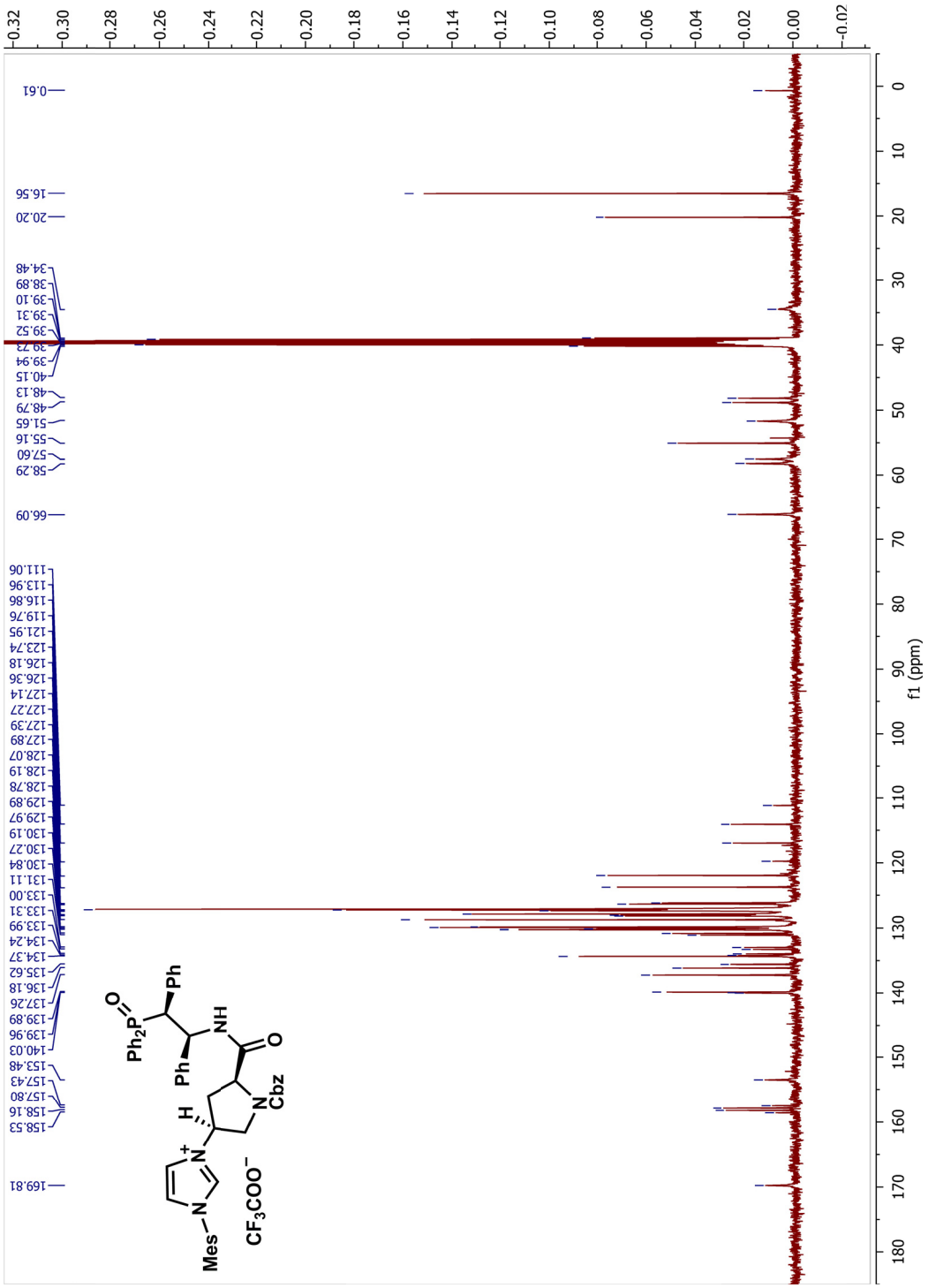

Figure 3.40: ^{13}C NMR (100 MHz, DMSO-*d*6, 353 K) of 3-((3*S*,5*S*)-1-(benzyloxycarbonyl)-5-((1*S*,2*S*)-2-(diphenylphosphoryl)-1,2-diphenylethylcarbamoyl) pyrrolidin-3-yl)-1-mesityl-1*H*-imidazol-3-ium trifluoroacetate (**3.55**).

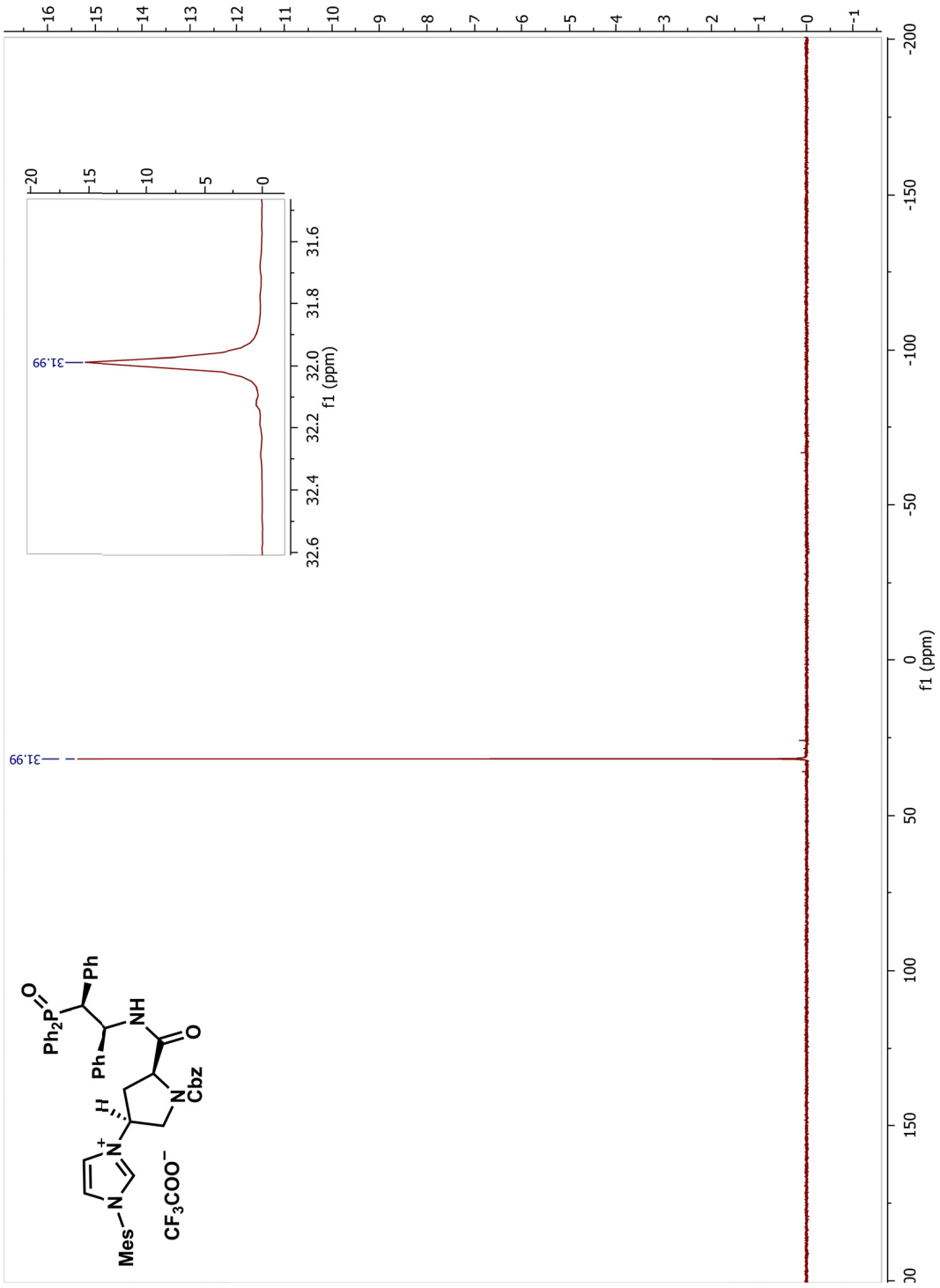

Figure 3.41: ^{31}P NMR (161 MHz, DMSO-*d*6, 353 K) of 3-((3*S*,5*S*)-1-(benzyloxycarbonyl)-5-((1*S*,2*S*)-2-(diphenylphosphoryl)-1,2-diphenylethylcarbamoyl) pyrrolidin-3-yl)-1-mesityl-1*H*-imidazol-3-ium trifluoroacetate (**3.55**).

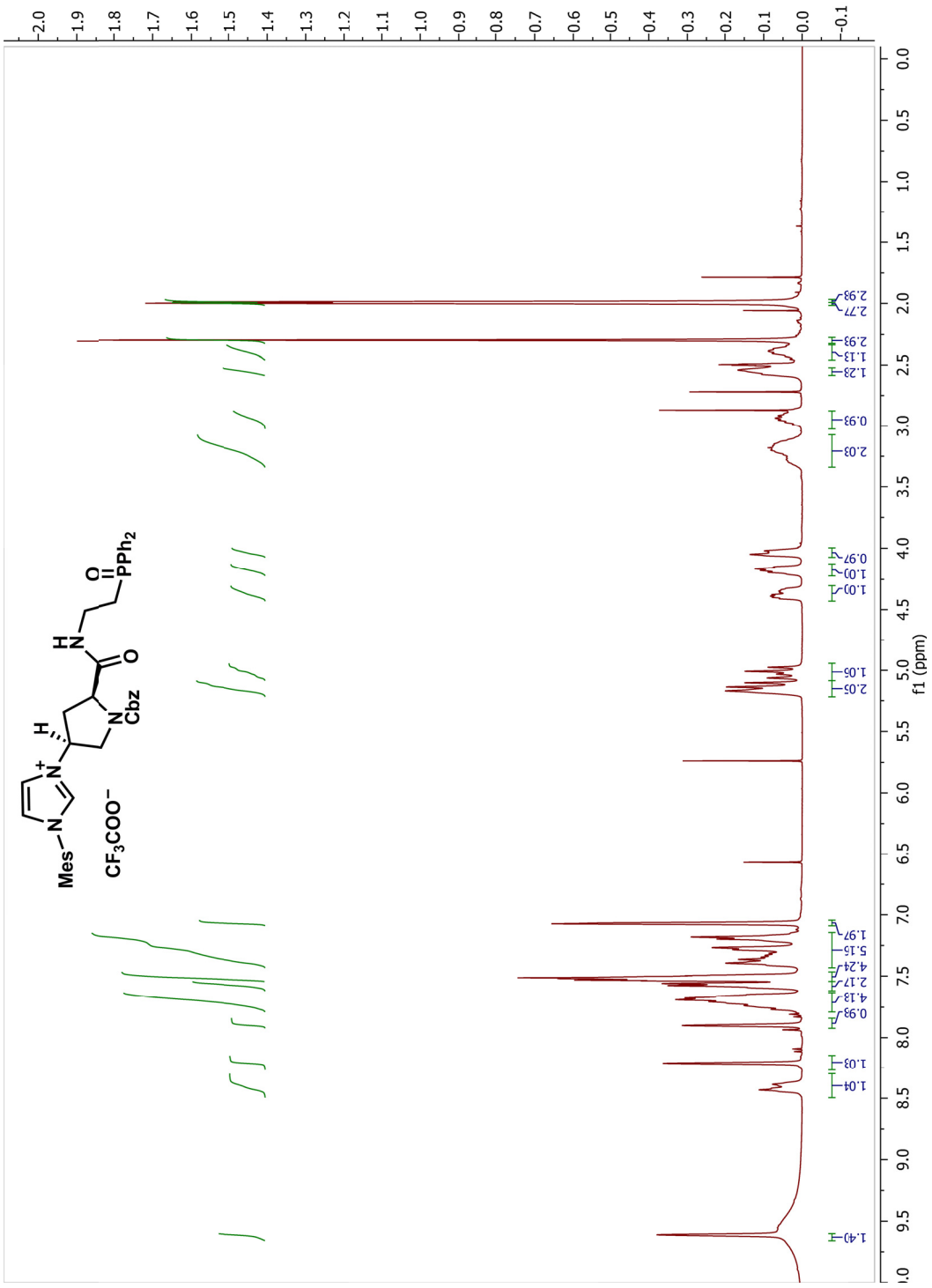

Figure 3.42: ^{1}H NMR (400 MHz, DMSO-*d*6, 293 K) of (*S*)-3-(2-(*tert*-butoxycarbonylamino)-3-methoxy-3-oxopropyl)-1-mesityl-1*H*-imidazol-3-ium trifluoroacetate (**3.61**).

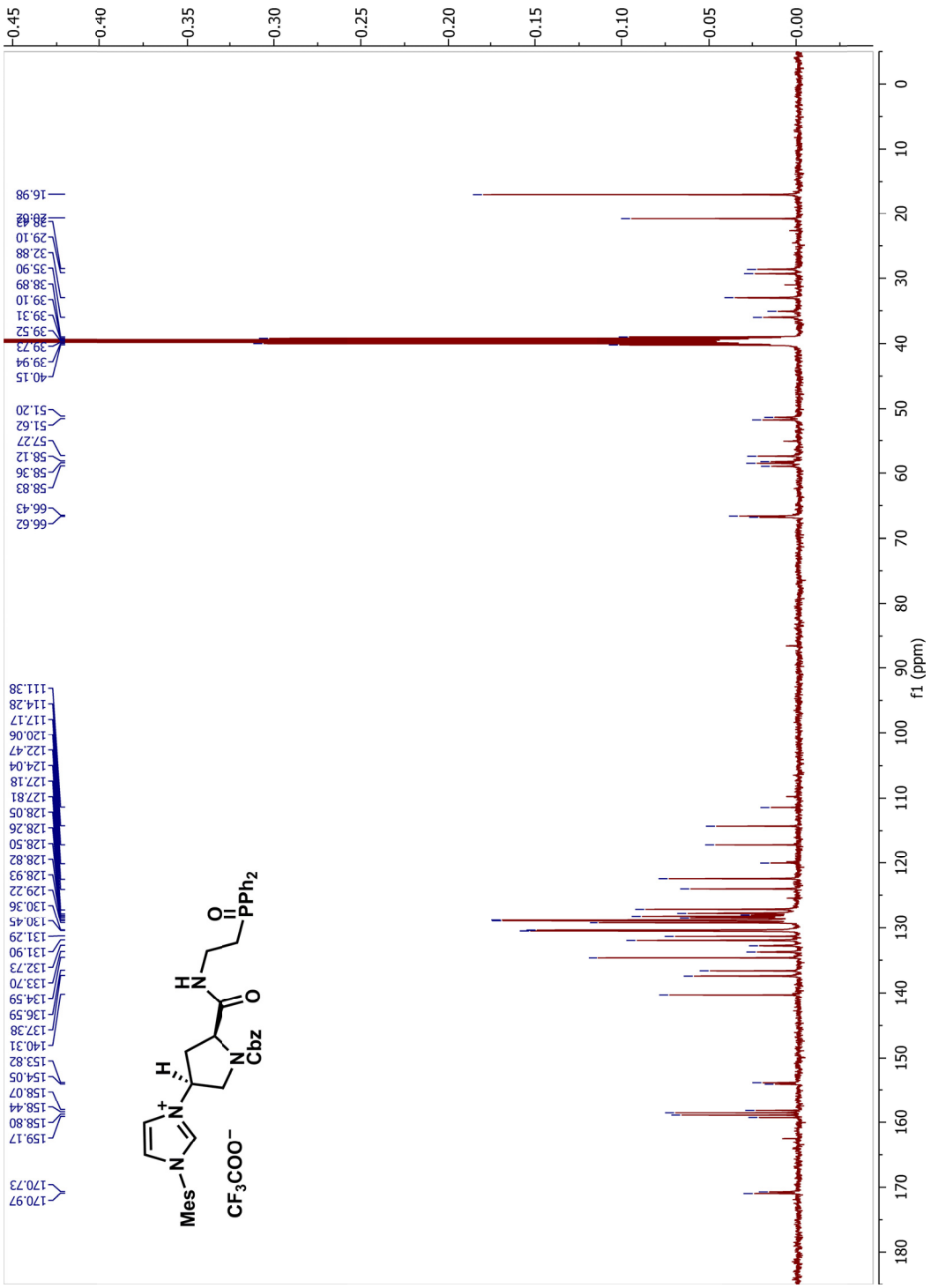

Figure 3.43: ^{13}C NMR (100 MHz, DMSO-*d*6, 293 K) of (*S*)-3-(2-(*tert*-butoxycarbonylamino)-3-methoxy-3-oxopropyl)-1-mesityl-1*H*-imidazol-3-ium trifluoroacetate (**3.61**).

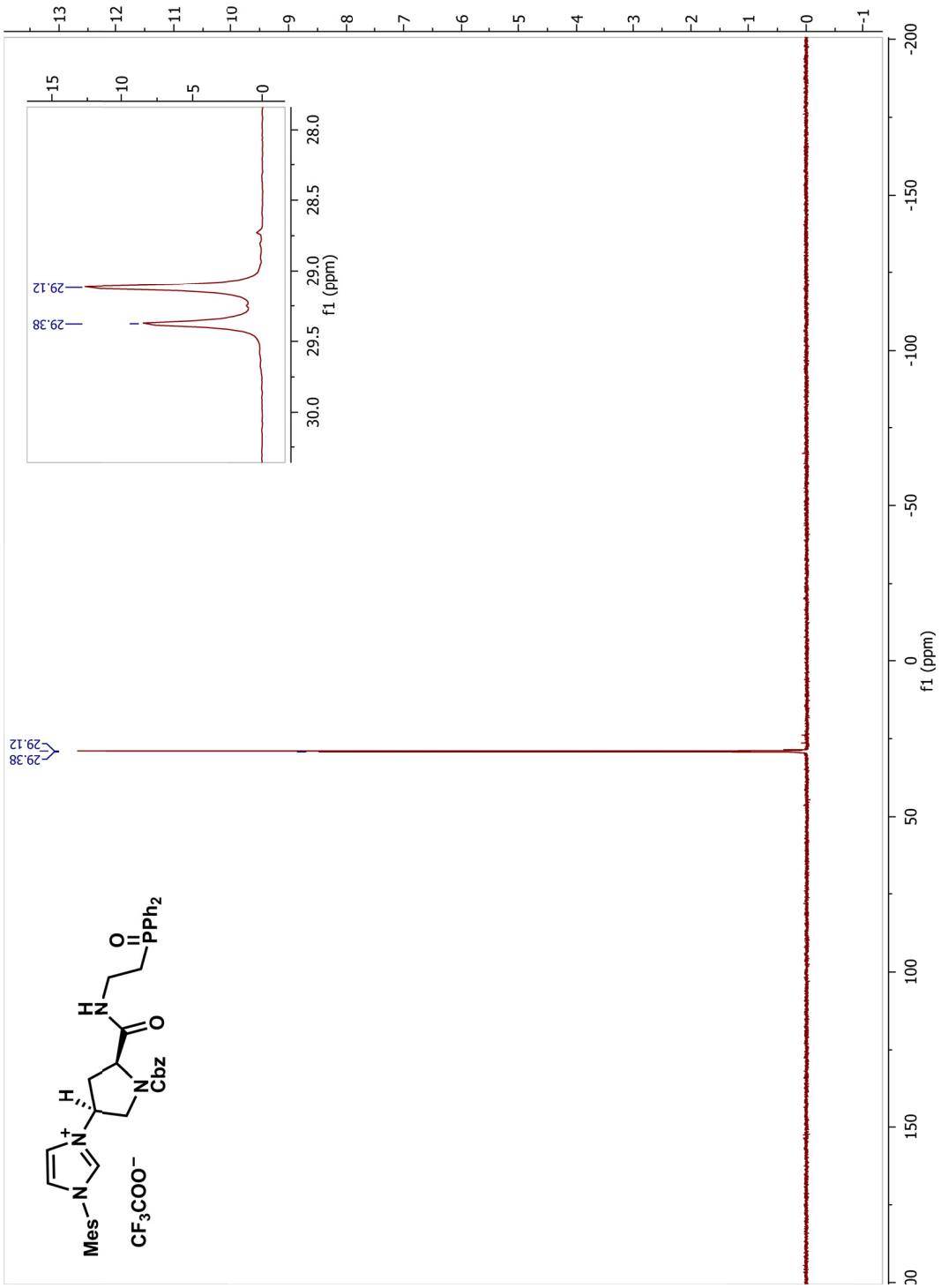

Figure 3.44: ^{31}P NMR (161 MHz, DMSO-*d*6, 293 K) of (*S*)-3-(2-(*tert*-butoxycarbonylamino)-3-methoxy-3-oxopropyl)-1-mesityl-1*H*-imidazol-3-ium trifluoroacetate (**3.61**).

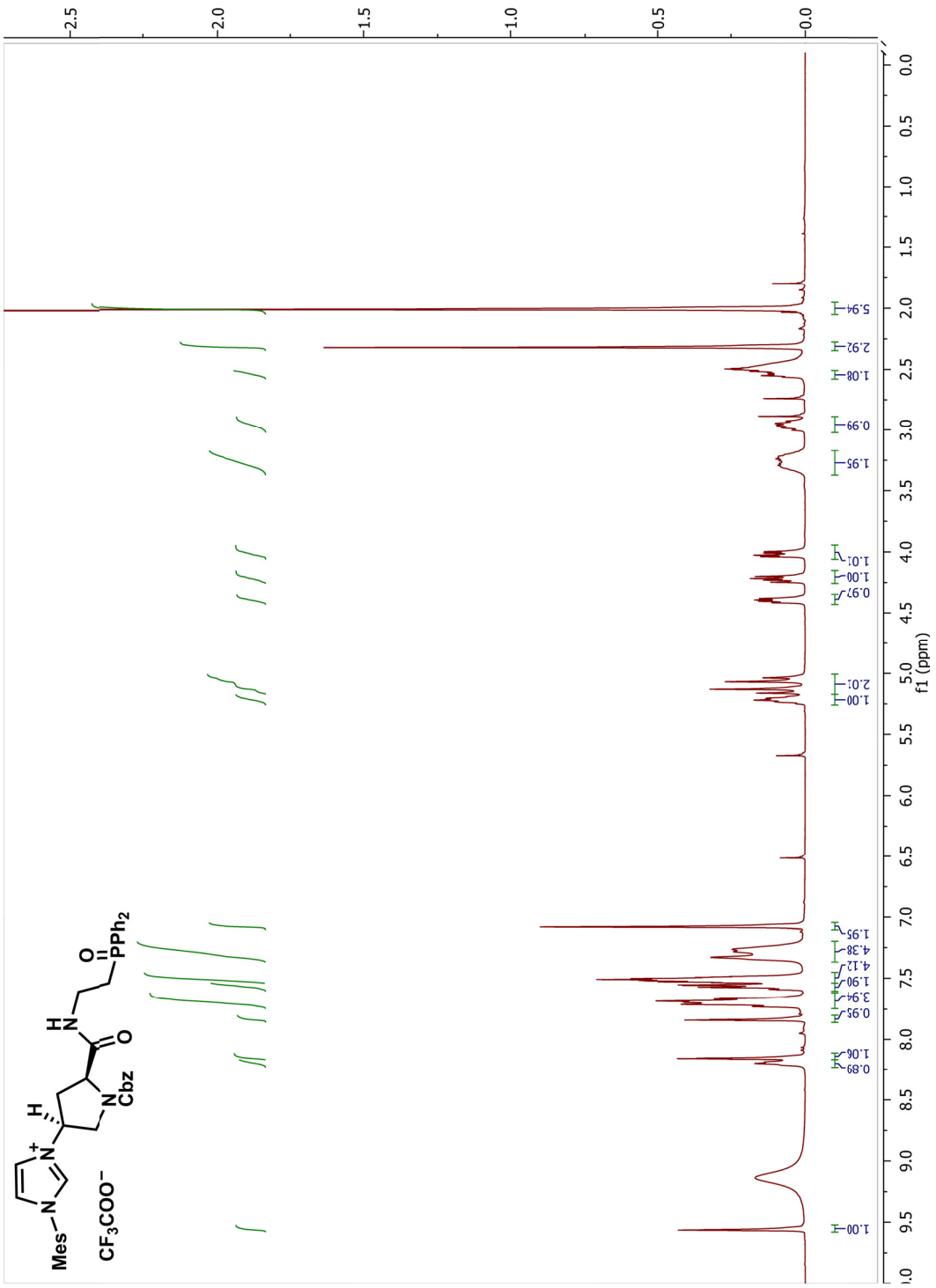

Figure 3.45: ^{1}H NMR (400 MHz, DMSO-*d*6, 353 K) of (*S*)-3-(2-(*tert*-butoxycarbonylamino)-3-methoxy-3-oxopropyl)-1-mesityl-1*H*-imidazol-3-ium trifluoroacetate (**3.61**).

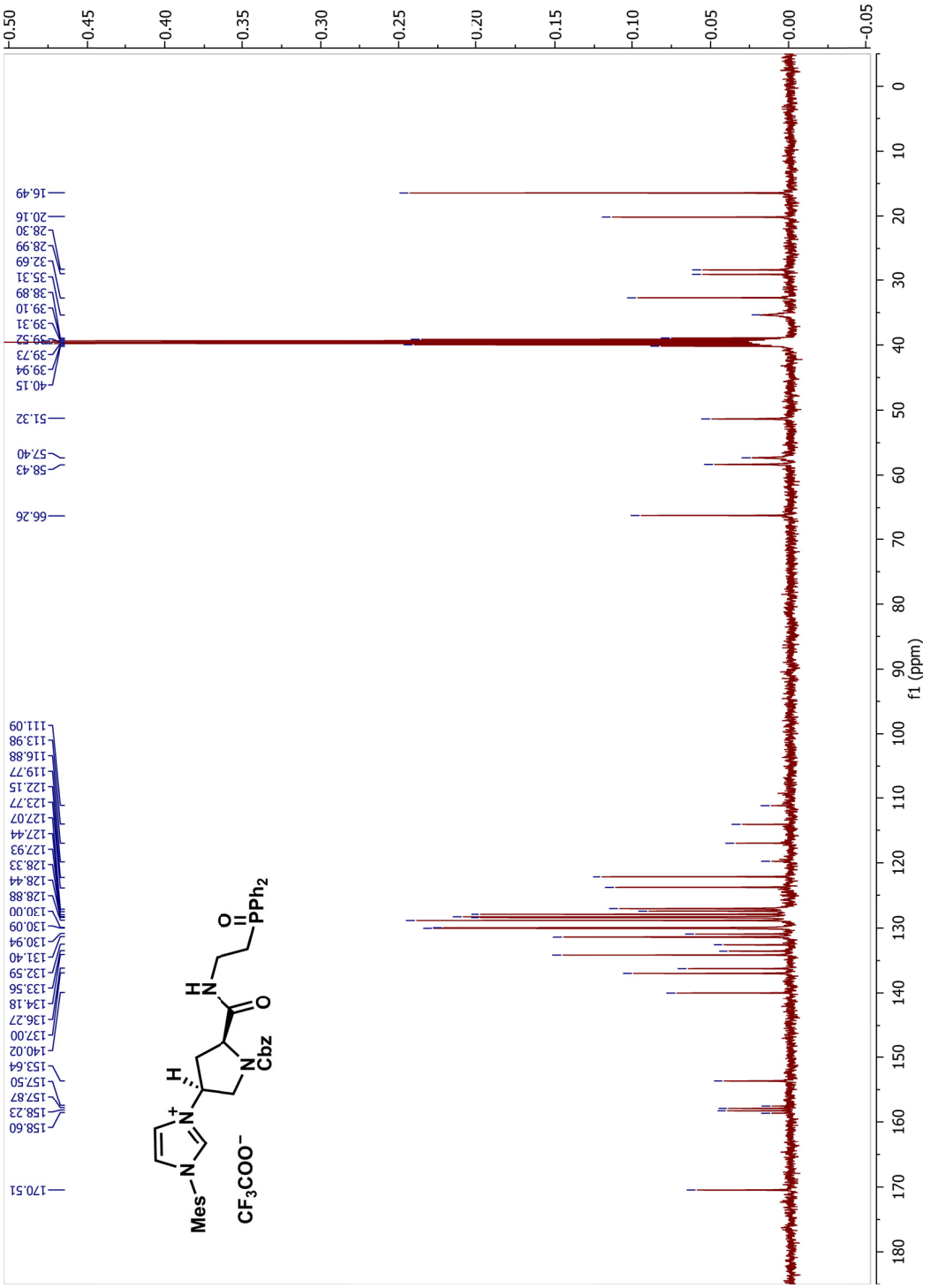

Figure 3.46: ^{13}C NMR (100 MHz, DMSO-*d*6, 353 K) of (*S*)-3-(2-(*tert*-butoxycarbonylamino)-3-methoxy-3-oxopropyl)-1-mesityl-1*H*-imidazol-3-ium trifluoroacetate (**3.61**).

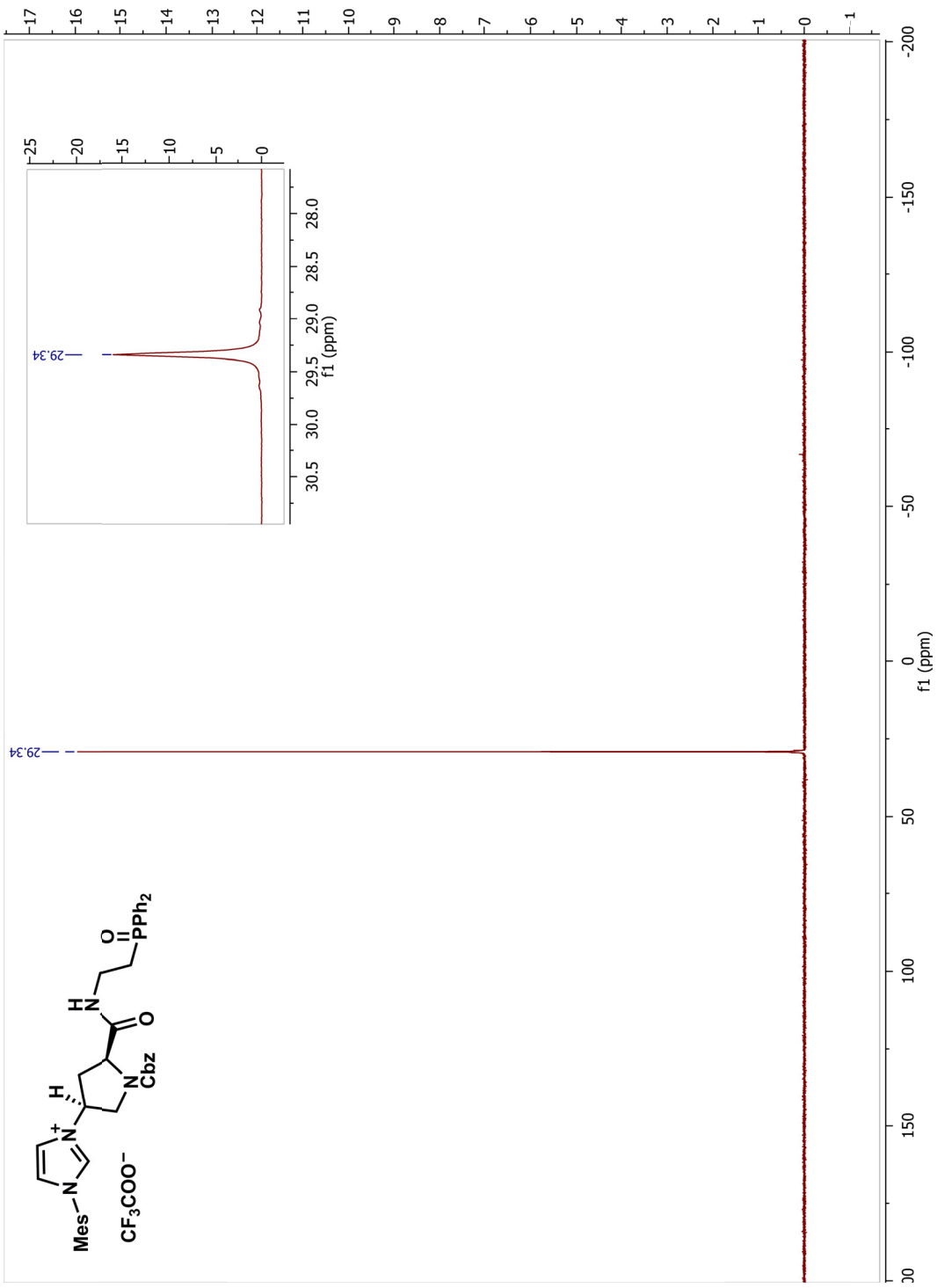

Figure 3.47: ^{31}P NMR (161 MHz, DMSO-*d*6, 353 K) of (*S*)-3-(2-(*tert*-butoxycarbonylamino)-3-methoxy-3-oxopropyl)-1-mesityl-1*H*-imidazol-3-ium trifluoroacetate (**3.61**).

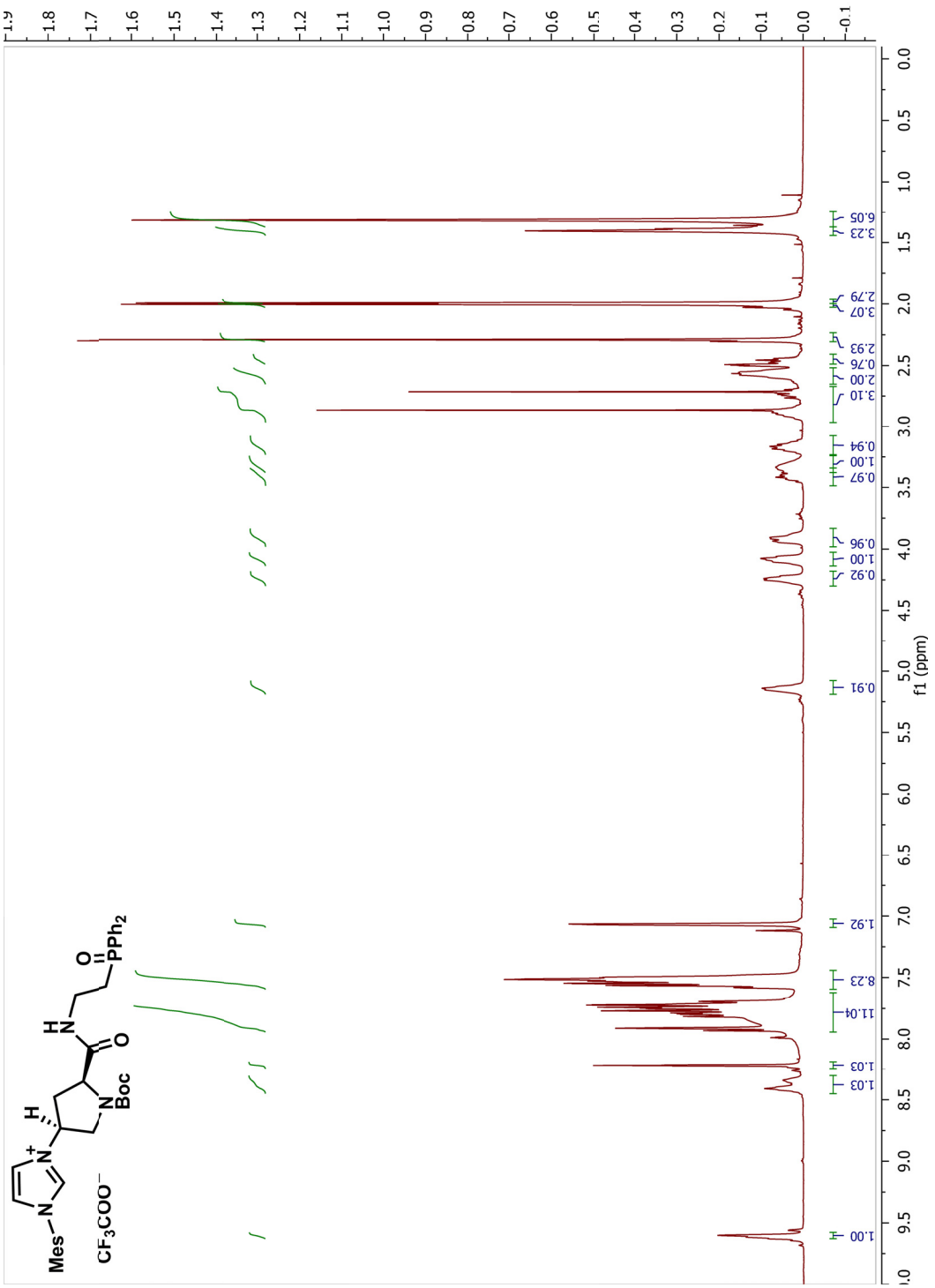

Figure 3.48: ^{1}H NMR (400 MHz, DMSO-*d*6, 293 K) of 3-((3*S*,5*S*)-1-(*tert*-butoxycarbonyl)-5-(2-(diphenylphosphoryl)ethylcarbamoyl)pyrrolidin-3-yl)-1-mesityl-1*H*-imidazol-3-ium trifluoroacetate (**3.62**).

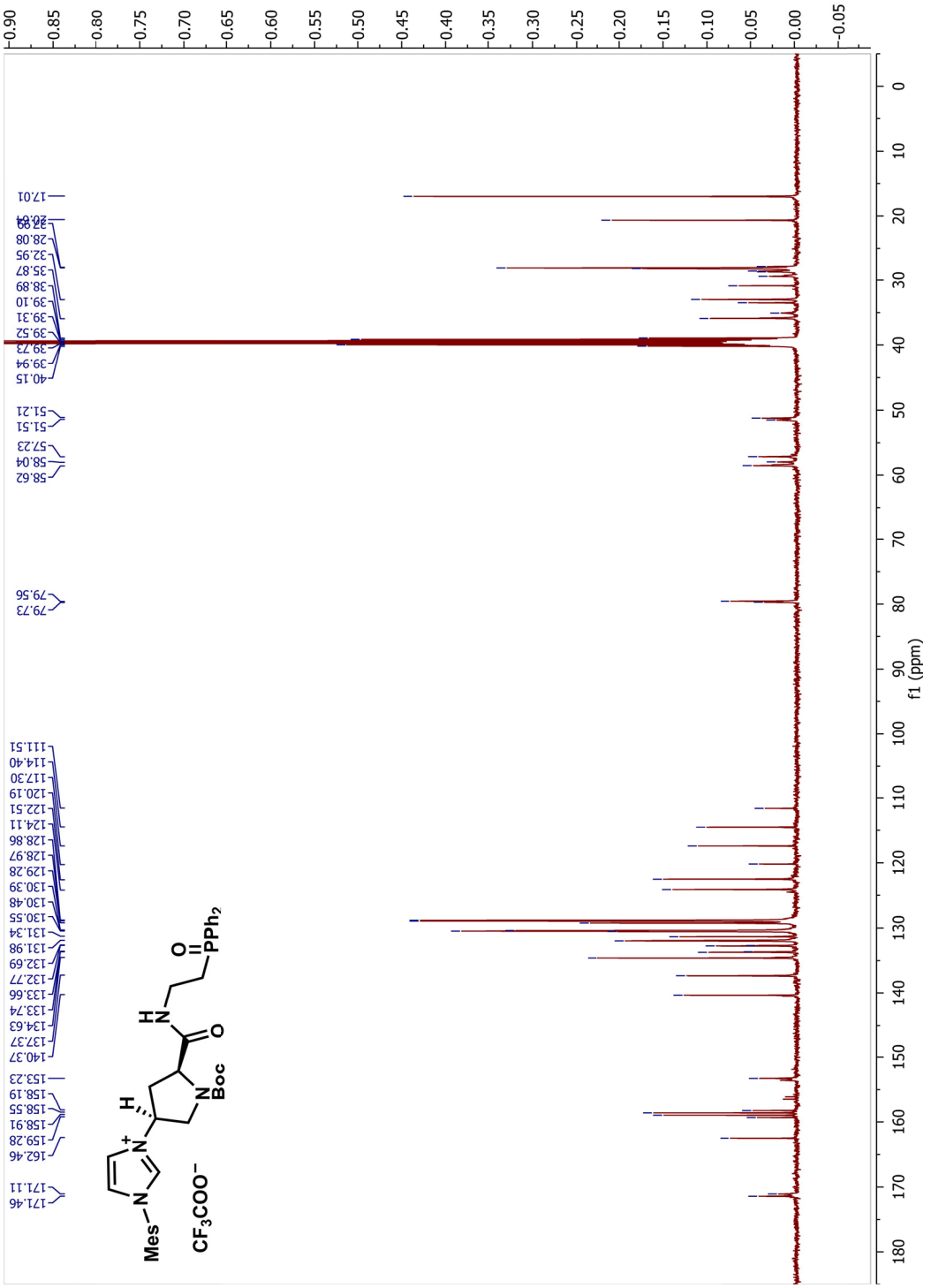

Figure 3.49: ^{13}C NMR (100 MHz, DMSO-*d*6, 293 K) of 3-((3*S*,5*S*)-1-(*tert*-butoxycarbonyl)-5-(2-(diphenylphosphoryl)ethylcarbamoyl)pyrrolidin-3-yl)-1-mesityl-1*H*-imidazol-3-ium trifluoroacetate (**3.62**).

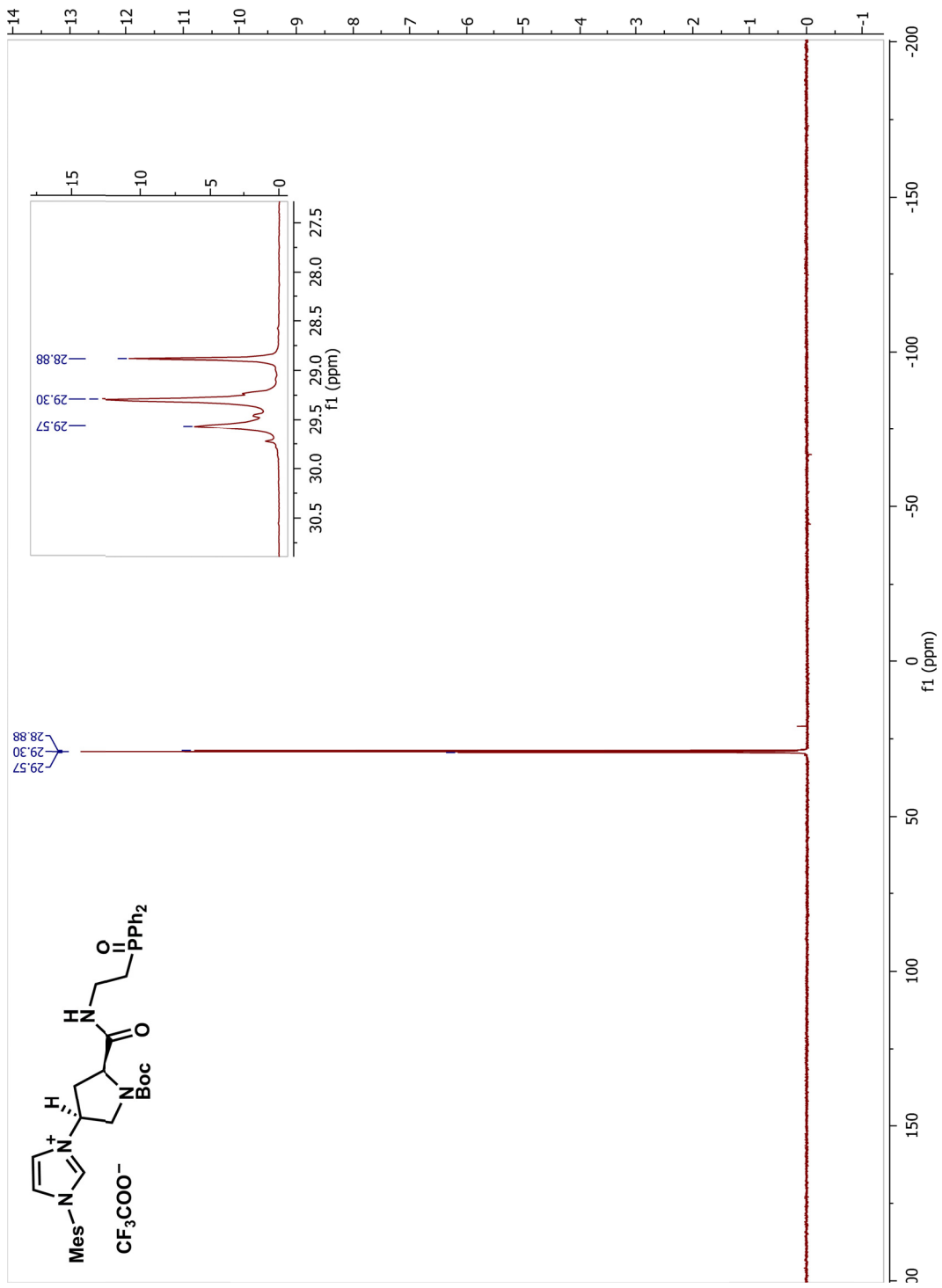

Figure 3.50: ^{31}P NMR (161 MHz, DMSO-*d*6, 293 K) of 3-((3*S*,5*S*)-1-(*tert*-butoxycarbonyl)-5-(2-(diphenylphosphoryl)ethylcarbamoyl)pyrrolidin-3-yl)-1-mesityl-1*H*-imidazol-3-ium trifluoroacetate (**3.62**).

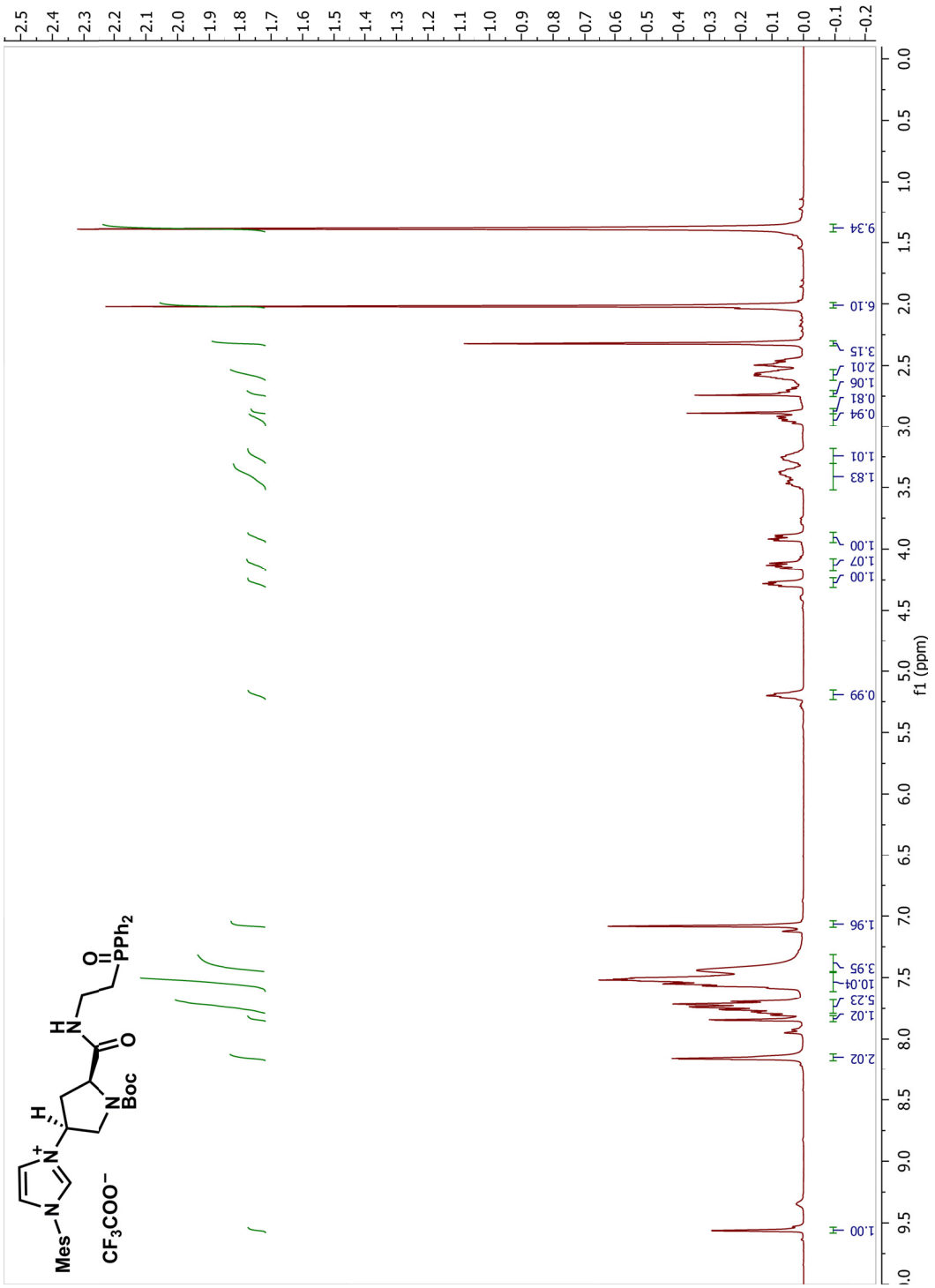

Figure 3.51: ^{1}H NMR (400 MHz, DMSO-*d*6, 353 K) of 3-((3*S*,5*S*)-1-(*tert*-butoxycarbonyl)-5-(2-(diphenylphosphoryl)ethylcarbamoyl)pyrrolidin-3-yl)-1-mesityl-1*H*-imidazol-3-ium trifluoroacetate (**3.62**).

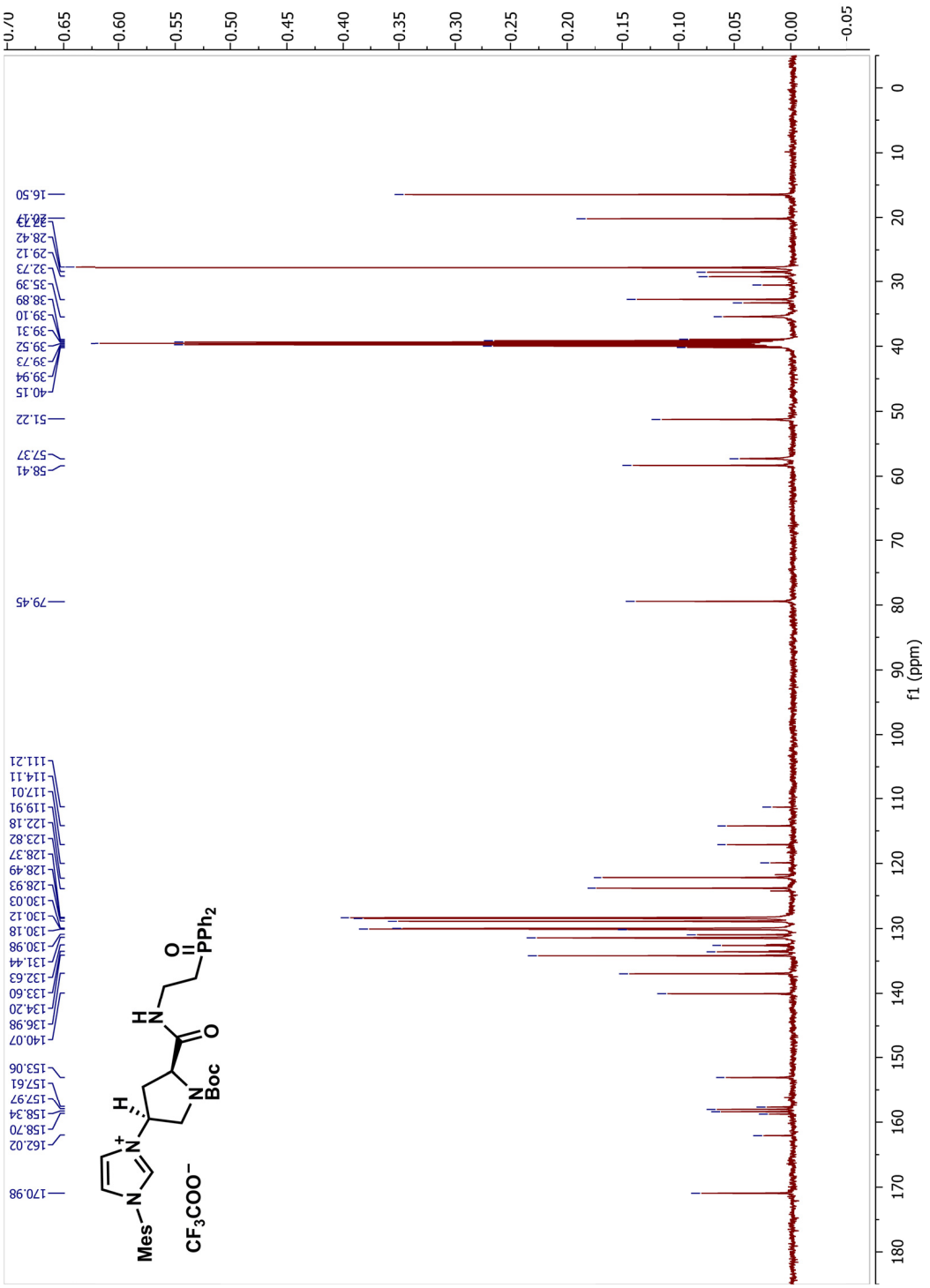

Figure 3.52: ^{13}C NMR (100 MHz, DMSO-*d*6, 353 K) of 3-((3*S*,5*S*)-1-(*tert*-butoxycarbonyl)-5-(2-(diphenylphosphoryl)ethylcarbamoyl)pyrrolidin-3-yl)-1-mesityl-1*H*-imidazol-3-ium trifluoroacetate (**3.62**).

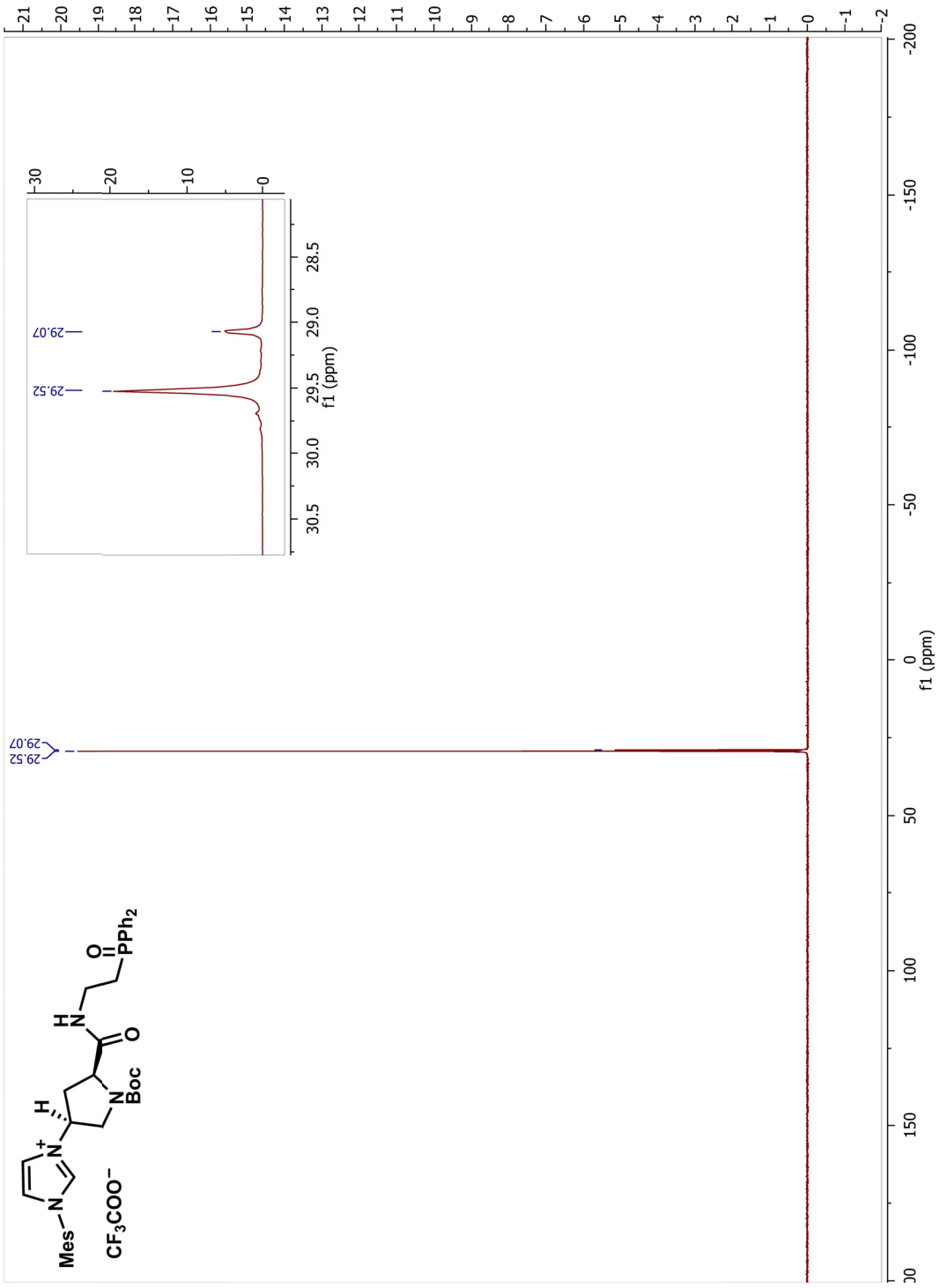

Figure 3.53: ^{31}P NMR (161 MHz, DMSO-*d*6, 353 K) of 3-((3*S*,5*S*)-1-(*tert*-butoxycarbonyl)-5-(2-(diphenylphosphoryl)ethylcarbamoyl)pyrrolidin-3-yl)-1-mesityl-1*H*-imidazol-3-ium trifluoroacetate (**3.62**).

CHAPTER 4 NHC LIGANDS IN ASYMMETRIC CATALYSIS

4.1 Synthesis of NHC Complexes

Most of the work in this section was shown in a published paper.[119] The most widely utilized strategies for the formation of NHC complexes are based on the transformations of the corresponding azolium salts.[166,167,4] The two most common methodologies are shown in Scheme 4.1 with imidazolium salts. We have used these methods extensively in this dissertation.

Scheme 4.1: Two common routes to the syntheses of NHC complexes

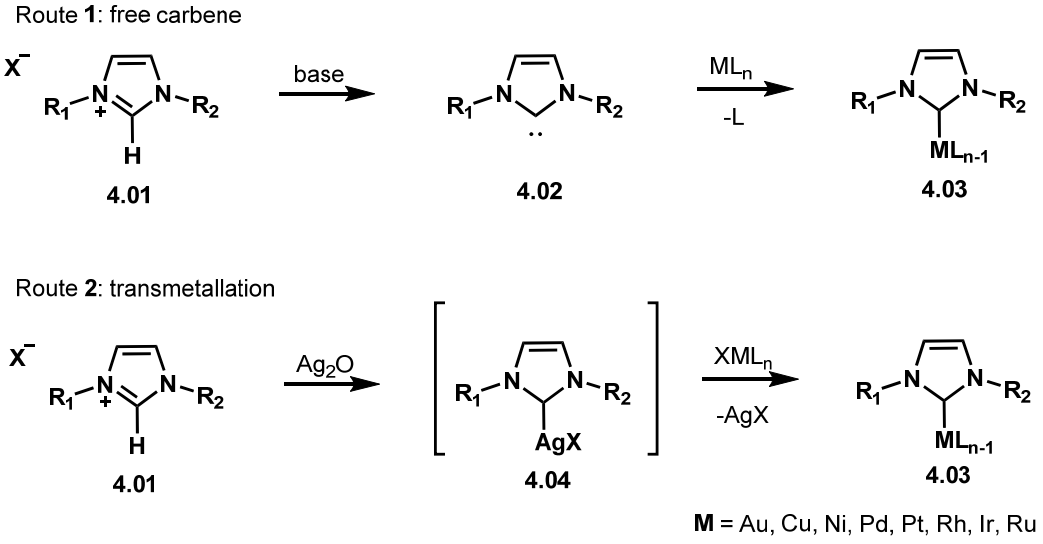

[119] Zhao, Y.; Gilbertson, S. R. *Org. Lett.* **2014**, *16* (4), 1033.

Free carbene is generated in Scheme 4.1, Route **1** by *in situ* deprotonation of the imidazolium salt in the presence of a base such as NaH or KO*t*Bu,[1,81,168] followed by the treatment with the desired metal source to afford the NHC complex **4.03**. This route is straightforward, easy to perform, and more importantly, no isolation of free carbene is required. However, one disadvantage of this methodology for the synthesis of carbene complexes is the basic conditions may decompose some ligands.

A relatively mild method (Scheme 4.1, Route **2**) to obtain a NHC complex is transmetallation from a silver-NHC complex.[169,170] because of the lability of Ag(I)-NHC bond, the NHC in such complexes can be easily transferred to a variety of other metals. Moreover, precipitation of the silver halide produced in the reaction can facilitate the transmetallation. This method is more suitable to prepare the carbene complexes since the more electron-donating saturated carbene forms a stronger bond with silver and thus the silver metal can be difficult to replace.

Scheme 4.2: Formation of rhodium-NHC **4.06**

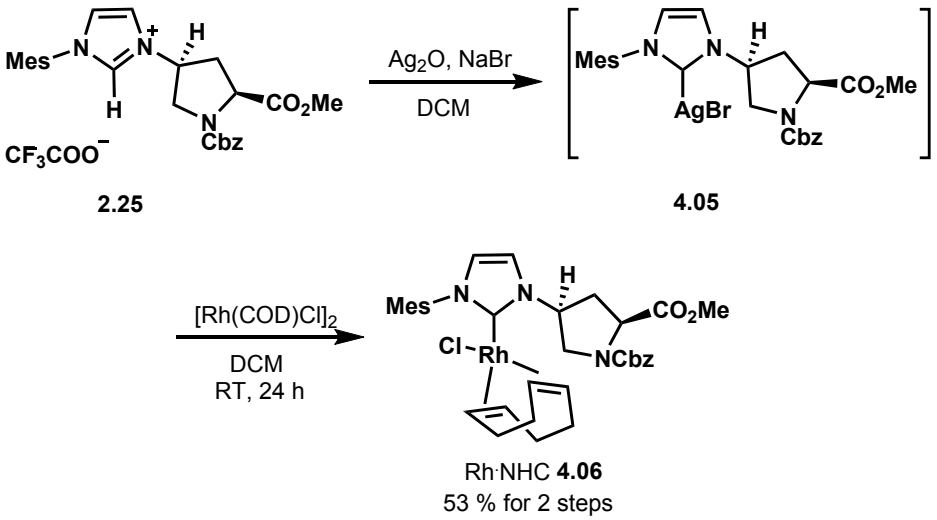

A number of our NHC precursors have been successfully complexed to rhodium (I). For example, imidazolium salt **2.25** was treated with silver (I) oxide in the presence of sodium bromide to generate silver-NHC **4.05**. Under the same condition without sodium bromide, no silver-NHC complex was noted to form. Transmetallation with rhodium cyclooctadiene chloride dimer easily afforded rhodium complex **4.06** (Scheme 4.2).

The other rhodium (I)-NHC complexes that were prepared are illustrated in Figure 4.1. These complexes are air stable and were purified by column chromatography.

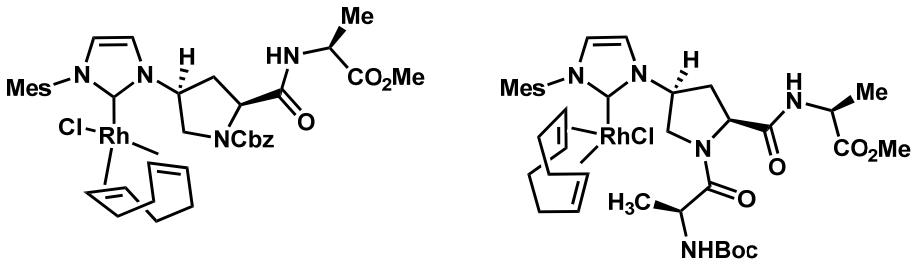

Figure 4.1: Isolated rhodium-NHC complexes.

4.2 Proline-NHC Ligands in Asymmetric Catalysis

The research with rhodium (I)-NHC complexes has been fruitful in a number of reactions catalyzing, hydrosilylation,[81,120,84] hydrogenation,[171,172] hydroformylation,[173,174] cyclization[175–180] and arylation reactions.[181] Rhodium complexes containing multi-dentate NHC ligands display superior stereoselectivity[182] in comparison to those with chiral mono-dentate NHC ligands.

One reaction we would like to apply our ligand system to is the 1,2-addition of boronic acids to aldehydes (Scheme 4.3).[183,184] To the best of our knowledge, there are no reports of highly enantioselective 1,2-addition of boronic acid to aldehydes using Rh-NHC complex as catalyst.[185]

Scheme 4.3: Rhodium-catalyzed addition of boronic acid to aldehyde

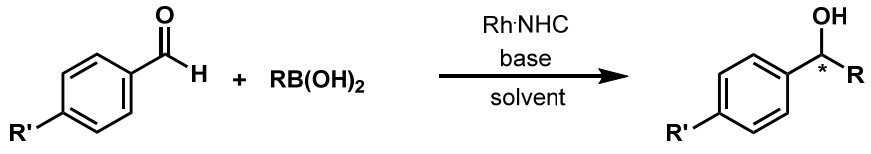

4.09 4.10 4.11

Numerous attempts to utilize the corresponding rhodium complexes of these mono-dentate NHCs (Figure 4.2) were unsuccessful in providing asymmetric environment for this reaction.

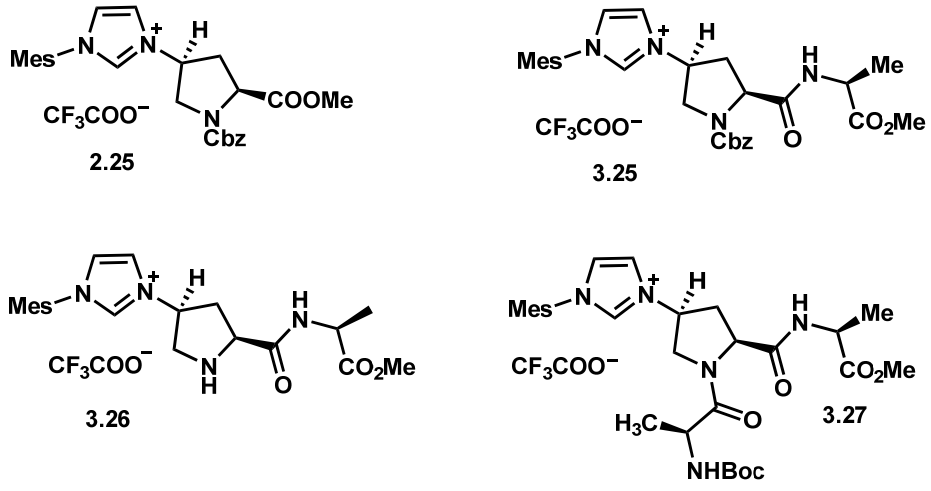

Figure 4.2: Imidazolium salts used in asymmetric catalysis.

The initial attempts were performed to catalyze the addition of phenyl boronic acid to *p*-anisaldehyde. Well defined catalyst **4.06** gave very low yields of desired alcohol **4.14** (Scheme 4.3). The *in situ* generation of NHC complex is more convenient (Scheme 4.5) and provided the reaction a higher conversion to product.

Scheme 4.4: 1, 2-Addition of boronic acid to aldehyde with Rh-NHC **4.06**

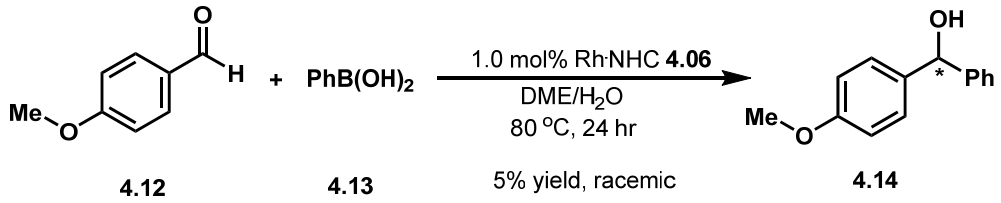

4.12 **4.13** 5% yield, racemic **4.14**

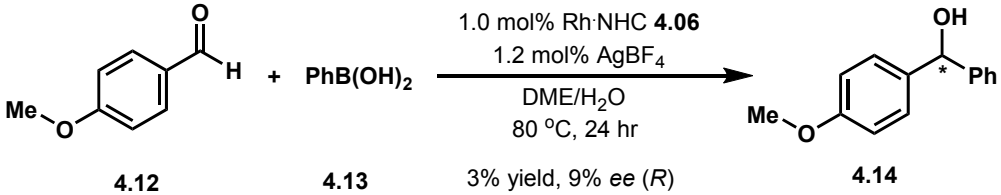

4.12 **4.13** 3% yield, 9% *ee* (*R*) **4.14**

Scheme 4.5: 1, 2-Addition of boronic acid to aldehyde with **2.25**

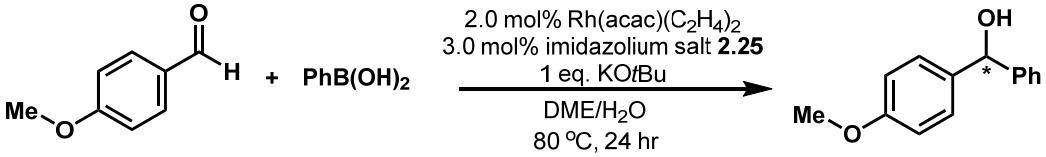

4.12 **4.13** 42% yield, racemic **4.14**

The reaction conditions screened are presented in Table 4.1. Using imidazolium salt **3.26** as NHC precursor, we obtained the alcohol **4.14** in 25% yield, 39% *ee* (entry 5).

Table 4.1: Initial condition screen of 1, 2-Addition of boronic acid to aldehyde

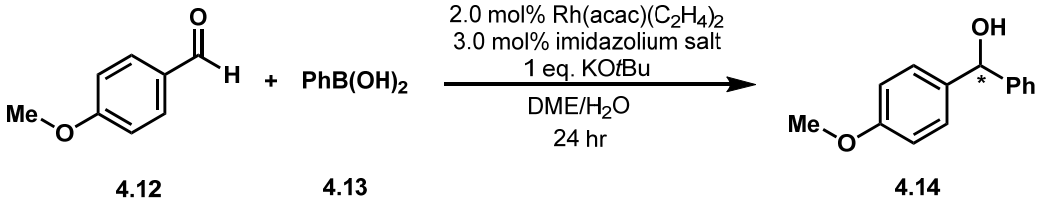

4.12 **4.13** **4.14**

Entry	Imidazolium salt	Temperature (°C)	Yield (%)	*ee* (%)
1	**2.25**	80	42	0
2	**2.25**	50	13	0
3	**2.25**	RT	N. R.	-
4	**3.25**	80	82	7 (*S*)
5	**3.26**	80	25	39 (*S*)
6	**3.27**	80	69	0
7	None	80	15	0

Unfortunately, this enantioselectivity could not be reproduced under the same conditions. Racemic products were obtained in the reactions using some other substrates (Table 4.2).

Table 4.2: Reaction scope using **3.26** as ligand precursor

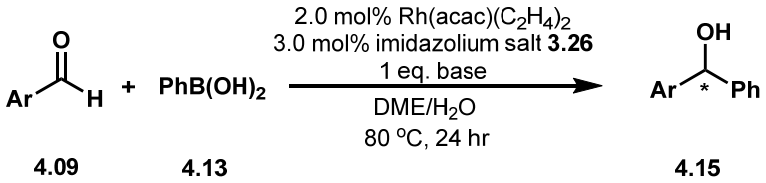

4.09 **4.13** **4.15**

Entry	Ar	Base	Yield (%)	*ee* (%)
1	4-MeOC_6H_4	KO*t*Bu	63	0
2	2-MeOC_6H_4	KO*t*Bu	81	0
3	3-MeOC_6H_4	KO*t*Bu	76	N. A.
4	1-Naphthyl	KO*t*Bu	75	0
5	4-MeOC_6H_4	None	Trace	-

A number of rhodium sources were used for the *in situ* generate NHC complexes with salt **2.25** and then employed in the addition of boronic acid to aldehyde (Table 4.3). The catalyst prepared from $[Rh(C_2H_4)_2Cl]_2$ was able to provide 19% *ee*.

Table 4.3: Conditions for 1, 2-Addition of boronic acid to aldehyde **1**

4.12 **4.13** **4.14**

Entry	Rh (I)	Temperature (°C)	Yield (%)	*ee* (%)
1	$Rh(acac)(C_2H_4)_2$	80	75	0
2	$[Rh(cod)Cl]_2$	80	66	0
3	$[Rh(C_2H_4)_2Cl]_2$	80	79	0
4	None	80	10	0
5[a]	$[Rh(cod)Cl]_2$	60	9	0
6	$[Rh(cod)Cl]_2$	RT	9	0
7	$[Rh(C_2H_4)_2Cl]_2$	60	27	19 (*S*)
8	$[Rh(C_2H_4)_2Cl]_2$	RT	15	0

a: Reaction conditions: Entry 5, 6, 7, 8 is in 0.5 mmol scale; Others are in 1.0 mmol scale.

Further reaction condition optimization failed to provide better enantioselectivity (Table 4.4, Table 4.5 and Table 4.6).

Table 4.4: Conditions for 1, 2-Addition of boronic acid to aldehyde **2**

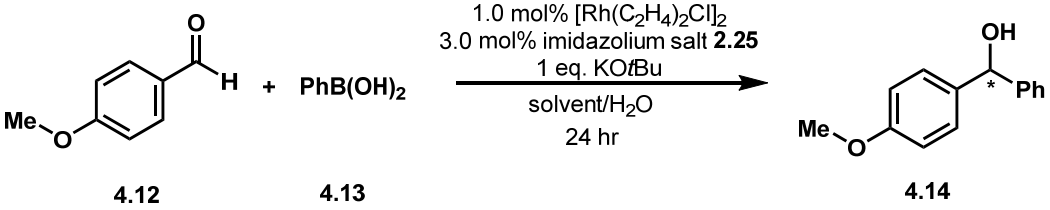

4.12 **4.13** **4.14**

Entry	Solvent	Temperature (°C)	Yield (%)	*ee* (%)
1	DME	60	27	19 (*S*)
2	DME	RT	15	0
3	$ClCH_2CH_2Cl$	60	58	0
4	$ClCH_2CH_2Cl$	RT	4	0
5	Toluene	60	37	0
6	Toluene	RT	Trace	-
7	Dioxane	60	60	0
8	Dioxane	RT	4	0
9	DMF	60	7	0
10	DMF	RT	N. R.	-

Table 4.5: Conditions for 1, 2-Addition of boronic acid to aldehyde **3**

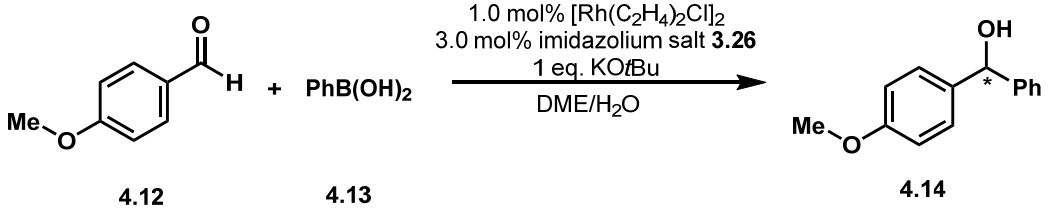

4.12 **4.13** **4.14**

Entry	Reaction time (hr)	Temperature (°C)	Yield (%)	*ee* (%)
1	24	60	39	0
2	48	RT	Trace	-
3	48	60	67	0
4[a]	24	80	89	0
5	24	80	62	0

a: Reaction conditions: Rh complex in a vial was added a solution of boronic acid and NHC salt in DME under N_2, *p*-Anisaldehyde, base and water was then added.

Table 4.6: Conditions for 1, 2-Addition of boronic acid to aldehyde **4**

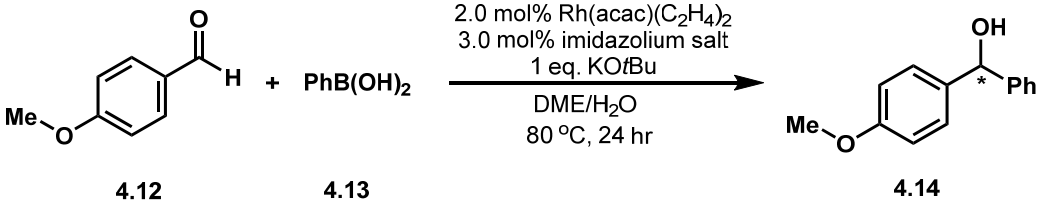

4.12 **4.13** **4.14**

Entry	Salt	Temperature (°C) /complex formation	Reaction time (min) /complex formation	Yield (%)	*ee* (%)
1	**3.26**	RT	10	19	0
2	**3.26**	RT	0	32	0
3	**3.26**	RT	60	27	9 (*S*)
4	**3.26**	60	60	10	17 (*S*)
5	**3.26**	80	60	18	10 (*S*)
6	**3.26**	60	60	8	17 (*S*)
7[a]	**3.26**	RT	10	15	0
8	**3.25**	RT	10	35	0
9	**3.25**	60	60	23	0

a: Reaction conditions: 2 mol% of imidazolium salt **3** was used.

Palladium-NHC was attempted and failed to afford the desired product (Table 4.7).

Bidentate NHC ligands will be employed next in the addition reaction due to the failure of mono-dentate ligand system. However, the initial NHC-phosphine oxide ligands we synthesized could not be converted to rhodium complex under a number of reaction conditions. More work will be done in the application of our NHC building blocks in asymmetric catalysis.

Table 4.7: Pd-catalyzed 1, 2-Addition of boronic acid to aldehyde

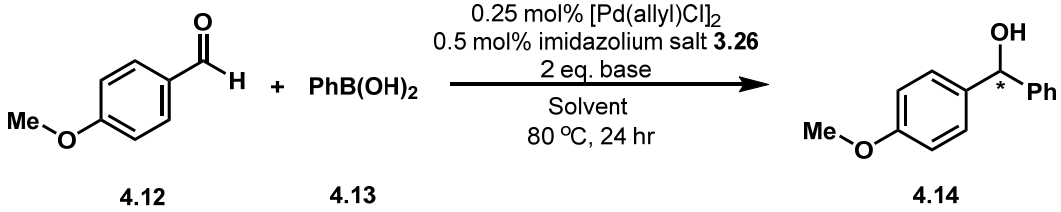

4.12 4.13 4.14

Entry	Base	Solvent	Yield (%)	*ee* (%)
1	CsF	DME	Trace	-
2	Cs_2CO_3	DME	6	0
3	KO*t*Bu	DME	N. R.	-
4	K_2CO_3	DME	9	0
5	K_2CO_3	DME/H_2O	12	0
6	K_2CO_3	Dioxane/H_2O	Trace	-
7	KOH	DME/H_2O	N. R.	-

4.3 Experimental Section

General Procedures:

All reagents were purchased from Sigma-Aldrich, Acros, Aapptec and Strem and used as received unless otherwise noted. Thin-layer chromatography was performed on silica gel 60 F_{254} pre-coated plates (0.25 mm) from Silicycle and components were visualized by UV light (254 nm) and/or 10% phosphomolybdic acid in ethanol stain. Flash chromatography was performed using Silicycle silica gel 230-400 (particle size 40-63 μm) mesh. Analytical high-performance liquid chromatography was performed on an Agilent 1100 Series instrument equipped with a Variable Wavelength Detector. Preparative HPLC was performed on a Gilson instrument equipped with a 321 pump, UV/VIS-155

detector and FC-204 fraction collector. ^{1}H and ^{13}C NMR were recorded on JEOL ECX-400 NMR spectrometer (400 MHz for ^{1}H NMR and 100 MHz for ^{13}C NMR) or JEOL ECX-500 NMR spectrometer (500 MHz for ^{1}H NMR and 125 MHz for ^{13}C NMR) in chloroform-*d* at ambient temperature and/or 318 K (45 ˚C) or in DMSO-*d*6 at ambient temperature and 353 K (80 ˚C, if necessary). In chloroform-*d*, chemical shifts were referenced to the residual chloroform-H peak at 7.26 ppm for ^{1}H NMR and 77.16 ppm for ^{13}C NMR. In DMSO-*d*6, chemical shifts were referenced to the residual DMSO-H peak at 2.50 ppm for ^{1}H NMR and 39.52 ppm for ^{13}C NMR. Chemical shifts are reported in parts per million (ppm, δ). Multiplicity are indicated as s = singlet, d = doublet, t = triplet, q = quartet, m = multiplet, br = broad resonance and the coupling constants (*J*) are reported in Hz. Liquid chromatography-mass spectrometry (LC-MS) was performed on a Thermo Finningan Surveyor instrument equipped with MSQ Plus single quadrupole detector. High resolution mass spectral data were recorded on an Agilent 6530 Accurate Mass Q-TOF LC/MS (high resolution ESI) and a Micromass (now Waters) Autospec Ultima mass Spectrometer (high resolution CI) from University of Texas at Austin, Mass Spectrometry Facility (MSF) of the Department of Chemistry & Biochemistry.

Procedure for synthesis of Rh-NHC complexes:

1 equivalent of imidazolium salt, 1 equivalent of silver oxide and 5 equivalents of sodium bromide were added to a sealed vial with septum. The vial was then evacuated and backfilled with nitrogen (twice). Dry degassed DCM was added to the vial and the mixture was allowed to stir overnight in the dark at room temperature. After filtration

over Celite 545, the solution was dried under reduced pressure to give the silver-NHC intermediate which was carried on to the next step without further purification.

The Ag-NHC complex was added to a solution of 0.5 equivalent of $[Rh(cod)Cl]_2$ in dry and degassed DCM and the mixture was stirred at room temperature for 24 hours. The yellowish suspension was filtered over Celite and then evaporation under reduced pressure gave a yellowish residue. The residue was washed with pentane three times and then purified by column chromatography.

Chloro(η^4-1,5-cyclooctadiene)(3-((3*S*,5*S*)-1-(benzyloxycarbonyl)-5-(methoxycarbonyl)pyrrolidin-3-yl)-1-mesitylimidazole-2-ylidene)rhodium(I) (4.06)

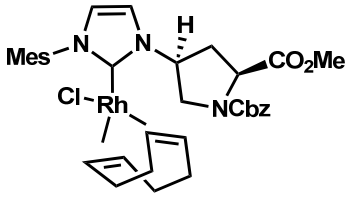

Yield for two steps: 53%. *The NMR spectra are reported for a mixture of two rotamers*: ^{1}H NMR (500 MHz, $CDCl_3$, 318 K) δ 7.41–7.27 (m, 5H), 7.24 (d, *J* = 1.5 Hz, 1H), 7.08 (s, 1H), 6.90 (s, 1H), 6.78 (d, *J* = 2.1 Hz, 1H), 6.66 (br s, 1H), 5.24 (d, *J* = 12.2 Hz, 1H), 5.15 (br s, 1H), 4.91–4.77 (m, 2H), 4.61 (dd, *J* = 28.0, 20.0 Hz, 1H), 4.54–4.39 (m, 1H), 3.79 (br s, 1.5H), 3.75–3.67 (m, 1.5H), 3.60 (s, 1H), 3.41 (s, 1H), 3.32 (d, *J* = 18.3 Hz, 0.5H), 3.09 (br s, 0.5H), 2.90 (s, 1H), 2.40 (s, 3H), 2.35 (s, 3H), 2.30–2.22 (m, 1H), 2.17–2.07 (m, 2H), 2.07–1.92 (m, 2H), 1.80 (s, 3H), 1.74–1.54 (m, 2H), 1.56–1.40 (m, 2H); ^{13}C NMR (125 MHz, $CDCl_3$, 318 K) δ 183.98 (d, $J_{Rh\text{-}C}$ = 51.5 Hz), 183.86 (d, $J_{Rh\text{-}C}$ =

51.8 Hz), 173.28, 172.83, 154.67, 154.26, 138.96, 137.16, 136.30, 136.01, 134.31, 134.19, 129.79, 129.74, 128.57, 128.32, 128.28, 128.16, 124.42, 117.50, 98.16 (d, J_{Rh-C} = 6.4 Hz), 97.56 (d, J_{Rh-C} = 6.2 Hz), 68.95, 68.65 (d, J_{Rh-C} = 14.3 Hz), 67.71, 67.65, 67.35 (d, J_{Rh-C} = 14.1 Hz), 58.82, 58.26, 52.48, 51.86, 37.34, 34.83, 31.04, 29.62, 27.64, 27.58, 21.11, 19.80, 17.82; LC/MS (ESI) calculated for $C_{34}H_{41}N_3O_4Rh$ $[M-Cl]^+$ 658.22, found 657.77 (t_R = 11.18 min); HRMS (CI^+) calculated for $C_{34}H_{41}N_3O_4ClRh$ $[M]^+$ 693.1841, found 693.1839.

Chloro(η^4-1,5-cyclooctadiene)(3-((3*S*,5*S*)-1-(benzyloxycarbonyl)-5-((*S*)-1-methoxy-1-oxopropan-2-ylcarbamoyl)pyrrolidin-3-yl)-1-mesitylimidazole-2-ylidene)rhodium(I) (4.07)

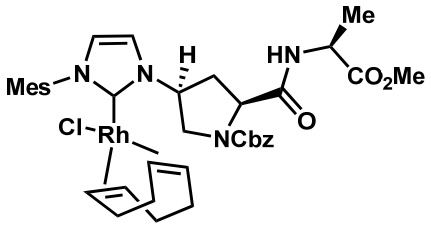

Yield for two steps: 45%. *The NMR spectra are reported for a mixture of two rotamers*: ^{1}H NMR (500 MHz, $CDCl_3$, 318 K) δ 7.54 (br s, 1H), 7.30-7.40 (m, 5H), 7.13 (br s, 1H), 6.94 (br s, 1H), 6.77-6.95 (m, 2H), 5.15-5.27 (m, 2H), 4.90-4.92 (m, 2H), 4.73 (br s, 0.5H), 4.64 (br s, 0.5H), 4.49-4.57 (m, 2H), 3.74 (s, 3H), 3.61 (br s, 1H), 3.34 (br s, 0.5H), 3.23 (br s, 0.5H), 3.09 (br s, 0.5H), 3.00 (br s, 0.5H), 2.88 (br s, 1H), 2.73 (br s, 1H), 2.39 (s, 6H), 2.20 (s, 3H), 1.99-2.06 (m, 1H), 1.84 (d, *J* = 6.9 Hz, 3H), 1.88-1.95 and 1.56-1.66 (m, 4H), 1.27-1.48 (m, 4H); ^{13}C NMR (125 MHz, $CDCl_3$, 318 K) δ 182.28 (d, J_{Rh-C} =

53.6 Hz), 182.18 (d, $J_{Rh\text{-}C}$ = 51.5 Hz), 173.09, 172.85, 171.48, 171,07, 155.46, 154.62, 139.02, 137.27, 135.89, 134.10, 129.89, 128.73, 128.51, 128.44, 128.31, 128.17, 124.57, 118.38, 98.62 (d, $J_{Rh\text{-}C}$ = 6.0 Hz), 97.31 (d, $J_{Rh\text{-}C}$ = 6.0 Hz), 68.03, 67.93, 67.26 (d, $J_{Rh\text{-}C}$ = 14.4 Hz), 66.12, 65.94 (d, $J_{Rh\text{-}C}$ = 14.4 Hz), 65.84, 65.73, 59.70, 59.50, 52.52, 52.27, 48.69, 34.15, 33.80, 31.60, 31.46, 29.83, 28.78, 28.64, 27.90, 21.19, 18.06, 18.02; LC/MS (APCI) calculated for $C_{37}H_{46}N_4O_5Rh$ $[M\text{-}Cl]^+$ 729.25, found 729.36 (t_R = 10.99 min); HRMS (CI^+) calculated for $C_{37}H_{46}N_4O_5Rh$ $[M]^+$ 764.2212, found 764.2212.

Chloro(η^4-1,5-cyclooctadiene)(3-((3*S*,5*S*)-1-((*S*)-2-(*tert*-butoxycarbonylamino)propanoyl)-5-((*S*)-1-methoxy-1-oxopropan-2-ylcarbamoyl)pyrrolidin-3-yl)-1-mesitylimidazole-2-ylidene)rhodium(I) (4.08)

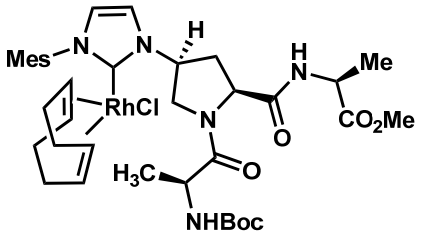

Yield for two steps: 41%. *The NMR spectra are reported for a mixture of two rotamers*: ^{1}H NMR (500 MHz, $CDCl_3$, 318 K) δ 7.50 (d, *J* = 5.0 Hz, 1H), 7.09 (br s, 1H), 6.92 (s, 1H), 6.80-6.75 (m, 2H), 5.46-5.42 (m, 1H), 4.98-4.86 (m, 2H), 4.85 (br s, 1H), 4.87-4.72 (m, 1H), 4.67-4.46 (m, 3H), 3.76 (s, 1.5H), 3.75 (s, 1.5H), 3.64-3.41 (m, 2H), 2.99-2.89 (m, 1H), 2.69-2.59 (m, 1H), 2.64-2.47 (m, 1H), 2.43 (s, 3H), 2.37 (s, 3H), 2.24-1.94 (m, 4H), 1.84 (s, 1.5H), 1.83 (s, 1.5H), 1.88-1.86 and 1.77-1.59 (m, 4H), 1.43 (s, 9H), 1.37-1.32 (m, 3H), 1.29-1.22 (m, 3H); ^{13}C NMR (125 MHz, $CDCl_3$, 318 K) δ 184.10 (d, $J_{Rh\text{-}C}$

= 48.0 Hz), 184.02 (d, J_{Rh-C} = 51.6 Hz), 173.20, 172.97, 172.78, 172.44, 171.15, 170.65, 155.37, 154.89, 139.01, 137.28, 136.15, 134.45, 134.35, 129.86, 129.81, 128.85, 128.39, 127.96, 124.67, 124.56, 118.11, 114.26, 98.40, 98.38, 97.90 (d, J_{Rh-C} = 6.0 Hz), 97.71 (d, J_{Rh-C} = 6.0 Hz), 69.05, 68.99, 68.88, 67.49 (d, J_{Rh-C} = 14.4 Hz), 67.07 (d, J_{Rh-C} = 14.4 Hz), 59.67, 59.31, 59.01, 52.78, 52.57, 48.69, 35.17, 34.98, 34.86, 33.87, 31.16, 30.96, 29.85, 29.72, 29.23, 28.58, 28.55, 28.23, 27.69, 27.57, 25.47, 22.78, 21.19, 19.92, 18.65, 18.24, 18.14, 17.94;

LC/MS (APCI) calculated for $C_{37}H_{53}N_5O_6Rh$ $[M-Cl]^+$ 766.31, found 766.33 (t_R = 10.85 min); HRMS (CI^+) calculated for $C_{37}H_{53}N_5O_6Rh$ $[M-Cl]^+$ 766.3051, found 766.3035.

APPENDIX C: NMR SPECTRA FOR CHAPTER 4

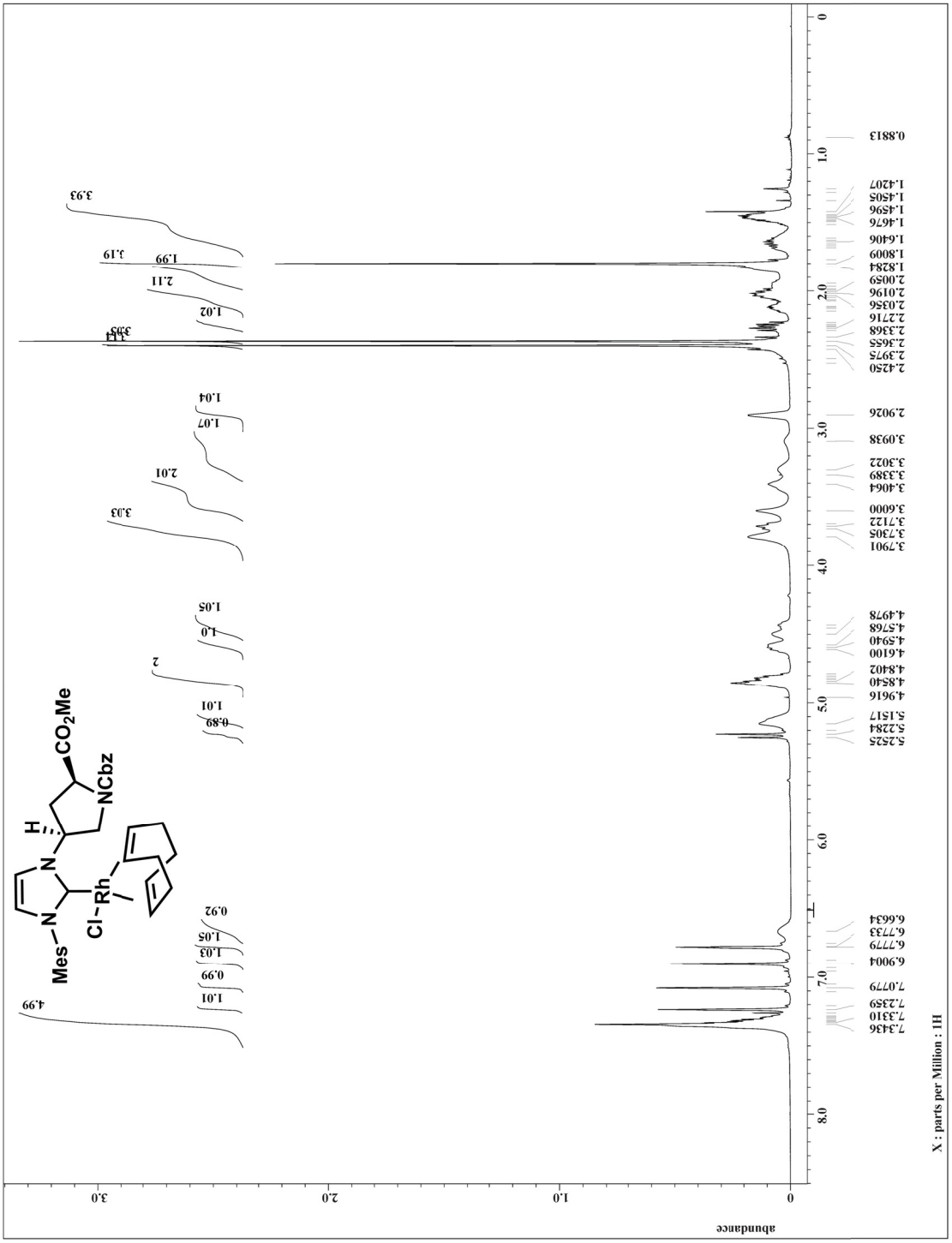

Figure 4.3: ^{1}H NMR (500 MHz, $CDCl_3$, 318 K) of Chloro(η^4-1,5-cyclooctadiene)(3-((3*S*,5*S*)-1-(benzyloxycarbonyl)-5-(methoxycarbonyl)pyrrolidin-3-yl)-1-mesitylimidazole-2-ylidene)rhodium(I) (**4.06**).

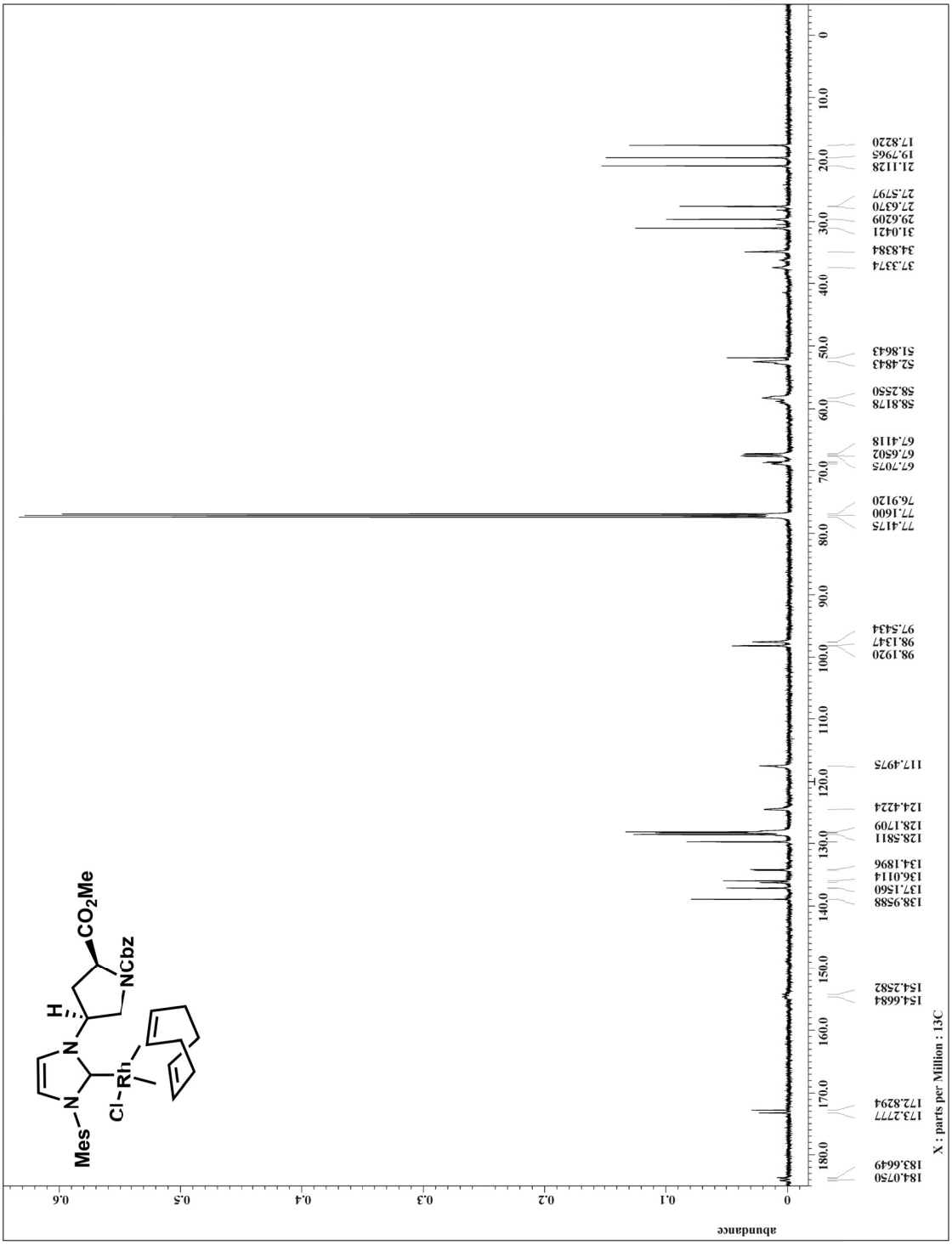

Figure 4.4: ^{13}C NMR (125 MHz, $CDCl_3$, 318 K) of Chloro(η^4-1,5-cyclooctadiene)(3-((3*S*,5*S*)-1-(benzyloxycarbonyl)-5-(methoxycarbonyl)pyrrolidin-3-yl)-1-mesitylimidazole-2-ylidene)rhodium(I) (**4.06**).

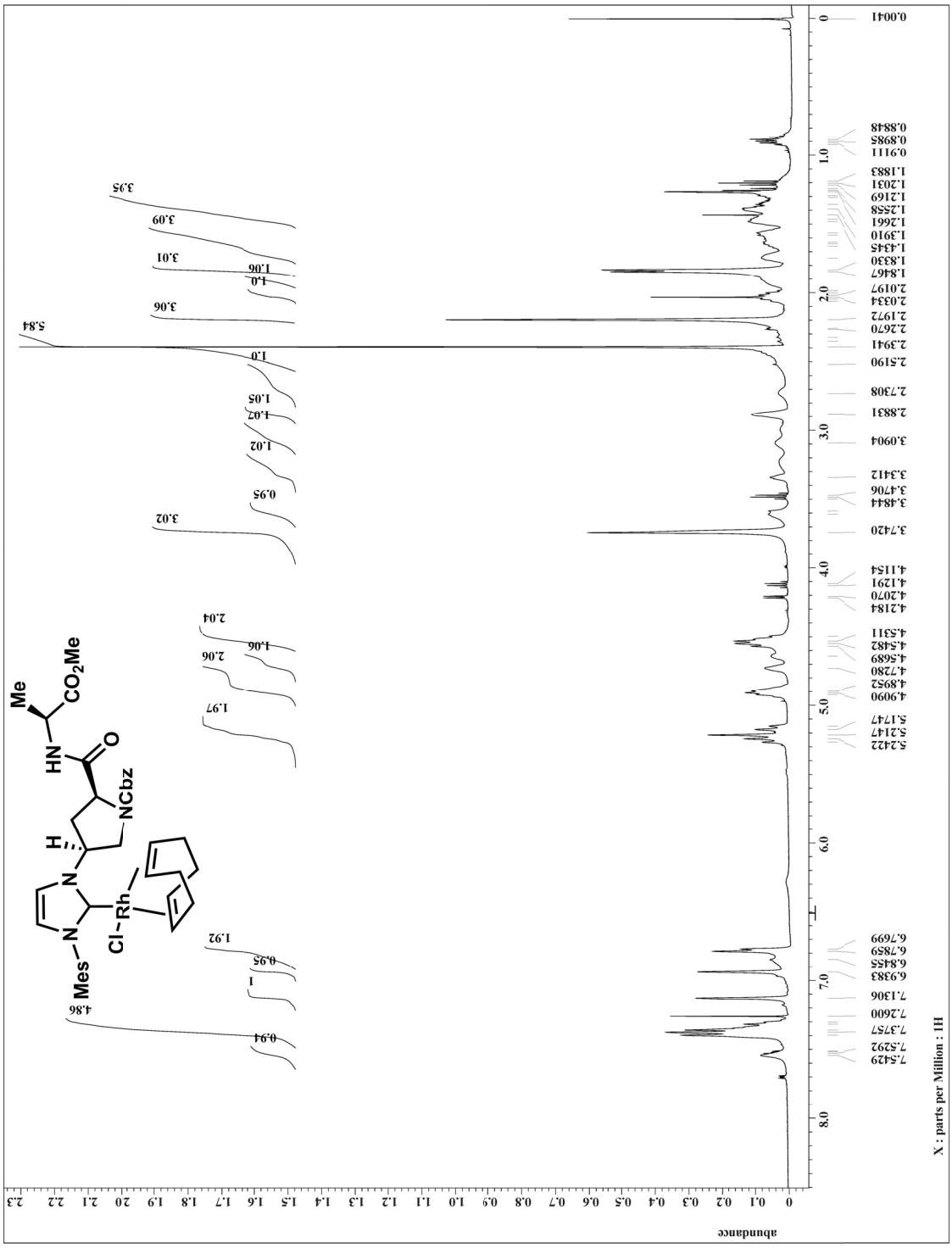

Figure 4.5: ^{1}H NMR (500 MHz, $CDCl_3$, 318 K) of Chloro(η^4-1,5-cyclooctadiene)(3-((3*S*,5*S*)-1-(benzyloxycarbonyl)-5-((*S*)-1-methoxy-1-oxopropan-2-ylcarbamoyl)pyrrolidin-3-yl)-1-mesitylimidazole-2-ylidene)rhodium(I) (**4.07**).

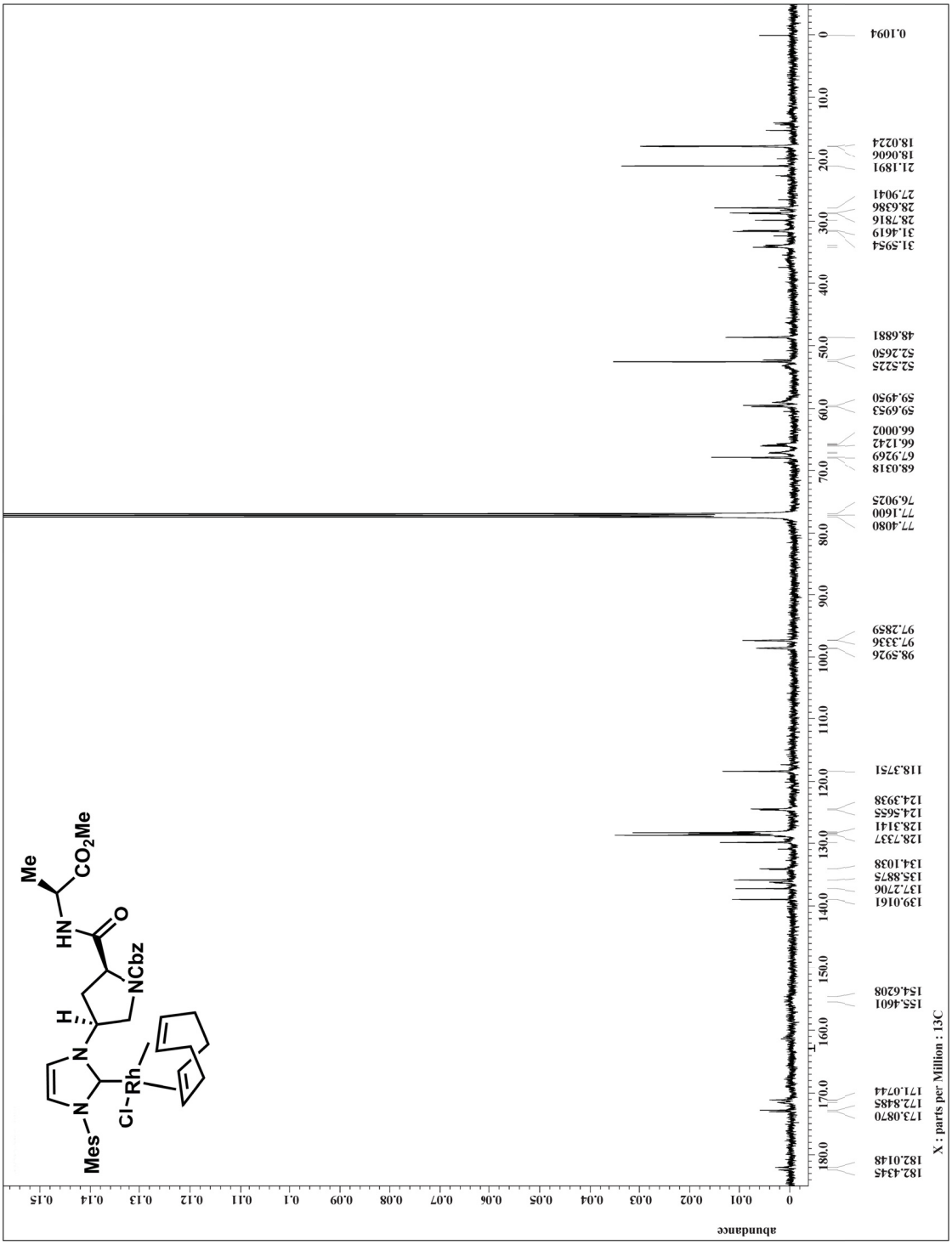

Figure 4.6: ^{13}C NMR (125 MHz, $CDCl_3$, 318 K) of Chloro(η^4-1,5-cyclooctadiene)(3-((3*S*,5*S*)-1-(benzyloxycarbonyl)-5-((*S*)-1-methoxy-1-oxopropan-2-ylcarbamoyl)pyrrolidin-3-yl)-1-mesitylimidazole-2-ylidene)rhodium(I) (**4.07**).

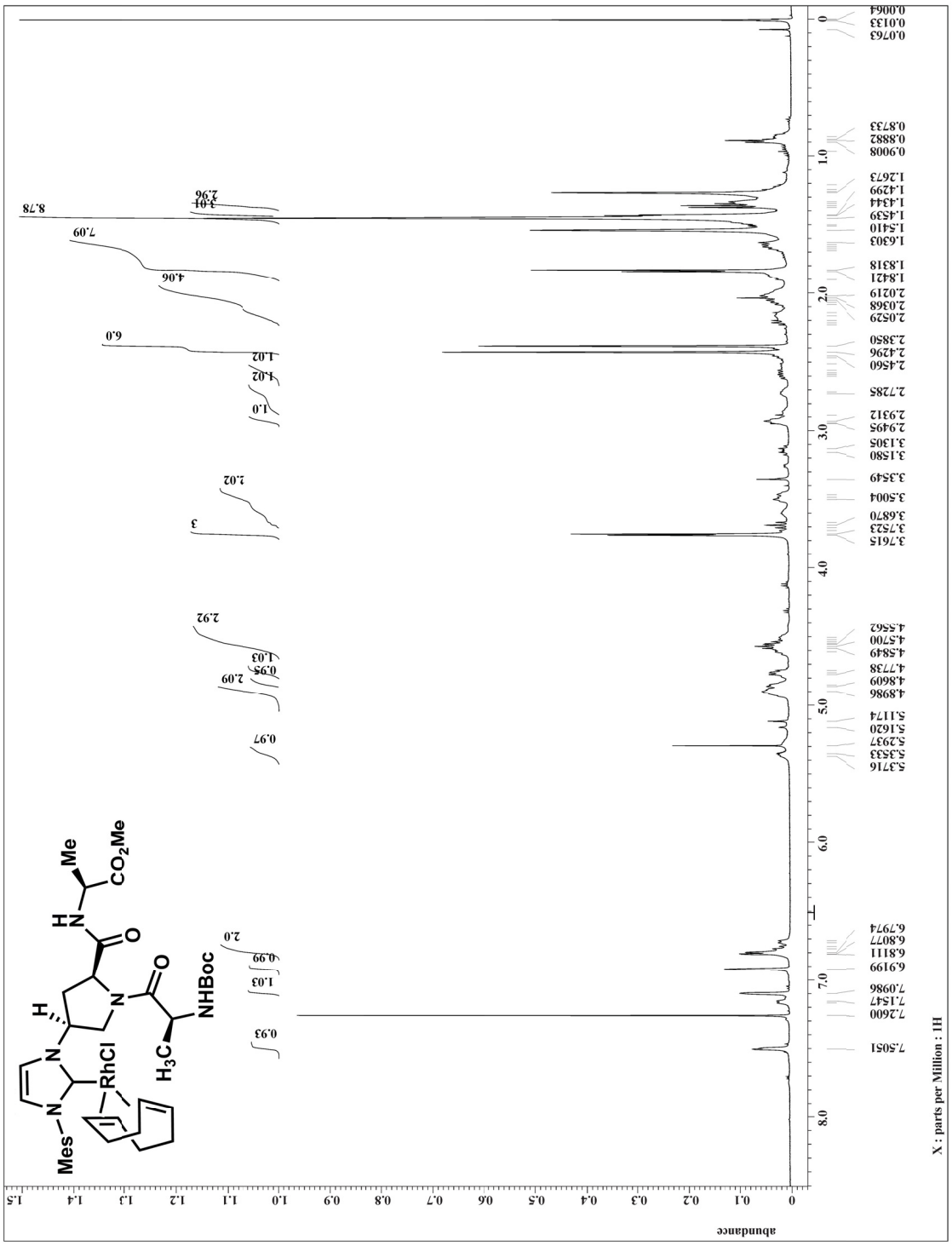

Figure 4.7: ^{1}H NMR (500 MHz, $CDCl_3$, 318 K) of Chloro(η^4-1,5-cyclooctadiene)(3-((3*S*,5*S*)-1-((*S*)-2-(*tert*-butoxycarbonylamino)propanoyl)-5-((*S*)-1-methoxy-1-oxopropan-2-ylcarbamoyl)pyrrolidin-3-yl)-1-mesitylimidazole-2-ylidene)rhodium(I) (**4.08**).

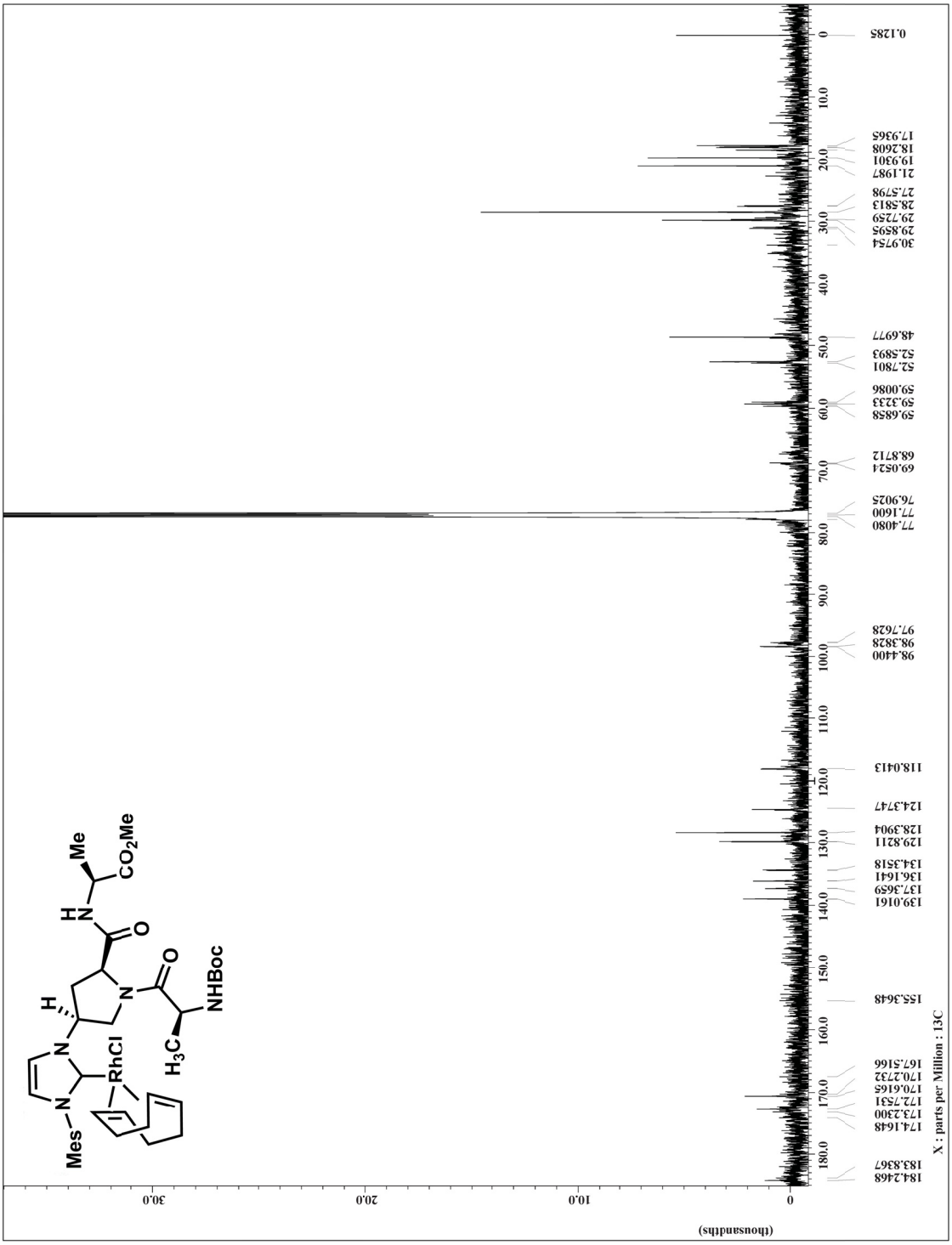

Figure 4.8: ^{13}C NMR (125 MHz, $CDCl_3$, 318 K) of Chloro(η^4-1,5-cyclooctadiene)(3-((3*S*,5*S*)-1-((*S*)-2-(*tert*-butoxycarbonylamino)propanoyl)-5-((*S*)-1-methoxy-1-oxopropan-2-ylcarbamoyl)pyrrolidin-3-yl)-1-mesitylimidazole-2-ylidene)rhodium(I) (**4.08**).

CHAPTER 5 SUMMARY

N-Heterocyclic carbenes have been widely employed as transition metal ligands and there is a significant need for structurally-diverse chiral NHCs. My work in this dissertation was to facilitate the synthesis of chiral NHC ligands by introducing novel NHC building blocks.

The facile cyclization of imidazolium ring failed to generate the desired product due to the steric hindrance and amino acid structural complexity. The synthesis of this type of proline-based imidazolium salts was achieved by alkylation of pre-existed mono-substituted imidazole using protected proline triflate as electrophile. Notably, the initial attempts of this transformation performed at room temperature gave a mixture of diastereomers. A single diastereomer was obtained if the reaction was maintained at low temperature. This method for the synthesis of NHC precursors is efficient requiring only two steps from commercially available proline derivatives.

These types of imidazolium salts have be used as building blocks for the synthesis of more sophisticated NHC precursors. The proline component of the ligand structure allows it to be combined with other functional groups including amino acids by simple amide bond formation. Removal and exchange of N- or C- protecting groups was performed to allow different coupling methods to be used. The proline-imidazolium was successfully incorporated into a tripeptide.

The approaches to a variety of bidentate ligand precursors was also reported. The other coordinating group was chosen to be phosphine oxide or oxazoline because of their potential use in catalysis. A number of phosphine oxide-imidazoliums were synthesized by standard amide coupling. The isolation of synthetic oxazoline-imidazolium could not be achieved without decomposition of the ligand.

A number of the ligands synthesized were bound to rhodium through transmetallation of a silver-NHC complex. The application of these ligands in asymmetric catalysis was as yet unsuccessful.

To summarize, the synthesis of proline-based N-heterocyclic carbene building blocks has been accomplished and they have been utilized to construct a variety of NHC precursors. Further research is being undertaken by other researchers in our laboratory toward the preparation of the next generation of bidentate ligands and the applications of these proline-based NHC ligands in stereoselective organometallic chemistry. There is significant potential of well-tuned bidentate ligands to be employed as highly competent asymmetric ligands in a number of reactions involving boronic acids in conjugate additions to enones and 1, 2-additions to aldehydes.

BIBLIOGRAPHY

(1) Bourissou, D.; Guerret, O.; Gabbaï, F. P.; Bertrand, G. *Chem. Rev.* **2000**, *100* (1), 39.
(2) Bertrand, G. *Carbene Chemistry: From Fleeting Intermediates to Powerful Reagents*; CRC Press, 2002.
(3) Canac, Y.; Soleilhavoup, M.; Conejero, S.; Bertrand, G. *J. Organomet. Chem.* **2004**, *689* (24), 3857.
(4) De Frémont, P.; Marion, N.; Nolan, S. P. *Coord. Chem. Rev.* **2009**, *253* (7–8), 862.
(5) Wanzlick, H. W. *Angew. Chem. Int. Ed. Engl.* **1962**, *1* (2), 75.
(6) Arduengo, A. J.; Harlow, R. L.; Kline, M. *J. Am. Chem. Soc.* **1991**, *113* (1), 361.
(7) Herrmann, W. A.; Elison, M.; Fischer, J.; Köcher, C.; Artus, G. R. J. *Angew. Chem. Int. Ed. Engl.* **1995**, *34* (21), 2371.
(8) Glorius, F. In *N-Heterocyclic Carbenes in Transition Metal Catalysis*; Topics in Organometallic Chemistry; Springer Berlin Heidelberg, 2007; pp 1–20.
(9) Leuthäußer, S.; Schwarz, D.; Plenio, H. *Chem. – Eur. J.* **2007**, *13* (25), 7195.
(10) Cavallo, L.; Correa, A.; Costabile, C.; Jacobsen, H. *J. Organomet. Chem.* **2005**, *690* (24–25), 5407.
(11) Díez-González, S.; Nolan, S. P. *Coord. Chem. Rev.* **2007**, *251* (5–6), 874.
(12) Dorta, R.; Stevens, E. D.; Scott, N. M.; Costabile, C.; Cavallo, L.; Hoff, C. D.; Nolan, S. P. *J. Am. Chem. Soc.* **2005**, *127* (8), 2485.
(13) Benhamou, L.; Chardon, E.; Lavigne, G.; Bellemin-Laponnaz, S.; César, V. *Chem. Rev.* **2011**, *111* (4), 2705.
(14) Jazzar, R.; Liang, H.; Donnadieu, B.; Bertrand, G. *J. Organomet. Chem.* **2006**, *691* (14), 3201.
(15) Kuhn, K. M.; Grubbs, R. H. *Org. Lett.* **2008**, *10* (10), 2075.
(16) Tennyson, A. G.; Lynch, V. M.; Bielawski, C. W. *J. Am. Chem. Soc.* **2010**, *132* (27), 9420.
(17) Benhamou, L.; César, V.; Gornitzka, H.; Lugan, N.; Lavigne, G. *Chem. Commun.* **2009**, No. 31, 4720.
(18) Benhamou, L.; Vujkovic, N.; César, V.; Gornitzka, H.; Lugan, N.; Lavigne, G. *Organometallics* **2010**, *29* (11), 2616.
(19) Biju, A. T.; Hirano, K.; Fröhlich, R.; Glorius, F. *Chem. – Asian J.* **2009**, *4* (12), 1786.
(20) Fürstner, A.; Alcarazo, M.; César, V.; Lehmann, C. W. *Chem. Commun.* **2006**, No. 20, 2176.
(21) Struble, J. R.; Bode, J. W. *Tetrahedron* **2008**, *64* (29), 6961.
(22) Struble, J. R.; Kaeobamrung, J.; Bode, J. W. *Org. Lett.* **2008**, *10* (5), 957.
(23) Makino, T.; Masu, H.; Katagiri, K.; Yamasaki, R.; Azumaya, I.; Saito, S. *Eur. J. Inorg. Chem.* **2008**, *2008* (31), 4861.
(24) Saba, S.; Brescia, A.-M.; Kaloustian, M. K. *Tetrahedron Lett* **1991**, *32*, 5031.

(25) Arduengo III, A. J.; Krafczyk, R.; Schmutzler, R.; Craig, H. A.; Goerlich, J. R.; Marshall, W. J.; Unverzagt, M. *Tetrahedron* **1999**, *55* (51), 14523.
(26) Delaude, L.; Szypa, M.; Demonceau, A.; Noels, A. F. *Adv Synth Catal* **2002**, *344*, 749.
(27) Leuthäusser, S.; Schmidts, V.; Thiele, C. M.; Plenio, H. *Chem—Eur J* **2008**, *14*, 5465.
(28) Fleckenstein, C.; Roy, S.; Leuthäusser, S.; Plenio, H. *Chem Commun* **2007**, 2870.
(29) Kantchev, E. A. B.; Ying, J. Y. *Organometallics* **2009**, *28*, 289.
(30) Fliedel, C.; Maisse-François, A.; Bellemin-Laponnaz, S. *Inorg Chim Acta* **2007**, *360*, 143.
(31) Waltman, A. W.; Grubbs, R. H. *Organometallics* **2004**, *23*, 3105.
(32) Vougioukalakis, G. C.; Grubbs, R. H. *Organometallics* **2007**, *26*, 2469.
(33) Hadei, N.; Kantchev, E. A. B.; O'Brien, C. J.; Organ, M. G. *J Org Chem* **2005**, *70*, 8503.
(34) Vougioukalakis, G. C.; Grubbs, R. H. *Chem—Eur J* **2008**, *14*, 7545.
(35) Ritter, T.; Day, M. W.; Grubbs, R. H. *J Am Chem Soc* **2006**, *128*, 11768.
(36) Winkelmann, O.; Linder, D.; Lacour, J.; Näther, C.; Lüning, U. *Eur J Org Chem* **2007**, 3687.
(37) Xu, G.; Gilbertson, S. R. *Org Lett* **2005**, *7*, 4605.
(38) Kuriyama, M.; Shimazawa, R.; Shirai, R. *Tetrahedron* **2007**, *63*, 9393.
(39) Clavier, H.; Coutable, L.; Guillemin, J. C.; Mauduit, M. *Tetrahedron Asymmetry* **2005**, *16*, 921.
(40) Tzur, E.; Ben-Asuly, A.; Diesendruck, C. E.; Goldberg, I.; Lemcoff, N. G. *Angew Chem Int Ed* **2008**, *47*, 6422.
(41) Jurcík, V.; Gilani, M.; Wilhelm, R. *Eur J Org Chem* **2006**, 5103.
(42) Steinke, T.; Shaw, B. K.; Jong, H.; Patrick, B. O.; Fryzuk, M. D. *Organometallics* **2009**, *28*, 2830.
(43) Prasad, B. A. B.; Gilbertson, S. R. *Org. Lett.* **2009**, *11* (16), 3710.
(44) Tiede, S.; Berger, A.; Schlesiger, D.; Rost, D.; Lühl, A.; Blechert, S. *Angew Chem Int Ed* **2010**, *49*, 3972.
(45) Kison, C.; Opatz, T. *Synthesis* **2006**, *21*, 3727.
(46) Sato, H.; Fujihara, T.; Obora, Y.; Tokunaga, M.; Kiyosu, J.; Tsuji, Y. *Chem Commun* **2007**, 269.
(47) Alexander, S. G.; Cole, M. L.; Morris, J. C. *New J Chem* **2009**, *33*, 720.
(48) Vasudevan, K. V.; Butorac, R. R.; Abernethy, C. D.; Cowley, A. H. *Dalton Trans* **2010**, *39*, 7401.
(49) Tapu, D.; Owens, C.; VanDerveer, D.; Gwaltney, K. *Organometallics* **2009**, *28*, 270.
(50) Hirsch-Weil, D.; Abboud, K. A.; Hong, S. *Chem Commun* **2010**, *46*, 7525.
(51) Ma, Q.; Ma, Y.; Liu, X.; Duan, W.; Qu, B.; Song, C. *Tetrahedron Asymmetry* **2010**, *21*, 292.
(52) Seo, H.; Hirsch-Weil, D.; Abboud, K. A.; Hong, S. *J Org Chem* **2008**, *73*, 1983.
(53) Saravanakumar, S.; Kindermann, M. K.; Heinicke, J.; Köckerling, M. *Chem Commun* **2006**, 640.
(54) Würtz, S.; Glorius, F. *Acc. Chem. Res.* **2008**, *41* (11), 1523.
(55) Grant, T. G.; Meyers, A. I. *Tetrahedron* **1994**, *50*, 2297.

(56) Peer, M.; de Jong, J. C.; Langer, T.; Rieck, H.; Schell, H.; Sennhann, P.; Sprinz, J.; Steinhagen, H.; Wiese, B.; Helmchen, G. *Tetrahedron* **1996**, *52*, 7547.
(57) Glorius, F.; Altenhoff, G.; Goddard, R.; Lehmann, C. W. *Chem Commun* **2002**, 2704.
(58) Altenhoff, G.; Goddard, R.; Lehmann, C. W.; Glorius, F. *Angew Chem Int Ed* **2003**, *42*, 3690.
(59) Altenhoff, G.; Goddard, R.; Lehmann, C. W.; Glorius, F. *J Am Chem Soc* **2004**, *126*, 15195.
(60) Würtz, S.; Lohre, C.; Fröhlich, R.; Bergander, K.; Glorius, F. *J Am Chem Soc* **2009**, *131*, 8344.
(61) Burstein, C.; Lehmann, C. W.; Glorius, F. *Tetrahedron* **2005**, *61*, 6207.
(62) Lohre, C.; Fröhlich, R.; Glorius, F. *Synthesis* **2008**, 2221.
(63) Suisse, J. M.; Bellemin-Laponnaz, S.; Douce, L.; Maisse-François, A.; Welter, R. *Tetrahedron Lett* **2005**, *46*, 4303.
(64) Suisse, J. M.; Douce, L.; Bellemin-Laponnaz, S.; Maisse-François, A.; Welter, R.; Miyake, Y.; Shimizu, Y. *Eur J Inorg Chem* **2007**, 3899.
(65) Bildstein, B.; Malaun, M.; Kopacka, H.; Wurst, K.; Mitterböck, M.; Ongania, K.-H.; Opromolla, G.; Zanello, P. *Organometallics* **1999**, *18*, 4325.
(66) Nolan, S. P. *N-Heterocyclic Carbenes in Synthesis*; 2006.
(67) Böhler, C.; Stein, D.; Donati, N.; Grützmacher, H. *New J Chem* **2002**, *26*, 1291.
(68) Jafarpour, L.; Stevens, E. D.; Nolan, S. P. *J Organomet Chem* **2000**, *606*, 49.
(69) Chien, C.-H.; Fujita, S.; Yamoto, S.; Hara, T.; Yamagata, T.; Watanabe, M.; Mashima, K. *Dalton Trans* **2008**, 916.
(70) Hintermann, L. *Beilstein J Org Chem* **2007**, *3*, 22.
(71) Huisgen, R. *Angew Chem Int Ed Engl* **1980**, *19*, 947.
(72) Taylor, E. C.; Turchi, I. J. *Chem Rev* **1979**, *79*, 181.
(73) Ogle, J. W.; Zhang, J.; Reibenspies, J. H.; Abboud, K.; Miller, S. A. *Org Lett* **2008**, *10*, 3677.
(74) Powell, A. B.; Bielawski, C. W.; Cowley, A. H. *J Am Chem Soc* **2010**, *132*, 10184.
(75) Powell, A. B.; Brown, J. R.; Vasudevan, K. V.; Cowley, A. H. *Dalton Trans* **2009**, 2521.
(76) Powell, A. B.; Bielawski, C. W.; Cowley, A. H. *J Am Chem Soc* **2009**, *131*, 18232.
(77) Kamijo, S.; Yamamoto, Y. *Chem. – Asian J.* **2007**, *2* (5), 568.
(78) Enders, D.; Niemeier, O.; Henseler, A. *Chem. Rev.* **2007**, *107* (12), 5606.
(79) Marion, N.; Díez-González, S.; Nolan, S. P. *Angew. Chem. Int. Ed.* **2007**, *46* (17), 2988.
(80) Campbell, C. D.; Ling, K. B.; Smith, A. D. In *N-Heterocyclic Carbenes in Transition Metal Catalysis and Organocatalysis*; Cazin, C. S. J., Ed.; Catalysis by Metal Complexes; Springer Netherlands, 2011; pp 263–297.
(81) Herrmann, W. A. *Angew. Chem. Int. Ed.* **2002**, *41* (8), 1290.
(82) Crudden, C. M.; Allen, D. P. *Coord. Chem. Rev.* **2004**, *248* (21–24), 2247.
(83) Lee, H.; Lee, C.-C.; Cheng, P.-Y. *Curr. Org. Chem.* **2007**, *11* (17), 1491.
(84) Herrmann, W. A.; Goossen, L. J.; Köcher, C.; Artus, G. R. J. *Angew Chem Int Ed Engl* **1996**, *35*, 2805.
(85) Enders, D.; Gielen, H. *J Organomet Chem* **2001**, *617−618*, 70.

(86) Lee, S.; Hartwig, J. F. *J. Org. Chem.* **2001**, *66* (10), 3402.
(87) Culkin, D. A.; Hartwig, J. F. *Acc. Chem. Res.* **2003**, *36* (4), 234.
(88) Sato, Y.; Yoshino, T.; Mori, M. *Org Lett* **2003**, *5*, 31.
(89) Powell, M. T.; Hou, D.-R.; Perry, M. C.; Cui, X.; Burgess, K. *J. Am. Chem. Soc.* **2001**, *123* (36), 8878.
(90) Gómez, M.; Muller, G.; Rocamora, M. *Coord. Chem. Rev.* **1999**, *193–195*, 769.
(91) Gade, L. H.; Bellemin-Laponnaz, S. In *N-Heterocyclic Carbenes in Transition Metal Catalysis*; Topics in Organometallic Chemistry; Springer Berlin Heidelberg, 2007; pp 117–157.
(92) Bongers, N.; Krause, N. *Angew Chem Int Ed* **2008**, *47*, 2178.
(93) Ravi, A.; Balaram, P. *Tetrahedron* **1984**, *40* (13), 2577.
(94) Aubry, A.; Cung, M. T.; Marraud, M. *J. Am. Chem. Soc.* **1985**, *107* (25), 7640.
(95) Imperiali, B.; Moats, R. A.; Fisher, S. L.; Prins, T. J. *J. Am. Chem. Soc.* **1992**, *114* (9), 3182.
(96) Imperiali, B.; Kapoor, T. M. *Tetrahedron* **1993**, *49* (17), 3501.
(97) Chung, Y. J.; Christianson, L. A.; Stanger, H. E.; Powell, D. R.; Gellman, S. H. *J. Am. Chem. Soc.* **1998**, *120* (40), 10555.
(98) Szpak, P. *J. Archaeol. Sci.* **2011**, *38* (12), 3358.
(99) Stewart, D. E.; Sarkar, A.; Wampler, J. E. *J. Mol. Biol.* **1990**, *214* (1), 253.
(100) Pal, D.; Chakrabarti, P. *J. Mol. Biol.* **1999**, *294* (1), 271.
(101) Ramachandran, G. N.; Sasisekharan, V. In *Advances in Protein Chemistry*; C.B. Anfinsen, M. L. A., John T. Edsall and Frederic M. Richards, Ed.; Academic Press, 1968; Vol. Volume 23, pp 283–437.
(102) List, B.; Lerner, R. A.; Barbas, C. F. *J. Am. Chem. Soc.* **2000**, *122* (10), 2395.
(103) Seayad, J.; List, B. *Org. Biomol. Chem.* **2005**, *3* (5), 719.
(104) Melchiorre, P.; Marigo, M.; Carlone, A.; Bartoli, G. *Angew. Chem. Int. Ed.* **2008**, *47* (33), 6138.
(105) Moyano, A.; Rios, R. *Chem. Rev.* **2011**, *111* (8), 4703.
(106) Gilbertson, S. R.; Xie, D. *Angew. Chem. Int. Ed.* **1999**, *38* (18), 2750.
(107) Gilbertson, S. R.; Fu, Z.; Xie, D. *Tetrahedron Lett.* **2001**, *42* (3), 365.
(108) Gilbertson, S. R.; Xie, D.; Fu, Z. *J. Org. Chem.* **2001**, *66* (22), 7240.
(109) Agarkov, A.; Greenfield, S.; Xie, D.; Pawlick, R.; Starkey, G.; Gilbertson, S. R. *Pept. Sci.* **2006**, *84* (1), 48.
(110) Gilbertson, S. R.; Wang, X. *Tetrahedron* **1999**, *55* (39), 11609.
(111) Gilbertson, S. R.; Collibee, S. E.; Agarkov, A. *J. Am. Chem. Soc.* **2000**, *122* (27), 6522.
(112) Greenfield, S. J.; Gilbertson, S. R. *Synthesis* **2001**, *2001* (15), 2337.
(113) Greenfield, S. J.; Agarkov, A.; Gilbertson, S. R. *Org. Lett.* **2003**, *5* (17), 3069.
(114) Leuthäußer, S.; Schmidts, V.; Thiele, C. M.; Plenio, H. *Chem. – Eur. J.* **2008**, *14* (18), 5465.
(115) Kappe, C. O. *Angew. Chem. Int. Ed.* **2004**, *43* (46), 6250.
(116) Fürstner, A.; Alcarazo, M.; Radkowski, K.; Lehmann, C. W. *Angew. Chem. Int. Ed.* **2008**, *47* (43), 8302.
(117) Liu, F.-Z.; Fang, H.; Zhu, H.-W.; Wang, Q.; Yang, Y.; Xu, W.-F. *Bioorg. Med. Chem.* **2008**, *16* (1), 578.

(118) Meena; Kumar, V. A. *Bioorg. Med. Chem.* **2003**, *11* (16), 3393.
(119) Zhao, Y.; Gilbertson, S. R. *Org. Lett.* **2014**, *16* (4), 1033.
(120) Herrmann, W. A.; Goossen, L. J.; Spiegler, M. *Organometallics* **1998**, *17* (11), 2162.
(121) Wang, A.-E.; Xie, J.-H.; Wang, L.-X.; Zhou, Q.-L. *Tetrahedron* **2005**, *61* (1), 259.
(122) Herrmann, W. A.; Gooβen, L. J.; Spiegler, M. *J. Organomet. Chem.* **1997**, *547* (2), 357.
(123) Gardiner, M. G.; Herrmann, W. A.; Reisinger, C.-P.; Schwarz, J.; Spiegler, M. *J. Organomet. Chem.* **1999**, *572* (2), 239.
(124) Yang, C.; Lee, H. M.; Nolan, S. P. *Org. Lett.* **2001**, *3* (10), 1511.
(125) Loch, J. A.; Albrecht, M.; Peris, E.; Mata, J.; Faller, J. W.; Crabtree, R. H. *Organometallics* **2002**, *21* (4), 700.
(126) César, V.; Bellemin-Laponnaz, S.; Gade, L. H. *Organometallics* **2002**, *21* (24), 5204.
(127) Perry, M. C.; Burgess, K. *Tetrahedron Asymmetry* **2003**, *14* (8), 951.
(128) Jodry, J. J.; Mikami, K. *Tetrahedron Lett.* **2004**, *45* (23), 4429.
(129) Ding, X.; Tang, W.; Zhu, C.; Cheng, Y. *Adv. Synth. Catal.* **2010**, *352* (1), 108.
(130) Occhipinti, G.; Jensen, V. R.; Törnroos, K. W.; Frøystein, N. Å.; Bjørsvik, H.-R. *Tetrahedron* **2009**, *65* (34), 7186.
(131) Cardinale, G. J.; Abeles, R. H. *Biochemistry (Mosc.)* **1968**, *7* (11), 3970.
(132) Buschiazzo, A.; Goytia, M.; Schaeffer, F.; Degrave, W.; Shepard, W.; Grégoire, C.; Chamond, N.; Cosson, A.; Berneman, A.; Coatnoan, N.; Alzari, P. M.; Minoprio, P. *Proc. Natl. Acad. Sci. U. S. A.* **2006**, *103* (6), 1705.
(133) Jarvo, E. R.; Miller, S. J. *Tetrahedron* **2002**, *58* (13), 2481.
(134) Movassaghi, M.; Jacobsen, E. N. *Science* **2002**, *298* (5600), 1904.
(135) Hajos, Z. G.; Parrish, D. R. *J. Org. Chem.* **1973**, *38* (19), 3239.
(136) Hajos, Z. G.; Parrish, D. R. *J. Org. Chem.* **1974**, *39* (12), 1615.
(137) Eder, U.; Sauer, G.; Wiechert, R. *Angew. Chem. Int. Ed. Engl.* **1971**, *10* (7), 496.
(138) Melchiorre, P.; Marigo, M.; Carlone, A.; Bartoli, G. *Angew. Chem. Int. Ed.* **2008**, *47* (33), 6138.
(139) Davie, E. A. C.; Mennen, S. M.; Xu, Y.; Miller, S. J. *Chem. Rev.* **2007**, *107* (12), 5759.
(140) Copeland, G. T.; Jarvo, E. R.; Miller, S. J. *J. Org. Chem.* **1998**, *63* (20), 6784.
(141) Jarvo, E. R.; Copeland, G. T.; Papaioannou, N.; Bonitatebus, P. J.; Miller, S. J. *J. Am. Chem. Soc.* **1999**, *121* (50), 11638.
(142) Sculimbrene, B. R.; Miller, S. J. *J. Am. Chem. Soc.* **2001**, *123* (41), 10125.
(143) Sculimbrene, B. R.; Morgan, A. J.; Miller, S. J. *J. Am. Chem. Soc.* **2002**, *124* (39), 11653.
(144) Imbriglio, J. E.; Vasbinder, M. M.; Miller, S. J. *Org. Lett.* **2003**, *5* (20), 3741.
(145) Aroyan, C. E.; Vasbinder, M. M.; Miller, S. J. *Org. Lett.* **2005**, *7* (18), 3849.
(146) Evans, J. W.; Fierman, M. B.; Miller, S. J.; Ellman, J. A. *J. Am. Chem. Soc.* **2004**, *126* (26), 8134.
(147) Revell, J. D.; Gantenbein, D.; Krattiger, P.; Wennemers, H. *Pept. Sci.* **2006**, *84* (1), 105.
(148) Kelly, D. R.; Roberts, S. M. *Pept. Sci.* **2006**, *84* (1), 74.

(149) Berkessel, A.; Koch, B.; Toniolo, C.; Rainaldi, M.; Broxterman, Q. B.; Kaptein, B. *Pept. Sci.* **2006**, *84* (1), 90.
(150) Gilbertson, S. R. In *In Progress in Inorganic Chemistry*; John Wiley & Sons: New York, 2001; Vol. 50, pp 433–471.
(151) Agarkov, A.; Uffman, E. W.; Gilbertson, S. R. *Org. Lett.* **2003**, *5* (12), 2091.
(152) Agarkov, A.; Greenfield, S. J.; Ohishi, T.; Collibee, S. E.; Gilbertson, S. R. *J. Org. Chem.* **2004**, *69* (23), 8077.
(153) Zaykov, A. N.; MacKenzie, K. R.; Ball, Z. T. *Chem. – Eur. J.* **2009**, *15* (36), 8961.
(154) Sambasivan, R.; Ball, Z. T. *Angew. Chem. Int. Ed.* **2012**, *51* (34), 8568.
(155) Chen, Z.; Vohidov, F.; Coughlin, J. M.; Stagg, L. J.; Arold, S. T.; Ladbury, J. E.; Ball, Z. T. *J. Am. Chem. Soc.* **2012**, *134* (24), 10138.
(156) Ball, Z. T. *Acc. Chem. Res.* **2013**, *46* (2), 560.
(157) Miller, S. J.; Copeland, G. T.; Papaioannou, N.; Horstmann, T. E.; Ruel, E. M. *J. Am. Chem. Soc.* **1998**, *120* (7), 1629.
(158) Hoveyda, A. H.; Hird, A. W.; Kacprzynski, M. A. *Chem. Commun.* **2004**, No. 16, 1779.
(159) Hird, A. W.; Hoveyda, A. H. *J. Am. Chem. Soc.* **2005**, *127* (43), 14988.
(160) Fu, P.; Snapper, M. L.; Hoveyda, A. H. *J. Am. Chem. Soc.* **2008**, *130* (16), 5530.
(161) Lalonde, M. P.; McGowan, M. A.; Rajapaksa, N. S.; Jacobsen, E. N. *J. Am. Chem. Soc.* **2013**, *135* (5), 1891.
(162) Filira, F.; Biondi, L.; Gobbo, M.; Rocchi, R. *Tetrahedron Lett.* **1991**, *32* (50), 7463.
(163) Canlas, G. M. R.; Gilbertson, S. R. *Chem. Commun.* **2014**, *50* (39), 5007.
(164) Zhang, X.; Liu, H.; Hu, X.; Tang, G.; Zhu, J.; Zhao, Y. *Org. Lett.* **2011**, *13* (13), 3478.
(165) Guo, R.; Lu, S.; Chen, X.; Tsang, C.-W.; Jia, W.; Sui-Seng, C.; Amoroso, D.; Abdur-Rashid, K. *J. Org. Chem.* **2010**, *75* (3), 937.
(166) Peris, E. In *N-Heterocyclic Carbenes in Transition Metal Catalysis*; Topics in Organometallic Chemistry; Springer Berlin Heidelberg, 2007; pp 83–116.
(167) Hahn, F. E.; Jahnke, M. C. *Angew. Chem. Int. Ed.* **2008**, *47* (17), 3122.
(168) Weskamp, T.; Böhm, V. P. W.; Herrmann, W. A. *J Organomet Chem* **2000**, *600*, 12.
(169) Wang, H. M. J.; Lin, I. J. B. *Organometallics* **1998**, *17* (5), 972.
(170) Garrison, J. C.; Youngs, W. J. *Chem. Rev.* **2005**, *105* (11), 3978.
(171) Allen, D. P.; Crudden, C. M.; Calhoun, L. A.; Wang, R.; Decken, A. *J Organomet Chem* **2005**, *690*, 5736.
(172) Herrmann, W. A.; Frey, G. D.; Herdtweck, E.; Steinbeck, M. *Adv Synth Catal* **2007**, *349*, 1677.
(173) Van Leeuwen, P. W. N. M.; Claver, C. *Rhodium Catalysed Hydroformylation*; 2000.
(174) Colquhoun, H. M.; Thompson, D. J.; Twigg, M. V. *Carbonylation: Direct Synthesis of Carbonyl Compounds*; 1991.
(175) Evans, P. A.; Baum, E. W.; Fazal, A. N.; Pink, M. *Chem Commun* **2005**, 63.
(176) Baik, M.-H.; Baum, E. W.; Burland, M. C.; Evans, P. A. *J Am Chem Soc* **2005**, *127*, 1602.

(177) Park, K. H.; Kim, S. Y.; Son, S. U.; Chung, Y. K. *Eur J Org Chem* **2003**, 4341.
(178) Gómez, F. J.; Kamber, N. E.; Deschamps, N. M.; Cole, A. P.; Wender, P. A.; Waymouth, R. M. *Organometallics* **2007**, *26*, 4541.
(179) Peng, H. M.; Webster, R. D.; Li, X. *Organometallics* **2008**, *27*, 4484.
(180) Gomes, L. F. R.; Trindade, A. F.; Candeias, N. R.; Gois, P. M. P.; Afonso, C. A. M. *Tetrahedron Lett* **2008**, *49*, 7372.
(181) Miyaura, N. *Bull Chem Soc Jpn* **2008**, *81*, 1535.
(182) Poyatos, M.; Mata, J. A.; Peris, E. *Chem Rev* **2009**, *109*.
(183) Duan, H.-F.; Xie, J.-H.; Shi, W.-J.; Zhang, Q.; Zhou, Q.-L. *Org. Lett.* **2006**, *8* (7), 1479.
(184) Morikawa, S.; Michigami, K.; Amii, H. *Org. Lett.* **2010**, *12* (11), 2520.
(185) Focken, T.; Rudolph, J.; Bolm, C. *Synthesis* **2005**, 429.